A SYSTEMATIC APPROACH TO DESIGN FOR LIFELONG AIRCRAFT EVOLUTION

A Thesis
Presented to
The Academic Faculty

by

Dongwook Lim

In Partial Fulfillment
of the Requirements for the Degree
Doctor of Philosophy in Aerospace Engineering

School of Aerospace Engineering
Georgia Institute of Technology
May 2009

A SYSTEMATIC APPROACH TO DESIGN FOR LIFELONG AIRCRAFT EVOLUTION

Approved by:

Dr. Dimitri N. Mavris, Advisor
School of Aerospace Engineering
Georgia Institute of Technology

Dr. Daniel P. Schrage
School of Aerospace Engineering
Georgia Institute of Technology

Dr. Carlee A. Bishop
Electronics Systems Laboratory
Georgia Tech Research Institute

Dr. Mark Costello
School of Aerospace Engineering
Georgia Institute of Technology

Dr. Taewoo Nam
School of Aerospace Engineering
Georgia Institute of Technology

Date Approved: 04/03/2009

To my parents, for their love and trust

and to Chanju, for everything

PREFACE

During my years in the Aerospace Systems Design Laboratory (ASDL) of the Georgia Institute of Technology, I have been very lucky to engage in some of the most exciting aerospace projects of the time. Some of these revolutionary systems included a 100 passenger commercial blended-wing-body aircraft that burns 20% less fuel than the state-of-art commercial transports; personal air vehicles (PAVs) with vertical takeoff and landing (VTOL) capabilities; compound helicopters cruising up to 300 knots; unmanned aerial vehicles (UAV) with inflatable wings that are launched from the Navy vessels; and a 5-inch wingspan micro-air-vehicles for a world competition. I was also involved in a next generation sizing and synthesis project in which advanced ways of designing revolutionary types of aircraft was investigated under sponsorship from NASA Langley Research Center. Yet, it is an irony that the I found my thesis topic from a more of an evolutionary way of designing new aircraft.

It was actually during the US Air Force CSAR-X project that I started to become curious about designing aircraft while accounting for future evolution. In 2006, the Air Force issued a request for proposal to acquire more than 250 helicopters to replace the aging HH-60 Black Hawk fleet, whose primary mission has been performing search-and-rescue for downed pilots. In this program, the vehicle selection among the candidates was subjected to a series of block requirements, given as Block 0, Block 10, and Block 10 plus. The fundamental difference between each of these three blocks' requirements was cruise speed. This requirement became progressively more demanding, increasing from 130 knots to 215, and finally to 250+ knots. Eventually, Boeing's proposal to provide a derivative version of the CH-47 Chinook won the contract, primarily because of its

growth potential to meet Block 10 and 10 plus requirements with minimal cost. The CSAR-X was one of the largest early-21st century U.S. acquisition programs, and its progressive requirements represent a larger trend in aerospace design.

My experience with this program influenced me greatly, and I began to ask how aircraft designers could predict and prepare for future growth. The ability to anticipate evolving requirements is especially important during the very early stage of the aircraft development process, when design freedom and potential for cost reduction are greatest, knowledge about the aircraft is the smallest, and thus program uncertainty is the greatest. I quickly realized that we confront similar problems in our daily lives. Buying a car or choosing a house to live in could fall into this category of decision-making where goals and needs vary in time. This is especially the case if one is expecting some sort of family growth. Even buying a pair of shoes for my two-year-old son and three-month-old daughter (at the moment of writing this thesis) involved a balanced decision making. On the one hand, there were the fitness and comfort the little ones would feel; on the other hand, there was the frequency with which a lazy father would have to prepare for new shoes, based on the forecasted rate of growth of children's feet.

It was this curiosity that led me on this long journey.

ACKNOWLEDGEMENTS

TABLE OF CONTENTS

LIST OF TABLES

LIST OF FIGURES

LIST OF SYMBOLS

C_{Di} drag-due-to-lift coefficient

C_{Do} zero-lift-drag coefficient

C_{Lmax} maximum lift coefficient

$\mathbb{E}_{\omega}[\Phi]$ expectation of Φ with respect to $\boldsymbol{\omega}$

f_{Θ} objective function of the Θth stage

$\mathbf{g}_{\Theta}$ design constraint vector of the Θth stage

L/D lift-to-drag ratio

$(\Phi_{\Theta}^{*})_s^p$ attribute Φ of strategy p in Θ^{th} stage under scenario s

$\hat{\Phi}$ attribute Φ evaluated after randomness is revealed

$\mathbf{x}_{\Theta}$ design variable vector of the Θth stage

$\boldsymbol{\omega}$ random variable vector

$\hat{\boldsymbol{\omega}}$ observed random variable

LIST OF ABBREVIATIONS

AFCEA	Armed Forces Communications and Electronic Association
AH	Ad-Hoc
AHP	Analytic Hierarchy Process
AIAA	American Institute of Aeronautics and Astronautics
ANN	Artificial Neural Network
AoA	Angle-of-Attack
ASDL	Aerospace Systems Design Laboratory
ATA	Advanced Tactical Aircraft
ATF	Advanced Tactical Fighter
BLISS	Bi-level Integrated System Synthesis
C2	Command and Control
CBO	Congressional Budget Office
CCDF	Complementary Cumulative Distribution Function
CDF	Cumulative Distribution Function
CG	Center of Gravity
CO	Collaborative Optimization
COEA	Cost and Operational Effectiveness Analysis
CVW	Carrier Air Wing
DCF	Design Commonality Factor

Dem/Val	Demonstration and validation
DetPP	Deterministic Preplanning
DLF	Design Load Factor
DMF	Decision Making Framework
DoD	Department of Defense
DOT&E	Director of Operational Test and Evaluation
DSM	Design Structure Matrix
DT	Development Test
DT&E	Developmental Testing and Evaluation
EA	Evolutionary Acquisition
EMD	Engineering and Manufacturing Development
EPA	Environmental Protection Agency
EvoLVE	Evaluation of Lifelong Vehicle Evolution
EVPI	Expected Value of Perfect Information
FLOPS	Flight Optimization
FRP	Full-Rate Production
FSD	Full Scale Development
FTM	Flight Test Matrix
GAO	General Accounting Office
GTM	Ground Test Matrix
HN	Here-and-Now

HQ	Handling Qualities
IOC	Initial Operational Capability
IOT&E	Initial Operational Test and Evaluation
JSF	Joint Strike Fighter
KPP	Key Performance Parameter
LEX	Leading Edge Extension
LHS	Latin Hypercube Sampling
LP	Linear Programming
LRIP	Low Rate Initial Production
LWOD	Launch Wind-Over-Deck
M&S	Modeling and Simulation
MALCCA	Military Aircraft Life Cycle Cost Analysis
MCS	Monte Carlo Simulation
MDO	Multidisciplinary Design Optimization
MoE	Measure of Effectiveness
MoFD	Method of Feasible Direction
MSII	Milestone II
MVP	Multivariate Profiler
ND	New Design
NP	Neutral Point
O&S	Operation and Support

OPEVAL	Operational Evaluation
ORD	Operational Requirements Document
OSD	Office of the Secretary of Defense
OT&E	Operational Testing and Evaluation
P3I	Preplanned Product Improvement
PDF	Probability Density Function
PfD	Perfect-fit Design
PMF	Probability Mass Function
PoD	Perfect over-Design
QFD	Quality Functional Deployment
R&D	Research and Development
RASS	Risk-Averse Strategy Selection
RCS	Radar Cross Section
RDT&E	Research, Development, Test, and Evaluation
RFP	Request for Proposal
RV	Random Variable
RWOD	Recovery Wind-Over-Deck
SAA	Sample Average Approximation
SAR	Selected Acquisition Report
SD	Spiral Development
SLEP	Service Life Extension Program

SM	Static Margin
SoS	System-of-Systems
SPR	Stochastic Programming with Recourse
SQP	Sequential Quadratic Programming
SRS	Simple Random Sampling
STAR	System Threat Assessment Report
StoPP	Stochastic Preplanning
T&E	Test and Evaluation
TAD	Two-stage Aircraft Design
TIES	Technology Identification, Evaluation, and Selection
TRL	Technology Readiness Level
UAV	Unmanned Aerial Vehicle
VSS	Value of Stochastic Solution
VTOL	Vertical Takeoff and Landing
WBS	Work Breakdown Structure
WOD	Wind-Over-Deck
WS	Wait-and-See
WTM	Wind Tunnel Test Matrix

SUMMARY

Modern aerospace systems rely heavily on legacy platforms and their derivatives. Several successful aircraft designs that were introduced a half decade ago are still in operation. Historical examples show that after a vehicle design is frozen and delivered to a customer, successive upgrades are often made to fulfill changing requirements. Given the long life of aerospace systems and the continual change of military, economic, and political conditions, an aircraft designer must seek optimum solutions subject to evolving requirements. Current practices of adapting to emerging needs with derivative designs, retrofits, and upgrades are often reactive and ad-hoc, resulting in performance and cost penalties. Recent DoD acquisition policies have addressed this problem by establishing a general paradigm for design for lifelong evolution. However, there is a need for a unified, practical design approach that considers the lifetime evolution of an aircraft concept by incorporating future requirements and technologies.

This research proposes a systematic approach with which the decision makers can evaluate the value and risk of a new aircraft development program, including potential derivative development opportunities. The proposed Evaluation of Lifelong Vehicle Evolution (EvoLVE) method is a two- or multi-stage representation of the aircraft design process that accommodates initial development phases as well as follow-on phases. One of the key elements of this method is the Stochastic Programming with Recourse (SPR) technique, which accounts for uncertainties associated with future requirements. The remedial approach of SPR in its two distinctive problem-solving steps is well suited to aircraft design problems where derivatives, retrofits, and upgrades have been used to fix designs that were once but no longer optimal. The solution approach of SPR is

complemented by the Risk-Averse Strategy Selection (RASS) technique to gauge risk associated with vehicle evolution options. In the absence of a full description of the random space, a scenario-based approach captures the randomness with a few probable scenarios and reveals implications of different future events. Last, an interactive framework for decision-making support allows simultaneous navigation of the current and future design space with a greater degree of freedom. A cantilevered beam design problem was set up and solved using the SPR technique to showcase its application to an engineering design setting. The full EvoLVE method was conducted on a notional multi-role fighter based on the F/A-18 Hornet.

With the proposed framework for decision making under evolving requirements and technologies, the decision makers would be able to systematically evaluate the advantages and disadvantages of various growth options for a given vehicle. Consequently, design decisions offering a long-term benefit could be achieved even in an ever-changing operational and/or technological development environment.

CHAPTER I

INTRODUCTION

Today's needs for aerospace systems—whether they fall in the military, commercial, or space sector—rely heavily on legacy platforms and their derivatives. Some of the more successful aircraft designs that were introduced a half decade ago are still in operation. The best example is the B-52 strategic bomber, which was first conceived at the end of World War II and produced between 1952 and 1962. It is projected to be operational well into the mid-21 century [1]. Also, many of Boeing's CH-47 Chinook medium-lift tandem helicopters, which were first produced in 1961, are still in operation and are planned to be operational at least until the 2030s, although many modifications and upgrades have been made to the original configuration over the past four decades. Manned space missions are still largely dependent on NASA's space shuttle, which is a 1970s legacy design with upgraded avionics. Historical precedents have shown that once a vehicle design is frozen and delivered to the customer, successive upgrades are often made to the original concept, whether such modifications were planned from its inception or not. Indeed, a large portion of the U.S. aircraft procurement programs are devoted to evolving existing designs rather than initiating new creations [2].

Considering the gradual lengthening of aircraft life cycles, it is expected that future aerospace systems will operate for a longer time, thus they are more likely to be under operational and technological environments that are far from the ones that are initially conceived. Because of tightening budgets and time constraints, increasingly competitive markets, and lengthening of aircraft operational life, retrofit and/or derivative

developments would be more common. In this context, it would be relevant to investigate the issues and challenges behind designing aerospace systems considering their lifetime evolvement and to formally structure a way to address such issues.

1.1 Organization of the Document

Throughout the study, the author has made efforts to adhere to the formal scientific method to define the problem, perform a literature search, and formulate and implement a new solution approach. Using this formalism, a series of **Observations, Research Questions**, and **Hypotheses** are presented whenever appropriate. An **Observation** is a formalized insight learned from experience, interview, or literature. Observations induce **Research Questions** that are formal inquires on what should be studied and answered. A **Hypothesis** proposes a solution to the problems defined by research questions. Hypotheses are proved or disproved through a series of experiments that are carefully planned and executed. The process is iterative, in which knowledge gained through the process requires revisiting the formulated research questions and hypotheses until they converge.

1.2 Motivation

1.2.1 Catalyst for Aircraft Upgrade/Retrofit/Derivatives

Aircraft design can be characterized as the process of finding an optimal combination of vehicle concepts and technologies to meet or exceed all imposed requirements. Defining or eliciting such requirements is often considered the beginning of the design process and is followed by exploring the concept and technology spaces in an attempt to converge towards a single design solution. After the solution is finally selected and frozen, the

external environment in which the vehicle system is to be utilized constantly changes over the course of its operational life. Enemy threats advance at fast rates as a result of adopting new technologies or combining existing ones in new ways. The commercial sector is subject to unexpected, disruptive events, such as the outbreak of Severe Acute Respiratory Syndrome (SARS) and the 9/11 terrorist attacks. Changes in the political climate also affect the doctrine of a nation, which is inexorably linked with its strategic approach to future weapon systems procurement. This can be seen in the effect on the West of the collapse of the Soviet Union.

Accordingly, customer requirements continually evolve in response to such variations in enemy threats, market conditions, and politics. Evolution in customer requirements, in turn, renders existing aerospace systems uncompetitive or even infeasible. Uncompetitiveness and infeasibility can be resolved by retrofitting existing productions, introducing derivative models, or designing another new system. Figure 1 illustrates the gradual and constant evolution of threat, market, and technology and also illustrates two different options to respond to the changing need. Figure 1 (a) shows an option to acquire another new system as a solution to requirement change. Another approach, shown in Figure 1 (b), is improving existing systems through smaller multiple capability improvements. The first approach is not always desirable due to time and budget constraints. The automobile industry follows this block improvement strategy. Automakers come up with minor updates on existing models every year and make major modifications every four years. Automakers' practice of making minor/major modifications in a one/four-year time span is certainly a balanced strategy considering

(a) New-New Strategy   (b) Block Improvement Strategy
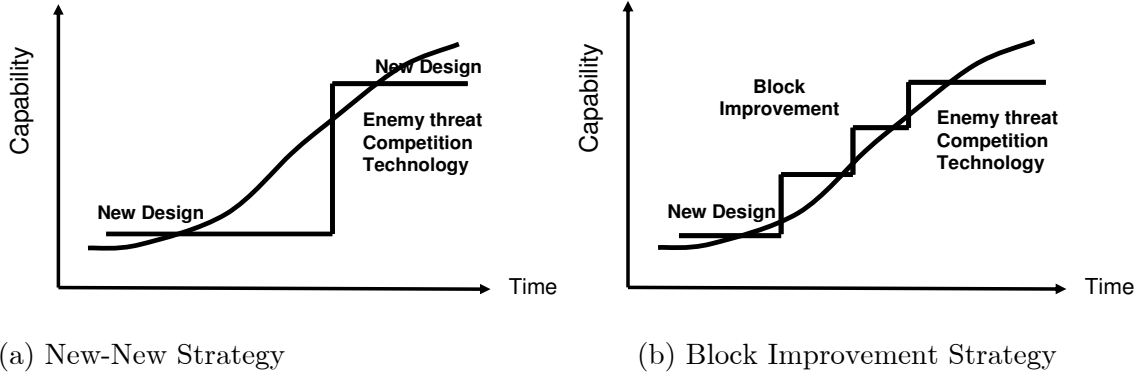
Figure 1: Evolution Capability and Threat over Time (adapted from [3])

competition, speed of technology advancement, customer need, cost associated with model changes, etc.

In summary, the two main drivers for upgrading an existing aerospace system are: (a) to adapt to evolving customer requirements; and (b) to maintain competitiveness by keeping pace with technological advancements. These observations are formally stated as follows:

Observation 1: *Aircraft designs evolve throughout their lives in order to meet constantly changing customer requirements and to keep competence through integration of new technologies.*

1.2.2 Trends in New Aerospace Systems Development

Since the first successful powered flight of the Wright brothers' Flyer I in 1903, aviation technology has advanced at a remarkable speed, expanding the capabilities of aerospace systems to an extent that was only possible in dreams a century ago. In the meantime, the complexity of such aerospace systems has been extraordinarily increased along with the development time and cost. A typical modern military aircraft development program
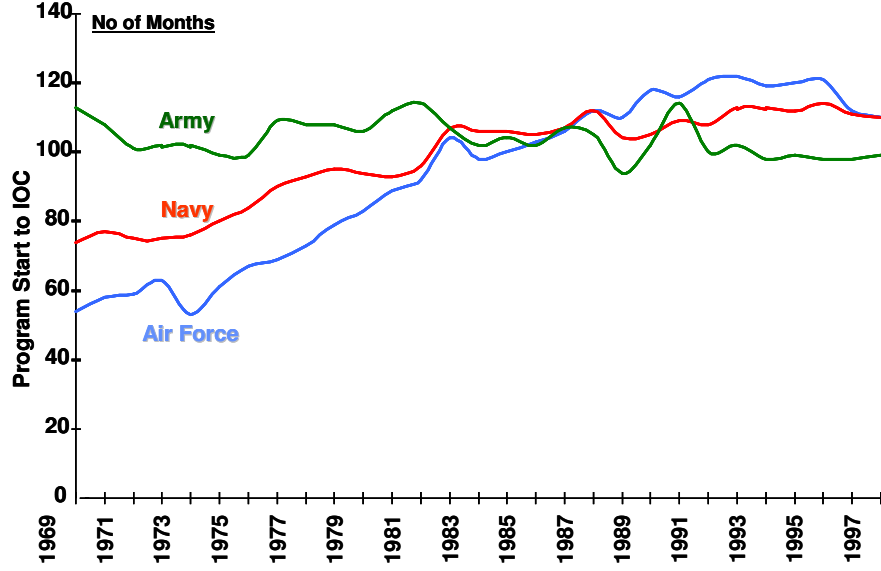
Figure 2: Average Acquisition Cycle Times [5]

involves multiple stakeholders, and thus multiple missions, multiple manufacturers, and even multiple countries.

With the growing complexity of aerospace systems, development time of a new aircraft has revealed a gradual increase from the early 1970s to the late 1990s. For example, Figure 2 shows the average acquisition time of the U.S. armed forces from 1969 to 1997. The figure shows a gradual increase in acquisition time in the case of the Navy and Air Force. In the 1990s, the U.S. Air Force and Navy acquisition programs took more than 100 months on average from project approval to initial operation capability (IOC). Specifically, in the case of the F-22 Raptor, it took more than two decades from the inception of the modern fighter jet to IOC [4].

Not surprisingly, such prolonged development time directly resulted in excessively higher-than-expected RDT&E and procurement cost. Empirical relationships between development cost and development time constructed from the Lean Aerospace Initiatives

(LAI) of MIT surveying 154 Air Force development programs shows in Eq (1) that development cost increases proportional to development time to the fourth power [5].

$$\$RDTE \approx (1.36 + 0.03\ T_{RDTE})^4 \qquad (1)$$

where $\$RDTE$ is the cost of RDT&E in million dollars and T_{RDTE} is time spent for RDT&E in months.

Such expanded development time and cost imposes high risk in the development of a new aircraft. The risk of program being canceled would increase due to unstable government funding or a lengthy period of time being necessary to reach the break-even point. Moreover, a long lead-in time to the IOC runs the risk of outdating most technologies embedded in the system, hampering technological competitiveness of newly fielded system.

Due to the ever-increasing time, cost, and risk of starting a new aircraft development program, modern aircraft systems are expected to be operational for a longer time, further aggravating the mismatch between the current operational, threat, market, and political environments and those defined when the program was first initiated. In order to close the gap between the actual and predicted requirements, modifying existing designs would become more common to not only aerospace systems but also any complex systems requiring a large amount of development time.

1.3 Background: Aircraft Design for Growth Potential

Modern aircraft designers are practicing provisions for growth potential within the setting of traditional aircraft design, consisting of conceptual, preliminary, and detail design phases. An illustration of conventional aircraft design processes that are

commonly found in publications such as Raymer [6], Roskam [7], Fielding [8], and Toreenbeek [9] are presented in Figure 3 along with the main design activities and the approaches to provide growth potential.

First of all, growth provisions, if any, can be allowed by permitting design margins in the sizing and synthesis process during the conceptual design. The allocation and appointment of the so-called margins are often based on expert opinion, engineering intuition, and historical precedents rather than analytical and rational methods. Additionally, modular design approaches and the use of standard components and common interfaces are practiced during the subsystem and component design phases [6].

However, more emphasis should be placed on the early phases of the design where design freedom is the largest and implication of the design decision is the greatest throughout the life of the system. Once a poor decision is made early on, the compensating effort by fine-tuning and optimizing at the sub-system level in later phases
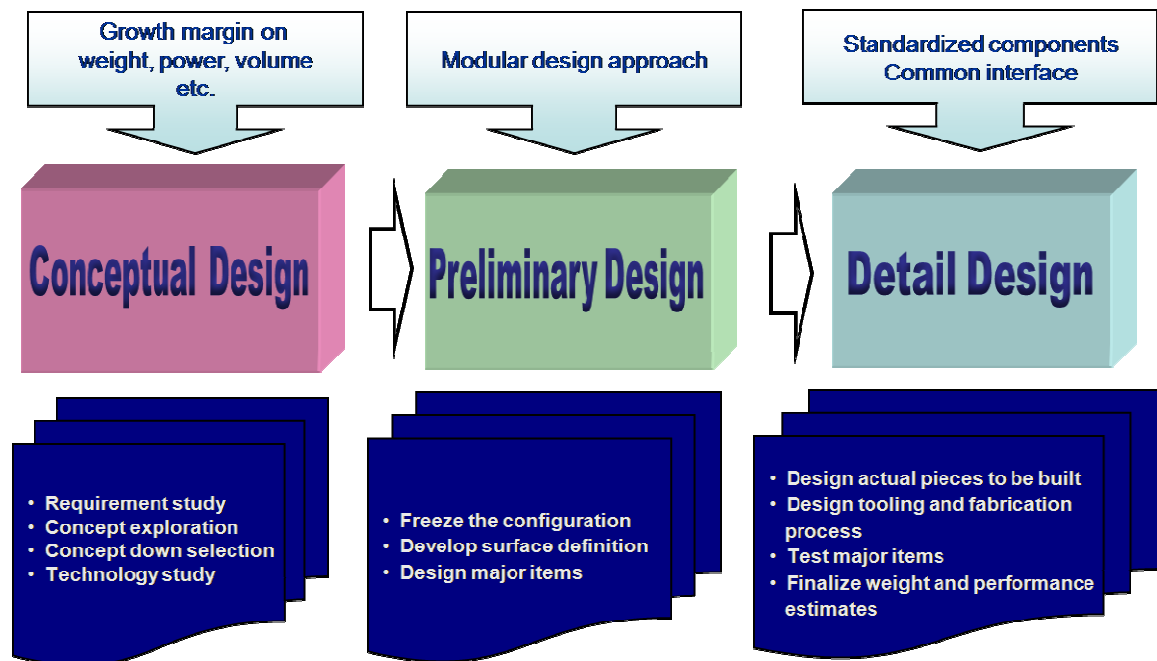
Figure 3: Traditional Aircraft Design Approach for Growth Potential

would be only marginal. This section examines the implication of design decisions during the aircraft sizing and synthesis process under evolving requirements.

The aircraft design process is about making a series of decisions to define vehicle attributes, which minimizes its objective function while satisfying all imposed constraints. In order to further discuss the concept of aircraft growth potential, consider the aircraft design process in numerical optimization terms

$$
\begin{aligned}
&\min_{\mathbf{x}} \ f(\mathbf{x}) \\
&\text{s.t.} \ \ g_i(\mathbf{x}) \leq 0 \ (i = 1, ..., l)
\end{aligned}
\tag{2}
$$

where f is the objective function, which embodies a quantity that is desired to be minimized or maximized, such as takeoff gross weight, life cycle cost, mission effectiveness, etc.; $\mathbf{x} \in \mathbb{R}^n$ is the design vector in n-dimensional space, parametrically representing the design decisions that influence the physical construct of the aircraft, such as wing area, aspect ratio, engine thrust, inclusion of specific technologies, etc.; and lastly, g_i $(i = 1,...,l)$ is the constraints that contain target metrics the final design needs to satisfy or exceed[*]. Here, the constraint functions could be formulated to include point-performance requirements, such as turn rate, acceleration, and takeoff field length; mission requirements, such as payload, range, and loiter time; and military specifications and/or commercial regulations on safety, noise, emissions, etc.

One aspect of solving the optimization problem is notionally illustrated in Figure 4. This figure shows an aircraft design space bounded by two dominant design variables—wing loading and thrust to weight ratio—and constrained by three representative point-

---

[*]Bold face differentiates vector properties from scalar properties throughout the document.

(a) At the moment design freezes   (b) After design is frozen
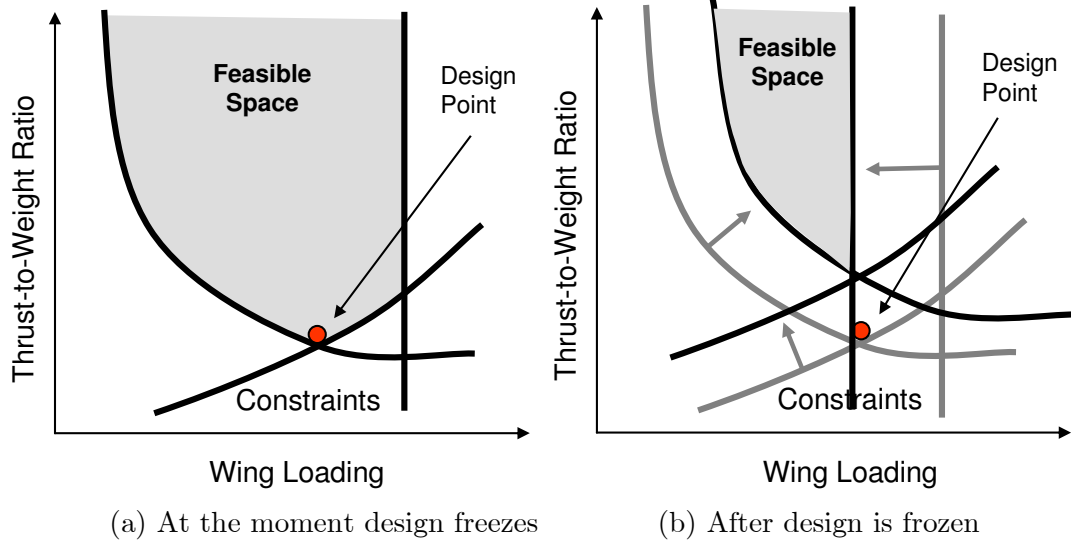
Figure 4: Aircraft Constraint Analysis

performance requirements: turn rate, takeoff field length, and landing field length. Any point design lying within the shaded region is declared to satisfy all prescribed constraints. Within this feasible space, a designer has the freedom to further optimize the aircraft in the direction of improving a given objective function's value. The feasible optimum is typically located on the edges of the feasible space; as shown by the red dot in Figure 4(a). Sometime after the design is frozen, however, the gap between the designed-in requirements and the actual requirements begins to be manifest as variable constraint lines. It is safe to presume that the requirements will likely evolve in the direction of increased capability (heavier payloads, extra weapons, longer range, etc.), shrinking the feasible space until design infeasibility occurs as illustrated in Figure 4(b).

As far as the infeasibility problem is concerned, two different solution approaches can be considered. One approach, shown in Figure 5(a), is to anticipate future changes in the design requirements and plan accordingly. By building in some margin for growth, the designer is trading current sub-optimality with future feasibility. Figure 5(b) shows an alternative strategy that does not incorporate any provisions for the future. Instead,

(a) Design with growth potential (b) Optimal design and upgrade
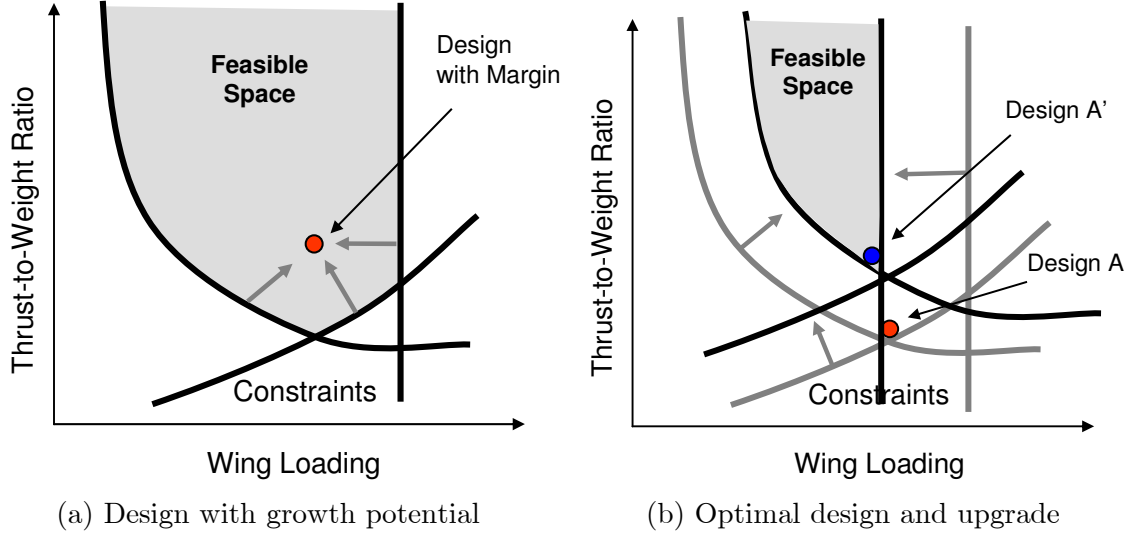
Figure 5: Two Strategic Responses to Evolving Requirements

an optimum design is first sought for the present requirements (Design A). Should the infeasibility problem occur later in the future, it is attempted to be addressed by creating a new vehicle (Design A') that can represent any one of the following cases: a retrofit of Design A, a derivative of Design A, or an entirely new design.

The strategy of designing-in growth margins from the beginning would result in an aircraft with an extended operational life. Without having to recourse to later upgrades, such a system could offer production cost savings in the long run. Nevertheless, this type of design-for-margin approach inevitably introduces conservatism and redundancy to the system, resulting in compromised vehicle performance and/or high operation and support (O&S) cost. In contrast, the build-now-and-upgrade-later strategy would yield a superior optimal solution—in terms of simplicity, compactness, and O&S cost—according to the present requirements.

An analogous case of embedding growth margins to an aerospace system is the design of a family of aircraft and a multi-role aircraft. It is not rare in a commercial aircraft design that a family of aircraft that are based on a common platform and
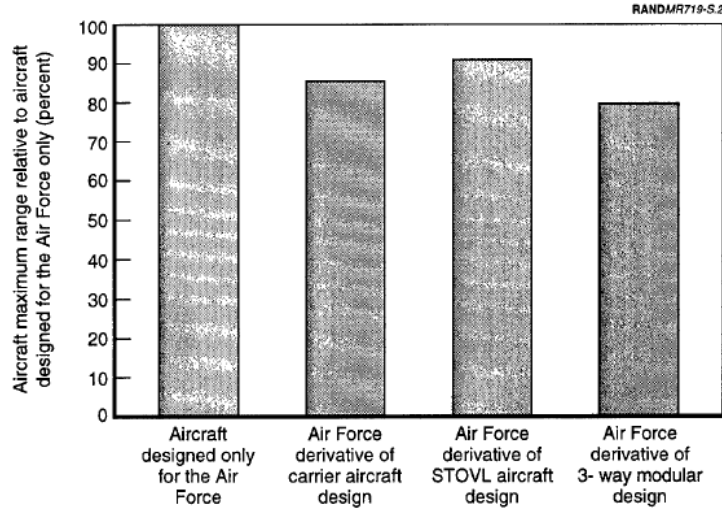
Figure 6: Impact of Commonality on Multi-Service Fighter Range [10]

standard parts is considered from the beginning to maximize the market capture with minimum cost. Often, the use of common features across the platform inevitably brings about some level of performance sacrifice.

Figure 6 shows the impact of commonality—that is, sharing an airframe configuration—on the performance of a military fighter designed for multiple customers' requirements. The measure of performance shown here is the relative maximum range of the multi-service fighter compared to that of an Air Force only version. It can be seen that the desire to make a single vehicle platform satisfy multi-service requirements stemming from different branches of the US armed services results in a notable reduction in the aircraft's maximum range.

Alternatively, if all four fighters were to possess the same maximum range, then the operating cost per flight hour of the multi-service versions would be higher. A case in point, the US Air Force rejected the N-102 proposal submitted by the then Northrop Corporation in 1953, citing that the proposed lightweight fighter's airframe would not be optimal for any particular engine [3]. This was a clear example of how the decision to

commit to an overly conservative design backfired—Northrop engineers had made the mistake of intending the N-102 airframe to be compatible even under the most speculative engine growth scenarios.

In contrast, the build-now-and-upgrade-later strategy would yield a superior optimal solution in terms of simplicity, compactness, and O&S cost. Because this approach also allows the identification of the best possible design from a mission-performance perspective, it was the preferred strategy of the U.S. government during the Cold War era when aircraft development operated under the paradigm of achieving the best possible performance. However, post-Cold War policies as well as the increasing competition in the global market imposed strict budgetary and scheduling constraints, making "the best performing aircraft strategy" obsolete.

The best modern strategy would thus likely fall somewhere between these two polar opposites, where the penalty of design modifications and the cost of over-design are balanced. In other words, some provisions for growth would have to be designed-in from the early development phases, while the very real possibility of having to also make upgrades to the original aircraft is concurrently acknowledged. From the standpoint of decision makers (e.g., policymakers, customers, manufacturers, designers, vendors, etc.), the heart of the matter is knowing what and how much growth provisions are necessary to hedge both the competitiveness and feasibility of the system against evolving requirements.

1.4 Research Objectives and Chapter Overview

Motivated by the need to consider the lifetime evolvement of an aircraft concept from its inception, the objective of this dissertation is to present a structured decision-making

framework that facilitates the systematic evaluation of either: (a) the advantages and disadvantages of various evolution options; or (b) a new production as a response to the evolution of potential requirements and/or technology advancement scenarios.

In the remainder of the study, some of the challenges a design engineer may face when conceptualizing an aircraft according to not only the present requirements but also its potential evolutionary growth are outlined. The case for a new approach that can account for such growth potential is presented throughout CHAPTERs II-IV by highlighting the limitations of state-of-the-art design practices and potential elements to overcome those limitations. The idiosyncrasies of the proposed approach, which is envisioned to have the greatest value in the conceptual aircraft design phase, are detailed in CHAPTER V. After some preliminary results and findings from a simplified proof-of-concept implementation of the proposed method are discussed in CHAPTER VI, a full implementation of the proposed method on an aircraft system design is presented in CHAPTER VII. Lastly, the conclusion and the roadmap for future research is presented in CHAPTER VIII.

CHAPTER II

MODERN SYSTEM DESIGN METHODS INCORPORATING VEHICLE EVOLUTION

The quest for a structured decision-making framework incorporating a lifelong aircraft evolution motivated in CHAPTER I begins with surveying established methods, processes, and philosophies that address the same or similar issues and goals in developing not only aerospace but also complex systems in general. The inquiry that is attempted to be answered in this chapter is formally stated as:

Research Question 1: *For a complex system development, how do decision makers intelligently and systematically prepare for and implement lifelong product evolution? Are there formal methods or strategies that incorporate future requirements and technologies in the initial design?* (**Observation 1**)

Not surprisingly, similar questions were asked in the past. For example Biery and Lorell [3] wrote, "In what ways, and to what extent, can designers adequately preplan for future system upgrades?" As such, a number of high-level strategies have been proposed and adopted over the years in the US military sector for acquisitioning new war fighting capabilities. These high-level strategies are henceforth referred to as participative or heuristic methods in this paper, due to their usefulness as guidance.

To answer the research question and formulate a new or improved approach later, a basic understanding of engineering design process is necessary. Thus, formal engineering

design methods in a broad sense are reviewed to provide a foundation for the proposition of a new design approach in the later chapters of the thesis. On a related note, an emergent trend in the aerospace domain has been the continual publication of advanced design methods. All of these formal strategies share the common goal of eliciting increased disciplinary and/or system-level knowledge earlier, rather than later, during product development to facilitate more informed decisions. A number of these existing methods were interpreted to be relevant for the issues of evolving aircraft requirements, technologies, and capabilities. The intricacies of the surveyed design methods are summarized under the heading of normative or rational methods, referring to their nature as formalisms for solution, rather than guidance.

2.1 Participative and Heuristic Methods

Three different but similar management strategies that attempt to address problems associated with the development of a complex system under evolving requirement and technology are identified and summarized here. They are pre-planned product improvement (P^3I), evolutionary acquisition (EA), and spiral development (SD). History, objectives, and applications of these methods are briefly discussed and compared.

2.1.1   Pre-Planned Product Improvement (P^3I)

A consensus was formed within the US government in the 1970s that, at the time, military procurement programs were too inefficient in terms of cycle-time and overall expense. For instance, prolonged development times directly led to excessively higher-than-expected RDT&E cost. Similarly, long lead-in times to IOC run the risk of outdating most embedded technologies as both customer needs and threat environments are likely to be different from those defined when the program was first initiated [11]. In

order to address such issues, a government acquisition strategy known as the pre-planned product improvement (P^{3}I) was introduced in the late 1970s. The key idea behind P^{3}I is the "design of a system from its origins to incorporate future performance enhancements [3]." Mackey also comments about P^{3}I, stating: "P^{3}I differs from past modification efforts in that it stresses preplanning for improvements while the system is still in the initial design stages [12]."

In April of 1980, the American Defense Preparedness Association (ADPA) sponsored a three-day seminar to discuss P^{3}I. In 1981, the Rand Corporation published a comprehensive report on its assessment of P^{3}I as an alternative strategy for aircraft acquisition [3]. As the Rand report pointed out, P^{3}I is based on the premise that a designer can anticipate needed improvements or possible changes in requirements well in the future. This assumption overlooked the uncertain nature of requirement and technology evolution and severely limited the usefulness of P^{3}I. Rand report mentioned the difficulties of forecasting the future, concluding that "preplanning very far into the future is an unworkable concept." Rand also recommended that the Air Force "adopt a P^{3}I strategy only for circumstances where subsystems are already in development but not mature enough to be incorporated in the initial version of the aircraft."

A few past attempts to incorporate the P^{3}I strategy into aircraft design were identified and reported as part of the case studies in §3.2. Those successful P^{3}I implementations were limited to the subsystem level technology integration and were planned for only short term.

2.1.2 Evolutionary Acquisition (EA)

A year after P^{3}I had been officially recognized by the ADPA, the Armed Forces Communications and Electronic Association (AFCEA) formed a task force to study a new acquisition strategy that appeared similar to P^{3}I for command and control (C2) systems [12]. Termed Evolutionary Acquisition (EA) by AFCEA, the strategy emphasizes the time-phased nature of system requirements and the notion of incrementally supporting technology maturation to reduce development cost, risk, and time [13]. Figure 7 graphically accentuates the differences between the traditional acquisition and EA procedures. In a traditional acquisition setting, the desired capability—defined to be bounded by the threshold and objective capabilities—is the only capability endeavored to be acquired. The EA strategy, however, advocates the initial acquisition of a core, baseline capability; preplanned and non-preplanned capabilities are subsequently added to the baseline capability on a needed basis.
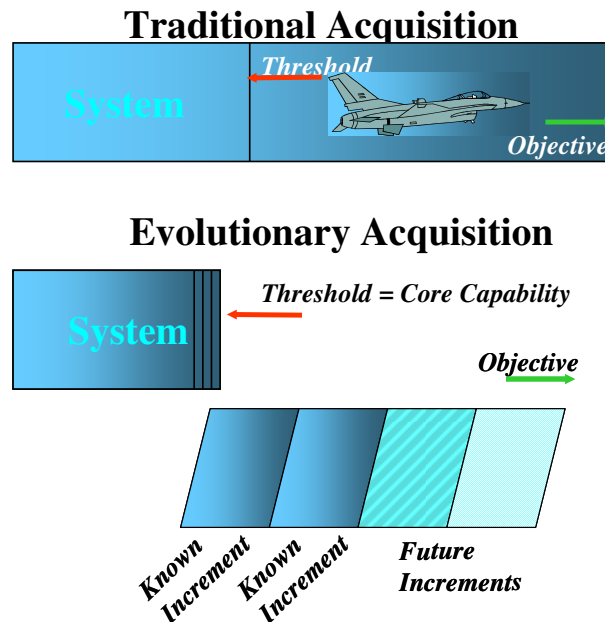
Figure 7: Traditional Acquisition vs. Evolutionary Acquisition [5]

EA was adopted as a preferred Department of Defense (DoD) strategy in 2000 for rapid acquisition of mature technology [14]. The US Air Force subsequently mandated the use of EA that leverages upon the *Spiral Development* (SD) process as the acquisition strategy for the C2 systems as a means of "quickly [adapting] to evolving requirements and ever-shortening technology life-cycles [15]." In December of 2004, the new National Security Space Acquisition Policy (NSSAP) 03-01 also mandated EA as the preferred acquisition approach to DoD space programs [16]. According to the Air Force instruction, EA is

> an acquisition strategy whereby a basic capability is fielded with the intent to develop and field additional capabilities as requirements are refined. The key concept is to rapidly develop and field useful increments of capability ... and to leverage user feedback in refining required capabilities for additional increments.

DoD defines SD as

> a method or process for developing a defined set of capabilities within one increment, providing opportunity for interaction between the user, tester, and developer communities to refine the requirements, provide continuous feedback and provide the best possible capability within the increment.

EA strategy relying on SD process is illustrated in Figure 8 from the DoD instruction 5000.1. The full capability is achieved by the baseline capability and three increments. In this process, the end-stage requirements are not known at the program initiation. As the spiral loops in the figure represent, requirements are refined through demonstration and risk management, and each increment provides the best possible capability to the user.
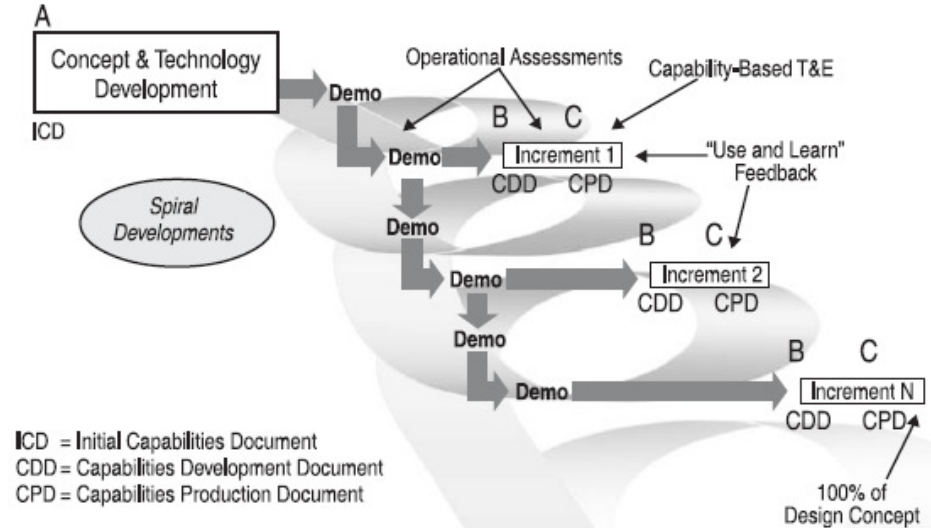
Figure 8: DoD's Evolutionary Acquisition and Spiral Development

2.1.3 Spiral Development (SD)

Although both EA and SD were adopted as DoD acquisition strategies, the concepts were developed independently. SD was developed by Barry Boehm [17] as a risk-driven management process for developing complex systems. SD originated from the software development community but has been successfully applied to complex or system-of-systems challenges in other domains, which include satellite constellation, unmanned aerial vehicles systems, space launch vehicles, unmanned ground vehicles, and the F/A-18E/F [18-23].

Being represented by the diagram originally proposed by Barry Boehm shown in Figure 9, spiral development calls for a "building block" approach to develop a complex system while capability is incrementally added through iterations with the users. The goal of this process is to reduce technological and budgetary risks associated with product development and to deliver the initial capability faster to the customer. The
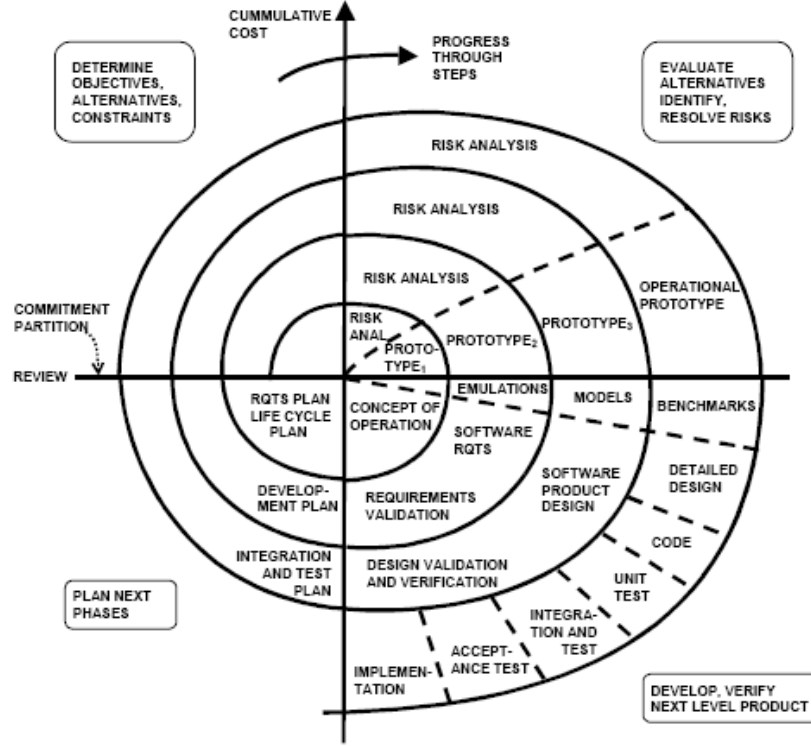
Figure 9: Original Spiral Development Diagram [18]

end-state of the product is, thus, not defined from the initial stage of the product development but gets refined depending on user feedback and technology maturation.

2.1.4 P³I versus EA and Challenges

Since the DoD embraced EA and SD, there has been some confusion as to the correct meanings behind the acronyms and the ways EA differs from P³I. For clarity, the Under Secretary of Defense issued a memorandum [19] defining EA, SD, and P3I on April 12, 2000. According to the memorandum,

> Evolutionary acquisition and spiral development are similar to pre-planned product improvement but are focused on providing the warfighter with an initial capability which may be less than the full requirement as a trade-off for earlier delivery, agility, affordability, and risk reduction.

In addition, the Air Force instruction also differentiates EA and P³I as follows:

Evolutionary acquisition differs from a Pre-Planned Product Improvement (P^3I) acquisition strategy in that future increments are not definitively planned and baselined until the current increment is about to be executed.

In summary, P^3I and EA are similar in that both strategies acquire capability incrementally, but the difference is that P^3I is more about preplanning for the upgrades on top of the initial, one hundred percent capability, whereas EA defines threshold and the full capability and achieves the full capability through multiple increments after the threshold is fielded. Moreover, these increments may or may not be pre-planned in the beginning of the program. Because of the uncertain nature of the evolution of threats and user needs, incremental capability is refined over time as the random variables are realized. This fundamental difference makes EA more relevant to situations in which unknown requirements and technologies are desired to be integrated. The Rand study on P^3I also pointed out its limitations of dealing with various sources of uncertainty, such as those originating from future requirements, funding, and technology.

Thus far, the conditions for implementing EA on a real aircraft development program have proved to be far from ideal [20]. A successful implementation of this recently adopted policy would require significant structural and attitudinal changes within organizations that include: the Congress, who funds the program; industry, who delivers the product; and the respective military departments, who deploy and operate the aircraft. The hot-button issue here is how, in the absence of steps to avert the risk of following a new paradigm, aircraft manufacturers can recognize the value of developing an aircraft in accordance with the EA philosophy?

2.2 Normative and Rational Methods

Although the new DoD's policy calls for a new paradigm of "design for system evolution" and also provides guidance to aircraft system managers and engineers, its usefulness is still limited as an acquisition strategy. This section of the chapter seeks formalized design methods the design engineers can use effectively to comply with the new acquisition policy. Although traditional aircraft design process was briefly introduced in §1.3, it is necessary to review the theoretical and procedural aspects of design in this study. Then, advanced, modern design methods with some of the relevant elements to this topic are reviewed.

2.2.1 Engineering Design Process

For many years, design has been in the realm of art rather than science. It was a more of a "trial-and-error" or an "ad-hoc" type of way to find a solution(s), which meets the need. A systematic work of design method or process was proposed by Morris Asimow [21] in 1962. Asimow's the *morphology of design* is a comprehensive process with seven phases from finding the need to plan, to creating the detailed sketch of the product, and planning for manufacture, sales, use, and disposal.

While Asimow's method provides a general guideline by which all engineering design problems at any hierarchical level can be attempted, the successful application of such method in a real world application requires various challenges to be hurdled. Especially, when the designed products are complex systems such as modern aircraft, where more than one customer expect multiple functions and the system is essentially the complicated interaction of subsystems, it could become extremely complicated to proficiently perform the tasks in the design methods.
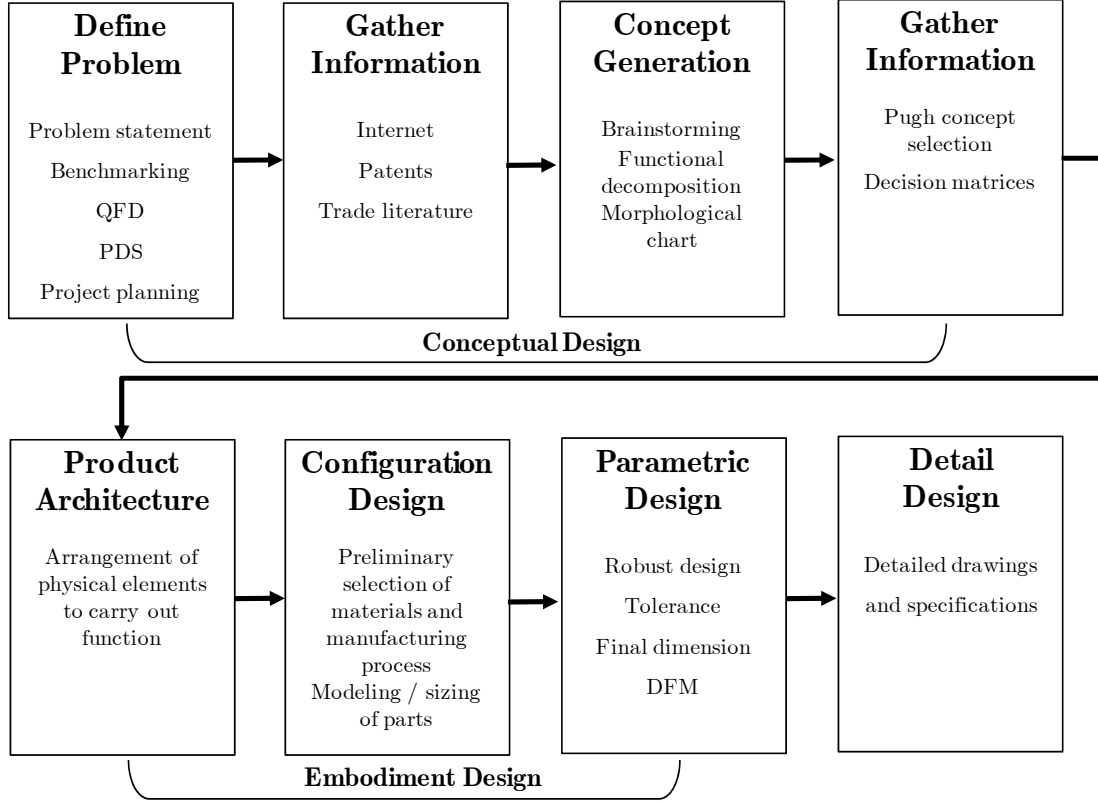
Figure 10: The Engineering Design Process by Dieter

Dieter [22] for example, adopts and modernizes the Asimow's method in an attempt to provide specific tools to facilitate the activities in the design phases. Especially, Dieter integrates some of the system engineering techniques into the early phases of the design process as shown in Figure 10. Among the elements in Dieter's design process, Quality Functional Deployment (QFD) under the step of "Define Problem" and Morphological chart under "Concept Generation" are introduced in more detail herein.

Quality function deployment is a tool that enables design engineers to analyze the wants and needs of a customer, prioritize them, and choose design characteristics and specifications in order to find a solution that meets these customer needs. This focus towards customer satisfaction is a way of ensuring that quality is built into the product. QFD was first developed in Japan in the early 1970s and was rapidly adopted by many

U.S. companies, including IBM, Texas Instruments, Chrysler, General Motors, Rockwell International, Hughes Aircraft, etc. [22-24]. The techniques have been proven in the domain of aerospace systems development as well. The DoD Joint Strike Fighter Program also employed QFD under the activity named Strategy-to-Task Technology QFD II Analysis [23] in the Integrated Product and Process Development (IPPD) framework that is introduced in the next section.

QFD is a graphical method that uses a QFD diagram also known as the *house of quality* because of its shape. The example QFD diagram shown in Figure 11 was created by the Georgia Tech graduate team for the 2002-2003 American Institute of Aeronautics and Astronautics (AIAA) aircraft design competition [24]. In the figure, the customer needs are placed on the left side. For each of the items that the customer wants, or the so-called "voice of customers", the customer importance ratings are quantified and placed in the diagram. Armacost [25] used Analytic Hierarchy Process with QFD to prioritize the customer needs. Analytic Hierarchy Process (AHP) is a multi-criteria decision-making technique that was developed by Saaty [26, 27] in the 1970s. Then, the design characteristics that can be controlled to meet customer requirements are placed under the roof of the house and mapped to the customer needs. Outcome of the QFD exercise is the list of engineering characteristics and their relative importance and target values, which can be used to construct evaluation criteria, constraint thresholds, and design objectives for the evaluation of design concepts. More interested readers are referred to [28, 29] for examples.

Engineering Characteristics

Customer Assessment

QuEST

Customer Requirements			Customer Importance	Lift-to-Drag Ratio	Cruise Altitude	Stall Speed	Wing Loading	Thrust-to-Weight Ratio	Takeoff Gross Weight	Required Structural Strength Factor	Structure Fatigue Life	Fuselage Volume	Engine Efficiency	High ByPass Ratio	Aircraft Static Stability	Systems handling Qualities	Utilization Level	Maintenance Cost	Production Cost	CAD/CAM system	Availability	RDT&E

Performance | Structure | Propulsion | S & C | Economics

Direction of Improvement: ↑ ↑ ↓ ↑ ↓ ↑ ↓ ↑ ↑ ↑ ↑ ↑ ↑ ↑ ↓ ↓ ↑ ↑ ↓

Customer Assessment legend:
- A318
- QuEST
- A717
- A737

Mission Requirements	Design range	4.0
	Cruise speed	4.0
	Lower takeoff fuel consumed	5.0
	Takeoff length	4.0
	Approach velocity	4.0
	Reserve mission capability	4.0
	Payload capacity	3.0
	Block fuel utilization efficiency	5.0
Environmentals	Operational emissions level	5.0
	Operational noise level	5.0
Economics	Acquisition price	5.0
	Direct operating cost	5.0
General Requirements	Entry into Sevice (2020)	4.0
	Airworthiness certification	5.0
	Cabin layout	4.0
	Better flying quality	3.0

Target Values: 15.0 | 40,000 | 100 | 120 | 0.3 | 125,000 | 3.5 | 20 | 13*13.6*103 | 0.9 | 12 | Optimize | Level 1 | 3,000 | minimize | 35 | maximize | maximize | Minimize

Units: ft | knot | lb/sqr ft | | lbs | | Years | cubic ft | | | | | FH/Year | | million $ | | |

Technical Difficulty: 4 | 2 | 4 | 3 | 4 | 4 | 3 | 3 | 2 | 5 | | 3 | 3 | 5 | 4 | 4 | 2 | |

Absolute Importance: 273.0 | 150.0 | 132.0 | 114.0 | 159.0 | 324.0 | 51.0 | 18.0 | 114.0 | 387.0 | 190.0 | 93.0 | 111.0 | 30.0 | 60.0 | 49.0 | 39.0 | 20.0 | 102.0

Relative Importance

Figure 11: The House of Quality [24]

A morphological analysis (MA) is a method that arranges the system functions and sub-functions in a logical order to enable the synthesis of numerous alternatives or configurations. Morphological analysis was invented by Zwicky in 1948 [30, 31] and has been used in a number of applications of policy making [32, 33], generation of scenarios and strategies for risk analysis [34], evaluation of military strategies [35], and synthesis of aircraft configurations [24]. The method is graphical and utilizes a matrix, often called a morphological matrix.

An example morphological matrix from [24] is presented in Table 1. As shown in the matrix, the system is broken down into different subcomponents and parameters necessary to the design solution. These subcomponents and parameters are listed vertically, and possible solutions to these different subcomponents and parameters are

Table 1: A Morphological Matrix [24]

	Design Attributes	1	2	3	4	5	6
Configuration	Vehicle Layout	Conventional	Joined Wing	Blended Wing Body			
	Wing Position	Joined Wing	High Wing	Low Wing	Mid Wing		
	Fuselage	Cylindrical	Area-Ruled	Oval	No fuselage		
	Engine Location	Under Wing	Tail Mounted	Over Wing	Rear Fuselage	Distributed	Embedded
	High Lift Devices	Conventional Slat & Flaps	Advanced Slat & Flaps	Circulation Control	Upper Surface Blowing (USB)		
	Controls	Tail Plane	Canard	Conventional	Hybrid		
	Number of Engines	2	3	4			
Propulsion	Engine Type	Electric	Turboprop	Turbofan	Advanced Turbofan		
	Nozzle Type	Separate Flow	Mixed-Flow				
Structure	Wing Materials	Aluminum Alloy	Composites	Hybrid			
	Fuselage Materials	Aluminum Alloy	Composites	Hybrid			

26

listed horizontally. Once this matrix is created, the designers can create various design concepts by combining different solutions to the subcomponents and parameters. The purpose of this method is to develop as many combinations of ideas as possible. By so doing, concepts that might not be considered ordinarily are generated.

While Asimow and Dieter focused on the steps and tasks of the design process, some presented philosophical aspects of design. Hill [36] compared the design method to the scientific method that was described briefly in the beginning of this thesis. The difference would be that the scientific method is to *discover* knowledge where as design method is to *create* a new product which advances the state-of-the-art of the field in some ways. Each step of the scientific method is matched to a step in the design method. For example, the synthesis of concept or alternative in the design process is the counterpart of generation of hypothesis. Vanderplaats [37] compared design to analysis, stating "analysis is the process of determining the response of a specified system to its environment… Design, on the other hand, is used to mean the actual process of defining the system… Clearly, analysis is a sub-problem in the design process because this is how we evaluate the adequacy of the design."

Suh [38] proposes the four distinct phases of the design process: the problem definition phase in which vague customer needs are embodied into a set of coherent requirements; the solution synthesis phase in which the functional requirements are decomposed and solutions are sought in the physical domain; an analytical phase in which quantitative evaluation of the generated solutions are made in terms of the requirements; and the feasibility check phase where conformance of the design to the requirements is evaluated. The process is graphically represented in Figure 12. While
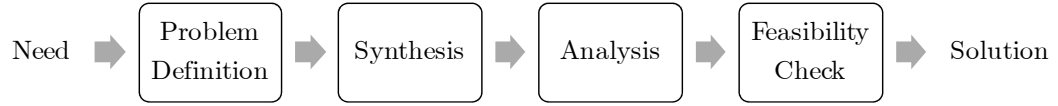
Figure 12: Four-Step Design Process Adopting Suh [38]

using different terminology, essentially identical three or four step models are also found in other literature. For instance, Jones's model of the design process [39] has the three steps of analysis, synthesis, and evaluation; Cross [40] proposed a model of exploration, generation, evaluation, and communication, the fourth step stressing the importance of effective delivery of the end product needs to the next process, such as production. It is very important to note that the design process is highly iterative within the phases and between the phases such that the designer often needs to go back to the previous stages to make changes and redo the following steps.

What is also important to consider in design process is to understand the hierarchical nature of design. Suh [38] philosophizes the hierarchical aspect in the functional domain and physical domain of problems as follows:

> There are two very important facts about design and the design process, which should be recognized by all designers: FRs and DPs have hierarchies, and they can be decomposed; FRs at the ith level cannot be decomposed into the next level of the FR hierarchy without first going over to the physical domain and developing a solution that satisfies the ith level FRs with all the corresponding DPs [in the physical domain] ... In the design of complicated systems, the hierarchical approach simplifies the design process a great deal

Therefore, it is important to consider in which hierarchy the designer should define problem and in which hierarchy the designer should compose solutions at a certain phase of the design process.

2.2.2 Aircraft Sizing

The traditional aircraft design process, consisting of conceptual, preliminary, and detail design phases, was briefly introduced in §1.3 to discuss the issue of planning for future vehicle upgrades in the traditional design process setting. This section further discusses the aerospace systems' specific design issues referred to as "aircraft sizing". While aerospace systems design can be conducted following the design processes introduced in this section, the systems intended to be operated in air require special attention to the vehicle's weight. Aircraft sizing, conducted as a sub-process of conceptual design, is defined by Ramer [6] as "the process of determining the takeoff gross weight and fuel weight required for an aircraft concept to perform its design mission." In addition, DeLaurentis [94] describes aircraft sizing as "a mathematical algorithm that determines the size and weight of an aircraft based on a specified mission and contributing disciplinary analyses." Anderson [41] lays outs seven intellectual pivot points for conceptual design as shown in Figure 13. While the process starts from the requirements and ends by down selecting the best design that meets all requirements, the iterative steps from 2-6 can be viewed as an aircraft specific sub-process of aircraft sizing. The traditional aircraft sizing process begins with estimating the weight of the airplane, which affects all downstream analyses resulting in calculated aircraft gross weight, including the structure, fuel, and payload. The process is repeated until the estimated weight and calculated weight converge.

Recently, Nam [42] suggested a more generalized and modern definition of aircraft sizing as the process of balancing available thrust, fuel (or energy), and volume with the required thrust, fuel (or energy), and volume determined by the point performance and

```
┌─────────────────────────────┐
│ 1. Requirements             │
└─────────────────────────────┘

┌──────────────────────────────────────────┐
│ 2. Weight of the airplane—first estimate  │
└──────────────────────────────────────────┘

┌──────────────────────────────────────────────┐
│ 3. Critical performance parameters             │
│      a.  Maximum lift coefficient $C_{Lmax}$   │
│      b.  Lift to drag ratio L/D                │
│      c.  Wing loading W/S                      │
│      d.  Thrust to weight ratio T/W            │
└──────────────────────────────────────────────┘

┌──────────────────────────────────────────────┐
│ 4. Configuration layout—shape and size of the  │
│ airplane on a drawing                          │
└──────────────────────────────────────────────┘

┌──────────────────────────────────────────────┐
│ 5. Better weight estimate                      │
└──────────────────────────────────────────────┘

      No  ┌──────────────────────────────────────────┐
          │ 6. Performance Analysis—does the design meet or │
          │ exceed requirements?                      │
          └──────────────────────────────────────────┘
                         │ Yes
          ┌──────────────────────────────────────────┐
          │ 7. Optimization—is this the best design?  │
          └──────────────────────────────────────────┘
```

Figure 13: Seven Intellectual Pivot Points for Conceptual Design [41]

mission performance requirements. Borer [43] formulated a method of sizing an aircraft for multiple missions that is particularly relevant in the design of military fighters. The sub-processes of the aircraft sizing are constraint analysis, mission analysis, and weight estimation, formally suggested by Mattingly [44] and Nam. A detailed review of conventional and modern aircraft design process is found in Nam [45] and Borer [46].

2.2.3   Modern System Design Methods

Various methods and processes to maximize system affordability were developed since the 1990s in the aerospace systems design community. Mavris and DeLaurentis [47] defined system affordability as "value to the customer, including a balance between benefits, costs, availability, and risks." The ideals and objectives of the design methods that were developed under the paradigm of "design for affordability" are in line with the

goals of P³I, EA, and SD in that better ways to reduce life cycle cost and development time and to improve customer satisfaction are sought.

Integrated Product and Process Development (IPPD) was a design process that was formally identified in the NCAT [48] as "a management methodology that incorporates a systematic approach to the early integration and concurrent application of all the disciplines that play a part throughout a system's life cycle." In order to improve product quality and reduce design time and life cycle cost, IPPD takes into account the product's entire life cycle during the early design phase. The IPPD process is enabled by the integrated product team (IPT) of all disciplines, such as design, production planning, manufacturing, maintenance, etc., to integrate not only the product development but also the process development for manufacturing and support [49].

Schrage [50] proposed a comprehensive IPPD formulation to help the U.S. Navy's acquisition reform effort and engineering education and training. The Generic IPPD methodology, as illustrated in Figure 14, consists of four key elements: quality engineering methods, computer-integrated environment, top-down design decision support process, and systems engineering methods. These elements are shown in the top portion of the figure. In the middle of the figure is the design process from identification of the need to decision making, which is essentially identical to the design processes reviewed in the previous section. The left and right elements of the design process are the key enablers or techniques. The system engineering methods on the right side of the figure are product design driven and are the key enablers in decomposing the problem. The other side of the flow contains the quality engineering methods that are process driven and recompose the solutions.
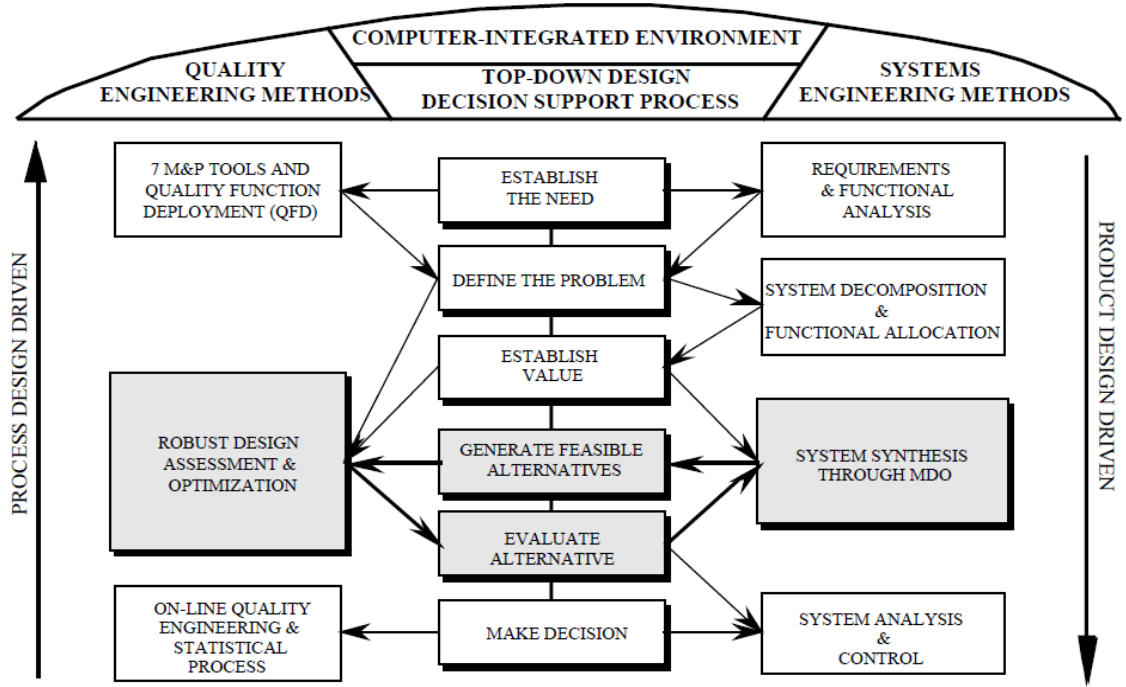
Figure 14: The Generic IPPD Methodology by Schrage [50]

Robust Design Simulation (RDS) by Mavris, one of the elements in the Generic IPPD method, is a systematic framework that identifies the design that not only performs well in the well-defined initial operational environment but also in a changing operational environment. RDS adopts the concept of quality and robustness from Taguchi methods and Six Sigma and creates a method that is tailored to aerospace systems design. RDS also incorporates uncertainty in aircraft operational environment. In Taguchi methods, the change in operational environment is captured by the *noise variables*, and then the best setting of the *control variables* minimizes the signal-to-noise ratio (S/N). In RDS, for a baseline aircraft configuration, the control variables and noise variables are identified. Alternative designs are created by using the Design of Experiment (DoE) techniques, and the variability due to noise variables are quantified using Monte Carlo analysis. The robust solution is found through maximization of the probability of an overall figure of merit achieving or exceeding a specified target.
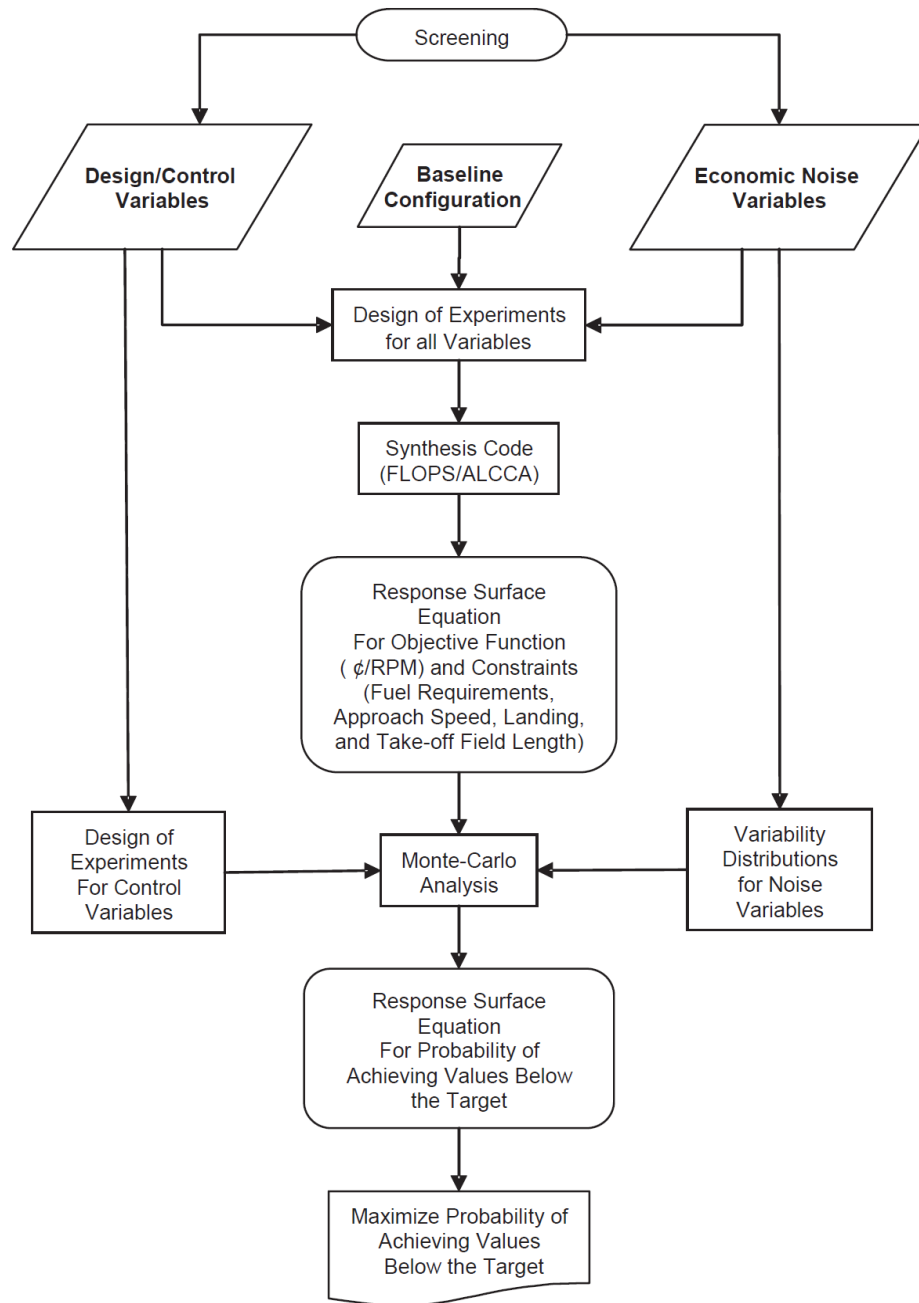
Figure 15: Flowchart of Robust Design Simulation [51]

Technology Identification, Evaluation, and Selection (TIES) by Kirby [52] prescribes a method to investigate, evaluate, and determine which technologies can be infused at the systems design stage. The key elements of TIES methods is the identification of potential technologies, their impact on the system being studied, compatibility with other technologies, and costs and risks associated with the further development of the interested technologies. The TIES methods have been successfully applied to the design of a high speed civil transport [53], a short haul civil tiltrotor [54], and an uninhabited combat aerial vehicle [55].

Mavris et al. suggested the Unified Tradeoff Environment (UTE) in which the combined effects of mission requirements, vehicle attributes, and technologies into one environment are assessed [56]. The UTE treats the requirements and technologies the same as vehicle design variables. Thus, impact of requirements, vehicle attributes, and technologies on the baseline vehicle is simultaneously studied. The UTE has been applied to the U.S. Army's Future Transport Rotorcraft, NASA's Short Haul Civil Tilt Rotor, and the development of the F/A-18E/F [56-60], to list a few.

Behind the advanced design methodologies introduced in this section are techniques that enable eliciting increased disciplinary and system-level knowledge earlier, for instance, surrogate modeling techniques such as Response Surface Methodology (RSM) [61] and Artificial Neural Network (ANN). The RSM approximates the complicated physical behavior of the model into 2nd order polynomials as known as Response Surface Equations (RSEs), which allow an instantaneous evaluation of aircraft performance characteristics. ANN based surrogate models are inspired by the structure of the human brain and are constructed by complex connections between the neurons. These ANN

based models' origin can be traced back to a 1943 article by neurophysiologist Warren McCulloch and mathematician Walter Pitts entitled "A Logical Calculus of Ideas Immanent in Nervous Activity" [62]. While many resources exist on the theory and application of neural networks to a wide range of problems, the DARPA Neural Networks Study by MIT's Lincoln Laboratory [63] is a comprehensive reference to the use of neural networks.

Surrogate modeling is further facilitated by systematically creating samples using Design-of-Experiment (DOE) techniques. Many types of DOE have been invented and applied to various engineering problems successfully. Among them, Box-Behnken designs by [64] and Central Composite Design (CCD) have been widely adopted in the domain of aerospace design along with RSM [65]. ANNs is known to work better with space-filling sampling techniques, such as Latin-Hypercube Sampling (LHS), developed by the Sandia Laboratory in 1981 [66].

One of the goals in the development of modern design methods was effective communication between the designers and the decision makers. As a means to facilitate more informed decision, visualization of the design space became important. As a result, visualization tools, such as prediction profilers, contour plots, and multivariate profilers, and surface profilers were introduced and used in aerospace systems design. Enabled by surrogate models in the background, these tools allow instantaneous design space exploration, involving the decision makers in the loop. For example, prediction profilers as shown in Figure 16 graphically represent the mapping between the system attributes and design requirement—range, speed, and payload. The slopes of the lines in each of the boxes are partial derivatives of the aircraft attributes with respect to the design

requirement evaluated for a particular design point, which the designer can change by moving the red vertical lines.
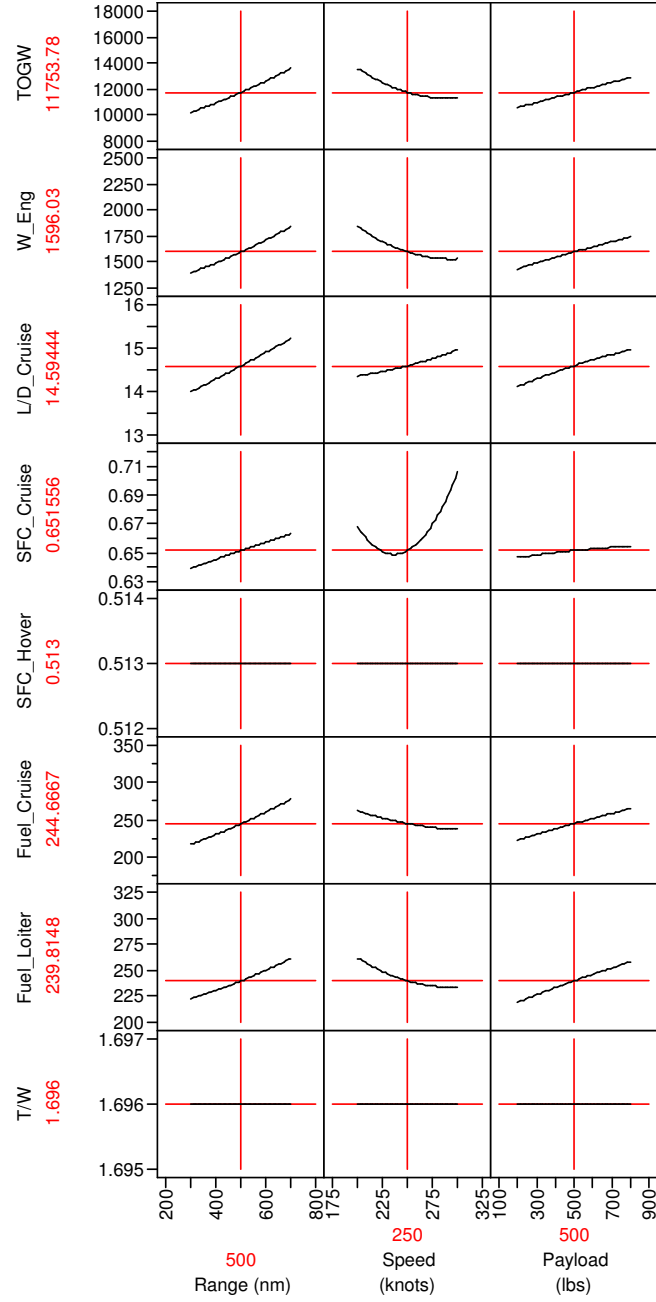
Figure 16: An Example Prediction Profiler [67]

2.3 Chapter Conclusion and Objective

The three strategies discussed in the section 2.1 can be viewed as system development strategies which can be adopted as managerial level design guidelines in dealing with problems of time-phased requirement change, technology maturation, and various source of uncertainties. Although EA and SD provide guidance to aircraft system designers, their usefulness is still limited as acquisition strategies or processes.

Historically design has been belonged to the realm of art rather than science. Recent efforts in brining the scientific process to design have been surveyed and reviewed in this chapter. Emerging methods in the aerospace systems design community are an effort to bring more knowledge into the early design process and to provide better traceability of design and customer satisfaction. Advanced methods, such as RDS, TIES, and UTE, provide for the means to incorporate technologies, requirements, and/or uncertainty into the sizing and synthesis process of an aircraft. However, those methods were developed to focus on finding a single design solution for the currently defined problem. The implementation of evolutionary aircraft development requires a design method that provides time-phased design solutions for a set of time-phased requirements and technology options.

In summary,

Observation 2: *While acquisition policies such as P³I, EA, and SD have established the paradigm of design for lifelong evolution and have been useful as design guidelines, a formalized method as to how contemporary aircraft designers can incorporate the theory into the aircraft design practice has been elusive.*

Conventional and modern design processes set up a single-stage design formulation with which the decision must be made here and now.

For aircraft designers to be able to capture future requirements and technologies in the current design, a fundamentally different design problem formulation is required. Such a new problem setup considering lifetime evolution of a complex system is formulated in the subsequent chapters.

CHAPTER III

CASE STUDIES ON AIRCRAFT EVOLUTION

As discussed in CHAPTER II, the paradigm for military system development has shifted from a single step approach to an evolutionary approach. Although much literature provides the needs and guidelines for such development philosophy, a design methodology as to how a system is designed in accordance with this philosophy has been missing.

From the perspective of aircraft design, a logical question that arises in preparing for such evolutionary development of a system is, "How can design engineers devise effective solutions incorporating evolving requirements and technologies?" A tie-in question that must also be addressed is, "What are the issues and challenges in preparing and implementing the provisional steps for the uncertain future?" These questions are formally stated as:

Research Question 2: *How can the traditional, single-stage design formulation be expanded to enable integration future design states and time-phased decision making? How can potential vehicle evolutionary paths be planned and quantitatively evaluated from the origin of the design?* (**Observation 2**)

Research Question 3: *What would be the barriers and challenges in implementing the preplanning strategy in aircraft design? What would be the elements needed to*

improve the current process to respond to the new policy of evolutionary acquisition? (**Observation 2**)

As one of the attempts to answer above questions, a three-part case study was performed to gain further insights into the implementation aspect of the pre-planning type strategies outlined in the previous section. The focus of such an exercise was to gain insights to which key aspects are missing or overlooked from the traditional aircraft sizing and synthesis process but are essential to the successful implementation of the pre-planning strategy. What follows is a brief summary of the key lessons learned from surveying the literature. The following questions were kept in mind when reviewing the past cases: What initiated the modification programs? To what extent have the vehicles been expanded over time? How were the modifications implemented? What constrained the growth of the vehicle? What attributed to the program's failure or success?

3.1 Part I: Aircraft Evolution Trends

The first part focuses on general trends associated with modification programs. This part quantitatively tracks the evolution history of some selected aircraft in the following categories: military fighter, military bomber, military rotorcraft, and commercial transport. The focus of this part of the case study is to answer a series of questions, such as: What initiated the modification programs? To what extent have the vehicles have been expanded over time? How were the modifications implemented? What constrained growth? Depending on the category an aircraft fell into, some common issues and pitfalls were identified.

3.1.1 Military Fighters: Northrop F-5, Lockheed Martin F-16, and Boeing F/A-18

For many military fighter jets, their evolution was driven by the need or desire to improve *lethality* and *survivability*. These objectives were endeavored to be achieved by a number of subsystem upgrades, such as a larger weapons payload, avionics enhancement, and more powerful propulsion systems. Consequently, the evolution trends of U.S. fighters show a gradual increase in both vehicle weight and available thrust. External pods to hold additional armament and fuel became unavoidable, which in turn increased both aircraft weight and drag. This inevitable degradation in vehicle performance was attempted to be offset by installing more powerful derivative engines whose gravimetric and volumetric characteristics did not change much. All the while, the airframe's geometry remained relatively fixed. The original wing shape and area were not modified as often, resulting in a continual increase in wing loading values. It would thus appear that whatever penalty a sub-optimal wing imparted on the vehicle's performance, it did not justify the cost of re-designing the wing.

3.1.1.1 Northrop F-5

Increase in weight over time is typical of most of aircraft as the customer established the need for more equipment and capability. F-5 was no exception to the trend. Figure 17 shows the evolution of weight and thrust of Northrop F-5. The takeoff gross weight more than doubled over its twenty-year evolutionary path from the T-38A to the F-5E. Engine thrust also increased in the order of 3350 lb (T-38A), 4080 lb (F-5A), 4300 lb (CF-5A), and 5000 lb (F-5E). The F-5G, which was the third generation F-5, weighed
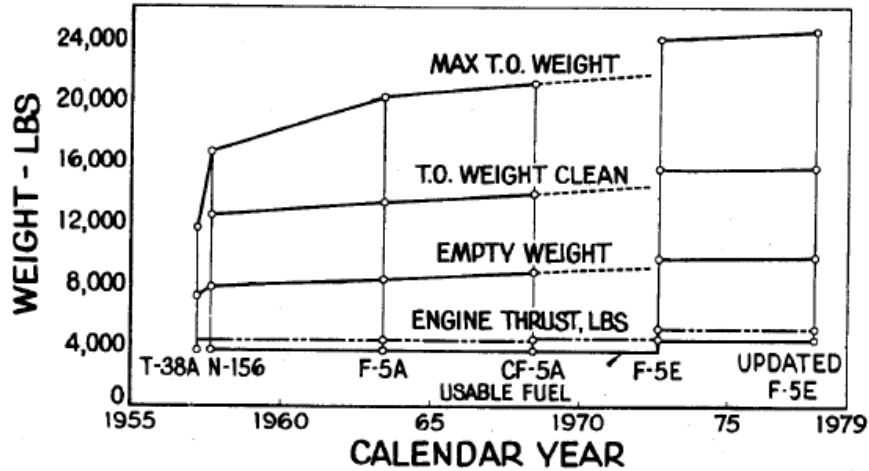
Figure 17: Northrop F-5 Weight and Thrust Growth [68]

26,290 lb with one F404-GE-100 engine rated at 17,000 lb (F-5G's immediate predecessor was a twin-engine design).

Northrop designed F-5 to be a low-cost, light-weight, multi-mission fighter, having foreign allies in mind. To appeal to diverse range customers other than the U.S. government, the design team stressed the flexibility and growth potential of the airframe. One example of design flexibility is the nose room of 40 cubic feet to accommodate various kinds of equipment according to the customer preference. Performance upgrade was facilitated by the advancements in engine technology. The maximum thrust of the GE-J85 engine used in the F-5 series increased from 1,150 lb for J85-5 to 8,160 lb for J85-13 to 10,000 lb for J85-21 with relatively small increase in engine weight and geometry. This allowed for upgrading of the F-5 propulsion system with minor modification to the airframe [3].

It is interesting to watch how wing area and wing loading has evolved in comparison. As evident from Figure 18, the wing was enlarged only one time. The wing area increased from 170 ft^2 to 186 ft^2 when the CF-5A was upgraded to F-5E. As a result of adding weight without updating the wing, wing loading gradually increased from its
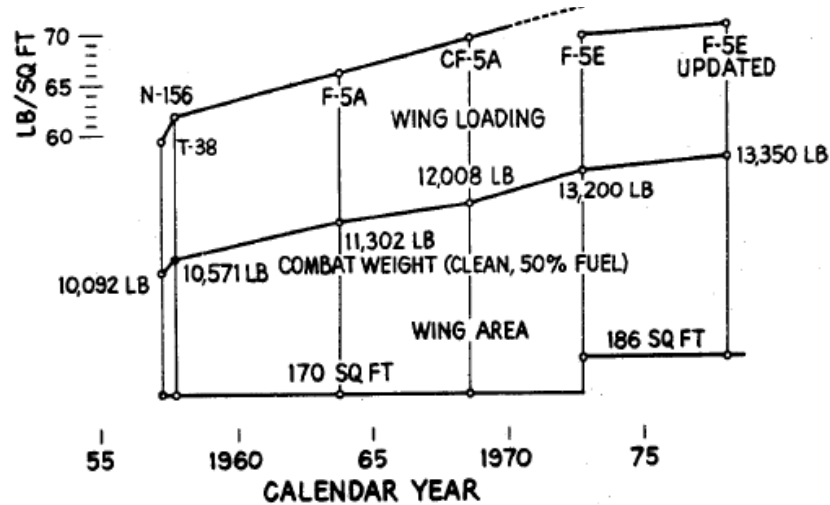
Figure 18: Northrop F-5 Wing Loading Growth [68]

originally designed wing loading of about 60 lb/ft^2 to 70 lb/ft^2. Wing loading is one of the most important design parameters and it seems that the penalty of having a wing at an off-design point did not offset the cost saving of keeping the wing design unmodified.

3.1.1.2   Lockheed Martin F-16 Fighting Falcon

Lockheed Martin's F-16 Fighting Falcon is one of the best-selling military aircraft in the world. Since the first production model was delivered to the U.S. Air Force in 1979, more than 4,000 F-16s have been produced, according to Lockheed Martin (www.lockheedmartin.com). The F-16 was originally designed as a lightweight, daytime, air-to-air fighter, but it has evolved into a multi-role, all-weather aircraft over the past twenty years. Having more than 110 different versions, the designation is tracked by block numbers. The evolution history of the F-16 is well documented by Hehs [69]. Starting from Block numbers 1 and 5, new block numbers were added whenever major upgrades were implemented. Almost every upgrade was accompanied by upgrades in avionics, weapon systems, and engines.

Expanding its realm from air superiority to include ground-attack and all-weather capability, more equipment and payload were added, leading to an inevitable increase in vehicle weight. For example, the empty weight of the Block 50 is 19,200 lb, which is about 24 percent heavier than the 15,600 lb Block 10. The wing area has undergone a 7 percent increase, growing from 260 ft^2 to 300 ft^2, representing the maximum possible growth before having to modify the fuselage. Both the horizontal and vertical tail areas also were enlarged by approximately 15 percent.

The evolution of the F-16 took advantage of the electronic revolution and advances in jet engine technology. The performance loss due to additional weight and drag (due to external attachments) was offset by the increase in the engine thrust from 23,000 lb on the YF-16 to 30,000 lb on the Block 50. Although the capabilities of radars, computers, and data links have been upgraded vastly, such electronic systems could be enclosed within the originally designed body thanks to the rapid advancements in electronic technology.

3.1.1.3 Boeing F/A-18 Hornet

The case study of the F/A-18 Hornet was conducted in two parts: the first part tracked the evolution history, focusing on the growth of the vehicle itself, and the second part focused on the historical background behind the birth of the F/A-18E/F program.

3.1.1.3.1 Evolution History of F/A-18 Hornet

The F/A-18 Hornet is a twin engine, mid-wing tactical fighter for the U.S. Navy. It is the first strike fighter of the United States designed to perform both air-to-air and air-to-ground missions. F/A-18 Hornet was derived from Northrop's YF-17, one of the contenders for the USAF's Light Weight Fighter Prototype program that was initiated

in April, 1972, along with the General Dynamics YF-16 [70]. Later in the 1970s, the U.S. Navy launched a program called the Navy Air Combat Fighter (NACF) program to procure a carrier-borne, multi-role fighter to replace both the A-7 and the F-4 and to complement the F-14 Tomcat. In May, 1975, McDonnell Douglas and Northrop as a subcontractor won the NACF to produce the F/A-18s [71].

Since the YF-17 was designed for the U.S. Air Force as a light weight fighter, a series of changes were made to the YF-17 to suit the needs of the Navy and to fulfill both fighter and attack missions when the F/A-18A was developed. Those changes included "catapult provisions, all-weather avionics, increased wing area, strengthened fuselage, strengthened landing gear, special arresting provisions for carrier operations, more internal fuel, a little more engine thrust, and a Sparrow missile capability [72]." The first generation of F-18s, designated as F-18A/B, went into operation in 1983. An upgraded version with updated missions and jamming devices, designated as C/D, became operational in 1993. Except for the early production models, the C/D versions were powered by F404-GE-402 enhanced performance engines.

In the 1990s, the need for a more capable Navy strike fighter was emerged, which called for another round of the F/A-18 upgrade program, designated as the F/A-18E/F program. F/A-18E/F, powered by upgraded F414-GE-400 engines, is significantly larger and more capable than the C/D versions while inheriting the traits of the previous versions. Jane's All the World Aircraft 2006-2007 summarizes the changes from the C/D to E/F version as follows:

> F/A-18E/F is a stretched version of C/D; landing weight increased by 10,000 lb; 2 ft 10 in fuselage plug; wing photographically increased by 100 ft2; larger horizontal tail surfaces; LEX increased to 75.3 ft2 from 56 ft2 of C/D; additional 3,600 lb of

internal fuel and 3,100 lb of external fuel; two more weapons hardpoints; air intakes redesigned to increase mass flow and reduce radar cross-section; F414-GE-400 engines; reduced observable measures by saw-toothed doors and panels, realigned joints and edges and angles antennas.

Figure 19 shows the geometrical characteristics and relative growth from YF-17 to F/A-18A and F/A-18E. F/A-18C, missing in the figure, is geometrically identical to the A version. F/A-18B, D, and F versions are two seat models of A, C, and E. They are identical except that the two seat versions have about 400 lb less internal fuel volume to accommodate another pilot [73]. While the geometric similarity between the versions is evident from the figure, wing area increased from 350 ft^2 to 500 ft^2; engine thrust increased from 15,000 lb to 22,000 lb per engine; empty weight even increased from 17,000 lb to 30,564 lb. The degree of growth from the C/D to E/F version was so dramatic that some government officials wanted to call the F/A-18E/F program a *new* aircraft program rather than an aircraft upgrade program[*]. Some of the major milestones and specifications of F/A-18 derivatives are summarized in Table 2.

---

[*]There was a disagreement between the government officials on the classification of the Super Hornet program as a major modification. A CRS report [74] to the Congress stated that "some observers describe the F/A-18E/F as an upgraded and larger version of the F/A-18C/D, with increased range and payload capacity and more space and weight observers assert that the differences between the baseline Hornet aircraft and the E/F model are so great that they would describe the Super Hornet as an entirely new aircraft." In 1994, as per the official request by Senator William V. Roth Jr., GAO investigated the matter. For more details on the issue, refer to the GAO report [75].
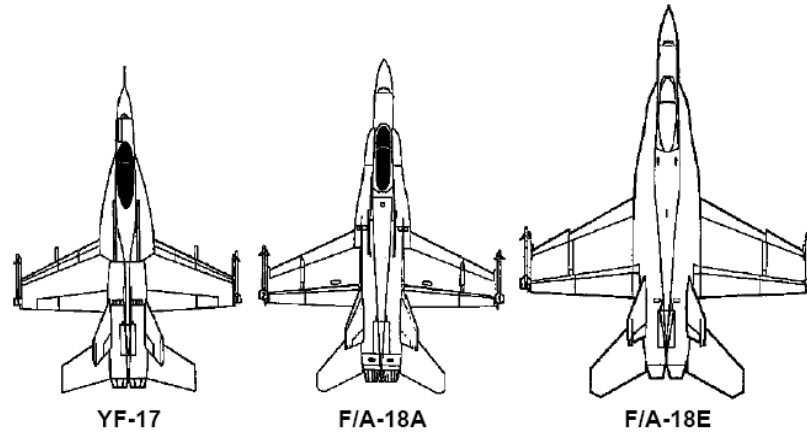
Figure 19: Evolution of F/A-18 [76]

Table 2: F/A-18 Hornet Missions, Specifications, and Milestones [70, 74, 76-79]

	YF-17	F/A-18A/B	F/A-18C/D	F/A-18E/F
Service	US Air Force	US Navy and Marines	US Navy and Marines	US Navy and Marines
Type	Prototype	Strike fighter	Strike fighter	Strike fighter
Mission capabilities	Day time air superiority	Escort and carrier-based interdiction	+Night attack	+Long-range, all weather
Manufacturer	Northrop	McDonnell Douglas	McDonnell Douglas	Boeing
Engine	J-101 Turbojet	F404-400	F404-402	F414-400
Thrust (SLS)	15,000 lb	16,000 lb	17,754 lb	22,000
Wing area	350 ft^2	400 ft^2	400 ft^2	500 ft^2
LEX area	46 ft^2	54 ft^2	54 ft^2	75.3 ft^2
Wing span	35.0 ft	37.6 ft	37.6 ft	42.9 ft
Empty weight	17,000 lb	21,830 lb	24,372 lb	30,564 lb
Internal fuel		10,860 lb	10,860 lb	14,700 lb
External fuel		6700 lb	6700 lb	9800 lb
First flight	June 9, 1974	November 18, 1978	September 3, 1987	December 1995
First Delivery	N/A	May 1980	1991	1999

3.1.1.3.2 Background of the F/A-18E/F Program

In the late 1980s, the U.S. Navy was facing a situation where they had to find some way to replace the aging F-14 in its air-to-air fighter role and the A-6E in its air-to-surface attack role. The U.S. Navy considered combinations of following options [80, 81]:

- SLEPs on A-6 and then buy JSFs to replace A-6
- Continued use of F/A-18C/D
- Upgrade F/A-18C/D to E/Fs (1,000 new productions)
- Upgrade F-14 to add attack capability, F/A-14D (600 new productions and 400 retrofits)
- Advanced Tactical Aircraft (ATA), later A-12 Avenger II
- Navy variant of F/A-22 (NATF)
- Carrier-capable version of F-117

The Advanced Tactical Aircraft (ATA) program began in 1983 as a long range, low observable, high payload medium-attack aircraft to replace the A-6, IOC in the mid-1990s. In January 1988, it was designated as the A-12. The program was terminated in January 1991, after disclosure of severe cost and schedule overruns and technical problems [82]. Procurement of Navy variant F/A-22 (NATF) was planned to start in 1999, when the F-14 would begin to retire in large quantities, based on the service life of 27 years. The consideration for NATF was dropped in 1991 [82]. The series of program cancellations was largely affected by the unexpected collapse of the Soviet Union. Since the carrier version of the F-117 was never endorsed by the Navy leadership, the only surviving options to modernize the U.S. Navy fleet by the early 1990s were the F-14D and the F/A-18E/F [74].

Evidence exist that the requirement for the F/A-18E/F—formalized in the ORD in 1991 and revised in 1997—was affected by the outcome of the F-14D program. In 1992, the House Armed Services Committee held a hearing on the Defense Acquisition Board

(DAB) review of the F/A-18E/F development program. In the hearing, various combinations of the F/A-18C/D, F/A-18E/F, F-14D, and STC-21 (a super Tomcat) were reviewed in terms of the procurement cost, operation and support cost, and capabilities. The conclusion from the hearing was that "F-14D [is] not as survivable in strike role, more expensive to procure, more expensive to operate and support, less capable in strike role [83]."

In addition, Bolkcom [81] reports in support of the E/F program that

> … the F-14's long-range air defense mission, known as the outer air battle, will be less important in the post-Cold War era, when naval aircraft are expected to be used at shorter ranges in littoral (off-shore) operations in Third-World scenarios… Navy officials emphasized in 1991-92 that affordability and inventory requirements were the driving factors in their support of the F/A-18E/F over the F-14D, whose higher-performance air-to-air radar and greater range and payload capabilities they considered less essential for fleet defense with the demise of a Soviet threat.

The F-14D program was truncated significantly, and a total of 37 new aircraft were constructed. Eighteen F-14As were remanufactured to D variants. The F-14D was first delivered in 1991 and completed its retirement from U.S. Naval service on March 10, 2006 [84].

On the other hand, the E/F program officially received Milestone IV/II approval in May, 1992, to start engineering & manufacturing development (EMD) [4]. Later, the production quantity of F/A-18E/F was also reduced several times from 1,000 in 1993 to 548 in 1997 and to 462 in 2003. The F/A-18E/F would be the only modern Navy Attack/Fighter aircraft until the procurement of JSF begins after 2010.

In conclusion, the evolution of the F/A-18 was largely affected by the unexpected change in the operational environment brought by the demise of Soviet Union. The requirement for F/A-18E/Fs formalized in the ORD in 1992 was affected by the outcome

of other U.S. Navy programs, especially the F-14D program. An interesting point is that while the unexpected collapse of the Soviet Union completely changed the needed capability of the U.S. Navy Air Wing in the 1990s and beyond and resulted in a series of program cancellations, the requirement for the F/A-18 still grew. An important lesson from this history is that the capability of a vehicle system should evolve in a way that it can offer more, not less, even in a situation where overall needed capability of the fleet decreases.

3.1.2   Military Helicopter: Boeing CH-47 Chinook

The Boeing CH-47 Chinook is a tandem, medium-lift helicopter for the U.S. Army and international customers. Since the first fully equipped CH-47A entered service in 1962, upgraded CH-47B and CH-49C went into production in the mid-1960s. In the mid-1970s, the need for the modernization of the U.S. Army's medium-lift helicopter was established. The U.S. Army decided to improve the existing CH-47 A, B, and C fleet instead of initiating a new development program to minimize cost and technological risk. Biery and Lorell [3] stated that "the Army estimated that a new development program would have cost from three to five times more in R&D funds than modification of the CH-47 without providing a commensurate improvement in capabilities." A total of 441 CH-47 A, B, and Cs were stripped and reassembled with the upgrades on seven subsystems as listed in Table 3. To extend the life of the CH-47 beyond 2030, Boeing subsequently upgraded CH-47Ds to CH-47Fs. Total 394 existing CH-47Ds are planned to be modified to CH-47Fs integrating the upgrades listed in Table 3 starting in 2003.

Table 3: CH-47 Major Modification Programs [11, 85]

Program	Upgraded Subsystems
A, B, and C to D	Composite rotor blades
	Improved Lycoming T55-L-712 engines
	Higher capacity transmission
	Upgraded electronics
	A multipoint suspension system for sling loads
	Advanced flight control system
	Improved APU with generator and hydraulic pump
D to F	Improved airframe structure to reduce vibration
	Structural enhancements
	Integrated cockpit control system
	Improved avionics with digital advanced flight control system
	More powerful engine with digital fuel controls (T-550L714 at 4900 SHP)
	Modularized hydraulics and triple cargo hooks

Some of the key specifications of CH-47 are summarized in Table 4. The evolution of the CH-47 clearly shows how growth can be manifest in both capability and weight. From the CH-46A to the MH-47E, the engine's horsepower increased from 2,650 hp to 4,867 hp while vehicle gross weight increased from 21,400 lb to 54,000 lb. Again, the basics of the airframe were relatively untouched. The rotor design also remained fixed except for the CH-47A, which had a slightly shorter rotor. It is thus not difficult to realize that modern CH-47s are operated at a disc loading that is 64% higher than that of the original design point. This is a testament to the ingenuity of Boeing engineers, as it represents doubling the load-carrying capability of the vehicle without significantly altering the rotor system. Nevertheless, it is questionable whether the newer, heavier versions can retain the same level of handling qualities, maneuverability, and agility.

Table 4: CH-47 Evolution [86-88]

Models	CH-47A	CH-47B	CH-47C	CH-47D	MH-47E
First delivery	1962	1967	1968	1982	1991
Empty weight	18,112	19,555	20,547	23,093	26,918
Gross weight (lb)	33,000	40,000	46,000	50,000	54,000
Payload weight (lb)	13,400	18,600	23,450	22,686	27,082
Ferry range (nm)	835	1,086	1,233	1,255	1,260
Power rating (hp)	2,650	2,850	3,750	4,500	4,867
Fuel capacity	621	621	1,129	1,068	2,068
Rotor diameter (ft)	59.1	60	60	60	60

3.1.3 Commercial Transport: The Boeing 737 Series

Although the case study has been conducted mostly focusing on military systems, a commercial transport was added to the study for comparison purposes. Boeing's 737 is the most successful commercial jet in history. Since its first delivery in 1967, more than 5000 B737s have been delivered to customers and more than 6,866 units have been ordered through the end of March 2006, according to the Boeing Company [89]. More than 10 different versions of the 737 have been introduced up to date, starting from the 737-100 of the 1960s to the most recent 737-900ER.

Table 5 summarizes major milestones of the 737 family, including first order, first flight, first delivery dates, etc. In accordance with the first order dates, the 737 series can be grouped together into three different groups. The first generation of the 737 includes 737-100 and 737-200, followed by the second generation from 300 to 500, and the third generation from 600 to 900 (or the Next Generation according to Boeing.) Different versions within each generation usually share the common design with either shortened or lengthened fuselage. For example, 737-400 and 737-500 are shortened and stretched

versions of 737-300. In addition, 737-600, 800, 900, and 900ER are shortened or stretched-body versions of 737-700.

General specifications for the 737 family were collected from various sources as shown in Table 6. The 737 family showed gradual increase in size, weight, and engine power. The 737-900ER is almost twice as heavy as the 737-100 and is powered by 187,700 lb maximum thrust General Electric CFM56-7 engine, compared to the 14,000 lb JT9D-9 installed in the 737-100. Not only the size and weight of the vehicle grew over time, but also the number of seats and range. Depending on the models, third generation models carry roughly twice the number of passengers a thousand more nautical miles than the first generation models.

It seems that Boeing took an approach of designing a family of aircraft rather than a single version. Major milestones of some derivative models show some hint of concurrent development. 737-400 and 737-500 are stretched and shortened-body versions of 737-300 and were introduced four and five years after the 737-300 was introduced respectively.

Table 5: Boeing 737 Series Introduction Dates [89]

Model	First Order	Rollout	First Flight	Certification	First Delivery
737-100	2/15/65	1/17/67	4/9/67	12/15/67	12/28/67
737-200	4/5/65	6/29/67	8/8/67	12/21/67	12/29/67
737-200C	2/15/66	8/12/68	9/18/68	10/1/68	10/30/68
737-200 Adv	7/16/70	3/26/71	4/15/71	5/3/71	5/20/71
737-300	3/5/81	1/17/84	2/24/84	11/14/84	11/28/84
737-400	6/4/86	1/26/88	2/19/88	9/2/88	9/15/88
737-500	5/20/87	6/3/89	6/30/89	2/12/90	2/28/90
737-600	3/15/95	12/8/97	1/22/98	7/1/98	9/19/98
737-700	11/17/93	12/8/96	2/9/97	11/7/97	12/17/97
737-800	9/5/94	6/30/97	7/31/97	3/13/98	4/22/98
737-900	11/10/97	7/23/00	9/1/00	3/1/01	5/16/01
737-900ER	7/18/05				

Moreover, the 747-600, 800, and 900 are based on the 737-700, having the same wings and empennage, but with different fuselage lengths and engine scales.

Figure 20 illustrates the evolution of the general arrangements from the 737-600 to the 737-900ER, which are significantly different in fuselage length. The 737-900ER is 36 ft longer than the 737-600. Comparing the body of a 737-600 to that of a 736-900ER, it is surprising that they have the same-sized wings (although the 900ER has winglets) as well as horizontal and vertical tails. It is thus likely that the wing design is not optimized for a specific version, but rather represents Boeing's strategy of saving manufacturing costs through platform sharing.

Designing a family of aircraft would entail a significantly different approach than designing for a single aircraft, balancing multiple missions and markets, cost, and design efficiency. A strategy or design methodology for an aircraft family development is a very interesting subject warranting further investigation, and is further discussed in §8.2.2 as part of the future research opportunities.

Table 6: Boeing 737 Series Specifications [79, 89, 90]

Model	TOGW (lb)	Range (nm)	Pax	Max Thrust (lb)	Wing Span	Length	# of Orders*
737-100	97,000	2,240	80/101	14,000	93ft 0 in	94 ft	30
737-200	107,000	2,400	88/113	14,500	93ft 0 in	100 ft	1,114
737-300	138,500	3,400	128/149	22,000	94ft 9in	109 ft 7 in	1,113
737-400	150,000	3,200	146/170	23,500	94ft 9in	119 ft 7 in	486
737-500	133,500	2,420	108/132	20,000	94ft 9in	101 ft 9 in	389
737-600	145,500	3,050	110/132	22,700	112 ft 7 in	102 ft 6 in	86
737-700	154,500	3,365	126/149	26,300	112 ft 7 in	110 ft 4 in	776
737-800	174,200	3,060	162/189	27,300	112 ft 7 in	129 ft 6 in	772
737-900ER	187,700	3,200	180/215	27,000	112 ft 7 in	138 ft 2 in	46

*as of 1 January 2001
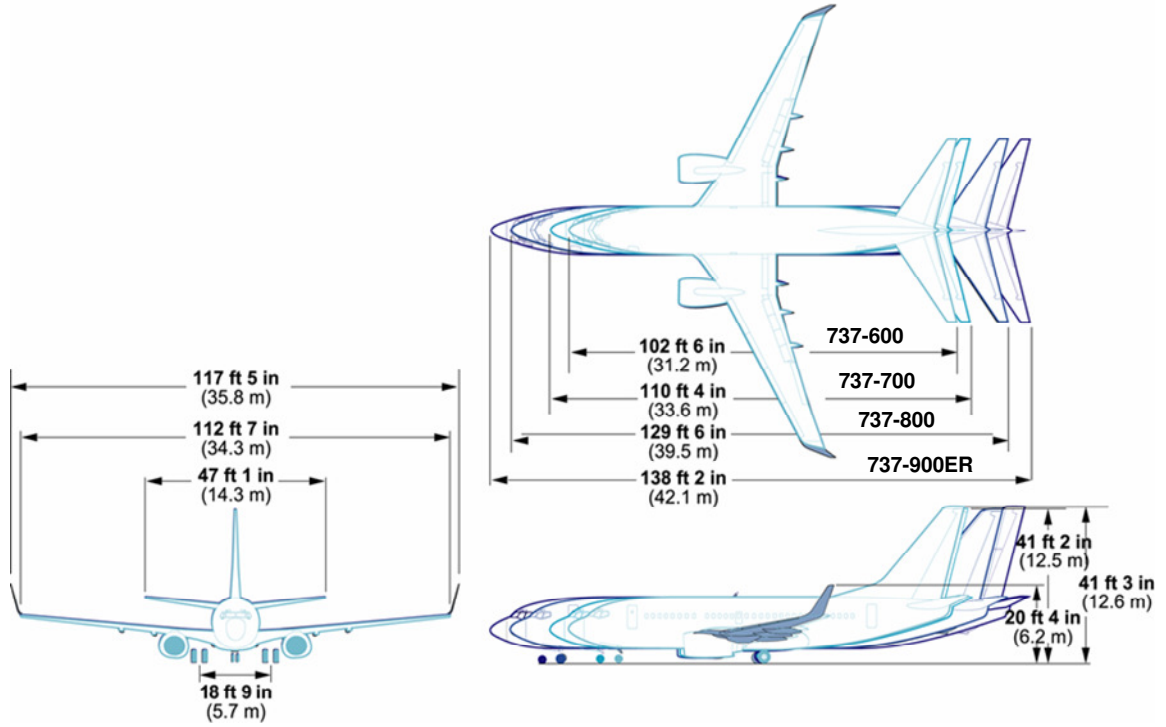
Figure 20: Boeing 737 Series General Arrangement [91]

3.2 Part II: Preplanned Aircraft Upgrades

The second part of the case study was devoted to identifying the attributes that acted as major contributors in determining the success or failure in upgrading/retrofitting existing aircraft. The study first collected cases in which growth provisions were pre-planned, regardless of whether they were actually implemented or not.

The Grumman F-14 evolved from the Navy's VFX program, which was supported by the Navy Fighter Study (NFS) in 1967. According to a Rand report [3]:

> The NFS placed great emphasis on growth potential in the new design so that when they became available advanced technology engines and avionics could be incorporated with little or no airframe modification. ... An important criterion determining the choice had been the growth potential exhibited by the Grumman design.

55

Grumman's proposal for the VFX design showed two major growth provisions. According to Mackey [12],

> The F-14 was designed from the start to incorporate an advanced engine, the F-401, the Navy's version of the Air Force's F-100 engine which was then in development. The aircraft was also designed to accommodate various avionics and armaments improvements, specifically in infra-red detection and targeting. Theses variants were subsequently designated the F-14B and the F-14C.

Incidentally, the F-14 development is considered to be one of the most successful P³I case.

Another very successful example of pre-panning is the design of the B-1B Lancer. A contract was awarded to the Rockwell International Corporation to develop the B-1B in 1982 when P³I was a popular movement within the aerospace community. The aircraft was designed "on the assumption that it would need to have a long and effective service life, and that its environment would be in constant change [92]." Therefore, the design team made a concerted effort to produce an airframe that was flexible and adaptable. For example, the wing was designed to sweep between 15 and 67.5 degrees in order to be effective in a wide range of mission profiles. A standard weapons interface, as per MIL-TSTD 1760, was adopted to allow the seamless integration of future war fighting capabilities. Reprogrammable avionics were adopted instead of, at the time, the more common hard-wired system. Lastly, an oversized engine was selected as a hedge against future thrust requirements. The F101-GE-102 engine, at the time, was under a separate P3I program anyway, representing the then-popularity of pre-planning.

EA was also reportedly successful in the development of the avionics system for the F/A-18E/F. Recognizing the tremendous difference in the rate of obsolescence between the electronics and airframe industries, the design team chose to inherit more than 90%

of the E/F version's electronics from the previous C/D system for the initial batch of production. Subsequently, pre-planned upgrades were made on an incremental basis that included [4]

> …improved cockpit instrumentation, a new and improved forward-looking infrared (FLIR), and an electronically scanned array for the radar. Other improvements have been added to the program during the past several years, including a reconnaissance pod, a helmet-mounted cuing system, and some integrated electronic defensive countermeasures.

The EA approach is thus considered instrumental to the successful development of the F/A-18E/F under time and budget constraints.

From the start, both multi-mission flexibility and growth possibilities were emphasized on the design of Northrop's F-5, because the company envisioned having international customers. Two distinctive growth provisions were integrated to the airframe, one of which was the inlet design. In the development of the F-5G, the inlets were shaped such that future, upgraded versions of the F404 engines could be installed. The shaping of the nose was also controlled to possess sufficient internal volume to cater to different customer requirements.

Similar to how the development of the F-5 designed-in growth provisions to the airframe, measures to ensure the production of stretched variants were conceived from the inception stages of the Boeing 727 [93]:

> From 1959 we had growth potential constantly in mind, and one of the limitations to growth potential is wing fuel capacity. In addition, we wanted to have an airplane that could be sold to the U.S. military, and we knew this would require longer range. Thus, we bent the front spar to allow the center section to have an increased fuel capacity (it is very thick as well).

Boeing engineers also decided to mount the engines under the wings, because such a configuration would allow for a wider center of gravity margin, should the fuselage be stretched later.

3.3 Part III: Challenges in Designing for Future

The last part mainly focuses on challenges in planning and executing modification programs. Both pre-planned and ad-hoc upgrade programs are studied. This part of the case study asks—what attributed to the program's failure or success? Special attention was paid to whether growth provisions were planned from the initial design or not and whether they are implemented and why.

One of the most challenging aspects of designing for growth potential is the fact that the future cannot be predicted with certainty. Uncertainties exist in forecasting the market dynamics, funding, customer requirements, technology availability, etc. From the aircraft manufacturers' standpoint, the biggest uncertainty would be what customers want in the future. Once the answer is figured out, the next question then is what they can offer in a response to the future need. The answer(s) to this question involves complex combinations of finance, competition, collaboration, and technological opportunities. Uncertainties from these sources imply that there is the inherent risk of wasted investment in preparing for growth in a prior manner.

Biery and Lorell [3] stated that one of the reasons for the N-102's rejection was the presence of technological risk: "reflecting on the pace of advances in air vehicle technology in the previous decade (1943-1953) the Air Force doubted anyone could adequately anticipate the direction of future technology." In their recommendations to the Air Force, the authors commented, "pre-planning very far into the future is [an]

unworkable concept," preferring instead to support pre-planning on a more restricted scope. That is, the risk of forecasting could be somewhat mitigated by limiting the provision for growth to specific sub-systems (e.g., engine, avionics, etc.) when they are still under development but not mature enough yet to be implemented on the initial production aircraft[*]. Many of the successful upgrade programs were indeed found to have planned for short-term, sub-system specific scenarios. The integration of newer technologies also did not occur until their readiness was close to maturation.

Besides the issue of uncertainty, there were cases when technology insertions failed to deliver the promised performance enhancement, regardless of whether such upgrades were pre-planned or not. Numerous modification programs suffered from unexpected, expensive design changes, schedule slippage, and cost over-runs, because physical constraints such as volume availability, maneuverability, and handling qualities were either overlooked or not analyzed with sufficient modeling and simulation.

The cases of the A-4 Sky Hawk and F-4/M Phantom from the Rand report [3] are good examples. In the case of the A-4 Sky Hawk upgrade program, a camel's hump-like structure was added behind the cockpit to compensate for the lack of volume to incorporate the new avionics system. The re-engining of the F-4K/M Phantom for the Royal Navy required entire redesign of aft-fuselage, inlets, and ducts of the vehicle, eventually costing more than developing a new aircraft. The case of the T-45 modification for aircraft carrier operation is a notorious example of an upgrade program gone wrong. Insufficient modeling and simulation work in the early design phases

---

[*]In the conceptual design phase, integration of technologies with technology readiness level 6 or higher is typically considered for a new aircraft, according to Mark Alber, Section Chief of Advanced Concept at Sikorsky Aircraft, Stratford, Connecticut [Interviewed on October 10, 2007, by the author].

prevented the deficiencies in aircraft handling characteristics from being identified until the operational testing phase, leading to extensive re-designs and tests. Due to this belatedly discovered problem, the original schedule had to slip several times, until the operational test was finally completed 10 years after full scale development had started [13].

The findings and lessons from the case studies on past aircraft modification programs are consolidated in the following observations. The observations then induce two research questions:

Observation 3: *Uncertainties associated with future requirements, market, government funding, and technology maturation made pre-planning into the far future difficult and risky.* (**Research Question 3**)

Observation 4: *Insufficient understanding of the key physical constraints through sufficient modeling and simulation early on often caused project delays, cost over-run, less-than-expected performance, and even infeasible design.* (**Research Question 3**)

Research Question 4: *How can a practical aircraft conceptual design methodology by which the lifetime evolvement of an aircraft is incorporated into the initial design under the presence of uncertainty be formulated? How can a decision-maker find a balanced design under the presence of uncertainty?* (**Observation 3**)

Research Question 5: *How can the possibility of having unexpected technical difficulties in upgrading existing designs be reduced?* (**Observation 4**)

3.4 Chapter Summary and Scope of the Research

This chapter reviewed the trends and issues of aircraft design evolution and long-term planning for such design modifications. Besides the technical barriers identified and summarized in the observations, social, political, environmental, and economic aspects related to a development program also played key roles during the decision-making process. In the case of commercial transport, market fluctuation and competition are the most important factors in planning for the development of a derivative aircraft. Thus, systematic market forecasting through system-of-systems (SoS) approach and game theoretic approaches would be relevant. However, to limit the scope of the problem, this study intends to focus on the technical challenges associated with designing aircraft for growth at the vehicle systems level. Since uncertainty in future requirements was identified as the key challenge when someone tries to incorporate future properties into a present physical entity, the goal of the study is solidified as the development of a new design methodology capable of quantitative evaluation of the evolution paths of a vehicle while incorporating requirement uncertainties at the vehicle systems level.

CHAPTER IV

DECISION MAKING UNDER UNCERTAINTY

People make decisions in their everyday lives, the consequences of which are governed by uncertainties. The decision-making process is often implicitly based on the anticipated probabilities of the future outcomes and associated consequences. People often predict the future by extrapolating their experiences. Other factors, such as irrational predilection, tolerance to loss, and fear also play roles during the process. Whether they are conscious of the decision they make or not, people have some internal logic to come up with a decision handling an uncertain future.

Historically, the senior leadership of organizations needed a more structured way to populate possible outcomes of uncertainty, i.e. scenarios, playing games with the conceivable scenarios, and making decisions, namely, *scenario planning* or *scenario analysis*. Mathematicians also developed a field of study named *stochastic programming* to address the issues of optimization under the presence of random variables. As an attempt to answer **Research Question 4**, these two distinctive areas of research related to decision making under uncertainty are reviewed in this chapter.

4.1 Stochastic Programming with Recourse

Stochastic programming (SP) is a sub-field of mathematical optimization that is concerned with making decisions under uncertainty. Here, the term "stochastic" means that the decision-making problem involves one or more modeled uncertainties in the form of random parameters, whereas the term "programming" is equivalent to

"optimizing" in the language of mathematics, and essentially refers to the process of converging at a decision. An underlying assumption in this field of study is that a decision maker either knows or is in the position to estimate the probability distribution of a random parameter and [94].

4.1.1 Formulation

Among the multitude of SP models, Dantzig [95] and Beale [96] formally introduced a multi-stage model in 1955 that would come to be known as stochastic programming with recourse (SPR). This branch of study deals with situations in which some corrective or "recourse" actions are allowed once the random parameters are realized, although the cost of such a posteriori recourse is not free. Shapiro and Philpott describe the two-stage recourse program as follows [97]:

> Here the decision maker takes some action in the first stage, after which a random event occurs affecting the outcome of the first-stage decision. A recourse decision can then be made in the second stage that compensates for any bad effects that might have been experienced as a result of the first-stage decision. The optimal policy from such a model is a single first-stage policy and a collection of recourse decisions defining which second-stage action should be taken in response to each random outcome.

Depending on the type of the objective function to be minimized, two-stage stochastic programming with recourse is further classified as *stochastic linear programming* and *stochastic non-linear programming* [98]. As a sub-field of stochastic linear programming, *stochastic integer programming* deals with discrete decision variables. Also, as the number of stages is expanded to more than two, the method falls into *stochastic dynamic programming*, the term coined by Bellman [99].

Since most engineering design problems deal with non-linear objective functions and constraints, the mathematical formulation is given in the most appropriate form to deal with non-linear functions:

$$\min_{\mathbf{x}} z \equiv f(\mathbf{x}) + \mathbb{E}_{\omega \in \Omega}\left[Q(\mathbf{x}, \omega)\right]$$
$$\text{s.t. } g(\mathbf{x}) \leq 0 \ (i = 1,...,l) \tag{3}$$

where $Q(\mathbf{x}, \omega)$ is the optimal value of the second-stage problem defined as

$$Q(\mathbf{x}, \omega) = \min_{\mathbf{y}} F(\omega, \mathbf{x}, \mathbf{y})$$
$$\text{s.t. } G(\omega, \mathbf{x}, \mathbf{y}) \leq 0 \ (j = 1,...,L) \tag{4}$$

where $\mathbf{x} \in \Re^{n_1}$ and $\mathbf{y} \in \Re^{n_2}$ represent the first and second-stage decisions in n_1 and n_2 dimensional space, respectively; $\omega \in \Omega$ is a random vector from a probability space $(\Omega, \mathfrak{F}, P)$ with set $\Omega \subseteq \Re^k$, a σ-algebra $\mathfrak{F} \subseteq \Omega$, and a measure P on $(\Omega, \mathfrak{F})$ such that $P(\Omega) = 1$; $Q(\mathbf{x}, \omega)$, called *the second-stage value function*, is the optimal value of the second-stage problem, given a first stage decision $\mathbf{x}$ and random parameter realization.

As evident from Eq. (3), the ultimate goal is to find the optimal first stage decision that minimizes the total expected cost, which is formulated as the summation of the first stage objective $f(\mathbf{x})$ and the expected penalty of correcting this first stage decision. It is important to realize that the optimal first stage decision is not an ideal solution under all possible outcomes of the random variable(s), but rather a decision that is well hedged against the risk of excessive corrections.

In most real-world engineering problems, analytical integration of the optimal value of the second-stage function $Q(\mathbf{x}, \omega)$ is impossible. In such a case, the expectation must be *estimated* through numerical integration. Numerical integration by assessing all possible

combinations of the random variable can be prohibitive, since the number of combinations exponentially grows as the dimension increases. Continuous random variables (N) can take an infinite number of combinations and even with discretization (d) with reasonable accuracy still produces d^N combinations.

The Monte Carlo Simulation (MCS) method relieves the issue of dimensionality by using random numbers. Essentially, MCS is about numerical integration with random numbers. Some more advanced Monte Carlo methods were introduced in the past, such as Quasi-Monte Carlo methods [100] and Sample Average Approximation (SAA) [97, 101]. These methods are known to improve the convergence rate under certain conditions.

In addition, two random sampling techniques—Latin Hypercube Sampling (LHS) and Simple Random Sampling (SRS)—are widely adopted, and their convergence properties have been studied in the past. According to the U.S. Environmental Protection Agency (EPA)'s Guiding Principle for Monte Carlo Analysis [102],

> Latin hypercube sampling may be viewed as a stratified sampling scheme designed to ensure that the upper or lower ends of the distributions used in the analysis are well represented. Latin hypercube sampling is considered to be more efficient than simple random sampling, that is, it requires fewer simulations to produce the same level of precision. Latin hypercube sampling is generally recommended over simple random sampling when the model is complex or when time and resource constraints are an issue.

Some other literature [103, 104] also supports that LHS converges faster than SRS in general. However, as past studies indicate, the performance of specific sampling methods depends on the problem at hand. The convergence rate depends on the type of random variables and the characteristics of the output. LHS is known to have advantage over SRS when the random variables are uniform and the output is an additive interaction between the inputs rather than multiplicative interactions. [105, 106] Therefore, the EPA

guide recommends the risk assessor investigate the stability and repeatability through repeated experiments before using Monte Carlo methods.

4.1.2 Value of Perfect Information and Stochastic Solution

In the setting of two-stage stochastic programming, two interesting quantities can be calculated to answer:

1. How much would one be willing to pay for the perfect forecast on the random variables?
2. How much is it worth to solve a stochastic problem rather than a deterministic problem?

4.1.2.1 Value of Perfect Information

The first question is answered by calculating *the expected value of perfect information* (EVPI), originally developed by Raiffa and Schlaifer [107]. Birge and Louveaux [94] state that, "the expected value of perfect information measures the maximum amount a decision maker would be ready to pay in return for complete (and accurate) information about the future." In the context of aircraft design, this value can be interpreted as the amount of money an aircraft manufacturer would be willing to pay to obtain the concrete future requirement by, for example, acquiring a future contract in advance.

To calculate EVPI, it is assumed that one can always predict the value of the random variable with certainty. For all possible realizations of the random variable—i.e. scenarios—the total cost of the two-stage problem is calculated. The average of the total cost is the *expected value of the optimal solution* or the *wait-and-see solution* (WS) coined by Mandansky [108].

$$WS = \mathbb{E}_{\omega \in \Omega} \left[\min_{\mathbf{x}} \left\{ f(\mathbf{x}) + Q(\mathbf{x}, \boldsymbol{\omega}) \right\} \right] \tag{5}$$

The wait-and-see solution is compared to the so-called *here-and-now* (HN) solution. The here-and-now solution is the expected value of the stochastic solution $\mathbf{x}^*$ that is obtained by solving Eq. (3)

$$HN = f(\mathbf{x}^*) + \mathbb{E}_{\omega \in \Omega}\left[Q(\mathbf{x}^*, \omega)\right] \tag{6}$$

Finally, EVPI is calculated as

$$EVPI = HN - WS \tag{7}$$

4.1.2.2   Value of Stochastic Solution

As discussed in the previous section, solving a stochastic problem is very expensive and time consuming. Thus, one might be interested in how much it is worth to pursue a stochastic problem rather than a deterministic problem.

One of the attempting ways to solve a stochastic problem easily is to transform it into a deterministic problem by replacing the random variables with their expected values. This is called the expected value (EV) problem [94] that is reduced from Eq. (3).

$$EV = \min_{\mathbf{x}} \left\{ f(\mathbf{x}) + Q(\mathbf{x}, \bar{\omega}) \right\} \tag{8}$$

where $\bar{\omega}$ is the expectation of ω.

For the optimal first stage decision $\tilde{\mathbf{x}}^*$ of the EV problem, the second-stage problem given in Eq. (4) is solved for all possible scenarios. This solution is called the *expected result of using the EV solution*, defined as

$$EEV = f(\tilde{\mathbf{x}}^*) + \mathbb{E}_{\omega \in \Omega}\left[Q(\tilde{\mathbf{x}}^*, \bar{\omega}, \omega)\right] \tag{9}$$

Finally, the value of stochastic solution (VSS) is defined as

$$VSS = EEV - HN \tag{10}$$

4.1.3 Adopting Stochastic Programming with Recourse to Aerospace Systems Design

> The recourse-based model makes a decision based on present first-stage and expected second-stage costs, i.e., based on the assumption that the decision-maker is risk-neutral.
>
> Nikolaos V. Sahinidis [109]

The recourse-based stochastic approach has been widely used in the fields of finance [110, 111], logistics and inventory planning [112], scheduling [113], transportation planning in a disaster such as an earthquake [114], in which decisions must be made "here-and-now" under uncertainties but corrective actions can also be taken to compensate for any unfavorable effects caused by randomness. In the context of aircraft design, unsatisfactory performance, sub-optimality due to technology obsolescence, violation of physical constraints, etc. are just a few examples of such unfavorable consequences. The underlying philosophy of SPR appears to be intrinsically compatible with the time-phased nature of engineering design. **Observation 5** formalizes this finding and immediately induces **Research Question 6**.

Observation 5: *The underlying philosophy of SPR is intrinsically compatible to the time-phased decision making process of aircraft design.*

Research Question 6: *Can the SPR formulation be seamlessly adopted to aircraft design? What are the limitations of SPR in the context of aerospace systems design? What are the technical and non-technical challenges?*

Since its inception in 1955, stochastic programming has been extensively studied and the solution approach has been well established as found in Shapiro [97], Linderoth [115], and Kall and Wallace [116]. However, while engineering design often involves non-linear, relatively small-scale problems with highly time-consuming analyses, the main focus of a technical approach in the field of stochastic programming is to solve large-scale, Linear Programming (LP) problems. The application of the SPR formulation to solve engineering design problems in a time-phased decision-making framework has been elusive.

As an attempt to address the concerns raised by **Research Question 6**, a two-stage cantilevered beam design problem was formulated and solved successfully in 2006, as presented in CHAPTER VI. The simple proof-of-concept study demonstrated the applicability of SPR in a two-stage engineering design problem setting. In 2008, Choi [117] applied SPR to a fuel cell based aircraft propulsion system design, considering the fact that the maturity of fuel cell technology far outpaces the aerospace systems development cycle, which, if implemented, renders the performance of the propulsion system highly uncertain. Choi showcased the applicability of the two-stage decision making setting of SPR by designing a propulsion system based on the currently known fuel cell performance at the first stage and redesigning it at the later phase of the aircraft development cycle, when more knowledge is gained about the particular technology.

Both of these examples demonstrated the applicability of SPR in engineering design problems, but besides the technical challenges, the explicit assumptions behind SPR also raised concerns. As an attempt to answer **Research Question 6**, a list of concerns pertinent to aerospace systems design was complied in **Observation 6** based on the

lessons from the case studies, the author's experience, and comments and feedback from engineers, scholars, practitioners, and mangers from industry and government after presenting the idea of adopting SPR into aerospace systems design that was first published by Lim [118] in 2006.

Observation 6: *The following characteristics of aerospace systems design seem incompatible to the assumptions and limitations of stochastic programming with recourse:*

- *While SPR assumes risk-neutral decision makers, those in the aerospace industry are often risk-averse.*
- *While SPR finds the optimum solution that is best on average, in aerospace development the stakes are very high that a single failure can cause irreversible consequences.*
- *While SPR requires a good definition of the random variables, the complex nature of aerospace development programs makes accurate predictions of the random variables (RV) very difficult. Even if the RVs can be predicted with accuracy, they could be wide in range and be highly correlated to each other, making integration of such RVs impractical.*
- *SPR is inflexible in handling multi-objectives, while complex systems design problems are often solved based on multi-criteria decisions.*
- *While SRP does not allow soft-constraints, non-optimal or even infeasible solutions are often permitted in aerospace programs for the sake of cost and schedule.*
- *Solving stochastic optimization problems with both continuous and discrete design variables is very difficult, which makes it hard to evaluate the future design and future technology combinations concurrently.*

First, the mathematical formulations of SPR, given in Eqs. (3) and (4), explicitly assume a risk-neutral decision maker. The optimum solution sought by solving the equations is *not* the ideal solution under every scenario. Rather, it is the best solution on average, which means that the optimum solution would incur the least amount of gross cost when the game is repeated many times under the same rules. It could be worse than some other decisions for a particular realization of random variables. Thus, if the stake of the game is so high and the participant can be eliminated from the game—for example, by filing bankruptcy or by being merged and acquired by the competitor—after playing the first game and losing too much, pursuing different strategies to avoid such an event would be necessary.

In addition, the optimum solution found by solving the stochastic equations is *only* optimum when the PDFs are correct. Assumptions in defining random variables inevitably introduce biases. Therefore, being able to come up with a reasonable definition of the random variable is important and difficult. Often the random variables are correlated to each other and variation of one affects the other. The complex structure of the random variables may render solving stochastic problems impractical.

SPR minimizes the sum of the first stage objective function and the penalty of making a corrective decision in the second stage, which requires that the objective function and the penalty be in a same unit, such as cost. The restriction on objective function in SPR may limit the extent of aerospace design problems, since most of them involve multi-attribute decision-making processes.

SPR finds the optimum solution within the feasible design space. All the constraints are viewed as hard constraints, violations of which are not permitted. In reality,

aerospace systems design problems often accept less than satisfactory performance for the sake of cost and/or schedule savings.

Finally, the use of SPR in aerospace design makes it very difficult to evaluate combinations of technologies. The exploration of a technology combinatorial space along with the optimization of continuous design variables is a very challenging problem in the realm of optimization and particularly difficult when random variables are involved. While *stochastic integer programming* formally deals with optimization with discrete variables, its application to a realistic aerospace systems design seems infeasible.

These issues concerning the implementation of SPR to aerospace design problems induced the following research questions.

Research Question 7: *How can the aerospace systems design process incorporate the concept of risk into the design loop? How can aerospace systems be optimized taking risk-averse decision makers into consideration?*

Research Question 8: *How can one integrate uncertainties into the decision-making process in the absence of accurate probability distributions? How can one draw meaningful observations when the random space is very large and complex?*

Research Question 9: *How can one explore options of aircraft design evolution without restrictions imposed by pursuing the optimization track?*

As an attempt to answer **Research Question 7** and **Research Question 8**, two fields of study are introduced in the subsequent sections.

4.2 Decision Making Under Risk

To answer **Research Question 7**, the concept of risk and optimization strategies incorporating risk are reviewed in this section. The concept of risk aversion was first formulated by Daniel Bernoulli in 1738 in *Specimen theoriae novae de mensura sorti*[*], in which he introduced and solved *St. Petersburg's dilemma*. The dilemma is about a man offered a game, the expected profit of which is infinite. When a choice was given to play the game or not, many people rejected it regardless of the infinite expectation because of the fear of losing money. A risk-averse decision maker may act irrationally and often choose the option with lower expected profit because he or she cannot tolerate the negative consequence of the other, supposedly more profitable option.

The most intuitive way to avoid a risky decision would be to choose a decision with the minimum loss under the worst-case scenario. This classical *min-max approach* can be readily used with the scenario-based analysis that is introduced in the next section. For example, one can solve the optimization with all scenarios and choose the strategy that shows the minimum cost when the worst scenario is realized.

In 1944, John Von Neumann and Oskar Morgenstern co-authored *The Theory of Games and Economic Behavior* [120], developing the *expected utility theory* to quantify risk in the setting of classical economic theory. Based on the assumption of a rational decision maker that maximizes their utility, the theory requires the creation of the utility function capturing risk. However, since a practical formulation of the decision maker's utility function is almost impossible, the theory was not widely used in the domain of numerical optimization.

*Originally published in 1738; translated by Dr. Lousie Sommer in January, 1954 [119]

More recently, two classes of formulations have been investigated to address risk under the study of stochastic programming. One approach is to introduce risk as an additional constraint:

$$
\begin{aligned}
&\min_{\mathbf{x}} \ \mathbb{E}_{\boldsymbol{\omega} \in \Omega} \Big[Z(\mathbf{x}, \boldsymbol{\omega}) \Big] \\
&\text{s.t.} \ \ \mathrm{Prob} \Big[Z \geq z_{\max} \Big] \leq \alpha
\end{aligned}
\tag{11}
$$

where Z is a measurable function, a smaller value of which is better; $z_{\max}$ is the limit or threshold value that Z should not exceed; $\alpha \in [0,1]$ is the threshold probability that is determined by the decision maker. This class of approach falls into the realm of Chance-Constraint Programming (CCP), which largely deals with optimization problems with probabilistic constraints. This branch of stochastic programming was conceived by Charnes and Cooper [121] in 1959 and has been widely adopted in engineering [122] and finance [123, 124]. The method is also known as Reliability Based Design Optimization (RBDO) in the structural engineering community and has been applied to structural optimization problems with probabilistic constraints [122, 125-128]. Recently, Nam [45, 129] incorporated and implemented the method to aerospace systems design applications.

The other class of formulations under the umbrella of stochastic programming combines the risk measure with the objective function so that the optimal decision minimizes the sum of objective function and the risk measure. Various risk measures have been investigated by several researchers. The classical risk measure proposed by Markowitz [130] in 1952 minimizes the sum

$$
\min \mathbb{E}[Z] + \lambda \cdot \mathrm{Var}[Z]
\tag{12}
$$

This mean-variance approach, also called *robust stochastic programming*, balances the minimum cost on average and its variability at the same time. The applications of robust stochastic programming are found in various engineering problems, such as power systems capacity expansion [131], chemical process planning [132], and telecommunications network design [133]. The use of variance as a dispersion measure has shortcomings, such as the mean and variance measure being realized in different units; variance penalizing the positive and negative deviation from the mean equally, and not preserving convexity of Z [101]. Various other forms of variability measures that are coherent, first-order stochastic dominance and convexity preserving have been proposed to overcome the shortcomings [134, 135].

Another type of approach minimizes the threshold value. by which cost function violates this value with a predetermined probability $\alpha \in [0,1]$

$$\min \ \mathbb{E}[Z] + \lambda \cdot \mathrm{VaR}_\alpha[Z] \tag{13}$$

where $\mathrm{VaR}_\alpha[Z] \equiv \min\{\gamma : \{\mathrm{Prob}[Z \leq \gamma] \geq \alpha\}$ is called value-at-risk (VaR). The VaR approach and its variations have been one of the standard methods of evaluating risks in the financial industry for portfolio optimization [136, 137] and derivative evaluation [138] and in the insurance industry for credit risk evaluation [111, 139, 140]. Rigorous mathematical backgrounds and discussions of various risk measures are found in [134].

4.3 Scenario Planning

Scenario planning, also known as scenario analysis, is one of the cornerstone methods in strategic decision-making along with sensitivity studies, contingency planning, time-series analysis, and so on. Scenario planning is widely used amongst high-level policy makers in

military, business, and government sectors rather than academia in order to facilitate decision making under uncertainty. While some literature provides formal step-by-step processes in how to create scenarios [141, 142] and when to use and how to use them [143], it has been in the realm of art rather than science. Although it might lack rigorous scientific evidence, it has proven its usefulness in variety of cases, such as the success of Dutch-shell company [144], which used scenario planning since the 1970s to evaluate its strategic options. Also, the Swedish Defense Agency [145] uses a formalized scenario analysis to establish its long-term military strategies. Management-consulting firm A.T. Kearney utilizes the method under the name of Global Radar Scenario Planning [146, 147]. Another management consulting company, the Futures Strategy Group, LLC., is one of the most active practitioners of scenario planning for a wide range of problems in the private and public sector [148, 149]. The Joint Planning and Development Office (JPDO) used scenario planning to predict future demand for air travel and to plan for the Next Generation Air Transportation System [150, 151].

In its essence, scenario analysis captures a handful of combinations of the random variables among the infinite combinations. Then, the alternative decisions, or strategies, are evaluated under these possible outcomes, called *scenarios*. Therefore, scenario analysis samples k outcomes from the scenarios space Ω, then solves k deterministic problems. The sampling of finite scenarios might include the extreme cases and average case. For example, the decision maker would want to evaluate the most extreme cases even though the probability of such an event is very low. Those possible outcomes, called *scenarios*, are the most plausible and/or meaningful representation of the entire probability space.

For example, consider an optimization problem with one random variable. The random variable is continuous and can take any value between the lower and upper limits. Within the ranges of the possible outcomes, one might consider only three—the minimum, average, and maximum values—and name them as worst, modest, and best cases scenarios. An optimization problem is then solved repeatedly to yield optimum solutions for the corresponding scenarios. Finally, patterns are observed within the optimum solutions and interpretations are made. The outcome of the scenario planning is a robust strategy(s) that will work across a range of plausible future outcomes.

This rather simple process is claimed to be advantageous over other strategic decision making methods, such as contingency planning and sensitivity study [141]. Contingency planning is a "what if" study tool where a decision maker investigates exceptional cases from the baseline by varying one uncertainty at a time. A sensitivity study perturbates one random variable at a time by a small degree such that the perturbation does not affect the state of the other variables. Therefore, sensitivity analysis is useful to see the influence of the random variables to the response near equilibrium points, but it is invalid on a large scale. However, scenario analysis is useful in exploring wide ranges of uncertainty collectively. It captures correlations between the random variables, thus the variation is made to all random variables at the same time in the most plausible ways. Thus, scenario analysis allows the policy makers to be exposed to a wide range of extreme events without overwhelming them by providing too much information.

The success of scenario planning largely depends on the creation of the scenarios. Many existing methods and techniques can be employed depending on the purpose of the

study and resource availability. The first questions that should be addressed are what is the scenario timeframe and what is the scenario scope [141]. Schoemaker [141] suggested a scenario creation method in ten steps as follows:

1. Define the Scope
2. Identify the Major Stakeholders
3. Identify Basic Trends
4. Identify Key Uncertainties
5. Construct Initial Scenario Themes
6. Check for Consistency and Plausibility
7. Develop Learning Scenarios
8. Identify Research Needs
9. Develop Quantitative Models
10. Evolve towards Decision Scenarios

Detailed descriptions and case studies are referred to [141]. Schwartz also presents the six steps of scenario creation checklist [142], which are, largely, similar to Schoemaker's. The methods of Schoemaker and Schwartz are intuitive and logical and have been successfully used in various business cases, but the methods lack the specific techniques to fulfill each of the steps.

Essentially, all the system engineering tools that are useful in engineering design process reviewed in §2.2.1 are applicable in identifying the source of uncertainty, random variables, and scenarios. For example, the system engineering tools, such as QFD, brainstorming, expert polls, Pareto analysis, AHP, and MA can be utilized. In addition, a statistical approach of collecting and analyzing past information can be useful as in the case of the calculation of the volatility of stock prices or oil prices in option pricing. Recently, Eriksson and Ritchey [145] used MA to generate operational and tactical scenarios for the Swedish Military using a computer tool that automatically generates

scenarios. Thomas [152] used MA for scenario generation in the application of risk assessment associated with a commercial air transport development.

4.4 Summary of the Chapter

A scenario-based approach can provide useful insights to the stakeholders and is especially useful when it is very difficult to assume the distribution of the random variables. If one can reasonably assume the distributions of the random variables, the formulation of stochastic programming with recourse can provide not only the optimum decision that is made now under the presence of uncertainty but also the collection of optimal recourse actions after the realization of uncertainty. The philosophy of stochastic programming with recourse is intrinsically compatible with a multi-stage process of developing a baseline aircraft and then retrofitting or newly manufacturing a derivative aircraft later. To address the issue of risk-averse decision makers, the traditional stochastic programming formulation can be complemented with some sort of risk measure.

CHAPTER V

PROPOSED SOLUTION

To be able to evaluate various growth options of an aircraft under potential market, threat, and technology evolution scenarios, a new aircraft design approach is warranted. The key elements of the new approach and the underlying philosophy behind the formulation are encapsulated in the hypotheses. Then, this chapter incorporates the identified elements into an evolutionary aircraft design approach considering the lifetime evolvement of an aircraft concept from its inception.

5.1 Hypotheses

5.1.1 Two-Stage Aircraft Design (TAD) Optimization

Hypothesis 1: *An expansion of the conventional, single-stage design process into a two or multiple stage process facilitates the quantitative and simultaneous exploration of future requirement, technology, and design evolution.* (**Research Question 2**)

The current, single-stage formulation of aircraft design problem solves,

$$
\min_{\mathbf{x}} f(\mathbf{x}) \\
\text{s.t. } g_i(\mathbf{x}) \leq 0 \ (i = 1, ..., l)
\tag{14}
$$

where f is the objective function; $\mathbf{x} \in \Re^n$ is the design vector in n-dimensional space; and $g_i \ (i = 1, ..., l)$ is constraints.

Hypothesis 1 proposes that the expansion of the current, single-stage problem setting into a two-stage problem setting would allow for the integration of the future problem into the current problem. **Hypothesis 1** is mathematically represented as follows:

$$\min_{\mathbf{x}_1} f_1(\mathbf{x}_1) + Q(\mathbf{x}_1)$$
$$\text{s.t. } g_{1_i}(\mathbf{x}_1) \leq 0 \ (i = 1,...,l_1)$$

(15)

where $Q(\mathbf{x}_1)$ is the optimal value of the second-stage problem defined as

$$Q(\mathbf{x}_1) = \min_{\mathbf{x}_2} f_2(\mathbf{x}_1, \mathbf{x}_2)$$
$$\text{s.t. } g_{2_j}(\mathbf{x}_1, \mathbf{x}_2) \leq 0 \ (j = 1,...,l_2)$$

(16)

Here, $\mathbf{x}_1 \in \Re^{n_1}$ and $\mathbf{x}_2 \in \Re^{n_2}$ represent the first- and second-stage decisions in n_1 and n_2 dimensional space, respectively; f_1 is the first-stage objective function and f_2 is the second-stage objective function; g_{1i}, $i = 1,...,l_1$ is the ith constraint of the first-stage problem and g_{2i}, $i = 1,...,l_2$ is the ith constraint of the second-stage problem. $Q(\mathbf{x}_1)$, called *the second-stage value function*, is the optimal value of the second-stage problem, given a first-stage decision $\mathbf{x}_1$. To differentiate vectors from scalars, bold face was used on the vectors.

In the context of aircraft design, the so-called first stage covers the time period of a new aircraft development program, while the subsequent stages encompass the follow-on derivative, upgrade, or retrofit programs. For the derivative design (second-stage) problem, the best modification strategy is sought by solving Eq. (6) in order to minimize the second-stage objective function (f_2) for a given set of first-stage decision variables and second-stage design requirements. The second-stage value function is intended to capture the cost of future design modifications and is constructed based on the degree of

technical difficulty and the difference between the decision variable settings of the first stage and the second stage.

The mathematical formulation proposed here enables Two-stage Aircraft Design (TAD) optimization and becomes the cornerstone of stochastic optimization, scenario-based analysis, and the creation of a framework for decision-making support that is proposed in the subsequent sections.

5.1.2 Adoption of Stochastic Programming with Recourse to TAD

Hypothesis 2: *When the probability density functions of future requirements are available, the best aircraft design that responds to future uncertainties and the set of aircraft modification schemes can be found by adopting stochastic programming with recourse formulation.* (**Research Question 4**)

The new formulation proposed in **Hypothesis 1** lacks the means to account for uncertainty, which exists in dealing with future problems unless a firm contract between the two parties is committed from the beginning. **Hypothesis 2** attempts to adopt the philosophy and mathematical formulations of the stochastic programming with recourse introduced in §4.1 as a means to incorporate uncertainty. **Hypothesis 2** is mathematically represented as follows:

$$
\begin{aligned}
&\min_{\mathbf{x}_1} \; f_1(\mathbf{x}_1) + \mathbb{E}_{\omega \in \Omega}\left[Q(\mathbf{x}_1, \boldsymbol{\omega})\right] \\
&\text{s.t.} \;\; g_{1i}(\mathbf{x}_1) \leq 0 \; (i = 1, ..., l_1)
\end{aligned}
\tag{17}
$$

$Q(\mathbf{x}_1, \boldsymbol{\omega})$ is the optimal value of the second-stage problem defined as

$$Q(\mathbf{x}_1, \boldsymbol{\omega}) = \min_{\mathbf{x}_2} f_2(\boldsymbol{\omega}, \mathbf{x}_1, \mathbf{x}_2)$$

$$\text{s.t. } g_{2j}(\boldsymbol{\omega}, \mathbf{x}_1, \mathbf{x}_2) \leq 0 \ (j = 1, ..., l_2) \tag{18}$$

where $\mathbf{x}_1 \in \Re^{n_1}$ and $\mathbf{x}_2 \in \Re^{n_2}$ represent the first and second-stage decisions in n_1 and n_2 dimensional space, respectively; $\boldsymbol{\omega} \in \boldsymbol{\Omega}$ is a random vector from a probability space $(\boldsymbol{\Omega}, \mathcal{F}, P)$ with set $\boldsymbol{\Omega} \subseteq \Re^k$, a σ-algebra $\mathcal{F} \subseteq \boldsymbol{\Omega}$, and a measure P on $(\boldsymbol{\Omega}, \mathcal{F})$ such that $P(\Omega) = 1$; $Q(\mathbf{x}_1, \boldsymbol{\omega})$, called *the second-stage value function*, is the optimal value of the second-stage problem, given a first-stage decision $\mathbf{x}_1$ and random parameter realization $\boldsymbol{\omega}$.

The inherent uncertainties in the requirements for the aircraft modification programs are modeled within the random parameter vector $\boldsymbol{\omega} \in \boldsymbol{\Omega}$. Due to this presence of uncertainty, the design of a derivative is performed in a probabilistic manner, and the *expected* outcome is fed into the first-stage problem.

5.1.3 Risk-Averse Strategy Selection

Hypothesis 3: *The quantification of risk associated with the random variables using*

Value-at-Risk for the evolution options would provide a risk-averse decision maker

the option to choose a strategy with the lowest probability to exceed the cost limit.

(**Research Question 7**)

As mentioned in **Observation 6**, the conventional SPR formulation lacks the ability to account for risk-averse decision makers. As a remedy to this deficiency, **Hypothesis 3** proposes a means to quantify and mitigate the risk associated with the evolution strategies by adopting Risk-Averse Stochastic Programming introduced in §4.2. Detailed discussion on creation of evolution paths or strategies are found in §5.4.3.

While various risk measures were proposed by many researchers as reviewed in §4.2, the author proposes a formulation that uses the probability of the cost function Z exceeding a certain threshold τ as a risk measure.

$$\text{Prob}\{Z > \tau\} \tag{19}$$

This formation falls into the category of the Value-at-Risk approach and seems suitable to the acquisition of military systems, where it is often crucial to keep the cost under a certain limit. When risk measure is evaluated for all the first stage optimum solutions of the evolution strategies, the least-risky evolution strategy can be found by solving:

$$\min_p \text{Prob}\left[\{f_1 + Q((\mathbf{x}_1^*)^p, \boldsymbol{\omega})\} > \tau\right] \tag{20}$$

where $Q((\mathbf{x}_1^*)^p, \boldsymbol{\omega})$ is the optimal value of the second-stage problem for the given first-stage optimal solution $(\mathbf{x}_1^*)^p$ under strategy $p = 1, ..., n$ defined as

$$
\begin{aligned}
Q((\mathbf{x}_1^*)^p, \boldsymbol{\omega}) &= \min_{\mathbf{x}_2} f_2(\boldsymbol{\omega}, (\mathbf{x}_1^*)^p, \mathbf{x}_2) \\
\text{s.t. } & g_{2j}(\boldsymbol{\omega}, (\mathbf{x}_1^*)^p, \mathbf{x}_2) \leq 0 \; (j = 1, ..., l_2)
\end{aligned}
\tag{21}
$$

This idea, named Risk-Averse Strategy Selection (RASS), finds the best strategy p among all the strategies. It should be noted that the first-stage optimal solutions $(\mathbf{x}_1^*)^p, p = 1, ..., p_n$ are still found by following the conventional SPR formulations.

5.1.4 Deterministic Scenario-Based TAD Optimization

Hypothesis 4: *Scenario-based analysis along with two-stage aircraft design optimization would allow the decision makers to investigate a wide spectrum of uncertainties deterministically to gain insight while avoiding the biases from inaccurate probability distributions.* (**Research Question 8**)

In the cases where an accurate and reliable prediction of the random variable is infeasible or a large number of random variables with high volatility and complicated correlation structure make the nature of random space very complex, pursing the stochastic two-stage aircraft design approach as proposed by **Hypothesis 2** and **Hypothesis 3** is not only difficult but also impractical.

Even though the issue of acquiring reasonable definition of the random variable is put aside for a moment, the idea of investigating and incorporating all the random space as in the stochastic programming approach can be too time-consuming and can overwhelm the decision makers with too much information. For instance, while the stochastic approach yields the first-stage optimum solution as a point-solution, it also yields myriads of second-stage design upgrade schemes. A large number of second-stage solutions, when they are produced by randomly sampled scenarios, can be very difficult for a human decision maker to interpret and can be meaningless. Instead, scenario analysis with only a handful of well-organized scenarios can provide much more insight with less computational effort.

In order to achieve the goal, first, the set of scenarios $\boldsymbol{\omega}_u, u = 1, \ldots, u_n$ are identified. With each of the scenarios, the deterministic, two-stage aircraft design optimization are solved repeatedly.

$$
\begin{aligned}
&\text{for } \forall u = 1, \ldots, u_n, \ \min_{\mathbf{x}_1} f_1(\mathbf{x}_1) + Q(\mathbf{x}_1, \boldsymbol{\omega}_u) \\
&\text{s.t. } g_{1i}(\mathbf{x}_1) \leq 0 \ (i = 1, \ldots, l_1)
\end{aligned}
\tag{22}
$$

where $Q(\mathbf{x}_1, \boldsymbol{\omega})$ is the optimal value of the second-stage problem defined as

$$Q(\mathbf{x}_1, \boldsymbol{\omega}_u) = \min_{\mathbf{x}_2} f_2(\boldsymbol{\omega}_u, \mathbf{x}_1, \mathbf{x}_2)$$

$$\text{s.t. } g_{2j}(\boldsymbol{\omega}_u, \mathbf{x}_1, \mathbf{x}_2) \leq 0 \ (j = 1, ..., l_2) \tag{23}$$

Then, u_n first-stage optimum solutions are gained for each corresponding prediction scenario, $(\mathbf{x}_1^*)^u, u = 1, ..., u_n$. Then, on top of these u_n Here-and-Now (HN) solutions, the second-stage optimization is solved again for each of the realized scenarios.

$$\text{for } \forall s, u : \min_{\mathbf{x}_2} f_2(\hat{\boldsymbol{\omega}}_s, (\mathbf{x}_1^*)^u, \mathbf{x}_2)$$

$$\text{s.t. } g_{2j}(\hat{\boldsymbol{\omega}}_s, (\mathbf{x}_1^*)^u, \mathbf{x}_2) \leq 0 \ (j = 1, ..., l_2) \tag{24}$$

where $\hat{\boldsymbol{\omega}}_s, s = 1, ..., s_n$ is the realized scenario. The result is $u_n \times s_n$ Wait-and-See (WS) solutions, $(\hat{\mathbf{x}}_2^*)_s^u, u = 1, ..., u_n, s = 1, ..., s_n$. If $u_n = s_n = 5$ for example, five first-stage solutions and twenty-five second-stage solutions are obtained. Along with these 5 HN designs and 25 WS designs, the aircraft attribute, such as performance or cost, evaluated at the optimum points, i.e.

$$(\mathbf{g}_1^*)^u, u = 1, ..., u_n, (\hat{\mathbf{g}}_2^*)_s^u, u = 1, ..., u_n, s = 1, ..., s_n$$

and

$$(f_1^*)^u, u = 1, ..., u_n, (\hat{f}_2^*)_s^u, u = 1, ..., u_n, s = 1, ..., s_n$$

Making comparisons with this set of designs and vehicle attributes often reveals important inequalities and equalities among the designs and vehicle attributes. The design can be visualized in the form of bar graphs to reveal the patterns without overwhelming the decision maker.

5.1.5 Framework for Two-Stage Design Space Exploration

Hypothesis 5: *A flexible and interactive tool built on the two-stage aircraft design formulation would allow the decision makers to effectively and concurrently explore the two-stage design space, evaluate evolution strategies, change assumptions, simulate scenarios, and thus make strategic decisions with a greater degree of freedom.* (**Research Question 9**)

The formulations proposed in **Hypothesis 2**, **Hypothesis 3**, and **Hypothesis 4** involve optimization loops. When the optimum solutions could be the most valuable information to the decision makers and engineers, they are simply point solutions that are only optimal under strict assumptions and scenarios. In the case in which uncertainty cannot be predicted reasonably, those point solutions can become meaningless when unexpected events occur. Another drawback of optimization is that all the constraints are treated as hard constraints and are strictly enforced. In reality, aerospace systems design problems often accept less than satisfactory performance for the sake of cost and/or schedule savings. More importantly, stochastic and deterministic optimizations solve a single objective rather than multiple objectives, lacking the capability of accounting for the possibility of conflicting interests between multiple stakeholders and entities. Finally, treating technology integration as a design variable can make optimization very difficult since technology combinations are inevitably discrete.

To quantitatively evaluate the vehicle growth options free from the restrictions listed above, a non-optimization approach is warranted. The goal becomes the creation of tools with which stakeholders can change the assumptions, apply the scenarios, and trade-off various requirements and figures of merit. It is envisioned that this goal will be

achieved by the use of an interactive, visual framework built based on the TAD environment. The framework(s) should be interactive—allowing almost instantaneous feedback to the decision-maker—and adequately visual for high-level decision makers to navigate various evolution scenarios and make strategic decisions. The framework should also allow every variable beyond the design variable $\mathbf{x}$ to be treated as an independent variable.

5.2 Synthesis of a New Method

Implementation of the proposed tasks into an actual aircraft design exercise requires recasting the aircraft design problem into the (f, $\mathbf{g}$, $\mathbf{x}$, $\boldsymbol{\omega}$) formulations. A comprehensive design methodology was formulated by adopting the elements that are found in the conventional engineering design process. The method, Evaluation of Lifelong Vehicle Evolution (EvoLVE), was initially constructed as a five-step process [118] in 2007 and has evolved into its current form. The EvoLVE method illustrated in Figure 21 consists of nine major steps. While the specifics of these steps are presented in the subsequent sections, they can be viewed as an expansion of the four-step engineering design process reviewed in §2.2.1. The first two steps are a two-stage problem definition, followed by a synthesis of solutions in the third and fourth steps. The fifth and sixth steps are modeling and simulation. The last three steps offer three different ways to explore the two-stage design space and make a decision. Steps 1, 3, and 5 are essentially identical to the first three steps of the conventional engineering design process by Suh and others in Figure 12. These three steps are shown in green outline to differentiate them from other steps created by the author.
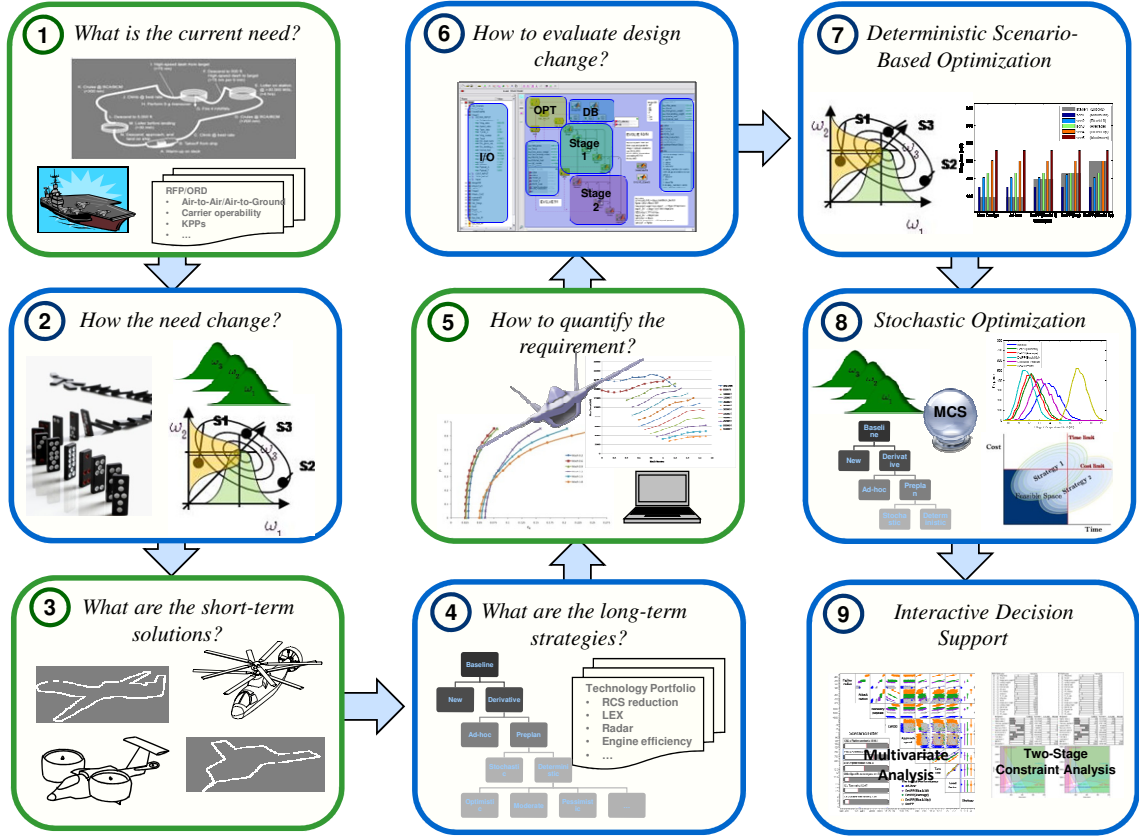
Figure 21: Overview of the EvoLVE Method

5.3 Present and Future Requirements: Steps 1-2

> The important thing [for a designer] to learn is that the ability to define the problem is the most important and difficult task in engineering.
>
> Nam P. Suh in *Principle of Design* [38]

The goal of the first two steps of the method is to identify what the customer wants now and in the future. These two steps define the set of requirements that are further arranged as objective functions, constraints, and risk measures for both the first- and second-stage design optimization. The definition of these elements in the future time frame inevitably introduces uncertainty. Therefore, future requirements take the form of random variables, probability measures, and scenarios.

5.3.1 The First-Stage Requirement

The first step of EvoLVE identifies the requirement for the current development program, or the first-stage requirement. The first-stage requirement defines what capability has to be built into the baseline system. The need for a new aircraft can be solicited in the form of a request for proposal (RFP) and made concrete in an operational requirement document (ORD). The requirements are often given as measures of effectiveness (MoE) and key performance parameters (KPPs), along with the mission profiles. Key performance parameters are defined below:

> Key performance parameters are capabilities or characteristics that the Joint Requirements Oversight Council designates as so significant that failure to meet the threshold value can cause the concept or system selected to be reevaluated or the program to be reassessed or terminated [153].

The KPPs constitute the first-stage constraint vector, $\mathbf{g}_1$ by definition.

MoEs provide a set of comprehensive goodness measures to evaluate a military system in terms of performance, cost, and program schedule. For a military system acquisition, MoEs are defined before the Milestone I review in order to provide justification to pursue a new military system. The Department of Defense defines MoEs as "a qualitative or quantitative measure of a system's performance or a characteristic that indicates the degree to which it performs the task or meets a requirement under specified conditions [154]." To give an example, the F/A-18E/F program's MoEs included: survivability/vulnerability, unit cost, strike mission radius, carrier suitability, fighter performance (such as turn rate, climb rate, and excess power), weapons system features, and armament flexibility [83]. Since the KPPs of the F/A-18E/F program included mission radius, carrier suitability, and fighter performance, the MoEs largely overlap with KPPs but are broader in scope.

In the absence of a concrete problem definition from the customer, the present or short-term need is identified by using system engineering methods, such as market analysis, QFD, operational analysis, etc. The QFD analysis introduced in §2.2.1 includes a proven method to translate the "voice of customers" to the "voice of engineers", which includes the aircraft system level requirements and relative importance rating.

Another question that must be answered in this step is "what does the customer want to avoid?" While customers have a clear goal to achieve, such as maximizing the net present value, maximizing the mission effectiveness, etc., they also have guidelines on what must be avoided in the worst-case scenario. The answer to this question would define the risk measure of the customer.

The outcome of Step 1 constructs objective f_1, constraints $\mathbf{g}_1$, and the risk measures that are used in later steps.

5.3.2 Evolution of the First-Stage Requirement

Step 2 solicits the long-term customer needs and translates them into the second-stage requirement. This step begins by taking the first-stage requirement and projecting it into the future time frame. It is important to define the scope in terms of time frame and degree of evolution of the requirement before such projection is made.

5.3.2.1 Emerging Needs and Time Frame

The time frame should be determined by asking when the variant or the derivative of the baseline aircraft is needed. For an acquisition program that follows the EA process, the customer is supposed to provide the timeline of the capability increments. Otherwise, the need for an upgrade is initiated by the events that affect what and how the baseline system should perform. For example, a new legislation requires 20% reduction of the

greenhouse gases by 2020. The a fighter/attack aircraft is expected to extend its mission spectrum in 2015 to cover the Close-Air-Support (CAS) role after the scheduled retirement of the aircraft or rotorcraft that currently performs the mission. These two scenarios would give a clear timeline as to when the baseline has to be upgraded either to maintain its competitiveness or to expand its market share. The time frame can be as far as the customer wants to consider, but about twenty years down the road would be the furthest future in a practical sense. On the other hand, the time frame can be as near as zero years if the second-stage program is concurrent to the first-stage program as in the case of the development of the Marine and the Navy variants of the F-35.

The scope of the problem is also bounded by determining what new capability, role, regulation, etc. are introduced on top of the first-stage requirement. For example, it is common that a military aircraft developed originally for an air-to-air role expands its capability to include air-to-ground, electronic warfare, etc., as the history of the F/A-18, F-16, and F-15 show. Commercial air transports are often customized as an extended-range version, a special cargo version, an executive or Presidential version, etc. When such capability expansion is considered in this step, it is important to bind the problem to only include "evolutionary" upgrades and avoid "disruptive" changes. For example, converting a subsonic air transport into a supersonic air transport is not practical. A supersonic fighter is not likely to be upgraded to have the VTOL capability unless such provision was embedded from the beginning.

Introduction of new missions brings in new elements to the baseline requirement set. For example, if a fighter developed for the Air Force is modified to have aircraft carrier capability, a series of carrier suitability requirements are added to form the new

requirement set. It is likely that the commercial jets in the future will be subject to stringent noise and emission regulations.

5.3.2.2 *Random Variables and Probability Measures*

Among the elements of the second-stage requirement, those that are likely to grow and those that are likely to remain constant at the current level are divided. Examination of the aircraft evolution trends of the class similar to the ones in CHAPTER III can provide insight into this process. For example, requirements on payload, range, and avionics weight are likely to increase. Especially, the modern trend is to constantly improve the electronic warfare suite, which in turn demands higher cooling and electrical power generation capacity. On the other hand, physical constraints, such as take-off field length, approach speed, and load factor are among the constraints that are not likely to change over time. Recent trends in fighter aircraft also show that the importance of stealthiness and radar power are increasing, while point performance requirements that were important during dog fighting decades ago, such as speed, turn rate, and excess power are becoming less critical to mission success.

Among the requirements that are likely to change over time, only those judged to be important and hard to predict with certainty are identified as random variables. Importance is judged by the sensitivity of the system level vehicle attributes to the change of the requirement. In general, if a new requirement can be fulfilled without affecting the vehicles' weight or drag, its impact to the system-level vehicle attribute would be minimal and thus unimportant.

The second criterion is the predictability of the requirement growth. The designer knows the future requirement with certainty if the customer specifies the growth of a

requirement from the beginning. For example, the customer places an order of 100 aircraft flying 1,000 nm at the cruise speed of Mach 0.8 carrying 200 passengers with a commitment of another 50 aircraft flying 1,200 nm at Mach 0.8 carrying 230 passengers, as an extended range variant. In another case, the same aircraft manufacturer gets an order of 100 aircraft flying 1,000 nm at Mach 0.8 with 200 passengers. This time the manufacturer does not have any other orders from other airlines, but it plans stretched version(s) in order to increase market capture. All three elements—range, speed, and number of passengers—significantly affect the attributes of the aircraft and are thus important. However, it is anticipated that the cruise speed would not increase, as the historical trend of commercial jets reveals. Then, the two remaining requirements—range and number of passengers—are random variables.

As the next step, the identified random variables have their values defined in the form of probability density functions (PDFs) or probability mass functions (PMFs). The full definition of the future requirement in probability space can be obtained by soliciting the potential customers, e.g. airlines. Conducting a market analysis of the past years and projecting it to the future would also identify the need for a particular class of airplanes. The Boeing Company's annual *Current Market Outlook* [155] forecasts the global commercial transport market up to 20 years from their study. Airbus also publishes *Global Market Forecast* [156] covering a 20-year time span. Alternatively, air vehicle level requirements may come from a System-of-Systems (SoS) level study involving all major aircraft manufacturers and airliners. A Monte Carlo study at the SoS level would provide probability distributions of air vehicle level attributes.

5.3.2.3   Scenario Development

The final task of **Step 2** is to capture the requirement uncertainty in the form of discrete
scenarios. In the case where probability distributions are not available or the cost of
pursuing a stochastic solution is prohibitive, the option of scenario-based analysis (**Step
7**) can be selected. This option requires at least two or more scenarios that capture the
probability space. The scenario generation starts from the higher hierarchical levels than
the level the design exercise is played in. At the higher hierarchical level, the source of
uncertainty is identified first. In the case of military aircraft, uncertainty comes from
changes in threat, theater, competition, politics, technology, regulation/deregulation, and
so forth. For each of the uncertainty sources, you may ask the relevant questions that
affect the current aircraft development most within the interested time frame. For
example,

- *Will the third world countries acquire air power that poses a threat to U.S. air
  power?*
- *Will Lockheed Martin win the second phase contract?*
- *Will the next administration cancel or truncate the program?*
- *Will the Royal Navy buy the aircraft? How many?*
- *If the Marine's new attack helicopter program is approved, will they purchase 300
  units of the Marine variant of the attack aircraft as promised?*
- *Will the current fighter program pass Milestone III and move on to FSD?*
- *Will the economic growth of the U.S. and the defense budget be maintained?*
- *Will a robot replace human pilots?*
- Will the delivery of the Navy variant of JSF be delayed?

Each of the questions constitutes a macro-level scenario. Then, the scenarios are mapped
into the set of aircraft system level parameters. For example, the question regarding the
Royal Navy purchase will affect the production quantity, weapons payload, the WOD
requirement, the bring back capability, etc. At the same time, the delay of JSF can

affect the production quantity as well as the mission coverage, which subsequently affects mission radius, radar range, etc. The scenario of emergent threats may require a Navy fighter with a better stand-off, which means a more powerful active radar, the Phoenix missile capability, etc. The mapping process can be done by a team of subject-matter experts using techniques such as QFD, expert polls, and brainstorming.

It is important to iterate the scenario generation process and only leave the important and meaningful ones. While no scientific rule prescribes how many scenarios are selected, at least three scenarios are recommended, for example, most probable, worst case, and best case. For example, the Joint Planning and Development Office (JPDO) studied the next generation air transportation system under three scenarios: the baseline air traffic demand scenario by FAA, the FAA scenario plus two times the growth rate, and the scenario of a shift to smaller aircraft and smaller airports [157].

The outcome of **Step 2** is the random variable vector ω and its definitions in the form of either or both the PDFs and the scenarios.

5.4 Baseline Platform, Technologies and Evolution

Strategies: Steps 3-4

Once the current and future problems are defined in **Steps 1** and **2**, the candidate solutions to respond to the needs are synthesized in **Steps 3** and **4. Step 3** down-selects a baseline platform(s) that has the greatest potential to meet the first and second-stage requirements. **Step 4** synthesizes the possible ways to respond to the evolving requirements. This step identifies the list of potential upgrade elements including

addition of new subsystems, features, and technologies. Another task in this step is to plan for the long-term development options or the evolution strategies.

5.4.1   The Baseline Platform

Step 3 synthesizes a large number of solution candidates and down-selects a baseline platform(s) with the greatest potential to meet the current and future requirements with the least cost for further evaluation. While engineering judgment is important to trim the alternative concept space and down select one or a few platforms as a baseline(s), the modern system engineering tools presented in §2.2.1 can be of use in this step. A particularly useful tool here is the morphological analysis [30], in which the required functions are decomposed, the alternative options for each said function are listed in the physical domain, and innovative concepts are identified through the recomposition process. Candidates for near-term technology substitution are also identified in this step.

The identified fusion of concept and technology can be qualitatively and quantitatively assessed using decision-making tools, such as the Pugh matrix [22] and Technique for Order Preference by Similarity to Ideal Solution (TOPSIS) [158]. Also, recently formulated qualitative tools, such as the Interactive Reconfigurable Matrix of Alternatives (IRMA) [159] or Qualitative Interactive Evaluation Tool (QuIET) [160], could prove to be useful in this step, as both are comprehensive tools containing elements of QFD, Morphological Analysis, TOPSIS, TRL, etc. The evaluation criteria for the assessment are available from **Step 1**.

The outcome of **Step 3** is the baseline platform, design space, and the near-term technology. The design space is defined by the vector of the first-stage design variables $\mathbf{x}_1$, along with the lower limit $\mathbf{x}_1^l$, and the upper limit $\mathbf{x}_1^u$. The design space should be

large enough to enclose designs that meet both the first- and second-stage requirements and should be refined at later steps as the modeling and simulation environment is created.

5.4.2 Upgrade Options and Long-Term Technology

For the given baseline platform identified in **Step 3, Step 4** synthesizes all the possible strategies brought about to effectively respond to the situations requirement evolution. Contemplation of the long-term solution would start by answering following two questions: what needs to be changed from the baseline aircraft and how can such a change be implemented? The first question is to identify the list of technical means to meet the second-stage requirement. The second question is to come up with managerial plans to implement capability upgrades, for example, either by retrofitting existing aircraft, producing variants, designing new airplanes, etc. The managerial alternatives in capability upgrade are called *evolution strategies* in this document and are further discussed in the next section.

An answer to the first question would identify the specific elements of upgrade, including the addition of new subsystems, features, and technologies. For example, based on the first-stage design, one can increase wing area, insert fuselage plugs, install external fuel tanks, enlarge vertical or horizontal tails, upgrade high-lift-device, increase engine thrust, increase engine efficiency, etc. Here, long-term technology candidates depending on the given time frame, technology maturity, and risk tolerance are identified as well. NASA's TRL is a technology maturity measure with a 1 to 9 scale

[161]. While **Step 3** only considers the technologies with high TRLs[*], **Step 4** might include the technologies with lower TRLs.

Mathematically, the outcome of **Step 4** is the new design variable vector $\mathbf{x}_2$. Sometimes, insertion of new technology cannot be modeled by continuous perturbation of the design variables. In such a case, it is necessary to add discrete variables to the second-stage design variable set $\mathbf{x}_2$. A mix of both continuous and discrete variables makes design space exploration and optimization very difficult.

5.4.3 Evolution Strategies

Another important task of **Step 4** is the managerial plan to effectively respond to the situations brought about by requirement evolution. Contemplation of the long-term strategy as to how design evolution will be implemented would start by answering following questions:

1. Do I upgrade the first-stage design or start from scratch?

2. (If upgrade,) Do I preplan for the future design from the beginning or solely focus on the first-stage requirement?

3. (If preplan,) Do I integrate future requirements deterministically or stochastically?

4. (If deterministically preplan,) Under which scenario do I preplan?

Answering the first question divides the second-stage program into either a new aircraft development program or a derivative aircraft development program. Once the

---

[*]In the conceptual design phase, integration of technologies with technology readiness level 6 or higher is typically considered for a new aircraft, according to Mark Alber, Section Chief of Advanced Concept at Sikorsky Aircraft, Stratford, Connecticut. [Interviewed on April 26, 2007, by the author]
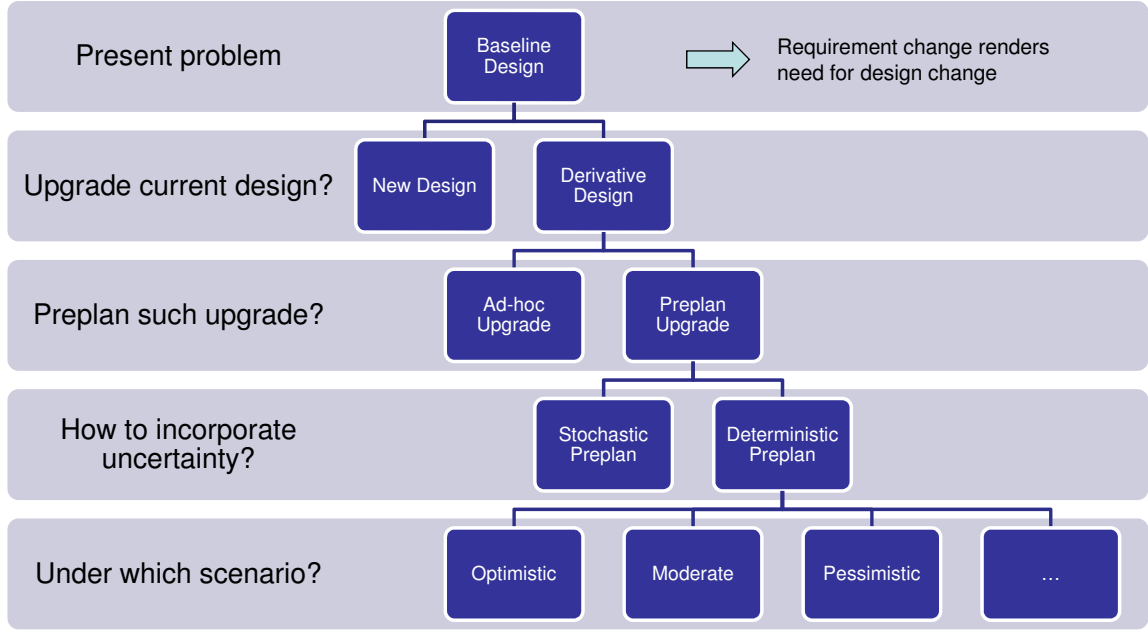
Figure 22: Taxonomy of Evolution Path

path of modifying the existing design is chosen, the path is further divided depending on whether such an upgrade is considered from the beginning of the first stage or not. Then, the option of preplanning future improvements from the beginning can be done either deterministically or stochastically, depending on how uncertainty is modeled and incorporated. Finally, since the path of deterministic preplanning requires selection of one particular scenario in the beginning, the maximum number of possible options is equal to the number of scenarios generated in **Step 2**. For example, in the case of the 200 passenger commercial transport example, up to three deterministic preplanning options can be generated by assigning the scenarios S_1, S_2, and S_3 to each of the options. Figure 22 shows a taxonomy of the vehicle evolution paths one can consider at the second stage, along with the criteria dividing the paths.

For the strategies falling under the derivative aircraft development track, the vehicle platform for the second stage should be held constant with the first stage since it is unreasonable to perceive a cross-platform jump as an evolutionary progression. However,

the new aircraft design option is free from this restriction, and any other platforms to serve the second-stage requirements best can be considered. Along with the evolution paths, the set of technologies that are applicable to the baseline platform is identified in this step. The subsequent sections discuss the options in detail along with corresponding design structure matrices (DSMs) and mathematical representations.

5.4.3.1 The New-Design Strategy

The first path of developing a new aircraft in the second stage, named as the New-Design (ND) strategy, sets up the first and second-stage problems completely independent to each other. In the first stage, an optimal design $\mathbf{x}_1^*$ is sought by minimizing f_1.

$$\min_{\mathbf{x}_1} f_1(\mathbf{x}_1)$$
$$\text{s.t. } g_{1i}(\mathbf{x}_1) \leq 0 \ (i = 1,...,l_1) \tag{25}$$

Then, later when changes in requirement call for a new design, a new optimization problem is solved.

$$\min_{\mathbf{x}_2} f_2(\mathbf{x}_2)$$
$$\text{s.t. } g_{2j}(\mathbf{x}_2) \leq 0 \ (j = 1,...,l_2) \tag{26}$$

Since the second-stage design is independent to the first-stage design, $\mathbf{x}_1$ does not affect the second stage. An example of pursuing this strategy would be using the F/A-18 for the first stage, then later purchasing the F-14, F-35, etc, instead of upgrading it.

Figure 23 is the DSM of the ND strategy. The boxes labeled "Stage 1" and "Stage 2" represent the contributing analyses that calculate f and $\mathbf{g}$ based on $\mathbf{x}$ for each strategy. Each stage is linked to an optimizer. The arrows between the boxes indicate
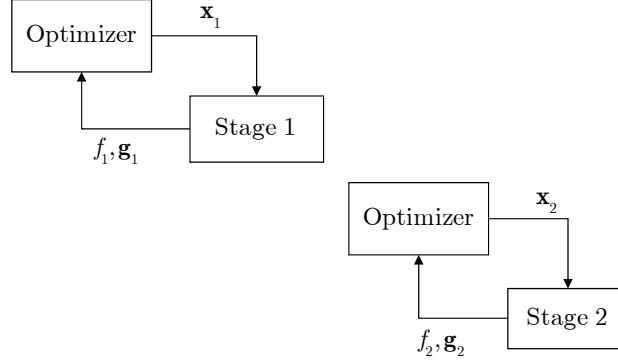
Figure 23: The New-Design Strategy

the direction of data flow. No arrows between the first- and second-stage problem shows that no data is exchanged between the two problems.

In order to assess the computational cost of pursuing the ND strategy, assume that the number of function calls in solving the stage 1 and stage 2 are n_1 and n_2 respectively. Then, the total number of function evaluations solving the entire problem is simply n_1 plus n_2. This number is compared to the computational cost of other strategies later. Inclusion of the ND strategy in the study provides a comparison point against which one of the worst derivative design strategies is compared to see to what extent introducing a derivative model would be cheaper than starting from scratch.

5.4.3.2   The Ad-hoc Upgrade Strategy

The option of introducing a derivative design in the second stage without preplanning was named the Ad-Hoc (AH) Strategy. As with the ND strategy, in the first stage, the design practice is to ensure the best design for the current, first-stage requirements by solving Eq. (25) with the AH strategy. No growth provision is considered or incorporated to the first-stage design x_1. Compared to the ND strategy, however, after the second-stage requirement is concretely defined, the AH strategy seeks the most effective way to
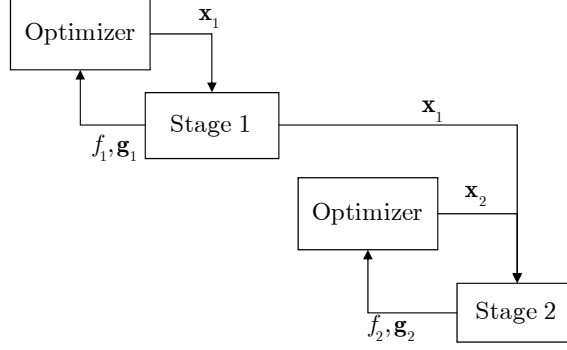
Figure 24: The Ad-Hoc Upgrade Strategy

modify the first-stage design to meet the new requirement rather than starting from scratch in the second stage by solving:

$$
\begin{aligned}
&\min_{\mathbf{x}_2} f_2(\mathbf{x}_1, \mathbf{x}_2) \\
&\text{s.t.} \ \ g_{2j}(\mathbf{x}_1, \mathbf{x}_2) \le 0 \ (j = 1, ..., l_2)
\end{aligned}
\tag{27}
$$

The objective function of the second-stage problem, f_2, either implicitly or explicitly includes the cost of modifying the design from the original state with other cost measures. In the case of aircraft acquisition, the cost of modifying an existing design is implicitly included in the RDT&E cost.

Figure 24 shows the difference of the AH strategy from the ND strategy, having a feed-forward loop from the stage 1 to stage 2 problem. Since the second-stage optimization is solved *after* the second-stage problem is defined, the total number of function evaluation is still in the order of n_1 plus n_2.

5.4.3.3 Deterministic Preplanning Strategy

Moving on to preplanning strategies, growth provisions are now considered in the first-stage design in order to reduce the cost of design modification in the second stage. Therefore the preplanning strategies must deal with the *uncertain* future requirements from the beginning. Depending on the way uncertainty is modeled and incorporated, the

preplanning strategies are classified into the Deterministic Preplanning (DetPP) strategy and the Stochastic Preplanning (StoPP) strategy. A DetPP solves a deterministic problem by selecting a future scenario among the discrete scenarios identified in **Step 2**. With a selected scenario $\boldsymbol{\omega}_u$, a DetPP performs the *"what-if"* study by solving a deterministic optimization given as

$$\min_{\mathbf{x}_1} f_1(\mathbf{x}_1) + Q(\mathbf{x}_1, \boldsymbol{\omega}_u)$$
$$\text{s.t. } g_{1i}(\mathbf{x}_1) \leq 0 \ (i = 1, ..., l_1)$$
(28)

where $Q(\mathbf{x}_1, \boldsymbol{\omega}_u)$ is the optimal value of the second-stage problem defined as

$$Q(\mathbf{x}_1, \boldsymbol{\omega}_u) = \min_{\mathbf{x}_2} f_2(\boldsymbol{\omega}_u, \mathbf{x}_1, \mathbf{x}_2)$$
$$\text{s.t. } g_{2j}(\boldsymbol{\omega}_u, \mathbf{x}_1, \mathbf{x}_2) \leq 0 \ (j = 1, ..., l_2)$$
(29)

The difference from the non-preplanning strategies, i.e. ND and AH, is that the first-stage optimization includes the cost function of the second stage so that it balances the cost of over-designing and upgrading. One important note is that since the second-stage optimization given in Eq (29) is based on the *predicted* second-stage requirement $\boldsymbol{\omega}_u$, after the actual second-stage requirement is revealed, the optimization must be resolved by solving:

$$\text{for } \forall k, \ \min_{\mathbf{x}_2} f_2(\hat{\boldsymbol{\omega}}_s, \mathbf{x}_1^*, \mathbf{x}_2)$$
$$\text{s.t. } g_{2j}(\hat{\boldsymbol{\omega}}_s, \mathbf{x}_1^*, \mathbf{x}_2) \leq 0 \ (j = 1, ..., l_2)$$
(30)

where $\hat{\boldsymbol{\omega}}_s$ is the realized scenario.

The DSM of DetPP in Figure 25 has a feedback loop from the second stage to the first stage, making the two problems interdependent. The feedback loop informs the
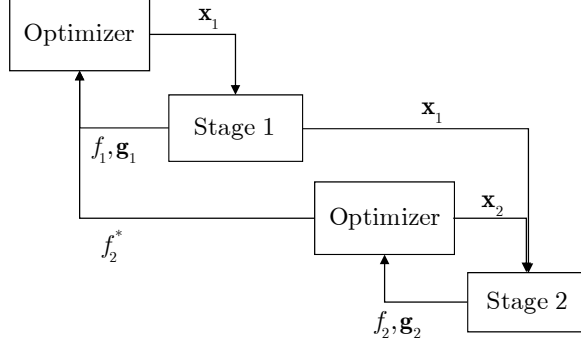
Figure 25: The Deterministic Preplanning Strategy

minimum second-stage cost f_2^* for a given first-stage design $\mathbf{x}_1$, and thus considerably increases the number of function evaluations to roughly in the order of n_1 times n_2.

The two-level optimization structure apparent from the DSM suggests the potential of utilizing some of the bi- or multi-level multidisciplinary design optimization (MDO) techniques in order to improve the efficiency of the optimization process. The MDO techniques, such as All-At-Once (AAO), Bi-Level Integrated System Synthesis (BLISS) [162], and Collaborative Optimization (CO) [163, 164] have been introduced and used in the community of MDO recently and proved their usefulness in aerospace design [165-168]. It seems that the problem structure of a deterministic preplanning strategy is compatible to all these methods. Therefore, it would be worth investigating such techniques in order to reduce the computational cost while maintaining efficiency.

Hypothesis 6: *Some bi-level MDO techniques are compatible to two-stage aircraft design optimization and potentially reduce the computational cost.*

5.4.3.4   *Stochastic Preplanning Strategy*

The StoPP deals with uncertainty by considering *all* combinations of the random variable realization, rather than just *one* combination as the deterministic counterpart

does. With all possible outcomes, the second-stage optimization problem is solved, and the average second-stage cost or the expectation is added to the first-stage objective function.

$$\min_{\mathbf{x}_1} \ f_1(\mathbf{x}_1) + \mathbb{E}_{\omega \in \Omega}\left[Q(\mathbf{x}_1, \omega)\right]$$
$$\text{s.t.} \ \ g_{1_i}(\mathbf{x}_1) \leq 0 \ (i = 1, ..., l_1)$$

(31)

where $Q(\mathbf{x}_1, \omega)$ is the optimal value of the second-stage problem defined as

$$Q(\mathbf{x}_1, \omega) = \min_{\mathbf{x}_2} \ f_2(\omega, \mathbf{x}_1, \mathbf{x}_2)$$
$$\text{s.t.} \ \ g_{2_j}(\omega, \mathbf{x}_1, \mathbf{x}_2) \leq 0 \ (j = 1, ..., l_2)$$

(32)

Again, for the given first-stage optimal solution $\mathbf{x}_1^*$ the second-stage problem is resolved after the realization of the random variables by solving

$$\min_{\mathbf{x}_2} \ f_2(\hat{\omega}, \mathbf{x}_1^*, \mathbf{x}_2)$$
$$\text{s.t.} \ \ g_{2_j}(\hat{\omega}, \mathbf{x}_1^*, \mathbf{x}_2) \leq 0 \ (j = 1, ..., l_2)$$

(33)

where $\hat{\omega}$ is the realized scenario.
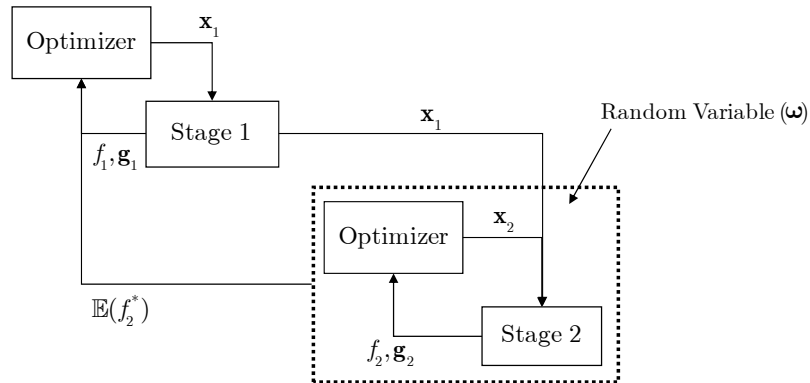
Figure 26: The Stochastic Preplanning Strategy

Comparison between the DSMs of deterministic and stochastic approaches (Figure 26) shows that the only difference between the two approaches is whether the first-stage optimization minimizes f_1 plus f_2^* or f_1 plus the *expectation* of f_2^*. This seemingly simple change inflicts enormous computational burden. Indeed, the expectation operation increases the number of second-stage function evaluations exponentially, making the StoPP very expensive to pursue. For example, if the number of random variables is d and each of them takes K number of scenarios (assuming finite outcomes), the total number of scenarios is K^d. The total number of function evaluations required to solve Eqs. (10) and (11) significantly depends on which solution technique is used and the desired accuracy of the integration or expectation operation, but it is roughly in the order of n_1 times n_2 times K^d.

5.5 Modeling and Simulation: Steps 5 and 6

Modeling and simulation is a process to develop a computer model that repeatedly quantifies the objective f and constraints $\mathbf{g}$ as a function of the design parameters $\mathbf{x}$. EvoLVE establishes the modeling and simulation in two following separate steps.

5.5.1 Conventional Modeling and Simulation

Step 5 is not different from the M&S process of conventional single-stage design processes. Therefore, this step involves collection, creation, and validation of physical relationships or analysis codes, by which the identified requirements are quantified in terms of the design variables and design parameters. The end product of **Step 5** is a validated computer model that evaluates f_1 and $\mathbf{g}_1$ for any design points in the design space $[\mathbf{x}_1^l, \mathbf{x}_1^u]$.

$$\mathbf{x}_1 \rightarrow \boxed{\text{Model}} \rightarrow f_1 \text{ and } \mathbf{g}_1 \tag{34}$$

Since such a model is required to pursue the conventional single-stage design, the organization might have a model already in hand. Then, **Step 5** can be skipped.

5.5.2 Scaling Laws and Upgrade Cost

While the model of the baseline vehicle established in **Step 5** should be adequate for a conventional single-stage design, expansion of the problem into two stages in EvoLVE also requires expansion of the model accordingly. **Step 6** prepares a model that maps the second-stage design variables to objectives and constraints.

$$\mathbf{x}_1 \text{ and } \mathbf{x}_2 \rightarrow \boxed{\text{Model}'} \rightarrow f_2 \text{ and } \mathbf{g}_2 \tag{35}$$

If the second-stage requirement calls for a new platform different from the first-stage vehicle, a new model is developed and validated as it was done in **Step 5**. Otherwise, the model developed in **Step 5** can be reused in **Step 6** with modifications.

First of all, to be able to provide feasible solutions after incorporation of the second-stage requirement, the first-stage design space $[\mathbf{x}_1^l, \mathbf{x}_1^u]$ needs to be expanded in terms of the number of design variables and the ranges of each design variable. This is not a trivial task because the functional relationship from $\mathbf{x}$ to $\mathbf{g}$ and f that was defined in **Step 5** may not be valid anymore. Incorporation of the second-stage requirement to the first-stage problem may require inclusion of some more design variables. Consider, for instance, the original requirement for a bomber that specifies a subsonic cruise speed and then the second-stage requirement demands a cruise speed in a high transonic regime. The change in the cruise speed requirement would add the consideration of wave drag in

the second stage. Then, the feedback loop from the second stage to the first stage makes it necessary to include the new design variables to calculate and reduce wave drag.

In traditional design practice, the design space is relatively small. Activities during design space exploration, such as sensitivity studies, trade-off studies, etc. involve a small perturbation of the design variables from the baseline within the range where the validated model remains valid. However, as the range of design change is much larger in EvoLVE than in a single-stage design practice, using the model validated at the baseline point can lead to erroneous results. Therefore, in **Step 6**, the scaling laws that capture the physical growth of the vehicle are developed and validated.

Another central task of **Step 6** is to develop a model that quantifies the cost of design modifications from one stage to the next. The cost of engine replacements, rating-up transmissions, integrating new avionics suites, etc. must be available in the same currency as the first-stage objective. The cost model should include the cost of integrating the technologies identified in **Step 4**.

5.5.3 Creation of a Two-Stage Aircraft Design Environment

Once the first-stage model is expanded to cover second-stage designs, and the second-stage model including the cost to change the first-stage design to the second-stage design is created and validated, the models are linked together to enable automatic execution. While the software architecture such an integrated M&S is built upon should not matter, it is required that the created M&S environment be also amenable to automatic execution and surrogate modeling, as the following steps are expected to require a significant computational overhead. The integrated modeling and simulation tool is named as the *Two-stage Aircraft Design* (TAD) environment in this text.

$$\mathbf{x}_1 \text{ and } \mathbf{x}_2 \rightarrow \boxed{\text{TAD}} \rightarrow f_1, \mathbf{g}_1, f_2, \text{ and } \mathbf{g}_2 \tag{36}$$

5.5.4 Surrogate Modeling and Challenges

To facilitate rapid evaluation of a plethora of design alternatives the creation of surrogate models is often necessary. To what level and with which modeling method depend on the problem in hand. With a given problem, one must consider the balance between the level of accuracy and the computational time available. For example, if one chooses to pursue the stochastic preplanning strategy, one should pre-estimate the computational cost of pursuing such strategy before attempting to solve it. As shown in Figure 26, solving SPR requires second-stage optimization whenever the global optimizer calls the second stage. Moreover, each second-stage function call requires a Monte Carlo simulation within the second stage. Assuming each second-stage optimization takes one minute to get f_2^*, ten thousand MCS runs are performed to calculate expectation $\mathbb{E}(f_2^*)$, and a first-stage optimization requires one hundred second-stage function evaluations, then the total second-stage function call requires 10^7 minutes or about nineteen years. In such a case, it would be practical to fit a surrogate model of f_2^*.

Once the extent to which surrogate models would replace actual models is known, a proper sampling technique(s) and surrogate modeling technique(s) are selected. Surrogate modeling methods, such as response surface methods (RSM) and Artificial Neural Networks (ANNs) have already been successfully applied to many engineering problems, including aerospace systems designs [56, 169, 170]. In addition, depending on the behavior of the model and surrogate modeling technique selected, a proper sampling technique and sample size should be determined.

EvoLVE is anticipated to render challenges in creating surrogate models. Since EvoLVE considers the future growth of a design and its requirements in the first stage, the design space that is explored is generally larger than the one in which the future growth is ignored. Fitting surrogate models covering a large design space can be difficult for two reasons: analysis codes often crash when an infeasible design point is evaluated, and the behavior of design space may become highly non-linear. In addition, since the second-stage problem is a function of the first-stage design, the number of design variables that must be included in the second stage is quite large. For example, if the number of design variables is ten for the first stage, the number for design variables in the second stage can be twenty, at least. In general, the number of sampling points for surrogate modeling increases rapidly as the number of independent variables increases, causing high computational cost.

5.5.5   Avoiding Pitfalls

As identified through case studies and encapsulated in **Observation 4**, past aircraft modification programs often suffered unexpected technical problems, resulting in cost and schedule overrun. In order to avoid the pitfalls of underestimating technical difficulty of modifying design, a special emphasis should be placed on modeling key physical constraints that are of particular importance to the future modification of the given baseline platform. If readily available, the deliberations of an integrated product team (IPT) can be utilized to further qualify the importance of the design constraints.

The sources for the most constraining factors of the derivative aircraft are different from one aircraft category to another—commercial/military, fixed wing/rotary wing, subsonic/supersonic, attacker/bomber/transport, etc. Therefore, case studies of similar

aircraft types would provide valuable insights as to which constraints are likely to be the most restrictive. For example, inadequate sonic boom mitigation has made the widespread emergence of commercial supersonic transport infeasible [53]. Supersonic fighters have very tight internal arrangements that do not allow much room for growth. Handling quality specifications is expected to be critical for the certification of derivative aircraft designs, if significant growth in vehicle weight, compared to that of the original, is forecasted. The issue of handling quality and safety degradation is further discussed in §8.2.7 as part of the future research opportunities.

5.6 Design Space Exploration: Steps 7-9

Once the environment for two-stage aircraft design (TAD) is established, the tool can be utilized in various ways. EvoLVE offers three distinctive options of using TAD in **Steps 7-9** to explore the two-stage design space simultaneously. **Steps 7** and **8** seek optimum designs for each of the strategies defined in **Step 4** under the scenarios defined in **Step 2** by solving two-stage optimization problems either deterministically or stochastically. The non-optimization track of **Step 9** allows exploration of the design space with a greater degree of freedom. While these options do not have to be exercised in the given order due to the iterative nature of the design process, it is recommended to follow the steps as given to minimize the need for rework.

5.6.1 A Deterministic Scenario-Based Approach to Two-Stage Aircraft Design Optimization

Step 7 explores the design space with all the non-stochastic strategies that are defined in **Step 4.** The ND and AH strategies seek the optimum solution by solving Eqs. (25)-(27),

and the DetPPs solve Eqs. (28) and (30). Optimizations are conducted in two phases: before, and after the uncertainty is realized. First, under the presence of uncertainty, the optimal first-stage solutions for each of the strategies, $(\mathbf{x}_1^*)^p$ and $(\mathbf{x}_2^*)^p$, are found, where $p = 1, \ldots, p_n$ is the strategy number. Then, on top of these here-and-now (HN) solutions, all the discrete scenarios $\boldsymbol{\omega}_s, s = 1, \ldots, s_n$ defined in **Step 4** are applied to see how well each strategy responds to the unexpected future requirement in a *posteriori* manner. For all the combinations of strategies and realized scenarios, the second-stage optimization problems are solved to yield the set of wait-and-see (WS) solutions $(\hat{\mathbf{x}}_2^*)_s^p, s = 1, \ldots, s_n$ and $p = 1, \ldots, p_n$. The hat symbol $\hat{\cdot}$ indicates that $\cdot$ is the state determined after the realization of the random variables.

For the 200-passenger commercial transport example, five deterministic strategies and three discrete scenarios were defined. The scenario-based approach applies all three scenarios to the five strategies to see which strategies works better under which circumstances. For example, $\text{DetPP}(S_2)$ predicts that scenario 2 would specify the second-stage requirements and preplan accordingly, yielding the first- and second-stage optimum strategies $(\mathbf{x}_1^*)_{u=2}^{\text{DetPP}(S_2)}$ and $(\mathbf{x}_2^*)_{u=2}^{\text{DetPP}(S_2)}$ where u is predicted scenario number. Then, after applying all three scenarios, a set of solutions $(\hat{\mathbf{x}}_2^*)_s^{\text{DetPP}(S_2)}, s = 1, \ldots, 3$ are found.

The scenario-based approach provides a manageable number of optimal designs, i.e. $(\mathbf{x}_1^*)^p$, $(\mathbf{x}_2^*)^p$, and $(\hat{\mathbf{x}}_2^*)_s^p$, along with cost f_1^*, $(f_2^*)^p$, and $(\hat{f}_2^*)_s^p$, and constraints $(\mathbf{g}_1^*)^p$, $(\mathbf{g}_2^*)^p$, and $(\hat{\mathbf{g}}_2^*)_s^p$ for $s = 1, \ldots, s_n$ and $p = 1, \ldots, p_n$. These states are compared in various different ways to yield meaningful observations and patterns. The patterns can provide general guidance and insights as to which strategies would outperform or underperform

in which situations. For example, comparisons between the first- and second-stage design can reveal how much growth potential is placed in what subsystem under what circumstances. The comparison between the design variables, e.g. wing area, engine thrust, landing gear, etc. can reveal which subsystem is more or less affected by which scenario. In addition, comparisons made between the constraints at the optimum points indicate the degree of growth potential imbedded in the optimal first-stage designs.

For an efficient communication, two terms are coined as follows:

A **PfD (Perfect fit Design)** is defined as an optimal first-stage design that is intended to minimize *only* first-stage cost function. Thus, it is the solution of the optimization problem,

$$
\begin{aligned}
&\min_{\mathbf{x}_1} f_1(\mathbf{x}_1) \\
&\text{s.t.} \ \ g_{1i}(\mathbf{x}_1) \leq 0 \ (i = 1,...,l_1)
\end{aligned}
\tag{37}
$$

A *PfD*, is the least expensive aircraft—and often smallest and lightest aircraft—among $(\mathbf{x}_1^*)^p$ and is obtained by applying non-preplanning strategies. However, the preplanning strategies may find the *PfD* the best design, even considering second-stage requirements, if embedding growth potential in the original design does not provide any long-term benefit.

A **PoD (Perfect over-Design)** is defined as an optimal first-stage design of a preplanning strategy that meets the predicted second-stage requirements without design modification. Since a *PoD* is over-designed from the beginning to meet the second-stage requirement, it does not have to be modified in the second stage if the actual scenario turns out be the predicted one. Therefore, $(\mathbf{x}_1^*)_u^p = (\hat{\mathbf{x}}_2^*)_s^p$ if $u = s$ where u is the anticipated scenario number and s is the realized scenario number. A *PoD* is the

opposite case of a *PfD* and is found when design change penalty dominates the cost of over-designing.

5.6.2   A Stochastic Approach to Two-Stage Aircraft Design Optimization

This step mainly focuses on pursuing the stochastic strategy defined in **Step 4**. The StoPP seeks an optimum first-stage design by solving Eqs. (31) and (32) using the continuous probability density functions of the random variables defined in **Step 2**.

Before the stochastic optimization is attempted, it is required that a technique to evaluate $\mathbb{E}(f_2^*)$, along with a proper sampling method and sample size be determined among the methods introduced in §4.1.1. In general, a minimum accuracy of 10^{-4} of the approximated $\mathbb{E}(f_2^*)$ is required in order to use the approximation in numerical optimization [97]. For a given approximation and sampling technique, the accuracy of approximation generally increases as the sample size increases at the cost of computational time. Since the convergence rate is largely affected by the matching of sampling techniques, the types of PDFs, and the relationship between the approximated functions and input, EvoLVE recommends the risk assessor investigate the stability and repeatability of the selected method through repeated experiments before moving to the next task.

After a proper approximation technique and sample size is selected, StoPP is solved in two phases: before, and after realization of the random variables. The first phase— under the presence of uncertainty—searches for the optimal first-stage decision $(\mathbf{x}_1^*)_\omega^{\text{StoPP}}$ that minimizes not only the first-stage objective but also the expected cost of corrective actions. The optimum solution under the stochastic strategy is compared to the optimum solutions of the deterministic strategies found in **Step 7.**

In the second phase, realizations of all the combinations of random variables are simulated on top of the already found $(\mathbf{x}_1^*)_{\boldsymbol{\omega}}^{\text{StoPP}}$. This is done by running a Monte Carlo simulation on Eq. (33) with the observed scenarios $\hat{\boldsymbol{\omega}} \in \boldsymbol{\Omega}$. The result of MCS is the collection of the optimal second-stage designs $(\mathbf{x}_2^*)_{\hat{\boldsymbol{\omega}}}^{\text{StoPP}} \in (\mathbf{X}_2^*)_{\boldsymbol{\Omega}}^{\text{StoPP}}$, where $(\mathbf{X}_2^*)_{\boldsymbol{\Omega}}^{\text{StoPP}}$ is the entire design set obtained from MCS. This process is repeated with all the optimal first-stage designs of other strategies to yield $(\mathbf{x}_2^*)_{\boldsymbol{\omega}}^{p} \in (\mathbf{X}_2^*)_{\boldsymbol{\Omega}}^{p}, p = 1, \ldots, p_n$.

The second-stage designs can be visualized using both PDFs and CDFs. Juxtaposition of the PDFs and CDFs of all the strategies can enable comparisons between the strategies on the entire spectrum of the random variable space. For example, a complementary CDF (CCDF) of the total and second-stage cost can visualize how much a strategy is susceptible to risk. A CCDF is the probability a random variable X assumes a value greater than or equal to some value x. A true CCDF of a real-valued random variable X is calculated for every real number x as:

$$F_C(X) = \text{Prob}(X > x) = 1 - \int_{-\infty}^{x} f(t)dt \tag{38}$$

where $f(t)$ is a PDF of the random variable X. Since analytical integration of $f(t)$ is impractical, an approximation of CCDF $\tilde{F}_C(X)$ is obtained by numerical integration.

Joint probability distribution or multivariate probability distribution visualizes more than one random variable simultaneously. An example bivariate distribution of both development cost and time is illustrated in Figure 27. The figure compares the probability distributions of two different strategies. Here, by imposing limits on cost and time, one can quantify which strategy has higher chance to meet both or either the cost and schedule limits.
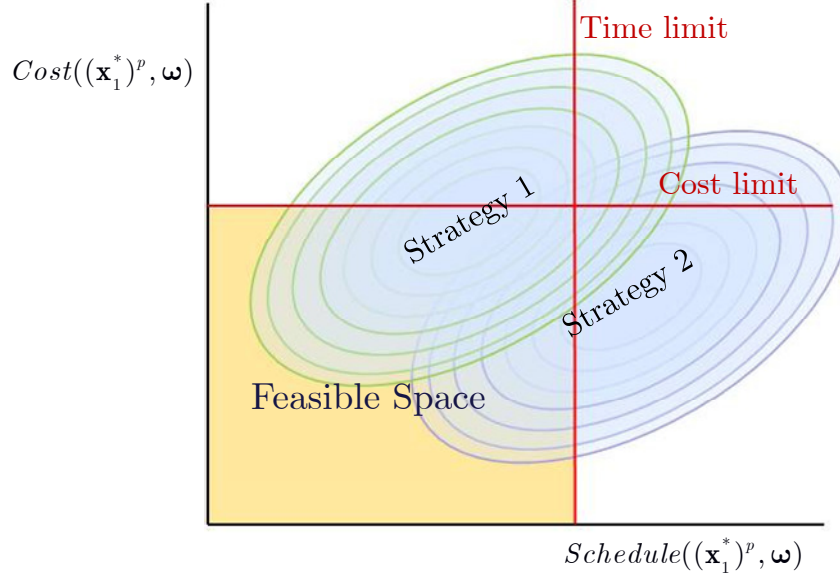
Figure 27: Risk Assessment using Joint Probability Distribution

The set of corrective actions for each of the strategies $(\mathbf{X}_2^*)_{\boldsymbol{\Omega}}^p, p = 1, ..., p_n$ is further processed by solving Eqs. (20) and (21) for a spending limit $\tau \in [0, +\infty]$. Then, the strategies are ranked in terms of the probability to exceed the spending limit, yielding the ranking function $RN : (p, \tau) \to r \in [1, ..., p_n]$, where r is the ranking, and p_n is the total number of strategies. Depending on how risk is perceived by the decision makers, the ranking function can be obtained using other risk-measures, such as the probability of exceeding the second-stage spending limit, the amount of loss when the project is canceled, the opportunity cost of losing potential foreign customers, or the variability of the second-stage cost.

In conclusion, the stochastic approach helps to identify the most risk-tolerant configuration against the modeled uncertainties, e.g., future changes in customer requirements, as a function of the decision-maker's own perception of risk.

5.6.3   Framework for Interactive Decision Making Support

The final step of the EvoLVE process is to create the framework for interactive decision-making support. In **Step 9**, all the restrictions applied to pursue optimization—a single objective, hard constraints, continuity of the design variables, restriction on the number of design variables and random variables, etc.—are removed, and a framework for decision-making support is created as per **Hypothesis 5**. While interactive, visual representation of the design space can take many different forms. Two-stage contour plots and two-stage multivariate profilers are proposed in this study.

Contour plots visualize the multi-dimensional design space in two-dimensions. One should select two design variables for each dimension, and then all the design constraints and system attributes are plotted in the space defined by the two design variables. The constraint analysis plot shown in Figure 4 is also a type of contour plot.

A sample two-stage contour plot is depicted in Figure 28. The plot was prepared using the commercial statistical software package JMP®. The left side of the figure depicts the first-stage design space and the right side shows the second-stage design space. Each plot has three parts. The top portion lists the design variables, two of which are selected to assume the axes of the contour plot in the bottom. The middle section is devoted to the list of system attributes, such as performance and cost, along with slide bars and an option for setting threshold values. For each attribute, lower or upper threshold values can be set up to create a constraint. The contour plot in the bottom displays the contour lines of all the system attributes. The current design point is indicated by the intersection point of the vertical and horizontal lines, and one can readily move the design point. When the design point changes, the values of all system

attributes are updated instantly. If constraints are set up, the constraint lines are drawn, dividing the design space into regions. The subset of design space is defined as *feasible space* if a design point within the region meets *all* constraints. The sample plot selects wing area and engine thrust as two interesting independent variables. The first-stage design space shown on the left has a narrow band of feasible space in white around wing area of 400 ft^2 and engine thrust of 18000 lb. The second-stage design space shows the feasible region around 500 ft^2 of wing area and 22000 lb of engine thrust.
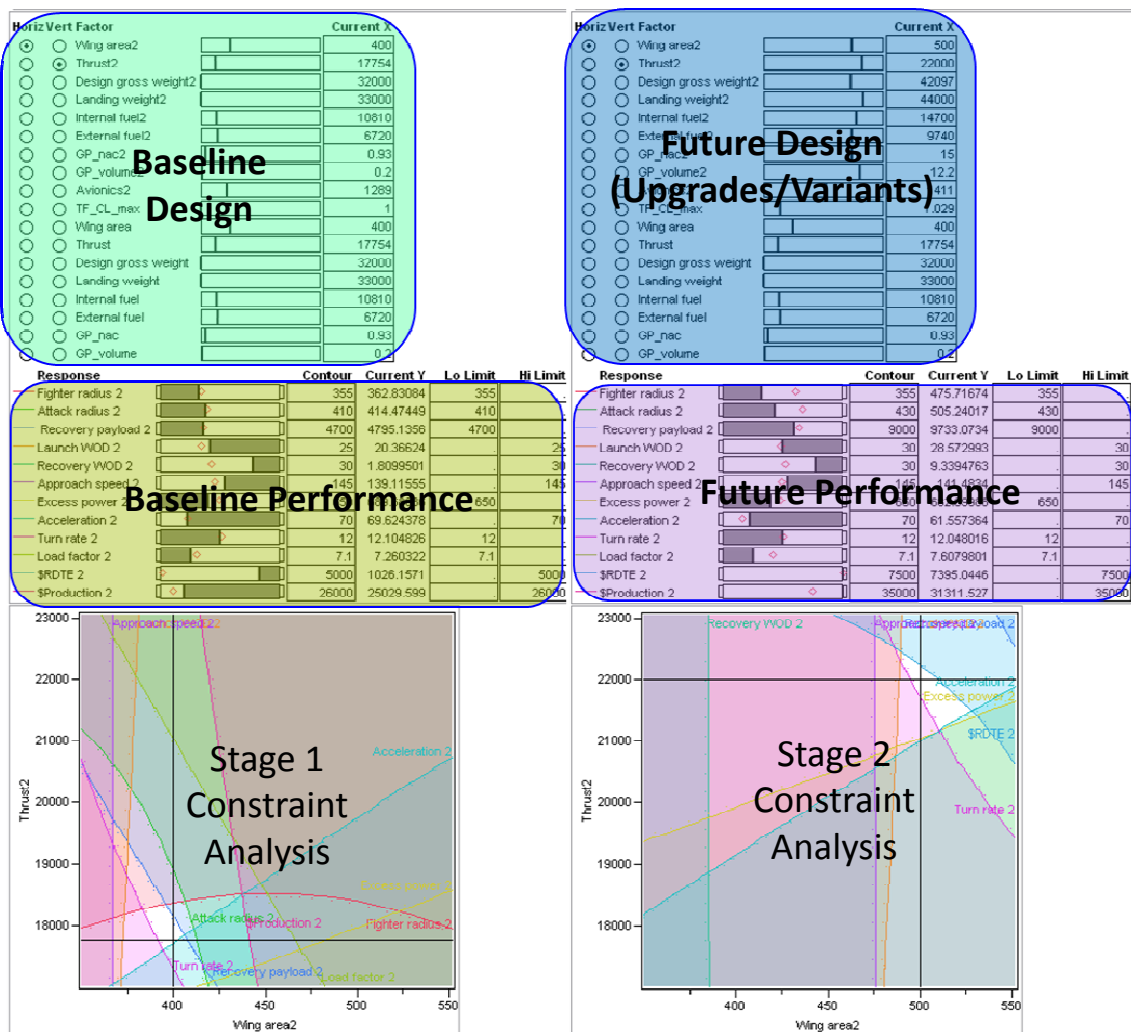
Figure 28: A Sample Two-Stage Contour Plot

While the first-stage constraint analysis alone allows various what-if studies for the current design problem, the second-stage constraint analysis expands the scope of investigation beyond the time frame of the first-stage problem. The two-stage constraint analysis tool allows various aircraft evolution studies including:

- What is constraining the design and where is growth potential?

- How does a change in future requirements affect aircraft performance?

- How does infusion of new technology open up the design space, and how much will it cost?

- How does the relaxation of less important constraints enable cost- and time-saving design alternatives?

Another potentially useful tool in this step is a multivariate profiler (MVP). A MVP gives the relationship between multiple variables shown at a time. Therefore, it allows simultaneous consideration of design variables and system attributes in all developing stages. While contour profilers display only two dimensions of multi-dimensional design space at a time, the multivariate plot presents the entire view of the design space interaction.

Figure 29 depicts an example MVP that was created using JMP® for a notional fighter. In a MVP, all the variable names are listed in the diagonal boxes of the plot. Each of the boxes shows interactions between the two variables comprising the intersection. A point in a box is one particular design, which is linked to the database created through repetition of design analysis. The data samples can be generated in various different ways: i.e. any combinations of parametric variations of the first-stage design, requirements, technologies, and the second-stage design.

Figure 29 was created based on the optimum first-stage designs under five aircraft evolution strategies. Random variation on the requirement is applied on the five baseline designs to see how these five optimum designs react to the future requirement evolution. Here, the design itself remains unchanged in the second stage, but aircraft performance changes due to either a more stringent requirement or the introduction of new technology. The highlighted points indicate the original performance of the aircraft. All other points are the future deviations from the original points. The color code shown in the far right column differentiates the five strategies. In the lower left corner of Figure 29 is a scenario filter, which filters the designs that do not meet a particular requirement scenario. For instance, one can impose a cost limit on the second stage and relax the turn rate constraint to see how more emphasis on affordability than fighter performance changes the fighter design.

As a final note, once the all steps of EvoLVE are executed, it is necessary to revisit the previous steps as more information about the problem at hand is gained.
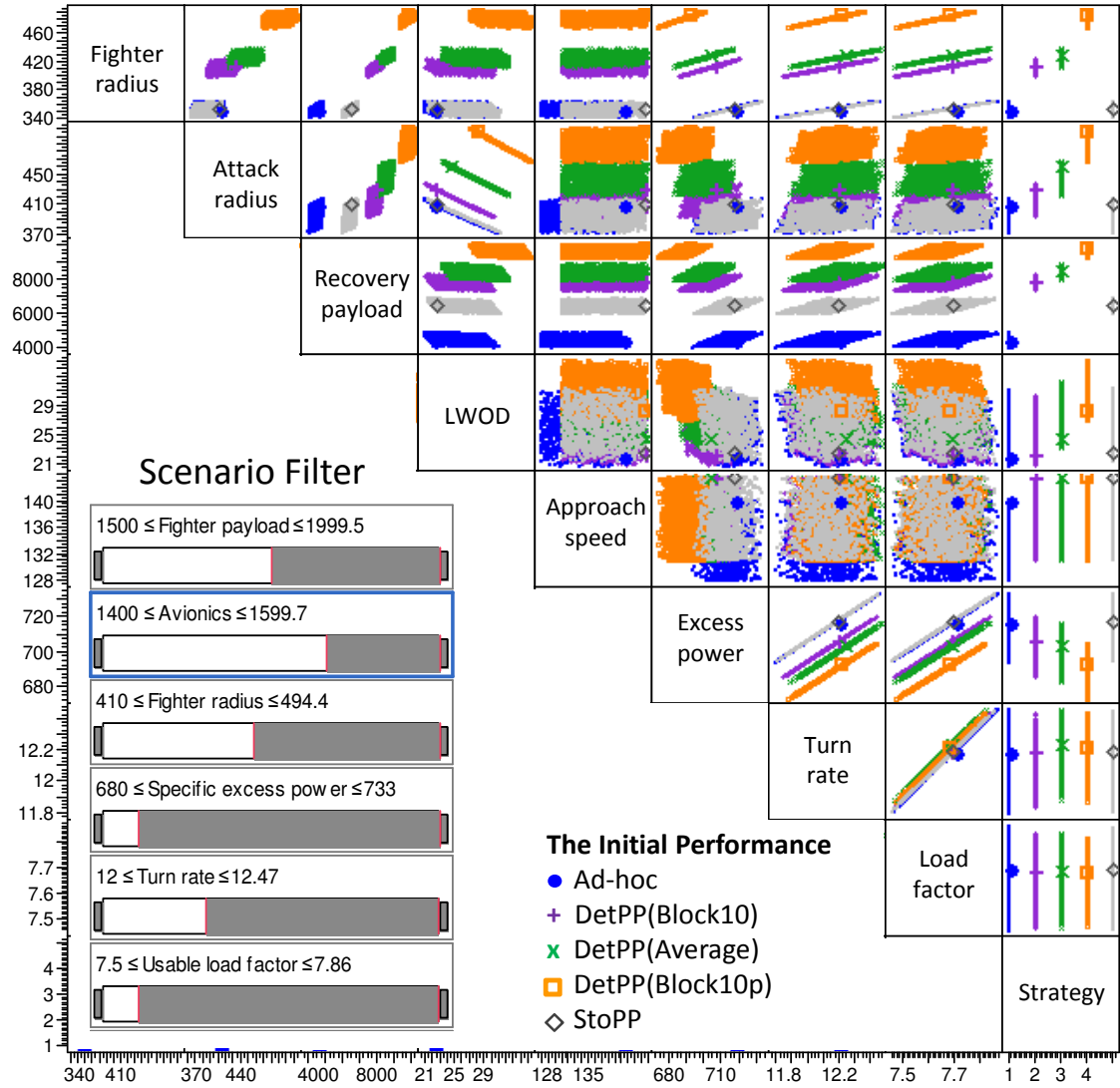
Figure 29: An Example Multivariate Profiler and Scenario Filter

CHAPTER VI

PROOF OF CONCEPT: A CANTILEVERED BEAM DESIGN

As a proof-of-concept study to the new approach proposed in the previous chapter, a two-stage cantilevered beam design problem is formulated and solved in this chapter. Since the main purpose of this study is to test the applicability of SPR on an engineering design problem consisting of two development stages, some of the steps of EvoLVE are either skipped or combined with other steps. A five segment cantilevered beam under a point transverse load is adopted from a problem presented by Vanderplaats [37]. The problem is then expanded to a two-stage design problem by imposing an uncertain second-stage requirement. The objective of the optimization is to minimize the total program cost, including RDT&E, production, operation, and design modification. Four design evolution strategies—ad-hoc upgrade, deterministic preplanning, stochastic preplanning, and new-design strategy—are defined and compared under various scenarios. Once the problem is set up, three experiments are designed and executed to test **Hypotheses 1**, **2**, and **4**.

6.1 Problem Setup

6.1.1   The Original Beam Design Problem

A cantilevered beam shown in Figure 30 consists of five segments. A point transverse load P is applied at the end of the beam structure. Design variables are the widths of each beam section b_i, $i = 1,...,5$. The goal of design is to find the minimum volume structure satisfying both of the two types of constraints, deflection and stress. The

deflection of the right end of each segment is constrained to be lower than a prescribed value. The deflection y_i at section i is calculated as follows:

$$y'_i = \frac{Pl}{EI_i}\left[L + \frac{l}{2} - \sum_{j=1}^{i} l_j\right] + y'_{i-1}$$

$$y_i = \frac{Pl^2}{2EI_i}\left[L - \sum_{j=1}^{i} l_j + \frac{2l}{3}\right] + y'_{i-1}l + y_{i-1} \qquad (39)$$

$$\text{where } I_i = \frac{b_i h_i^3}{12} \text{ and } y_o = y'_o = 0$$

where y'_i deflection of segment i

y'_i derivative of y with respect to x

l_i length of segment i

E Young's modulus (same for all segments)

P applied load

I_i moment of inertia of segment i

h_i height of segment i (twenty times the width of the segment)

$P = 50,000$ N
$E = 2.0\text{x}10^7$ N/cm²
$l_i = 100$cm
$\bar{\sigma} = 14,000$ N/cm²
$\bar{y} = 2.5$ cm

Cross section
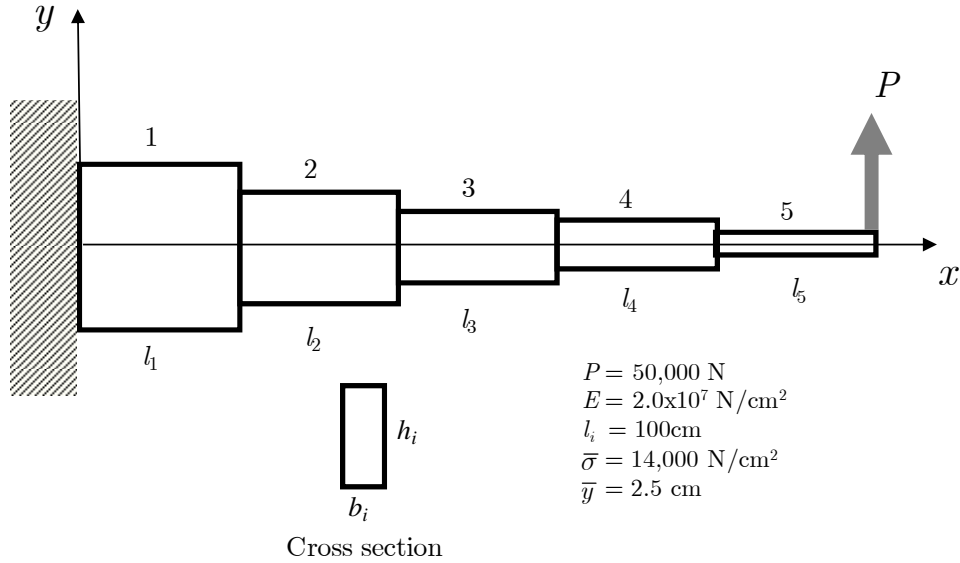
Figure 30: A Five-Segment Cantilevered Beam [37]

In addition, the bending stress, which is largest at the left end of each segment, is also constrained. The bending stress (σ_i) at section i is calculated as:

$$\sigma_i = \frac{M_i h_i}{2 I_i} \tag{40}$$

where $M_i = P\left[L + l_i - \sum_{j=1}^{i} l_j \right]$ is the bending moment at the left end of segment i; L is total length of the beam (500 cm); P is the applied load (50,000 N).

The original beam design problem is formally formulated as a constrained optimization problem as follows:

$$\min_{b_i} V = \sum_{i=1}^{5} b_i h_i l_i, \ i = 1,\ldots,5 \tag{41}$$

$$\text{s.t.} \ \frac{\sigma_i}{\overline{\sigma}} - 1 \le 0, \ \frac{y_i}{\overline{y}} - 1 \le 0$$

where $\overline{\sigma}$ is the maximum allowable stress (14,000 N/cm^2) and $\overline{y}$ is the maximum allowable deflection (2.5 cm).

6.1.2 Expansion of the Problem

The beam problem described in the previous section is adapted and redefined here. First, the beam design problem is expanded to a two-stage beam design problem, in which a beam is designed for the present applied load (P_1) and modified later to meet the future applied load (P_2) as illustrated in Figure 31. It is assumed that the future requirement is more demanding than the current one, thus the beam structure should become stronger to increase its load-carrying capability. The first-stage problem is the same as the original problem, i.e. same requirements and constraints, except for that the optimization routine minimizes overall program cost instead of the beam volume. The
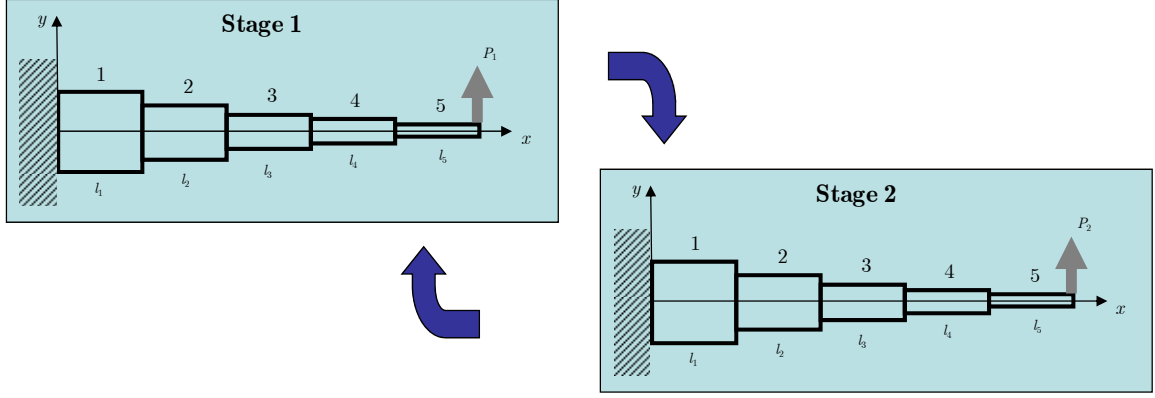
Figure 31: Illustration of the Two-stage Cantilevered Beam Design Problem

overall program cost is the sum of the cost of the new beam development program (stage 1) and the beam modification program (stage 2). The objective of the optimization is to find the best beam design for stage 1, which minimizes the overall program cost.

In stage 2, the objective function to minimize is the program cost of beam modification program, including the penalty of design modification. The requirement of stage 2, i.e. the applied load, is a random variable ω. Because of the uncertainty associated with the applied load in the stage 2, the stage 2 cost cannot be evaluated deterministically but probabilistically. Thus, the expectation of stage 2 cost is calculated for all realizations of the random variable. The mathematical representation of the problem is now expressed as follows:

In stage 1,

$$\min_{\mathbf{b}_1} f_1(\mathbf{b}_1) + \frac{1}{(1+r)^{t_{12}}} \mathbb{E}_{\omega \in \Omega} \left[Q(\mathbf{b}_1, \omega) \right]$$

$$\text{s.t. } g_{1i}(\mathbf{b}_1) < 0, \, (i = 1, ..., 10)$$

(42)

where $\mathbf{b}_1$ stage1 beam width vector

         f_1 stage 1 objective

         r risk-free discount rate

         t_{12} time span between stage 1 and 2

$\mathbb{E}[*]$ expectation of *

Q stage 2 objective

ω random variable

g_{1i} stage 1 deflection and stress constraints

In the second stage, for a given $\mathbf{b}_1$ and a realization of the random variable following optimization problem is solved as

$$Q(\mathbf{b}_1, \omega) = \min_{\mathbf{b}_2} \left[f_2(\mathbf{b}_2, \omega) + H(\mathbf{b}_1, \mathbf{b}_2, \omega) \right]$$
$$\text{s.t. } g_{2i}(\mathbf{b}_2, \omega) < 0, \ (i = 1, ..., 10)$$

(43)

where $\mathbf{b}_2$ stage 2 beam width vector

f_2 stage 2 cost

H design modification penalty

g_{2i} stage 2 deflection and stress constraints

In this experiment, the first-stage applied load P_1 is fixed at 50,000 lb. The stage 2 applied load P_2 is identified as a random variable. For simplicity, it was assumed that the random variable takes a finite number of outcomes, and a probability mass function (PMF) was assigned to the random variable as follows:

$$\text{PMF}(\omega) = \left(75,000, \ 0.2\right), \ \left(100,000, \ 0.5\right), \ \left(150,000, \ 0.3\right)$$

(44)

where the first values in the parentheses are the applied load P_2, and the second values are the probabilities associated with them. These three possible outcomes of ω constitute three scenarios that are defined as Scenario 1, 2, and 3, under which P_2 is 75,000, 100,000, and 150,000 respectively.

6.1.3 Evolution Strategies

Four different beam development strategies are formulated. They are new-design, ad-hoc upgrade, deterministic preplanning, and stochastic preplanning strategies. The new-design and ad-hoc upgrade strategies are non-preplanning strategies. In the new-design strategy, a new beam design is introduced in stage 1. Then, another new design is prepared in the second stage as necessary. Thus, the stage 1 and stage 2 designs are completely independent each other. The new-design strategy is later compared to one of the best new-derivative strategies to see to what extent introducing a derivative model would be more beneficial than starting from scratch. With the ad-hoc upgrade strategy, no provision for the future is made. In the first stage, the design practice is to ensure the best design for only the current, given requirement. No growth provision is incorporated. Then, after the second-stage requirement is concretely defined, a derivative version of the stage 1 design is sought to meet the new requirement with minimal cost. The cost in the second-stage problem includes the cost of modifying the design from the original design as well as the cost of producing and operating the derivative.

With the deterministic preplanning strategy, the second-stage requirement is known or predicted to take a certain value. Growth provisions are planned in the first-stage design in order to reduce the cost of design modification. Thus, the objective function of the first-stage problem is expanded from f_1 to Q. A feedback from stage 2 to stage 1 makes the stage 1 and 2 interdependent. Mathematically, the deterministic preplanning solves Eqs. (42) and (43) with the absence of uncertainties. Thus, a random variable becomes a deterministic variable, and the second-stage objective Q is evaluated

deterministically. Finally, the stochastic preplanning strategy solves Eqs. (42) and (43) with the random variable defined in Eq. (44).

6.1.4 Cost Modeling

A hypothetical cost model was created as a final step of problem set up. The elements of the stage 1 and 2 program cost (f_1 and f_2) are research, development, test, and evaluation (RDT&E) cost, production cost, and operation and support (O&S) cost. The cost of changing the design in stage 2 is captured separately in P_2. The RDT&E cost was assumed to be \$70,000 for stage 1 and zero for stage 2. It was assumed that the stage 2 RDT&E cost was included in the penalty function.

Production and O&S cost for stage 1 and 2 are calculated based on the weight of the beam segment. Production cost at stage Θ ($\$Production_\Theta$) is simply ten times the total weight of the beam of the stage. The O&S cost ($\$OS_\Theta$) is the sum of segment weight multiplied by a coefficient $\alpha_{\Theta i}, i = 1,\dots,5$. Finally, design modification penalty is calculated based on the difference between the stage 1 and stage 2 design. For this problem, only the quadratic relationship between the differences of the design variable values to the cost was modeled.

$$f_\Theta = \$RDTE_\Theta + \$Production_\Theta + \$OS_\Theta$$

$$\$Production_\Theta = \sum_{i=1}^{5} 10(Weight)_{\Theta i}$$

$$\$OS_\Theta = \sum_{i=1}^{5} \alpha_{\Theta i}(Weight)_{\Theta i} \tag{45}$$

$$Weight_{\Theta i} = Volume_{\Theta i} \times \rho$$

$$H = \sum_{i=1}^{5} \beta_i (b_{1i} - b_{2i})^2$$

where $\Theta \in [1,2]$ is index for stage, $i = 1,\ldots,5$ is index for beam segment, $\$RDTE_1$ and $\$RDTE_2$ were fixed at \$70,000 and \$0, respectively, and $\rho = 0.00785$ kg/cm^3 is material density.

The values for the coefficients α and β are determined by the following rules. For each of the beam segments, subjective ratings for O&S cost and design modification penalty are assigned as presented in Table 7. The rating scale is low, mid, or high. For example, the contribution of beam segment 1 to the O&S cost is assumed to be medium, where it is assumed to incur high penalty if its design is modified in the second stage. A rationale behind this is that beam segment 1 and 5 interface with the outer environment, so their modification would cause compatibility issues and thus incur high cost. For example, the first beam segment or B_1 is clamped to the supporting wall, and redesigning the first beam segment is subject to additional constraints, such as interface and regulations. According to the rating, the numerical values of the O&S and penalty cost coefficients are assigned in Table 8 presented below.

Table 7: The O&S and Penalty Cost Coefficient Schedule

Beam Segment	O&S	Penalty
1	mid	High
2	high	Low
3	mid	Mid
4	low	Low
5	high	High

Table 8: The Values of the O&S and Penalty Cost Coefficients

Scale	$\alpha_{\Theta i}$ (O&S)	β_i (Penalty)
Low	20	5,000
Mid	80	10,000
High	150	40,000

6.2 Experiment I: Comparison of the Four Strategies

Once a hypothetical two-stage cantilevered beam problem is formulated, the problem is solved for the four development strategies. The new-design and ad-hoc upgrade strategies solve the first-stage problem independent to the second-stage problem. Then, the second-stage problem is solved for after the second-stage requirement is known. The deterministic preplanning strategy predicts the second-stage applied load to be at 100,000 lb and examines the possibility of having growth potential in the original design. The stochastic strategy sees all three scenarios and the probability of having such a scenario and seeks an optimum first-stage design that is supposed to work best on average. Once the optimum first-stage beam designs for each of the strategies are obtained, they are tested with the three scenarios by solving the second-stage optimization in a posteriori manner to see how well each strategy responds to each scenario.

6.2.1   Total Program Cost Comparison

Table 9 provides the total program cost of the four strategies under three different scenarios. Figure 32 graphically compares how much each strategy costs under a specific scenario. A comparison from the scenario point of view reveals that no strategy is best for the all scenarios. When the actual realization of the second-stage requirement turned out to be 75,000 lb (Scenario 1), ad-hoc strategy met the requirement with the smallest cost. For Scenario 2 and 3, however, both of the preplanning strategies cost less than the two non-planning strategies. Deterministic preplanning strategy cost the least under Scenario 2. The stochastic preplanning cost the least under Scenario 3.

It is easily seen from the figure that for the ad-hoc upgrade strategy, the total cost increases rapidly as the second-stage applied load increases. The ad-hoc strategy was the best under Scenario 1 but the worst under Scenario 3. The deterministic preplanning strategy, on the other hand, was the best among all four strategies when the predicted P_2 was equal to the actual P_2, as expected. The stochastic preplanning strategy performed the best under scenario 3, but more importantly, it cost the least on average as compared in the bottom row of the table.

Table 9: Total Program Cost of the Four Strategies under the Three Scenarios

Scenario	Applied Load	New-Design	Ad-Hoc	Det. Planning	Stoc. Planning
1	75,000 N	206,962	154,532	155,794	159,212
2	100,000 N	215,772	181,245	166,345	167,101
3	150,000 N	231,540	249,184	208,618	201,031
Average	n/a	218,740	196,284	176,917	175,702
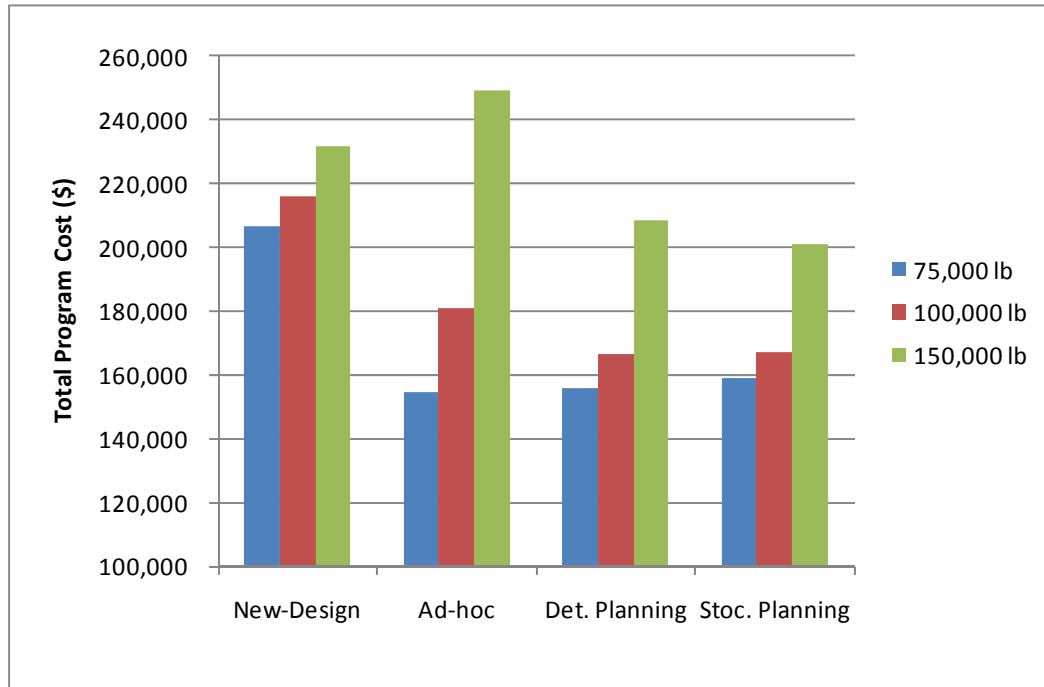
Figure 32: Total Program Cost Comparison

6.2.2 Optimum Design Results under Different Strategies

This section compares how each of the beam segments at each stage was sized under the four strategies. The second-stage design is only finalized after the actual second-stage requirement becomes realized. The study was conducted with the realized second-stage requirement P_2 to be 100,000 lb; that is, Scenario 2 was realized. The results were non-dimensionalized by dividing the value by the design value of the new-design strategy. Symbol $b_{\Theta i}$ represents the beam width of the ith segment in stage under strategy p.

Figure 33 shows the optimized values of b_{11} and b_{21} of the four strategies. Both the new-design and ad-hoc strategies sized the beam segment 1 to meet the given first-stage applied load and then increase the beam width in the second stage by about 20%. However, two preplanning strategies over-sized b_{11} to such an extent that it is close to b_{21}. The oversizing tendency of b_{11} is attributed to the fact that the cost of changing b_{11} is very high and the cost incurred by oversizing it is relatively small. Thus, both deterministic and stochastic preplanning strategies identified that sizing b_{11} to meet the
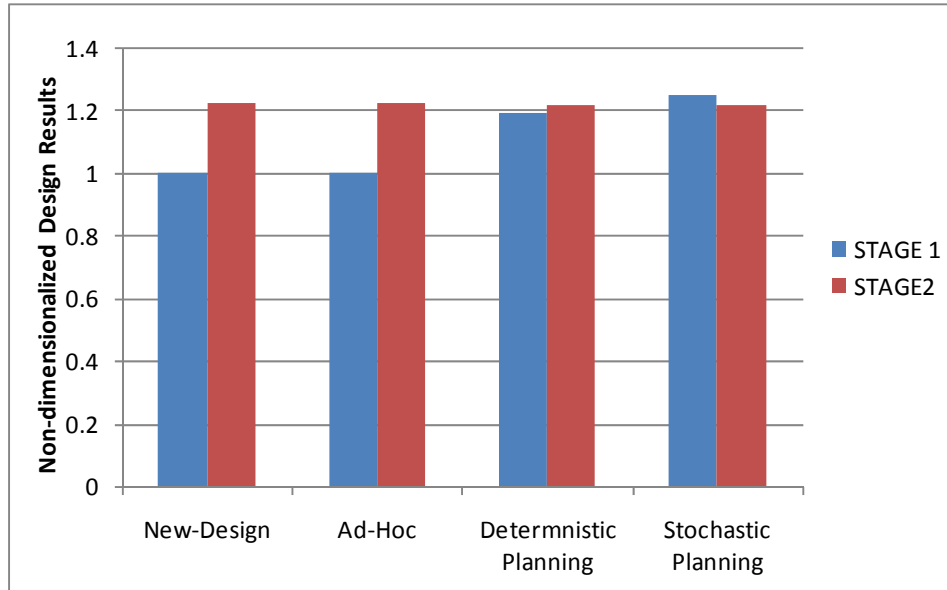
Figure 33: Optimum Widths of the Beam Segment 1
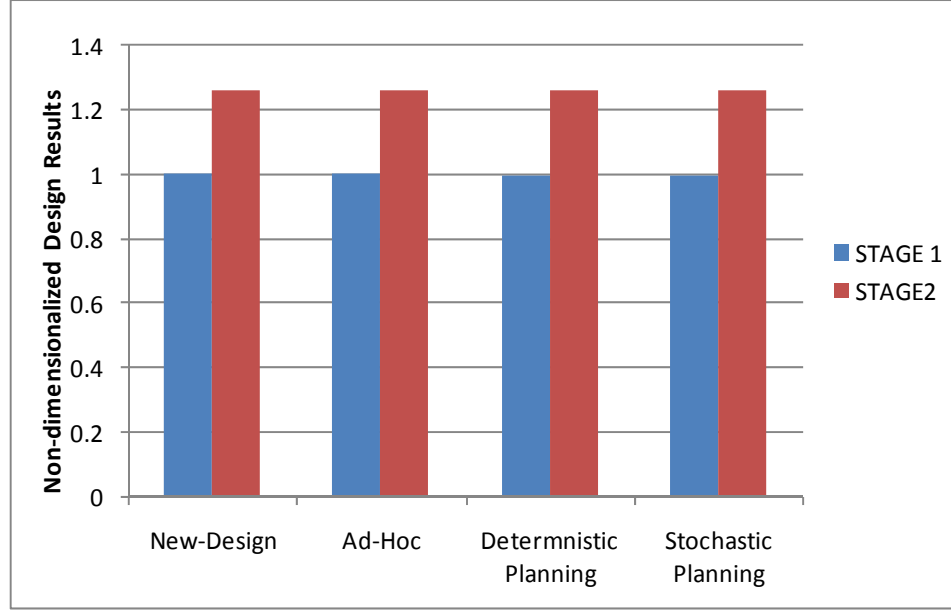
Figure 34: Optimum Widths of the Beam Segment 2

second-stage requirement from the beginning was cheaper in the end.

Figure 34 compares the widths of the beam segment 2. In contrast to the results of the beam segment 1, none of the four strategies overdesigned the beam segment 2 in the first stage. The result can be interpreted as the cost of overdesigning segment 2 outweighs the cost of upgrading it later.

Finally, the optimum widths of the tip section b_{15} and b_{25} are compared in Figure 35. Again, the non-preplanning strategies sized the beam segment to meet the given first-stage applied load requirement. Then, the preplanning strategies oversized b_{15} but not as much as they oversized b_{11}. The stochastic preplanning oversized more than the deterministic strategy because it accounted for the fact that there is a 30% probability of P_2 being 150,000 lb.

The comparison of the optimum solution from the design point of view reveals that the preplanning strategies allocate growth margin on each of the beam segments in a very different way. Beam segment 1 was overdesigned and segment 2 was not

134
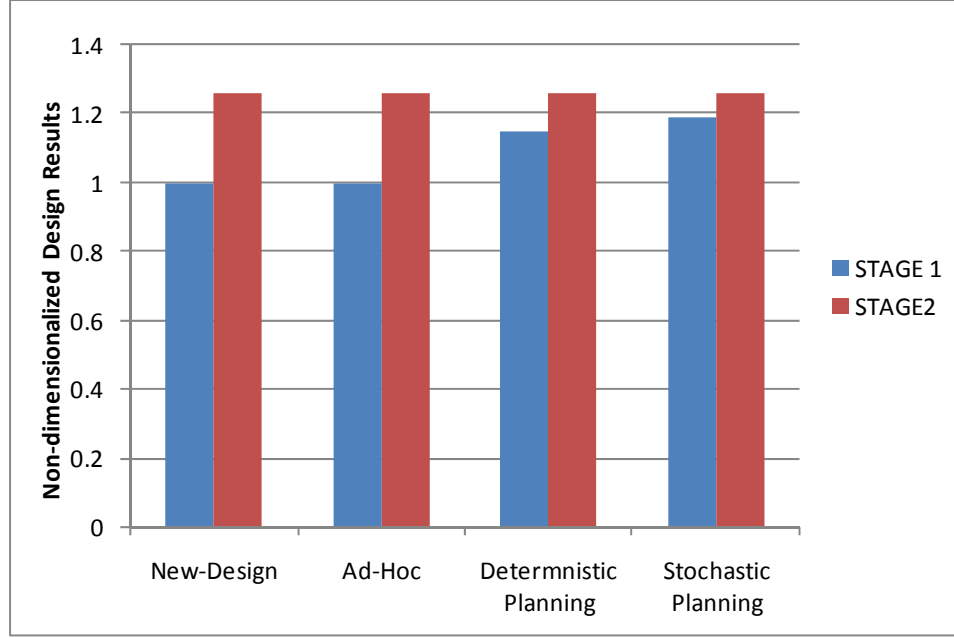
Figure 35: Optimum Widths of the Beam Segment 5

overdesigned at all under the both the deterministic and stochastic preplanning strategies. The result shows that the new method can quantify the allocation of growth potential on the subsystems in a way that balances the cost of overdesigning and the cost of modifying the existing design later.

6.3 Experiment II: Growth Limit

The previous section showed that the new-design strategy cost more than other strategies cost, at least when P_2 is between 75,000 and 150,000 lb. However, this may not be the case if P_2 increases further. The question is when would it be beneficial to start from scratch rather than modify the existing design? What would be the absolute growth limit to a design? The query is answered by comparing the new-design strategy to the best derivative development strategy. The best derivative design strategy is the deterministic preplanning strategy with the complete knowledge of the second-stage

requirement from the beginning. The total problem costs of these two strategies were calculated for the increasing second-stage beam load and were compared in Figure 36.

The total cost under the derivative development strategy based on the perfect prediction was less than the developing a new product strategy when the P_2 was less than 32,500 lb. Then, because of a sharp increase in the modification cost, the rate of change of the total cost under the derivative development case was higher, making it more expensive than the new-design strategy when P_2 was larger than 32,500 lb. This experiment shows that for this beam design problem, the absolute growth limit of the first-stage design is 32,500 lb. If P_2 grows larger than 32,500 lb, no cost benefit exists in upgrading the existing design. Rather, it is cheaper to start from scratch.
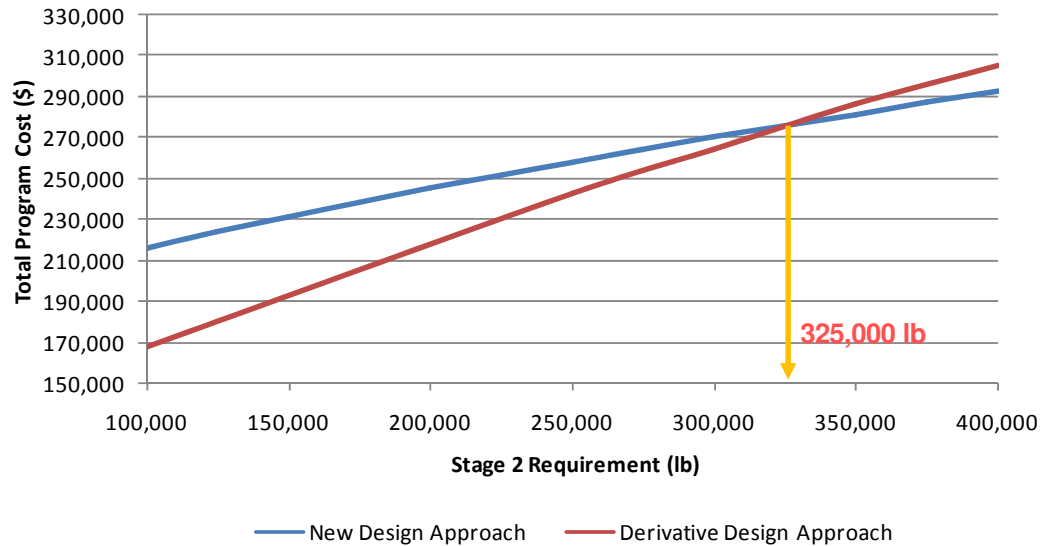
Figure 36: Total Cost of the New-Design and the Deterministic Planning

6.4 Experiment III: Value of Perfect Information and Stochastic Solution

In this experiment, two quantities that are valuable in the domain of stochastic programming with recourse—namely, value of perfect information (EVPI) and value of stochastic solution (VSS)—are calculated.

6.4.1 Value of Perfect Information

To calculate EVPI, it is assumed that one can always predicted the value of the random variable with certainty. For all possible realization of the random variable—i.e. scenarios—the total cost of the two-stage problem is calculated. Then, the average of the total cost is the expected value of the optimal solution or the wait-and-see solution (WS) as:

$$WS = \mathbb{E}_{\omega \in \Omega} \left[\min_{\mathbf{b}_1} f_1(\mathbf{b}_1) + \frac{1}{(1+r)^{t_{12}}} Q_2(\mathbf{b}_1, \boldsymbol{\omega}) \right]$$

$$\text{s.t. } g_{1i}(\mathbf{b}_1) < 0, (i = 1,...,10)$$

(46)

where Q_2 is as given in Eq. (43). Since ω takes only three outcomes, Eq. (46) is solved by transforming it to three deterministic equivalents, and the results are summarized in Table 10. Each column of the table is the optimum solution and the total cost for each scenario.

Table 10: The Wait-and-See Solution for Each Scenario

Scenario	P_2 (N)	Total Cost ($)
1	75,000	154,872
2	100,000	166,345
3	150,000	193,404

Then, the expected cost is calculated as

$$WS(\$) = 0.2(154,872) + 0.5\left(166,345\right) + 0.3\left(193,404\right) = 172,168 \tag{47}$$

The wait-and-see solution is compared to the so-called *here-and-now* (*HN*) solution. The *HN* is the expected value of the stochastic solution $\mathbf{b}^*$ calculated as:

$$HN = \min_{\mathbf{b}_1} f_1(\mathbf{b}_1^*) + \frac{1}{(1+r)^{t_{12}}} \mathbb{E}_{\omega \in \Omega}\left[Q_2(\mathbf{b}_1^*, \omega)\right] \tag{48}$$

where $\mathbf{b}_1^*$ is the optimum first-stage beam design obtained in the previous section. HN is readily obtained using the results in Table 9 as

$$HN(\$) = 0.2(159,212) + 0.5\left(167,101\right) + 0.3\left(201,031\right) = 175,702 \tag{49}$$

Finally, $EVPI(\$) = HN - WS = 175,702 - 172,168 = 3,534.$

6.4.2 Value of Stochastic Solution

Solving a stochastic programming problem is generally very expensive and time consuming. So, it is possible that one can ask himself if pursuing a stochastic approach is really worthy of the time and effort. One of the attempts to solve a stochastic problem easily is by simplifying it by replacing the random variables to their expected values. This is called the expected value (EV) problem [94]. In the beam example, this greatly simplifies Eq. (42) to

$$EV = \min_{\mathbf{b}_1} f_1(\mathbf{b}_1) + \frac{1}{(1+r)^{t_{12}}} Q_2(\mathbf{b}_1, \bar{\omega})$$
$$\text{s.t. } g_{1i}(\mathbf{b}_1) < 0, \ (i = 1,...,10) \tag{50}$$

where $\bar{\omega} = E(\omega) = 0.2(75,000) + 0.5(100,000) + 0.3(150,000) = 24,500 \ [\text{N}].$

For the optimal first-stage design $\tilde{\mathbf{b}}_1^*$ of the EV problem, the second-stage problem given in Eq. (43) is solved for all possible scenarios. This solution is called the expected result of using the EV solution (EVV), defined as

$$EVV = f_1(\tilde{\mathbf{b}}_1^*) + \frac{1}{(1+r)^{t_{12}}} \mathbb{E}_{\omega \in \Omega}\left[Q_2(\tilde{\mathbf{b}}_1^*, \bar{\omega}, \omega) \right] \tag{51}$$

Again, Eq. (29) is solved by converting it to its deterministic equivalent. The optimization results for each scenario are in Table 11.

Table 11: Result of Using the Expected Value Solution

Scenario	P_2 (N)	Total Cost ($)
1	75,000	159,014
2	100,000	167,323
3	150,000	201,364

Then, the expected value is calculated as

$$EVV(\$) = 0.2(159,014) + 0.5(167,323) + 0.3(201,364) = 175,874 \tag{52}$$

Since HN is \$175,702 from the previous section, $VSS(\$) = 175,874 - 175,702 = 172$.

6.5 Hypothesis Test

Hypotheses 1, **2**, and **4** were proved though three experiments with a two-stage cantilevered beam design problem. Experiment I, II, and III showed that by expanding a classical, one-stage design problem to a two-stage problem incorporating future requirements: (a) cost associated with the four beam design evolution options was evaluated with three requirement evolution scenarios; (b) the right amount of growth provisions to minimize the overall cost were quantified for each of the beam segments; and (c) the growth limit of a given design was identified. These three evidences

collectively prove **Hypotheses 1** and **4**. Presence of uncertainty imposes risk in designing for the future. **Hypothesis 2** claims that the risk can be mitigated by assigning probabilities to the random variables and minimizing the expected cost. In experiment I, although the deterministic preplanning strategy found the optimal stage 1 and stage 2 design solutions with minimal cost when the predicted and actual future requirements were close, the stochastic approach cost the least on average, which supports **Hypothesis 2**. In addition, EVPI calculated in experiment III provided the value of knowing the accurate future requirement in advance, which provides the decision makers very valuable knowledge they can exploit through trading managerial options.

CHAPTER VII

APPLICATION TO A NOTIONAL MULTI-ROLE FIGHTER DESIGN

EvoLVE was implemented on a notional multi-role fighter design based on F/A-18 Hornet and Super Hornet. Based on the evolution history of F/A-18, a hypothetical requirement was created in order to test the efficacy of EvoLVE in aerospace systems design and prove the hypotheses. A scalable computer model of F/A-18 Hornet was created and validated using public domain data of the A, C, E versions. The modeling and validation process is extensively documented in §7.6 and §7.7.

The study is not intended to recreate the evolution of F/A-18 but utilizes the historical example, especially the upgrade program from the C/D to E/F versions, in order to validate the computer models and create a test case as realistic as possible. Therefore, the study is based on a hypothetical time frame, background, and requirement, and thus the optimized vehicles at the end of the study are *not* new versions of the F/A-18 *but* are notional fighters that perform very similar missions.

Although this study was primarily conducted in 2008, the clock was rewound by twenty years as if the notional multi-role fighter program started in 1988. This is when the F/A-18C/D was being developed and a plan for the E/F version was being formulated by McDonnell Douglas and the U.S. Navy [171]. This time frame has a significant meaning because it was when the Cold War between the Western World and the Soviet Union was at its culmination and the sudden collapse of the Soviet Union in 1991 was not anticipated.

This chapter starts with the rationale behind the selection of the test case as a notional multi-role fighter based on the F/A-18C among many other options. Then, the EvoLVE process **Steps 1** to **9** are presented. Some of the finding are discusses at the end of the chapter.

7.1 Selection of the Baseline Aircraft and Time frame

First, military aircraft were preferred to commercial aircraft. Military aircraft design is driven by rather complicated, yet solid requirements. Design usually starts from well-defined needs, the documentation of which is often available to the public. In opposition to common sense, requirements and aircraft performance data for military aircraft are easier to obtain from public sources than those of commercial aircraft, because military airplanes are funded by taxpayers. As a downside, modeling military aircraft is generally more challenging because they are usually designed to perform more than one mission. Each of the missions is associated with a mission profile(s) and internal/external storage configurations. The mission profiles may cover both super-sonic and sub-sonic regimes. Commercial transports fly rather simple missions. The key performance parameters are range and payload (or the number of passengers), and the design is mostly driven by one factor, economics. However, it is harder to obtain accurate and comprehensive data on commercial aircraft, for they are proprietary.

Another criterion for model selection was time frame and availability of adequate evolution history. A modern time frame was preferred to enable a game-play in the context of modern doctrine. The ways fighters were operated in the battlefields in the early Cold War era and after the Cold War era were very different from each other. Time frame dictates the external environment that determines design requirements.

Time frame is also related to the richness of evolution history and data availability. While first and second generation jet fighters, such as F-86, F-4, and F-5 have interesting evolution histories, their design specifications are not well-documented digitally. The fourth generation fighters, such as F-22 and F-35 not only lack the evolution history but they are also classified. Performance and cost data of the fighters that were developed in the 1970s and 1980s are well-documented and less sensitive than the modern fighters, such as F-22 or F-35, and many of them have more than one derivative.

Among many fighters, the F/A-18 and the F-16 met the above criteria, and the decision was made to pursue the F/A-18. The F/A-18 had a unique history that made it a perfect candidate for the validation of EvoLVE. As summarized in §3.1.1.3, the F/A-18, as the first multi-role fighter in history, took two evolution steps: from the original version of A/B to C/D, and then from C/D to E/F. The C/D versions were retrofits of A/B, keeping most of the subsystem unchanged except the engines and avionics. However, the E/F versions were "resized" or photographically scaled up from C/D to provide for significantly more capability. Although the DoD designated the upgrade from C/D to E/F as a "major modification", the E/F version has only 10% in common with the C/D version.

This major capability upgrade provides for a very good example case, against which a scalable aircraft model can be validated. EvoLVE requires a vehicle model at the baseline requirement and a series of scaling laws to be able to quantitatively capture the impact of requirement growth in the future. Such scaling laws are calibrated using both physics and actual vehicle evolution data. Those scaling laws are considered more valid

within the range of the initial and a derivative aircraft design points, and extrapolation beyond the actual data might introduce the danger of not capturing important physics. While many other derivative aircraft possibly provide such data points, the F/A-18's wide expansion of both vehicle geometry and capability through an evolutionary upgrade minimizes the need for extrapolation.

In conclusion, the two derivative versions of the F/A-18 provide two vital and rare aircraft growth examples, which can be benchmarked to generate plausible growth strategies and scenarios.

7.2 The First-Stage Requirement: Step 1

The first-stage requirement is either given from the customer or formulated by the aircraft manufacturer using the conventional system engineering tools, such as market analysis, brainstorming, QFD, etc. In this application, it is assumed that the hypothetical first-stage requirement is given from the US Navy in the form of ORD issued in FY1988. ORD defines a specification of a fighter aircraft in terms of the KPPs with associated mission profiles. A summary of the hypothetical ORD is given as[*]:

> A new fighter aircraft performing both fleet air defense and attack role for the US Navy is being developed to replace F-4 on fighter missions and A-7 on attack missions. The vehicle shall reach IOC in 7 years (FY 1995), and the goal is to minimize the acquisition cost while meeting or exceeding all imposed key performance parameters (KPPs). The KPPs shall be evaluated with the two given mission profiles. Production quantity of the vehicle is 627 units for the US Navy.

---

[*]The hypothetical mission and requirement is very close to those of F/A-18C/D and E/F that are summarized in APPENDIX B.

The KPPs and their thresholds are defined in Table 12. The conditions for the KPPs are the mission profiles given in the following section. These requirements and KPPs constitute the first-stage objective (f_1) and constraints ($\mathbf{g}_1$).

7.2.1 Mission Profiles

The interdiction (hi-lo-lo-hi) and fighter escort with medium altitude combat are depicted in Figure 37 and Figure 38. The figures are attached with the tables of fuel usage, range, speed, altitude, and throttle setting conditions for each of the mission segments. These mission profiles are the standard mission profiles found in MIL-STD-3031 [172].

Interdiction mission profile includes fuel to warm-up, take-off, accelerate to climb speed, military power climb, cruise at best cruise altitude and Mach number, 50 nm penetration at 2000 ft before expending the air-to-ground bombs, cruise back, descent without distance credit, and reserve of 3500 lb of fuel.

The fighter escort mission includes fuel to warm-up, take-off, accelerate to climb speed, military power climb, cruise at best cruise altitude and Mach number, combat at 15000 ft expending half the missiles and ammunitions, return to the base, and reserve. The reserve mission includes 20 minute sea level loiter at best endurance speed, plus 5 percent of the initial fuel. These two mission profiles, interdiction and fighter escort, are used as the design missions of the notional fighter with the following external store conditions:

Attack configuration: two AIM-9s, FLIR, NAVFLIR, four MK-83 bombs, and three external fuel tanks (see Figure 51 for the allocation of the hard points)

Fighter configuration: two AIM-9s at the wing tips and two AIM-7s at the two fuselage stations (see Figure 52 for the allocation of the hard points)

145

	Segment	Fuel	Time	Distance	Speed	Altitude	Thrust Setting
A	Warm-up, Takeoff	20 min @ ground idle + 30 sec @takeoff/maximum A/B + fuel to accelerate from obstacle clearance to climb speed @ IRT					
B	Climb				Minimum time climb schedule	Takeoff to optimum cruise	Intermediate
C	Cruise				Optimum cruise	Optimum cruise	
D	Descent	None	None	No credit		End cruise to 2000 ft press alt.	
E	Penetration			50 nm	0.8 Mach	2000 ft press alt.	
F	Combat	One 2000ft energy exchange + one 180 deg turn at Virt - 50 ktas, expend air-to-ground stores					Max A/B
G	Withdrawal			50 nm including accel	0.8 Mach	2000 ft press alt.	
H	Climb				Minimum time climb schedule	2000 ft press alt. to optimum cruise	Intermediate
I	Cruise				Optimum cruise	Optimum cruise	
J	Descent	None	None	No credit		End cruise to landing	
K	Reserves	4000 lbs of fixed fuel					

Figure 37: Interdiction Mission Profile (Hi-Lo-Lo-Hi)

	Segment	Fuel	Time	Distance	Speed	Altitude	Thrust Setting
A	Warm-up, Takeoff	20 min @ ground idle + 30 sec @takeoff/maximum A/B + fuel to accelerate from obstacle clearance to climb speed @ IRT					
B	Climb				Minimum time climb schedule	Takeoff to optimum cruise	Intermediate
C	Cruise				Optimum cruise	Optimum cruise	
D	Descent	None	None	No credit		End cruise to 15,000 ft press alt.	
E	Combat	One 360 deg turn @Mach 1.2 (max A/B) + two 180 deg turn @ Mach 0.9 (max A/B), expend half of ammo and missiles.					Max A/B
F	Climb				Minimum time climb schedule	15,000 ft press alt. to optimum cruise	Intermediate
G	Cruise				Optimum cruise	Optimum cruise	
H	Descent	None	None	No credit		End cruise to landing	
I	Reserves	20 min + 5% of initial fuel		No credit	Maximum endurance	Sea level	

Figure 38: Fighter Escort Mission Profile (Medium Altitude Fighter Sweep)

7.2.1.1   Key Performance Parameters

The key performance parameters and their threshold values are listed in Table 12. The KPPs are classified in three categories: mission performance, carrier suitability, and fighter performance. Mission performance measures the one-way unrefueled range for the two design missions. For the fighter escort mission, mission radius is measured using internal fuel only without external fuel tanks. The aircraft will fly the fighter escort mission profile in Figure 38 with two AIM-9s and two AIM-7s. The interdiction radius is measured by flying the mission profile in Figure 37 in attack configuration, i.e. three external fuel tanks. The size of the external fuel tanks is a design variable and will be determined later. The carrier suitability is measured by four parameters: recovery payload, launch wind over deck (LWOD), recovery wind over deck (RWOD), and approach speed. The definitions, calculation procedures, and equations of these parameters are provided in §7.6.5.

To measure the fighter's point-performance, five parameters—combat ceiling, specific excess power, acceleration, turn rate, and usable load factor—are used. All these metrics shall be measured in the combat configuration: two AIM-9s, two AIM-7s, and 60% of total internal fuel. In addition, all the fighter performance parameters are measured at maximum power with afterburners on. Specific excess power is measured during one-g level flight at Mach 0.9 at 10,000 ft. Acceleration from Mach 0.8 to 1.2 is conducted at 35,000 ft. Sustained turn rate is measured at 15,000 ft. Detailed definitions and calculation procedures are provided in §7.6.6.1.

Table 12: The Key Performance Parameters of the First Stage

Category	Key Performance Parameters	Threshold	Unit
Mission	Fighter escort mission radius	> 350	nm
Performance	Interdiction mission radius	> 360	nm
Carrier	Recovery payload	> 6000	lb
Suitability	Launch wind over deck	< 30	knot
	Recovery wind over deck	< 15	knot
	Approach speed	< 150	knot
Fighter	Combat ceiling	$> 50,000$	ft
Performance	Specific excess power at 0.9M/10,000 ft	> 600	hp
	Acceleration from 0.8M to 1.2M at 35,000 ft	< 70	sec
	Turn rate at 15,000 ft	> 11.5	rad/sec
	Usable load factor	> 7.5	g

7.3 Evolution of the Requirement—Random Variables and Scenarios: Step 2

The main distinction between EvoLVE and conventional single-stage aircraft design processes is that EvoLVE expands the problem beyond the current (single-stage) problem in order to incorporate the future into the current design from the origin. Expansion of the conventional single-stage design process to the two-stage design process starts with identifying evolution paths of the requirements.

In order to predict what will happen to the vehicle-level requirement in the future, it is natural to start from the operational environment where the vehicle is being utilized. This system-of-systems type study would be based on projections of both enemy and friendly force capability under plausible SoS level scenarios, such as theater-level conflict scenarios, and can provide the future requirement of the baseline vehicle in a deterministic or probabilistic manner.

The Congressional Budget Office (CBO) conducted a SoS level study involving F/A-18 in 1987. The results plan Navy aircraft force projections into the 1990s and are introduced in §A.1. The study was conducted at the US Navy Air Wings level including F/A-18 in the European theater under the influence of Soviet Union bombers and fighters. The CBO study suggested how the requirements of F/A-18 should evolve towards the 1990s.

While not available to the public, a system specific System Threat Assessment Report (STAR) of the F/A-18 was created by the Naval Maritime Intelligence Center (NAVMIC), including a detailed description of threat projections. Although such information was not completely available to the author, it is not difficult to reason that such studies led to the ORD of the F/A-18E/F, part of which is introduced in APPENDIX B.

It is envisaged that such independent SoS level studies by CBO and NAVMIC could more systematically identify the random variables and the probability functions at the vehicle system level. The potential of concurrently applying EvoLVE at two different hierarchical levels is proposed in §8.2.4 as part of the future research opportunities.

In the current study however, the random variables along with the associated Probabilities Density Functions (PDFs) were defined trying to follow the actual evolution of the F/A-18's requirements as closely as possible. Among the requirements that changed from the F/A-18C/D to E/F, the most significant four parameters—fighter escort radius, interdiction mission radius, recovery payload, and avionics weight—were identified as the random variables. Then, triangular PDFs were assumed for all random

variables. Triangular PDFs are determined by three parameters: minimum (a), most-likely (m), and maximum values (b) as follows:

$$f(z \mid a, m, b) = \begin{cases} \dfrac{2(z-a)}{(b-a)(m-a)} & \text{for } m \le z \le b \\[3em] \dfrac{2(b-z)}{(b-a)(b-m)} & \text{for } m \le z \le b \\[3em] 0 & \text{otherwise} \end{cases} \tag{53}$$

The list of random variables and their assumed probabilities are in Table 13. The minimum and maximum values of the random variables are slightly higher than the F/A-18C/D's and E/F's requirements, respectively, so that most of the requirement space defined by the random variables is covered by the actual evolution history of the F/A-18C/D and E/F. The most likely values of the random variables are the average of the minimum and maximum values. Finally, it was also assumed that the random variables are independent of each other. The triangular PDFs of the four random variables are illustrated in Figure 39.

Table 13: Random Variables and Probability Density Functions

	Stage 1	Stage 2				Unit
	Baseline	Min	Most Likely	Max	Function Type	
Fighter escort radius	350	350	420	490	PDF/Triangular	nm
Interdiction radius	410	410	460	510	PDF/Triangular	nm
Recovery payload	4,500	7,000	8,400	9,800	PDF/Triangular	lb
Avionics weight	1,289	1,300	1,400	1,500	PDF/Triangular	lb
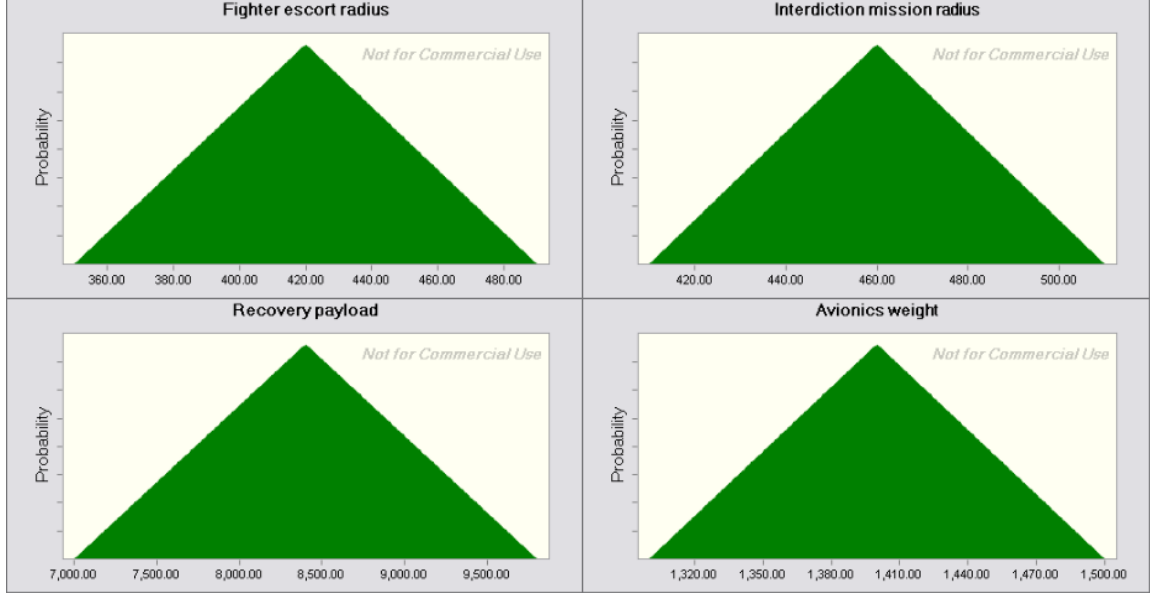
Figure 39: Triangular Probability Density Functions of the Random Variables

Combinations of the realization of the random variables constitute scenarios, and those continuous random variables $\boldsymbol{\omega} \in \boldsymbol{\Omega}$ in a probability space $(\boldsymbol{\Omega}, F, P)$ with $\boldsymbol{\Omega} \subseteq \Re^4$ as defined in Table 13 can generate an infinite number of scenarios. In this section, however, only five scenarios $\boldsymbol{\omega}_s$, $s = 1 \dots, 5$ were selected from the infinite set in $\boldsymbol{\Omega}$ and are provided in Table 14. The five scenarios were numbered in a way that each of the requirements gets more demanding as s increases, i.e. $\omega_{1v} < \omega_{2v} < \omega_{3v} < \omega_{4v} < \omega_{5v}$ where ω_{sv} is the vth element of the sth scenario vector $\boldsymbol{\omega}_s$ defined as:

$$\boldsymbol{\omega}_s = \begin{bmatrix} \omega_{sv} \\ \omega_{sv} \\ \omega_{sv} \\ \omega_{sv} \end{bmatrix} \tag{54}$$

The first and last scenarios $\boldsymbol{\omega}_1$ and $\boldsymbol{\omega}_5$ are the minimum and maximum bounds of the PDFs of $\boldsymbol{\omega}$ as defined in **Step 2**. The third scenario $\boldsymbol{\omega}_3$ is the expected values of the PDFs, i.e. $\boldsymbol{\omega}_3 = \overline{\boldsymbol{\omega}} \equiv \mathbb{E}(\boldsymbol{\omega})$. Two other scenarios are based on either the F/A-18E/F's

requirements or actual performance. The forth scenario ω_4, named *Block 10 plus* scenario, is very close to the actual F/A-18E/F's performance. The second scenario ω_2, named *Block 10* requirement, is based on the F/A-18E/F's threshold requirement given in Table 62.

Table 14: The Five Discrete Scenarios for the Deterministic Study

| Scenario Number | ω_1 | ω_2 | ω_3 | ω_4 | ω_5 |
Scenario Name	Minimum	Block 10	Average	Block 10p	Maximum
Fighter escort radius, ω_{s1}	350	410	420	475	490
Interdiction radius, ω_{s2}	410	430	460	504	510
Recovery payload, ω_{s3}	7,000	8,000	8,400	9,700	9,800
Avionics weight, ω_{s4}	1,300	1,350	1,400	1,411	1,500

7.4 Baseline Design: Step 3

Once the current requirement and its evolution paths in the future are defined, the next step is to find out how those requirements would be met. In this step, the candidate solutions to the corresponding functional requirements are synthesized in the physical domain and a baseline platform(s) is down-selected based on both qualitative and quantitative evaluations.

In this study, since the baseline platform was selected as a notional multi-role fighter based on the F/A-18C, the geometrical characteristics of the F/A-18 are introduced first and a subset of the F/A-18's geometric parameters are selected as design variables. All four variants of the Hornet (A, B, C, and D) are geometrically identical. The geometrical traits of the F/A-18 family, including the latest E/F versions, contain: a fixed oblique shock inlet; a moderate swept, low aspect ratio wing with NACA 65A airfoil and variable camber; area-ruled wing/body integration; large, highly-swept leading

edge extensions (LEXs); two low-bypass ratio, afterburning turbofans; and a twin tail. Dimensional data of the F/A-18 were obtained from NASA Technical Memorandum 107601 [173] and summarized in Table 15.

Table 15: F/A-18 Hornet Dimensional Data [173]

Total Airplane		Leading Edge Extension	
Net Wetted Area	2028 ft²	Planform Area	56 ft²
Overall Length	56 ft	Wetted Area	210 ft²
Overall Height	15.3 ft	Leading Edge Sweep	43 deg
Fuselage		Incidence	6 deg
Length	53 ft	**Horizontal Tails**	
Maximum Width	7.6 ft	Exposed Area	88.1 ft²
Wetted Area	890 ft²	Wetted Area	176 ft²
Wing		Aspect Ratio	2.4
Area	400 ft²	Taper Ratio	0.46
Wetted Area	562 ft²	Leading Edge Sweep	47.2 deg
Span	37.42 ft	c/4 Sweep	42.8 deg
Aspect Ratio	3.5	Dihedral	-2 deg
Root Chord	15.86 ft	Span	14.67 ft
Tip Chord	5.52 ft	Root Chord	8.23 ft
Mean Aerodynamic Chord	11.52 ft	Tip Chord	3.79 ft
Leading Edge Sweep	26.7 deg	Mean Aerodynamic Chord	6.28 ft
c/4 Sweep	20 deg	Airfoil	NACA 65A
Taper Ratio	0.35	Thickness at Root	6 % chord
Dihedral	-3 deg	Thickness at Tip	2 % chord
Twist	4 deg	**Vertical tails**	
Incidence	0 deg	Area	52 ft² each
Airfoil	NACA 65A	Wetted Area	104 ft² each
Thickness at		Aspect Ratio	1.2
Wing Station 56.876	5 % chord	Taper Ratio	0.4
Wing Station 145.39	3.5 % chord	Leading Edge Sweep	41.3 deg
Tip Chord	3.5 % chord	c/4 Sweep	35
Leading Edge Flaps		Root Chord	9.42 ft
Type	Plain	Tip Chord	3.75 ft
Area	48.4 ft²	Mean Aerodynamic Chord	6.99 ft
Span	13.8 ft	Airfoil	NACA 65A
Trailing Edge Flaps		Thickness at Root	5 % chord
Type	Single Slotted	Thickness at Tip	3 % chord
Area	61.9 ft²	**Rudders**	
Span	8.72	Area	7.72 ft² each
Ailerons		Span	5.21 ft
Type	Single	Percent Chord	
Area	24.4 ft²		
Span	5.68 ft		
Percent Wing Span	68.9 – 100 %		

While almost all the geometrical parameters in the above table are used in **Step 5** to create a F/A-18 model, only a small subset of such parameters are identified as design variables. The design *parameters* are fixed throughout the study at the value of the F/A-18C while the design *variables* are varied to *resize* the vehicle *photographically*: the geometric traits of the F/A-18 family are preserved, and the size of subsystems, such as wing, tails, fuselage, engines, etc. are varied.

The set of twelve design variables were finalized as listed in Table 16 after much iteration between **Steps 4-6**. The design variables are the minimum variables to sufficiently scale the vehicle and calculate $\mathbf{g}_1$ and f_1. The first five variables (from x_1 to x_5) define the shape of the wing. Engine thrust, x_6, is the maximum sea level static thrust of one engine, and the number of engines was fixed at two.

Reference weight for design load factor (DLF), x_7, is the reference gross weight by which the structural design of the vehicle is determined. Design load factor was fixed at 7.5 g's, which gives the ultimate load factor of 11.25 g's after the typical 1.5 times margin. Therefore, the vehicle is design to withstand up to 11.25 g's at x_7. This weight should be equal to or greater than the actual combat weight, which is the gross weight in combat configuration with 60% of the internal fuel.

Operational landing weight, x_8, is the reference gross weight by which landing gears are designed. Therefore, x_8 must be equal to or greater than the actual aircraft landing weight for safe landing. Landing weight also affects several carrier-suitability requirements, such as approach speed, bring back weight, and wind-over-deck speeds, which are calculated in §7.6.5.

Internal and external fuel weights, x_9 and x_{10}, are usable fuel weights that are carried internally or externally. JP-5 fuel at 6.8 US gallon/pound was assumed. Reference thrust for aft-body sizing, x_{10}, is the reference engine thrust to size the aft-fuselage section where two turbofan engines and related subsystems including inlets and nozzles are mounted internally. The value of x_{10} should be equal to or greater than the engine thrust, x_6. Finally, fuselage length, x_{12}, was used to scale the forward and mid fuselage where avionics and equipments are placed.

While the baseline values of the variables are not very meaningful, they are listed in the table defining the baseline aircraft $\mathbf{x}_0$. Note that the baseline design is slightly different from the F/A-18C. Justifications for the selection of the design variables and more detailed descriptions are provided in **Steps 5** and **6** when appropriate.

Table 16: Design Variables and the Baseline Notional Fighter

Symbol	Name	Baseline	Unit
x_1	Wing area	400	ft^2
x_2	Wing aspect ratio	3.5	n/a
x_3	Wing taper ratio	0.35	n/a
x_4	Wing t/c	0.042	n/a
x_5	Wing sweep angle	20	deg
x_6	Engine thrust	17,754	lb
x_7	Reference weight for DLF	32,000	lb
x_8	Operational landing weight	33,000	lb
x_9	Internal fuel weight	10,810	lb
x_{10}	External fuel weight	6,720	lb
x_{11}	Reference thrust for aft-body sizing	17,920	lb
x_{12}	Fuselage length	53	ft

7.5 Evolution Strategies: Step 4

Step 4 identifies the alternatives to meet the future requirements defined in **Step 2**.

While the baseline platform selected in **Step 3** was to respond to the first-stage

requirement identified in **Step 1**, **Step 4** formulates the possible ways or strategies to

meet the evolving (growing) requirement. In addition, the set of candidate technologies

that will be considered in the second-stage design are also identified.

7.5.1 Aircraft Evolution Strategies

Six aircraft evolution strategies were defined, including a New-design (ND), the Ad-hoc

(AH) upgrade strategy, three Deterministic preplanning strategies (DetPPs), and the

Stochastic preplanning strategy (StoPP).

The question, "what would be the best way to meet the long-term requirement?",

would be ideally answered by considering not only the new requirement but also the

projection of the friendly force structure at the Navy Air Wing fleet level, such as a

retirement schedule of the existing fleet and other planned naval aircraft development

programs. The study expanded to the SoS level would identify multiple ND strategies.

For example, the option of upgrading F/A-18C/D can be compared against purchasing

F-14D, F-35, ATA, NATF, AFX etc. as the US government did (see §3.1.1.3) by

assigning them to each of the ND strategies. However, inclusion of multiple platforms

requires modeling and simulation of all included platforms, and thus is avoided. In this

study, all the alternatives were limited to a version of the F-18-like notional fighter to

bind the problem. Therefore, the ND strategy considered here is assumed as another

notional fighter design based on F-18 and is developed in isolation from the first-stage design so that no cost savings utilizing commonality from its predecessor is allowed.

The DetPP requires that the designer choose only one particular realization of the random variables or a scenario. Typically, the designer chooses a handful of scenarios, such as the worst case, most likely, and the best case to cover the random space and compare the results. In this study, a scenario-based study was performed by selecting three scenarios ω_2, ω_3, and ω_4 and assigning them to three DetPP strategies. These three DetPP strategies were named DetPP(Block10), DetPP(Average), and DetPP(Block10p), following the scenarios names assigned to them.

Finally, the StoPP is solely determined by preplanning for the future, incorporating *all* possible scenarios in the probability space $(\Omega, \widehat{\mathfrak{F}}, P)$ defined in Table 13. Table 17 summarizes the six strategies evaluated in this study.

Table 17: The Vehicle Evolution Strategies

Strategies	New Design	Ad-Hoc Upgrade	Moderate Det. Upgrade	Average Det. Upgrade	Aggressive Det. Upgrade	Stochastic Upgrade
Number	1	2	3	4	5	6
Predicted scenario	-	-	ω_2	ω_3	ω_4	$\omega \in \Omega$

7.5.2 Technological Opportunities

Technological development over time often provides options to open up the design space or improve the existing system. A potential technology candidate that can be applied to the second-stage design is identified in this **Step 4**. In order to retain the similarity to the actual F/A-18 evolution history, the following four technologies were considered:

- LEX upgrade for higher C_{Lmax}
- Low RCS capability
- Conformal fuel tank
- New engine core

All of these technologies were either applied or considered when the F/A-18C/D was upgraded to the E/F. The F/A-18E/F's LEX was not only enlarged from that of the C/D but also redesigned to increase the maximum lift capability of the vehicle, which favorably impacted the vehicle's takeoff, landing, and approach performance. Details of C_{Lmax} increase are found in §7.6.2.2.

Another important upgrade from the C/D to the E/F versions was the reduction of the RCS to reduce observability and thus, increase survivability. The reduction of radar cross section (RCS) was not achieved by redesigning the fuselage, wings, and tails, but was accomplished by realigning the surface edges, filling the gaps between the panels and openings, and coating the navigation lights, canopy, and wind shields with metalized paint [174]. Figure 40 illustrates the RCS reduction treatments applied to the F/A-18E/F.
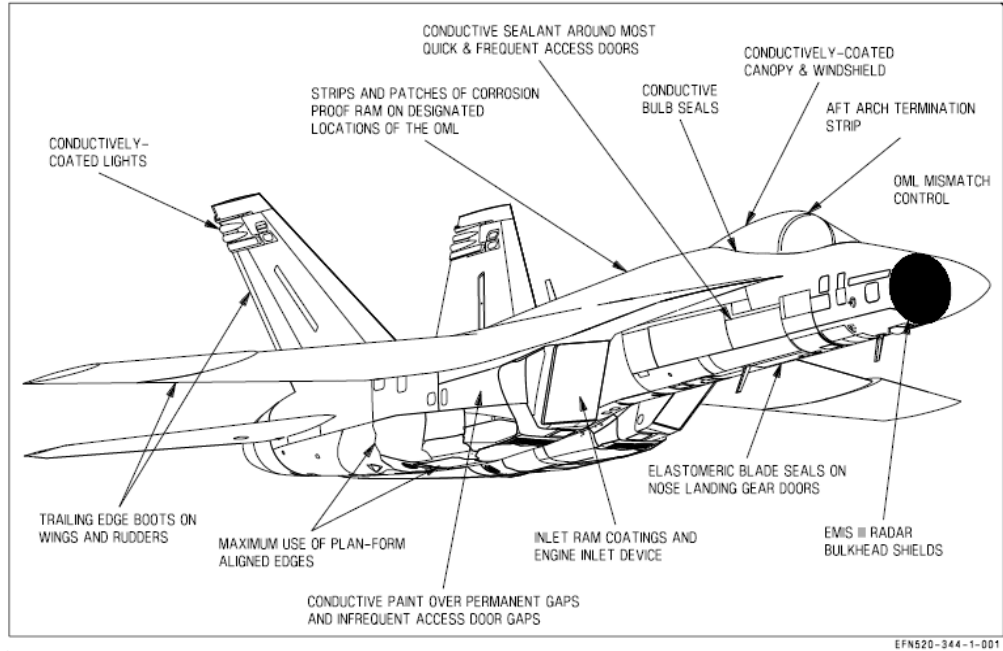
Figure 40: RCS Reduction of the F/A-18E/F [175]

Conformal fuel tank is a technology by which the fuel capacity of an aircraft can be augmented without severely degrading the aerodynamic efficiency of the vehicle. Compared to the conventional external fuel tanks that are mounted under the fuselage or wings using pylons, conformal fuel tanks add significantly less drag, which enables a better range increase per gallon of fuel added. However, they cannot be jettisoned during flight, unlike conventional external fuel tanks.

The conformal fuel tank is a matured technology as it is found under the wing roots of the F-15 Strike Eagle as shown in Figure 41 or behind the cockpit of the F-16. The technology was also considered to improve the range capability of the F/A-18C/D by McDonnell Douglas [76] but has not been implemented so far. Despite the dismissal of the technology in the Super Hornet program, it was included in this work because the technology was necessary to create and calibrate the cost model. More details about all the listed technologies and the modeling process are provided in **Step 6**.

Figure 41: Conformal Fuel Tanks of the F-15 Strike Eagle [176]

7.6 Modeling and Simulation I: Step 5

In **Step 5**, a modeling and simulation environment of the baseline vehicle, defined in **Step 3**, is created and validated. A computer simulation model of the F/A-18C was developed by the author to conduct this study. The model was validated using public domain data as exhaustively as possible. The modeling and simulation process was largely based on NASA's Flight Optimization System (FLOPS) [177]. However, computer codes were written to calculate some of the aircraft performance that FLOPS does not calculate. In the subsequent sections, the process of geometry, aerodynamics, weight, and propulsion modeling and validation are described. Then, an entire aircraft system is synthesized and validated against the actual F/A-18 data collected in APPENDIX B using various mission profiles. It is important to note that the F/A-18 model was created as a *scalable* model. Therefore, system weight, drag polar, and engine performance were not hard coded but calculated as a function of design parameters.

7.6.1 Limitation of the Model

The entire modeling process was done using strictly publicly available information only. No classified or proprietary data were consulted or utilized during the modeling and calibration process. A complete data set of a specific F/A-18 version was not available. Instead, the public domain information was available piecewise. For example, the weight breakdown of the C version with a 404-GE-402 engine was available, whereas the F/A-18 performance manual was available with the 404-GE-400 engines and the 414-GE-400 engines only. Drag polars at some altitudes and Mach numbers were available on the A/B/C/D variants. Mission profiles that the fighters actually flew were not identified completely, thus those conditions had to be assumed to follow the standard military mission profile given in the MIL-STD-3031 [172].

7.6.2 Aerodynamics Modeling

Aerodynamics modeling was conducted in three parts. The first part briefly introduces the aerodynamic characteristics that are unique to the F/A-18 family in relation to its geometric traits. Then, drag polar of the clean configuration is generated and calibrated. The second part discusses aerodynamics at a high angle-of-attack (AOA). The third part models drag increment due to external stores.

7.6.2.1 *Aerodynamic Characteristics and Drag Polar in Clean Configuration*

All of the F-18 Hornet family, from the YF-17 to the F/A-18E/F Super Hornet, uses the NACA 65A airfoil [173, 178]. The NACA 65A airfoil is an uncambered high-speed laminar flow airfoil with a maximum thickness of 50% [179]. The most distinctive geometric and aerodynamic feature of the F/A-18 is its variable camber wing and leading edge extension (LEX) [70]. The wing's leading edge (LE) flaps and trailing edge
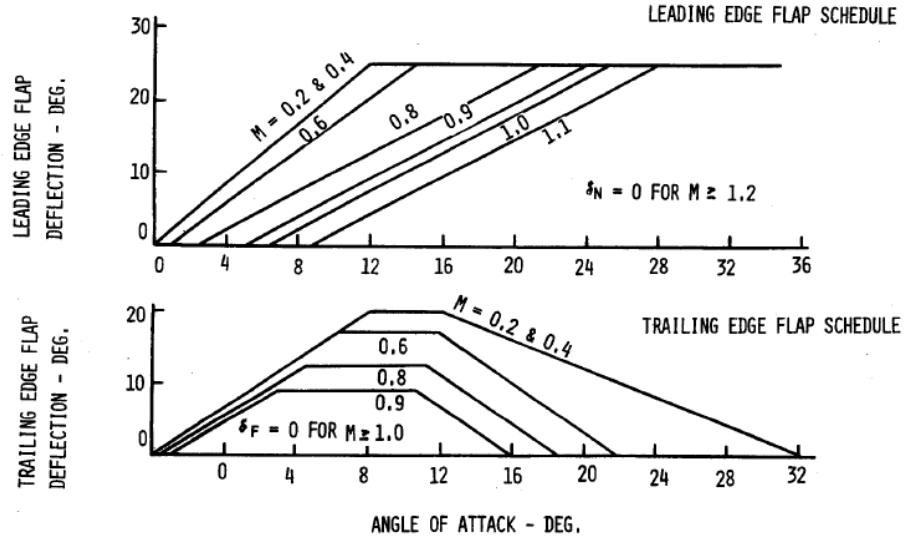
Figure 42: F/A-18 Flap Deflection Schedules [180]

(TE) flaps are automatically deflected according to the Mach number and AOA to improve maneuverability by reducing drag-due-to-lift. Both leading and trailing edge flap deflection schedules are provided in Figure 42. LEX produces high-energy vortices, which increase the maximum lift and control system effectiveness at a high angle of attack [78]. When used with a variable cambered wing, the F/A-18's highly cambered LEX synergistically increases subsonic maximum lift, reduces both subsonic and supersonic drag-due-to-lift, and improves lateral control effectiveness.

The effect of variable camber and LEX on the F-18 was studied by Patierno [70]. Figure 43 compares drag-due-to-lift at Mach 0.8 of the basic F-18 wing, the basic wing with LEX, and the variable camber wing with LEX. The figure clearly shows that the synergistic effect of variable camber and LEX in solid line creates significantly less drag-due-to-lift at all angles of attack tested than the same wings without variable camber or LEX.
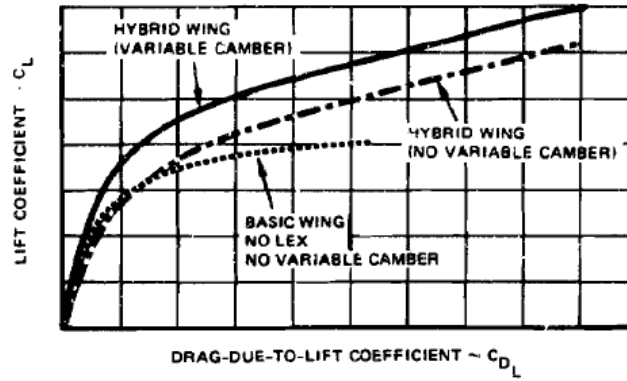
Figure 43: Effect of LEX and Variable Camber [70]

The F/A-18's drag polar was generated using the internal aerodynamics module of FLOPS. The aero module in FLOPS uses the Delta method, an empirical drag correlation technique developed from nineteen subsonic and supersonic military aircraft and fifteen advanced or supercritical airfoil configurations, according to NASA CR 151971 [181]. Regarding the applicability and limitation of the method, NASA CR 151971 states that:

> [t]he Delta Method may be used for estimating the clean wing drag polar for cruise and maneuver conditions up to buffet onset, and to approximately Mach 2.0. … The method is applicable to wind tunnel models as well as to full-scale configurations. … Results obtained using this method to predict known aircraft characteristics are good and agreement can be obtained within a degree of accuracy judged to be sufficient for the initial processes of preliminary design.

Since the method lacks the capability to model those sophisticated effects of LEX and wing camber scheduling, the aero model created in FLOPS was calibrated using actual drag polar of the F/A-18. F/A-18 drag polar data were collected from several public domain sources. Among them are NASA TM 3414 [182], which shows F/A-18 drag polar at Mach 0.9 in Figure 44 and zero-lift-drag coefficients (C_{Do}) and maximum lift-to-drag-ratio (L/D_{max}) at Mach 0.6, 0.9, and 1.3 in Figure 45. Moreover, Siewert [180] provides trimmed lift coefficient versus drag-due-to-lift curves at Mach 0.6, 0.8, and

0.9 with various LE and TE flap scheduling as shown in Figure 46, Figure 47, and Figure 48. The effect of optimal LE and TE flap deflection is to significantly reduce the lift-related drag in Mach 0.6 and 0.8 as observed in the figures. The external store configurations were not stated in the references, so it was assumed that the data are for the clean configuration—no external stores but the two AIM-9s at the tips.

C_L for several load factors					
	Load factor, g units				
A/C	1.0	1.5	2.0	2.5	3.0
X-29A	0.243	0.365	0.486	0.608	0.729
F-15C	0.166	0.249	0.332	0.415	0.498
F-16C	0.202	0.303	0.404	0.505	0.606
F/A-18	0.220	0.330	0.440	0.550	0.660
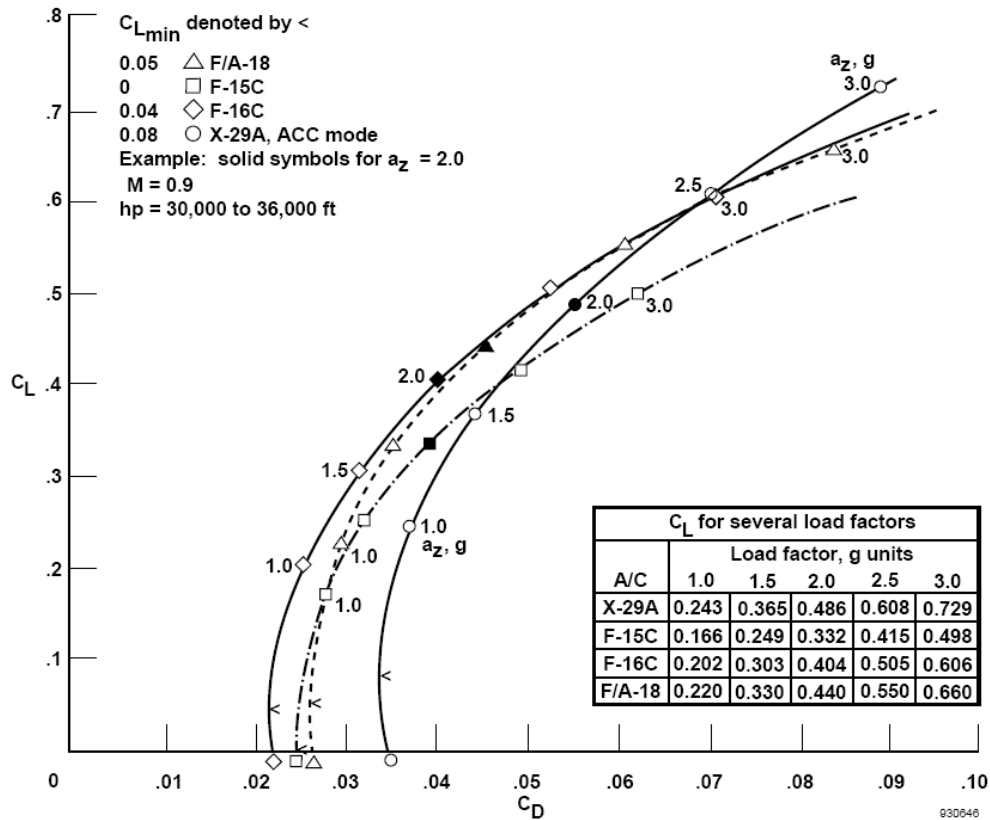
Figure 44: F/A-18 Drag Polar at Mach 0.9 [182]
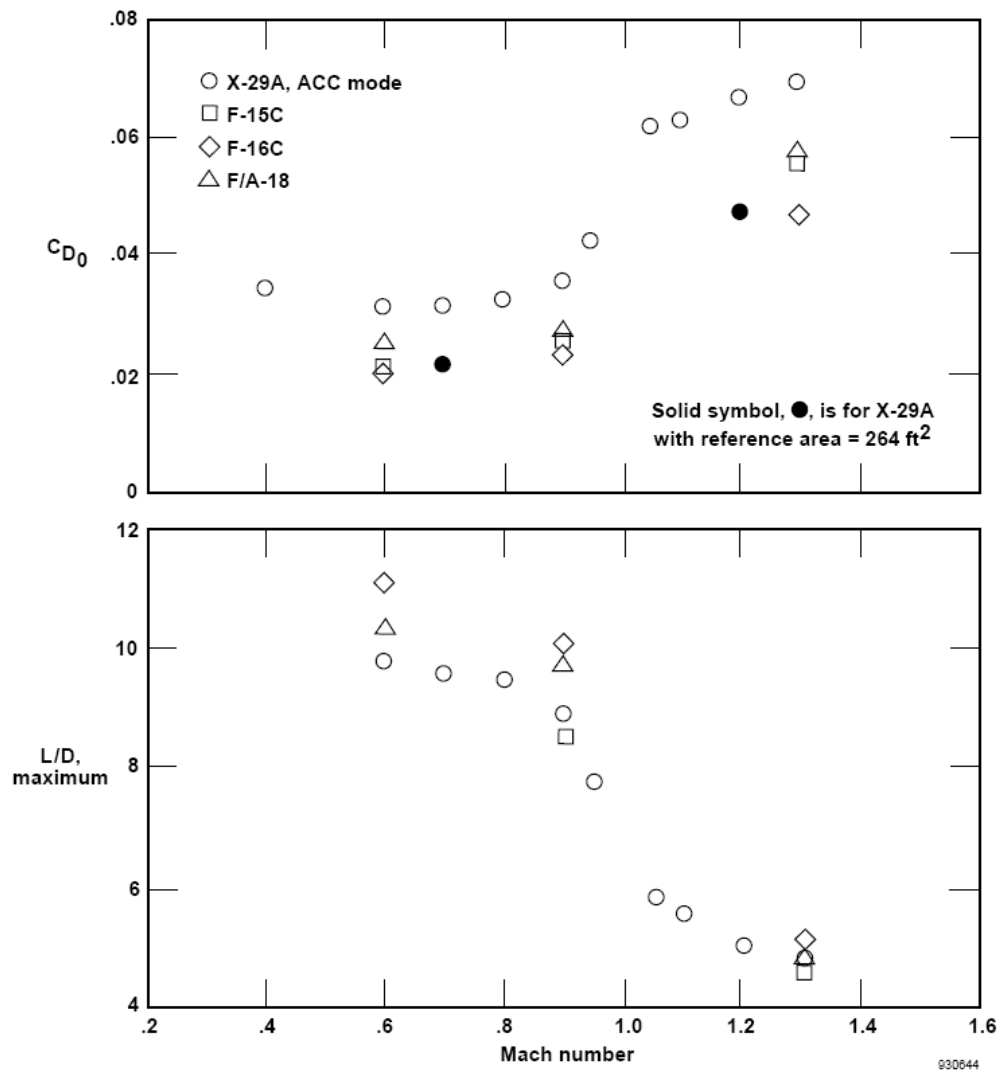
Figure 45: F/A-18 Zero Lift Drag Coefficient and Maximum L/D [182]
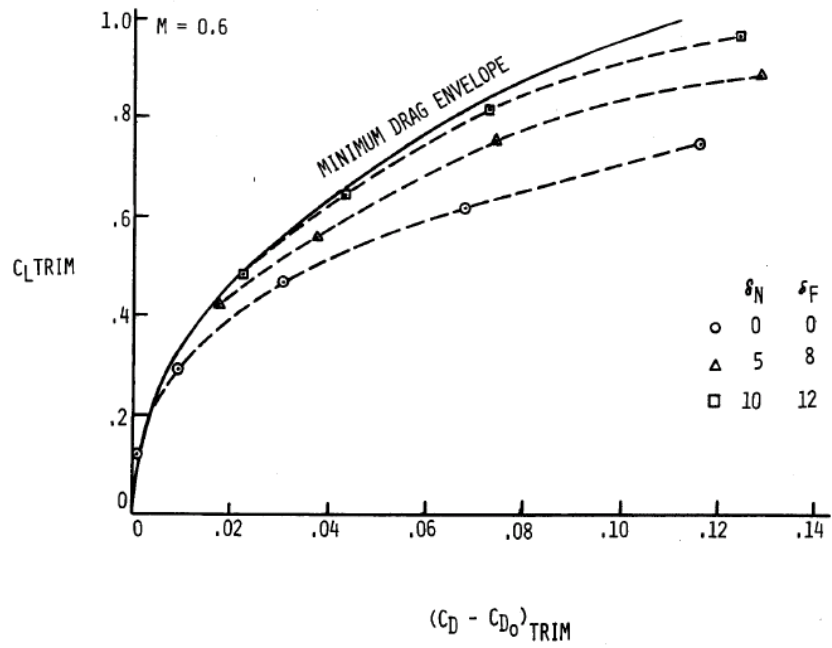
Figure 46: F-18 Trimmed Drag-Due-to-Lift at Mach 0.6 [180]
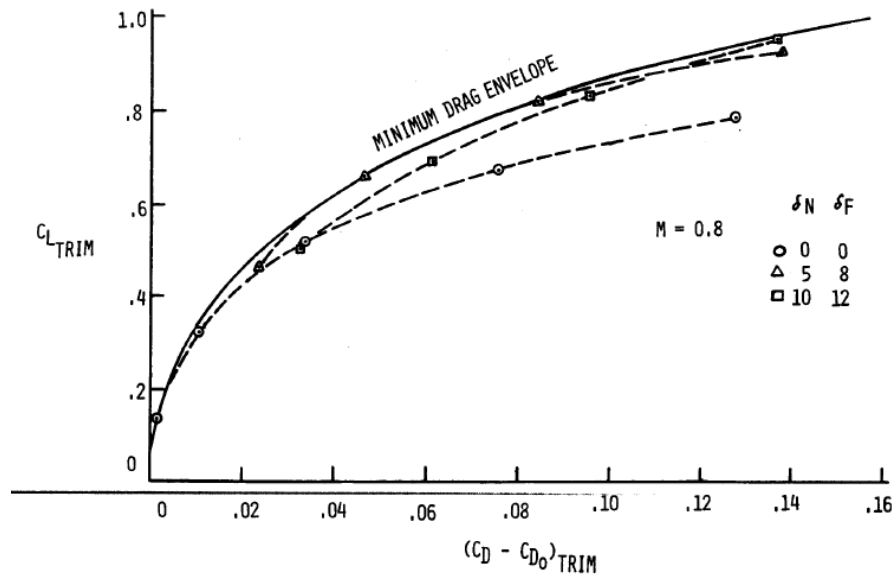
Figure 47: F-18 Trimmed Drag-Due-to-Lift at Mach 0.8 [180]
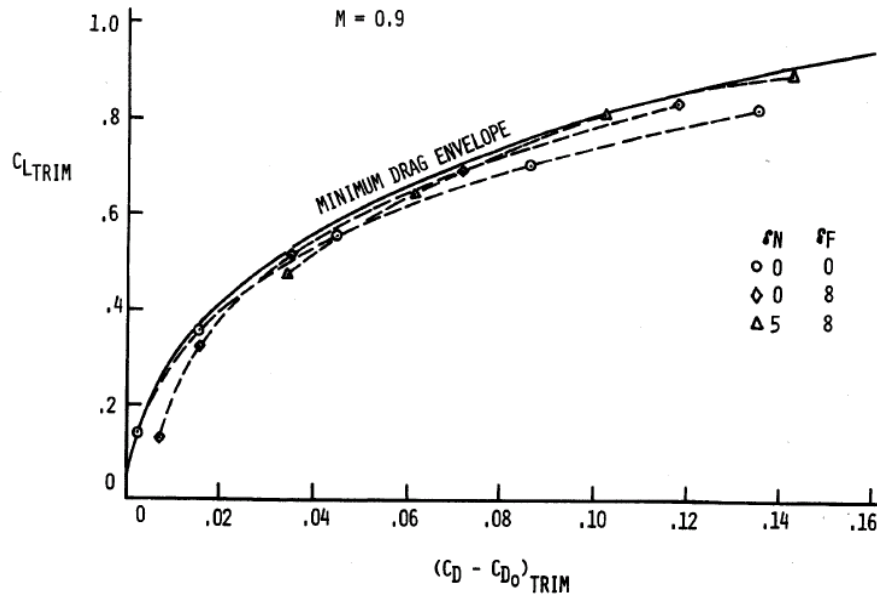
Figure 48: F-18 Trimmed Drag-Due-to-Lift at Mach 0.9 [180]

FLOPS calculates zero-lift-drag based on wetted areas, form factors, and skin friction drag coefficients for each body part and sums them up. The skin friction drag coefficient is a function of Reynolds number, and thus varies with altitude. Zero-lift-drag data used for calibration was assumed to be at 36,000 ft, which is approximately the best cruise Mach number of the F/A-18 [183]. Wetted areas were calculated rather than hard coded so that parametric variation of the vehicle geometry updates the wetted area and zero-lift-drag. To calculate the drag-due-to-lift of the F/A-18 while accounting for the effects of LEX and variable camber, a very low value of the induced drag correction factor in FLOPS was used to match the minimum drag envelopes in Figure 46, Figure 47, and Figure 48. The baseline drag polar generated using FLOPS is plotted in Figure 49 at Mach numbers from 0.2 to 1.8 in 0.3 increments. The general trend is that as the Mach number increases at low subsonic speed, C_{D_o} decreases slightly and starts to increase from Mach 0.6 to Mach 0.9. Then, C_{D_o} increases dramatically in the transonic regime and then decreases again. Also, the drag-due-to-lift coefficient (C_{D_i}) is constant through the

169

subsonic regime and decreases in the supersonic regime. These trends agree with the general trend of drag polars found in other fighters, such as the F-15 Eagle [184]. In addition, the drag polar matches the actual F/A-18's drag polar at Mach 0.6, 0.8, and 0.9. In the supersonic regime, zero-lift-drag at Mach 1.3 matches the actual data.
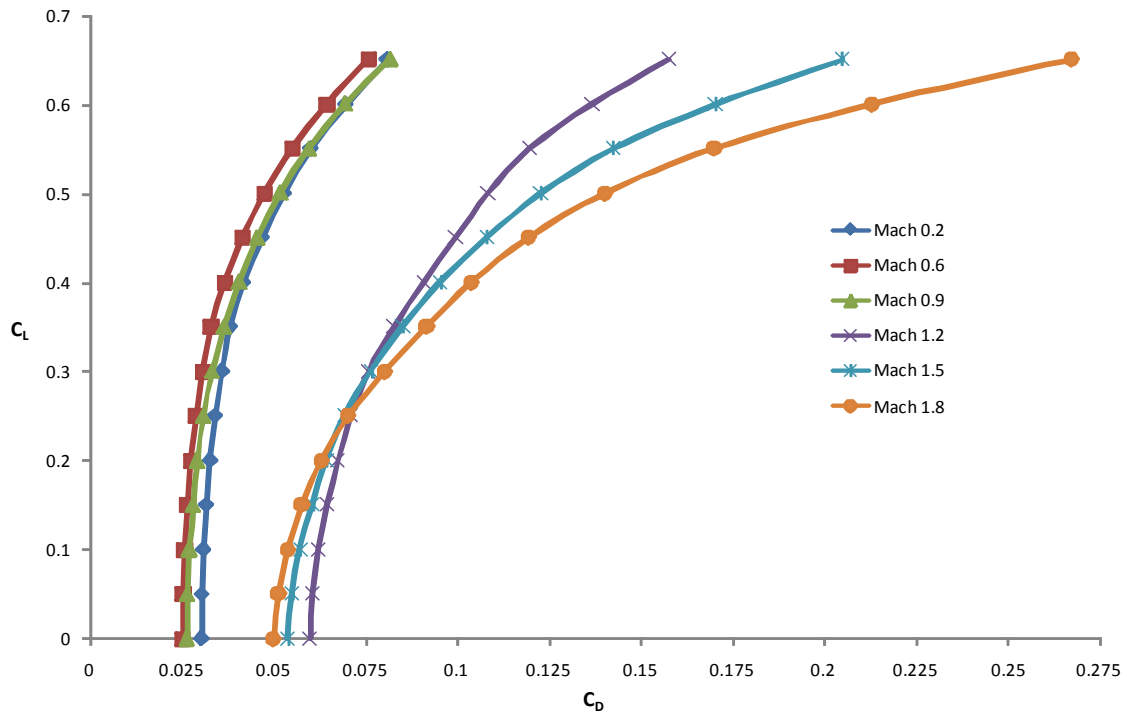
*36,000ft; No external stores but one AIM-9s at each wing tip

Figure 49: F/A-18 Drag Polar Generated in FLOPS

7.6.2.2   High Angle of Attack Aerodynamics during Maneuver and Landing

To check conformance to some of the point performance requirements, such as approach speed and maximum instantaneous turn rate, accurate estimation of high angle of attack aerodynamic coefficients are essential. The F/A-18 boasted unprecedented high angle-of-attack flight capability enabled by high-energy vortex systems generated by the forebody and LEX. Due to the interaction of this vortex system with the vehicle body, aerodynamics at high angles of attack are highly unsteady and non-linear and, thus, very difficult to estimate [185].

Highly sophisticated computational fluid dynamics (CFD) techniques are often used to simulate such physical phenomenon, complemented by wind tunnel tests during and after preliminary design stages. At least four independent wind tunnel tests were conducted with four different scaled models (0.03-, 0.06-, and 0.16-scale) and a full-scale production model of the F/A-18. References [185-190] report some of the wind tunnel test data at a high angle of attack with/without various attachments, such as a nose boom and LEX fences. In particular, Hall [185] compared the three different F/A-18 wind tunnel test data sets for the maximum lift coefficient C_{Lmax} at the maneuver configuration of the leading edge (LE) flap deflection at a maximum value of approximately 34° and the trailing edge (TE) flap deflection angle at 0° as shown in Figure 50. Hall stated that "the values for the numerical maximum of C_L and the respective alpha at which it occurs are 1.79 at alpha = 38° for the (NASA Langley) 30-by 60-Foot Tunnel, 1.81 at alpha = 40° for the (NASA Langley) 7- by 10-Foot High Speed Tunnel, and 1.82 at alpha = 40° for the (NASA Ames) 80- by 120-Foot Wind

Test	M_∞	β, deg	$R_c/10^6$	Grit
0.16-scale F/A-18 in 30x60	0.08	0.0	1.00	No Grit
0.06-scale F/A-18 in 7x10	0.30	0.0	1.37	Nose Ring
Full-scale F/A-18 in 80x120	0.15	0.0	12.36	No Grit

*LE Flaps at 34° and TE Flaps at 0°
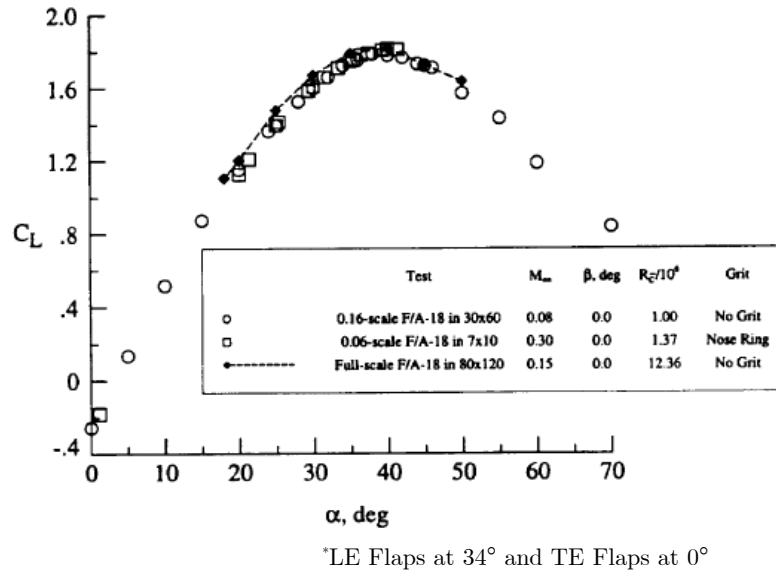
Figure 50: F/A-18 Lift Coefficient from Three Wind Tunnel Tests [185]

Tunnel." In the modeling of the F/A-18, a C_{Lmax} of 1.82 was used for instantaneous turn rate calculation.

7.6.2.3 Drag Increment Due to External Stores

The external stores a military combat aircraft are required to carry may increase the drag of the vehicle and thus degrade the vehicle's mission and point performance. Therefore, it is essential to accurately model the drag increment due to various external store combinations at all operating speeds.

External store drag was obtained for the two primary missions—interdiction and fighter escort available from the F/A-18 NATOPS Flight Manual [183]. Figure 51 and Figure 52 show the external stores for the interdiction and the fighter escort mission. The figures also show the drag contribution of each store item. In addition to the drag of each item, depending on the relative locations of such items, interference drag is added.

172

Interference drag increases with Mach number, and a comprehensive interference drag schedule is provided in the flight manual.
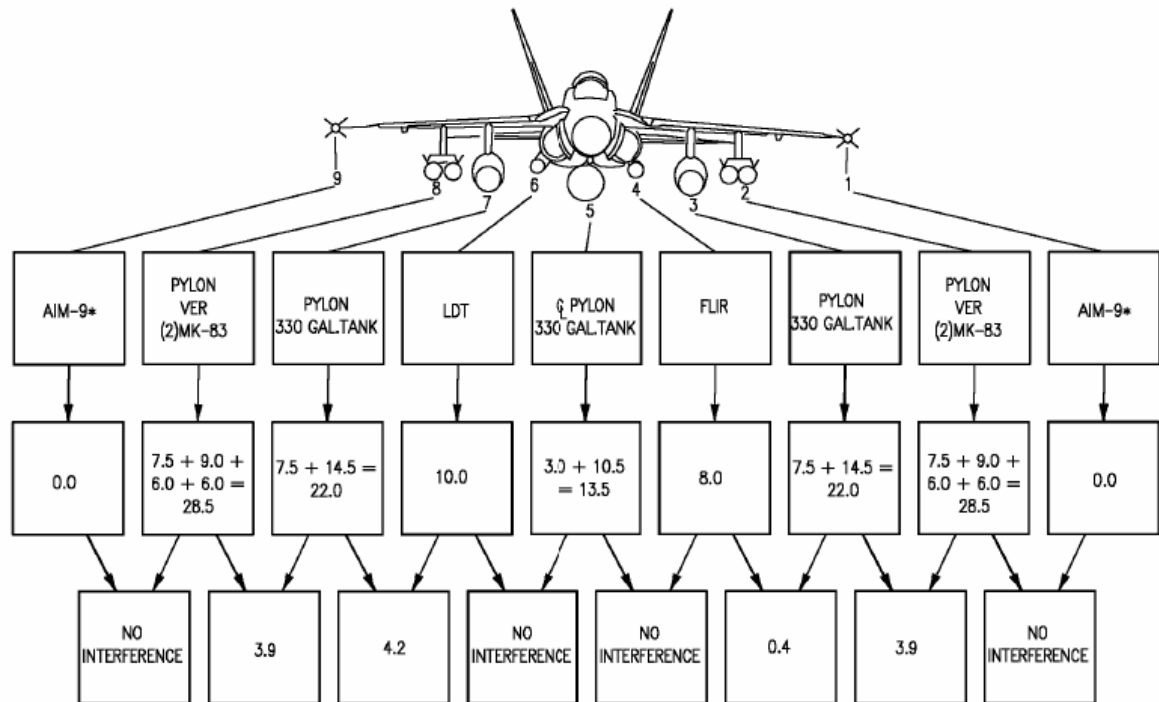
Figure 51: External Stores for the Interdiction Mission [183]
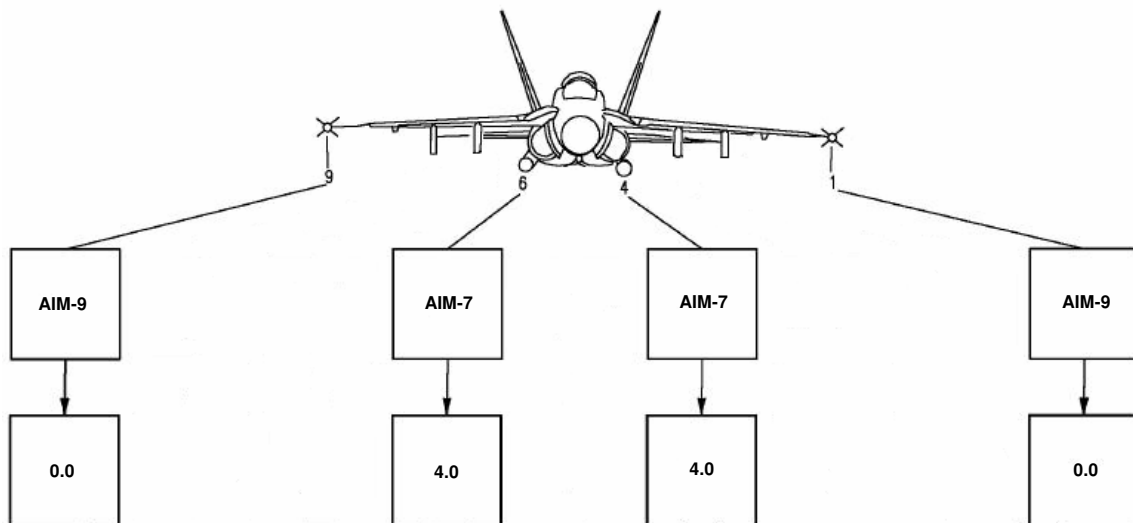
Figure 52: External Stores for the Fighter Escort Mission [183]

Total store drag for the interdiction and fighter escort configurations is given in Table 18. The total store drag of the interdiction mission is about 150 counts and increases with Mach number. The fighter escort mission has only 8 counts of additional drag due to two AIM-7's. During combat, the attack mission requires expending all four MK-83 bombs, and the fighter mission requires expending half the missiles and ammo. Two AIM-9 sidewinders are attached, one at each wing tip, as a default, and the absence of one reduces drag by 2.3 counts.

Table 18: F/A-18 Store Drag in Counts

Mission	Interdiction		Fighter Escort	
Mach	before combat	after combat	before combat	after combat
0.6	142.5	128.5	8	1.7
0.7	146.5	131.5	8	1.7
0.8	152.5	136.5	8	1.7
0.85	168.5	146.5	8	1.7

7.6.3 Weight

Empty and gross weights of the F/A-18 family are available in many sources with large discrepancies. Since the gross weight of the vehicle would depend on external stores, such as external fuel tanks, missiles, bombs, etc., it would be meaningless to compare gross weight without knowing the exact configuration. However, even operating empty weight differs as much as 2,000 lbs depending on the source, largely because of the fact that even within the same version an aircraft may come with different engines and equipments. In addition, non-unique definitions of "empty weight" seem to be used. In this document, all terms and definitions related to aircraft weight abide by MIL-STD-3013 [172] as follows:

Weight Empty: Weight empty is defined as the weight of the air vehicle, complete by model design definitions, dry, clean, and empty, except for fluids in closed systems, such as the hydraulic system. Weight empty includes total structure group, propulsion group, flight controls group, avionics group, auxiliary power plant group, electrical group, etc.

Basic Weight: Basic weight is defined as the weight empty adjusted for standard operational items, such as unusable fuel, engine oil, oxygen, and all fixed armament.

Operating Weight: Operating weight is defined as the sum of basic weight plus such factors as crew, crew baggage, steward equipment, emergency equipment, special mission fixed equipment, pylons, racks, and other nonexpendable items not in basic weight. It is equivalent to takeoff gross weight less usable fuel, payload, and any items to be expended in flight.

Payload: Payload is defined as any item which is being transported and is directly related to the purpose of the mission, as opposed to items necessary for the mission. Payload can include—but is not limited to—passengers, cargo, passenger baggage, ammunition, internal and external stores, and fuel which is to be delivered to another air vehicle or site. Payload may or may not be expended.

Takeoff Gross Weight: Takeoff gross weight is defined as the sum of the operating weight, usable fuel weight, payload items required to perform a particular defined mission, and other items to be expended during flight.

Following the definitions provided above, the weight breakdown of the F/A-18C was constructed based on published data. Table 19 shows a detailed breakdown of the F/A-18C weight empty (We), operating weight, payload, fuel, and takeoff gross weight (TOGW) for both fighter escort mission and interdiction mission. While the F/A-18C's weight empty could have increases over time, one fixed representative weight was used in this study due to lack of information on such continuous weight evolution. The F/A-18C's weight empty of 24,372 lb, found in a Government Accounting Office (GAO) document [191], is the weight of the LOT XVIII production model but is used here to represent all F/A-18Cs. The F/A-18C crew, unusable fuel, engine fluid, gun, ammo, and

chaff weight data are also from the same reference. Weights related to external stores, including missiles, pylons, launchers, pods, fuel tanks, and both internal and external usable fuel are from the NATOPS Flight Manual for the F/A-18A/B/C/D [183]. External stores condition and weight depend on whether the aircraft is in attack or fighter configuration. Among external store items, those that are not expendable during the mission were classified as operating weight. The F/A-18 in fighter configuration carries internal fuel of only 10,810 lb, while attack configuration carries 10,810 lb of internal and 6,720 lb of external fuel when all three 330-gallon tanks are attached. The fuel weight used throughout the study is based on JP-5 at a standard day density of 6.8 lb per gallon. The sum of operating weight, payload, and usable fuel gives the takeoff gross weight of 34,966/47,783 lb (fighter/attack) for the F/A-18A and 37,508/50,325 lb (fighter/attack) for the F/A-18C.

Table 19: F/A-18C Weight Breakdown

		Weight per Unit	# in Attack	# in Fighter	Attack Weight	Fighter Weight
Weight Empty					**24,372**	**24,372**
Crew					180	180
Crew Equipment					59	59
Unusable Fuel					207	207
Engine Fluid					114	114
Gun					204	204
400 Rounds Ammo					100	100
Chaff					52	52
SUU-63	Wing Pylon	310	4	0	1,240	0
SUU-62	Centerline Pylon	139	1	0	139	0
ASS-38	Target FLIR	353	1	0	353	0
ASQ-173	Laser Detector	165	1	0	165	0
BRU-33/A	Vertical Ejector Rack	175	2	0	350	0
Operating Weight					**27,535**	**25,288**
FPU-8/A	External Fuel Tank	290	3	0	870	0
MK-83	1000 lb Bomb	1,000	4	0	4,000	0
AIM-9	Sidewinder	195	2	2	390	390
AIM-7	Sparrow	510	0	2	0	1,020
Payload					**5,260**	**1,410**
Internal Fuel					10,810	10,810
External Fuel		2,240	3	0	6,720	0
Usable Fuel					**17,530**	**10,810**
Takeoff Gross Weight					**50,325**	**37,508**
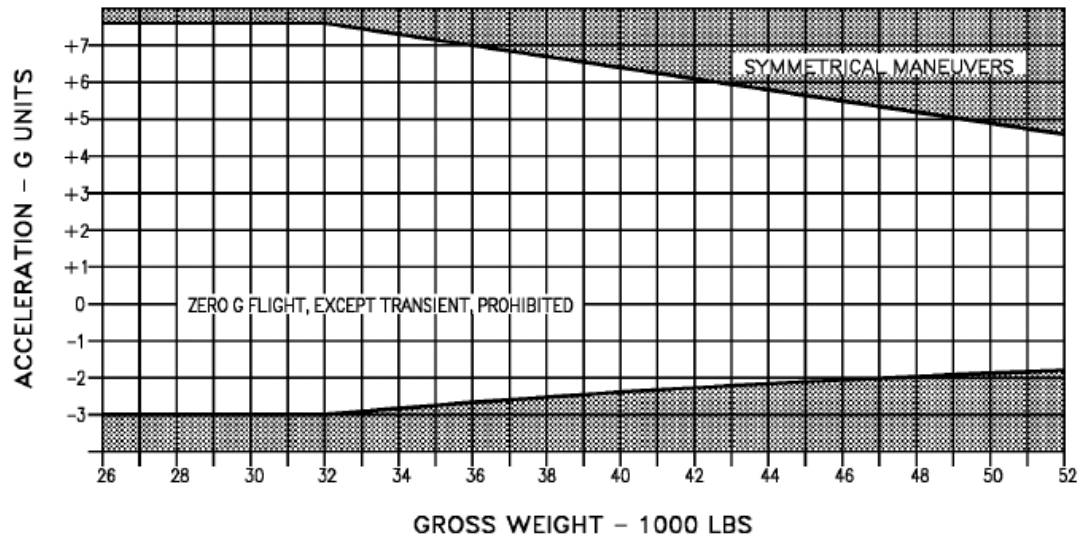
Figure 53: F/A-18A/B/C/D Acceleration Limitations [183]

FLOPS calculates aircraft weight based on designed structural limit and aircraft weight at the limit. Structural limit is defined by two criteria: how many g's an aircraft can pull in symmetric maneuvers at specific loading and weight conditions; and speed limit. Figure 53 shows the F/A-18A/B/C/D's structural limits during symmetrical maneuvers in both clean and fighter configurations. The F/A-18 initially had a design load factor (DLF) of 7.5 g's with up to 32,000 lb of gross weight.

The F/A-18E/F was designed for the same load factor, but the weight was increased to 42,097 lb as shown in Figure 54 [175]. This reference weight was used as a design variable, named *Design weight for DLF*. Comparison of this variable to the combat weight can be a measure of a vehicle's growth potential in terms of structural strength. For example, if *Design weight for DLF* is 45,000 lb while actual combat weight is 42,000 lb, the vehicle's combat weight can increase further (up to 3,000 lb) without compromising its maneuver capability. Speed limits for all F/A-18 models in basic
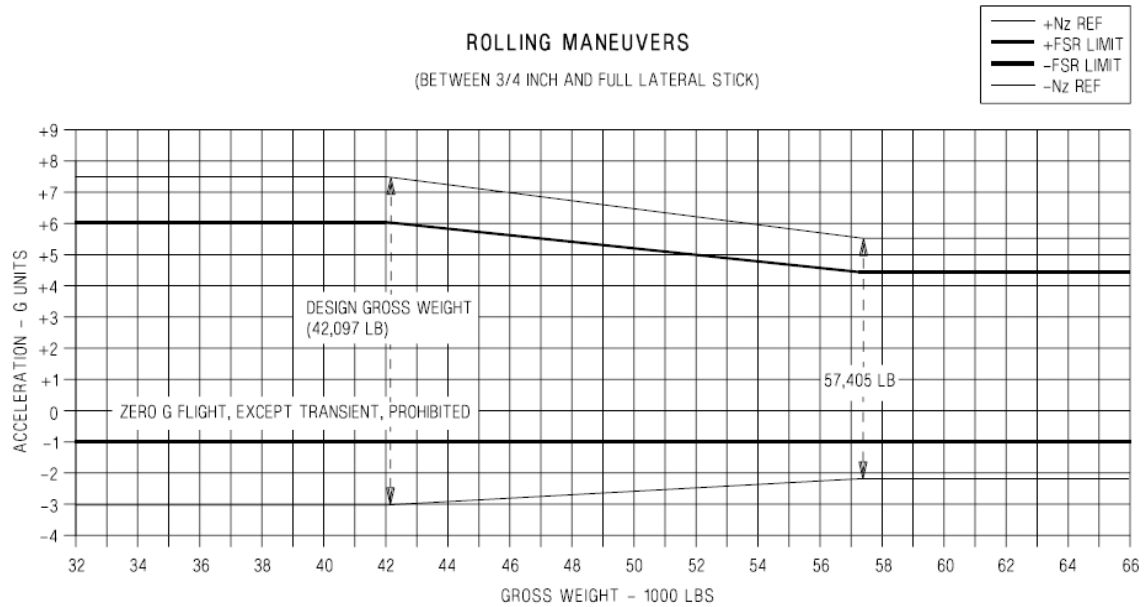
Figure 54: F/A-18E/F Acceleration Limitations [175]

configuration were Mach 2.0 at or above 35,000 ft. Speed limits are reduced if the altitude is lower than 35,000 ft or if configuration changes on flaps, landing gear, external stores, etc. are made.

FLOPS calculates landing gear weight based on the maximum landing weight and aircraft type, i.e., carrier based or land based. Carrier maximum landing weight for the F/A-18A/B/C/D was 33,000 lb until 1994 and was then raised to 34,000 lb [191]. To be able to clear for a 34,000 lb landing, restrictions are applied to arresting gear, asymmetric loading conditions, and recovery wind over deck [183]. The F/A-18E/F was designed to land at up to 44,000 lb. While landing gear weight is determined by the maximum landing weight, it can be inferred from the history that the original F/A-18's landing gear was designed with some level of safety margin. In sizing landing gear, a safety margin of 5 percent was added to the maximum operational landing weight.

As a final note, it was necessary to calculate the weight of the F/A-18A and the F/A-18E. The F/A-18A's weight empty of 21,830 lb was found from Young [76]. Then,

it was assumed that only weight empty is different from the C version and all other weight elements are the same. A detailed discussion and weight breakdown of the F/A-18E is provided in §7.7.4 and in Table 31.

7.6.4 Propulsion System Modeling and Calibration

F/A-18s are powered by two General Electric F404 or F414 turbofan engines, depending on the version. F/A-18A/Bs and early productions of C/Ds are powered by F404-GE-400 engines, and more recent C/D versions are powered by the enhanced performance derivative of F404-GE-400, designated as F404-GE-402. F/A-18E/Fs are powered by two F414-GE-400 engines. F404-GE-400 is a derivative of the General Electric YJ101 turbojet engine, developed to power the US Air Force's YF-17 aircraft [192]. The F404 turbofan engine is a two-shaft augmented low bypass ratio turbofan with three-stage axial fans, seven-stage axial HP compressors, a single piece annular combustion chamber, and a single-stage axial HP turbine. F404-GE-402 engines provide performance improvements made possible by applying the latest technology and materials to the turbine and afterburner sections of the engine [193]. According to the engine manufacturer, General Electric [194],

> The F404-GE-402 Enhanced Performance Engine (EPE) provides higher power, improved fuel efficiency and increased mission capability for the F/A-18C/D Hornet. The enhanced engine retains the proven design characteristics of the baseline F404, while achieving increased performance through improved thermodynamic cycle and increased temperature.

The F414-GE-400 is "an evolutionary engine based on the F404 [4]." The F414 used the F412 core, a non-afterburning derivative of the F404 that was partially developed for the A-12 program [82]. The F414 provides about 20% thrust increase over the F404

while keeping the engine size the same. Basic configurations and performance metrics of the F404 and F414 are summarized in Table 20.

Table 20: General Specifications for the F404-GE-400 [175, 183, 192, 194-196]

	F404-GE-400	F404-GE-402	F414-GE-400
Fan	Three-stage axial	Three-stage axial	Three-stage axial
Bypass Ratio	0.32*	0.29*	0.29
Airflow (lb/sec)	142	142	not listed
HP Compressor	Seven-stage axial	Seven-stage axial	Seven-stage axial
OPR	26*	26	27.2
Turbine Inlet Temp. (°F)	2,459	2,534	2,757
Combustion Chamber	Single-piece annular	Single-piece annular	Single-piece annular
HP Turbine	Single-stage axial	Single-stage axial	Single-stage axial
LP Turbine	Single-stage axial	Single-stage axial	Single-stage axial
Nozzle	Convergent-divergent	Convergent-divergent	Convergent-divergent
Length (in)	154*	154	154
Max Diameter (in)	35	35	35
Weight, dry (lb)	2,195*	2,282	2,445
Military Thrust (lbf)	10,700	10,800	14,327
Max Thrust (lbf)	16,000	17,754	22,000
SFC, Mil Thrust (lb/lbf.h)	0.81	0.81	0.84
SFC, Max A/B (lb/lbf.h)	1.85	1.74	not listed
Application	F/A-18A/B/C/D	F/A-18C/D	F/A-18E/F
Low Rate Production	1979		1996
Unit Cost ($K)	not listed	not listed	3564

(*found in multiple sources and discrepancies exist, manufactures' official websites took priority)

The F404-GE-400 was modeled with QNEP [197], an engine cycle and performance analysis program developed for the US Navy. QNEP is an upgraded version of NEPCOMP [198] and is now part of NASA Langley's FLOPS for engine cycle analysis. With given engine architecture and parameters, QNEP performs both on-design and off-design point engine cycle analysis and writes an engine deck, which gives installed thrust and fuel flow in various combinations of altitudes, Mach numbers, and engine throttle settings.

The F404-GE-400 was modeled with the known engine parameters, and its performance was compared to the published data. Engine performance data is extremely proprietary and is published only under very limited conditions. However, actual maximum sea level installed thrust at five different Mach numbers were found in one of the GAO reports [191] and duplicated in Table 21. Installed thrust calculated by QNEP was calibrated to match the actual data at the sea level condition.

Table 21: F404-GE-400 Maximum Installed Thrust at Sea Level

Mach Number	Altitude	Maximum Installed Thrust (lbf)
0.8	Sea Level	17,182
0.9	Sea Level	16,927
1	Sea Level	16,488
1.1	Sea Level	15,487
1.2	Sea Level	14,500

Calculated maximum thrust at various Mach numbers and altitudes by QNEP is plotted in Figure 55. The maximum thrust at sea level matches the published data. As altitude increases, thrust decreases. The variation trend with Mach number and altitude is similar to the trends found on the Rolls-Royce RB211-535E4 [199] turbofan and a 30,000-lb notional turbofan engine in [6]. Validation of the maximum installed thrust at above sea level was achieved indirectly by comparing the actual and calculated F/A-18 point performance data in §7.6.6.
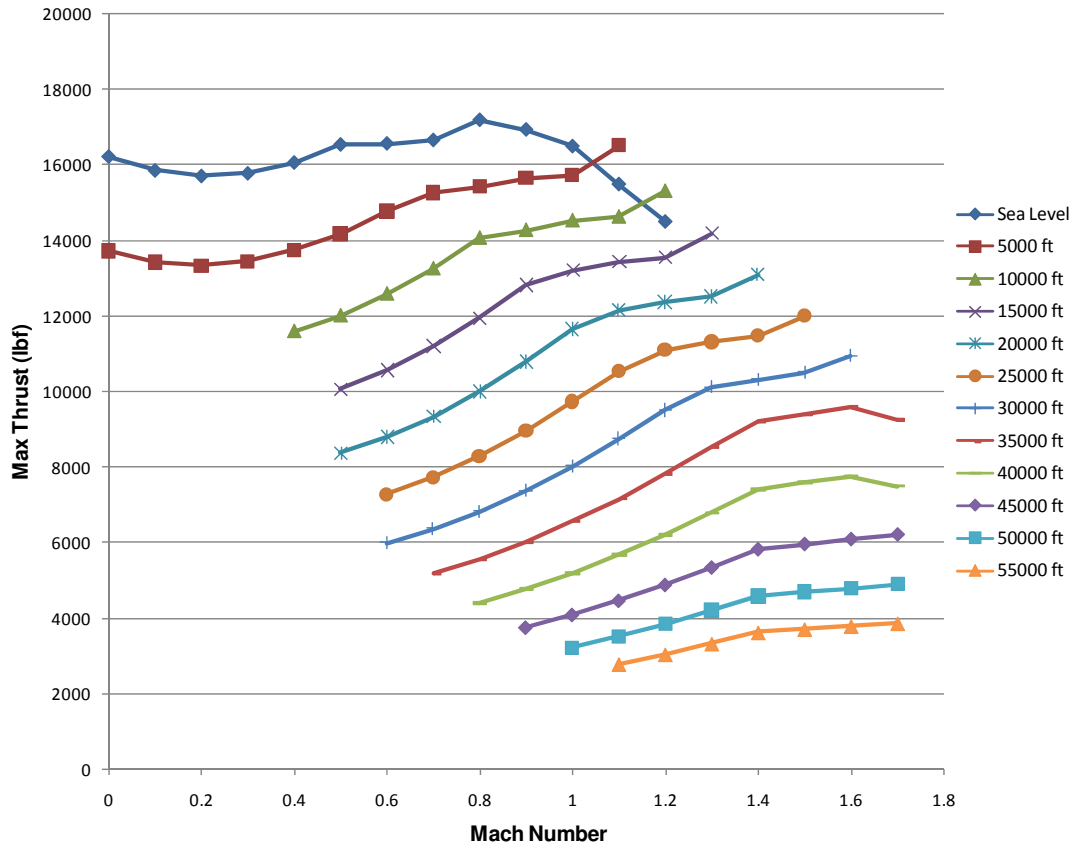
Figure 55: F404-GE-400 Maximum Installed Thrust Calculated from QNEP

Although the specific fuel consumption (SFC), a direct measure of the engine efficiency, of F404 was not available, fuel flow of the F/A-18 at various combinations of vehicle gross weight, altitude, Mach number, and store drag conditions is available from the NATOPS flight manual [183]. Engine efficiency of the F404 QNEP model was calibrated using these data. Table 22 shows comparisons of the calculated and actual fuel flow at various combinations of flight conditions that cover most of the flight envelope that are described by the interdiction and fighter escort mission profiles as given in Figure 37 and Figure 38. The comparison shows that the errors are reasonably small in both supersonic and subsonic flight regimes.

Table 22: Comparison of Calculated and Actual Fuel Flow of the F404-GE-400

Drag Index (count)	Weight (lb)	Altitude (ft)	Speed (Mach)	Calculated Fuel Flow (lb/hr)	Actual Fuel Flow (lb/hr)	Error (%)
DI=150	42000	0	0.8	17172	17351	-1.03
	42000	5000	0.8	14334	14444	-0.76
	38000	10000	0.8	11821	11740	0.69
	38000	15000	0.8	9557	9547	0.11
	38000	20000	0.8	7963	7927	0.45
	38000	25000	0.8	6697	6689	0.12
	42000	30000	0.8	5873	5968	-1.60
	46000	30000	0.8	6235	6237	-0.03
	50000	30000	0.8	6933	6594	1.37
	38000	35000	0.8	5033	5014	0.38
	42000	35000	0.8	5505	5364	2.63
	30000	40000	0.8	4011	4025	-0.36
	34000	40000	0.8	4490	4391	2.25
DI=0	34000	35000	0.85	3479	3577	-2.75
	38000	35000	0.85	3787	3829	-1.09
	30000	40000	0.85	3037	3085	-1.57
	34000	40000	0.85	3416	3390	0.76
	38000	40000	0.85	3861	3779	2.17
DI=8	34000	35000	1.5	33988	34596	-1.76
	34000	15000	1.15	49680	49683	-0.01

7.6.5 Carrier Suitability

Key performance parameters for carrier suitability are approach speed, launch and recovery wind over deck (WOD), and carrier recovery payload. These metrics are calculated for the F/A-18 in attack configuration. The minimum WOD required is the minimum ship speed required to ensure safe launch and recovery of carrier-based air vehicles. Thus, a small minimum WOD requirement is desired to allow for flexible ship operation.

7.6.5.1 Approach Speed

Historically, different organizations have used different methods to estimate approach speed, often basing estimates on the stall speed multiplied by a safety factor S_f.

$$V_{app} = S_f \cdot V_{stall,landing} \tag{55}$$

where $V_{stall,landing}$ is the stall speed of an aircraft at landing configuration.

$$V_{stall,landing} = \sqrt{\frac{2 \cdot W_{landing}}{S \cdot \rho \cdot C_{L\max,landing}}} \tag{56}$$

where $W_{landing}$ is aircraft gross weight at landing, S is wing area, ρ is air density, and $C_{Lmax,landing}$ is the maximum lift coefficient of the aircraft at landing configuration.

Since 1953, for a military aircraft, a safety factor of 1.2 was required by MIL-A-8629 [200] based on the power-off stall speed for landing, but industries started using a criteria based on power-on stall speed for landing. [201] Updated modern military standards provides more complicated means to estimate approach speed, as in MIL-STD-3013 [172], considering not only aerodynamic capability but also longitudinal acceleration, pilot field of view (FOV), stability and control requirements per MIL-

HDBK-1797 [202], and control system limits. Safety margin based on the stall speed is defined as follows [172]:

For land-based aircraft: a speed that corresponds to 120-percent (120%) of the out-of-ground effect power-off stall speed in the approach configuration, gear down

For carrier-based aircraft (with the air vehicle in the landing configuration and on a 4° glide slope on a 89.8°F day, zero wind): one-hundred-ten-percent (110%) of the power-on stall speed using the thrust (power) required for level flight (V_{spa}) at 115-percent (115%) of V_{sl}, the power-off stall speed

It is not clear whether the F/A-18's specification was prepared following MIL-STD-3013. Even if it were, the coupling of thrust and lift would have made parametric estimation of the F/A-18's approach speed, which updates as vehicle parameters change, quite difficult. Therefore, a rather simple, fixed safety factor multiplication method as in Eqs. (55) and (56) was used to obtain such factors from actual F/A-18 stall and approach speed data.

Table 23: F/A-18 Stall and Approach Speeds

	A/B	C/D	E/F	Units
Stall Speed	112	114	114	knots
Approach Speed	139	141	140	knots
Wing Area	400	400	500	ft^2
Landing Weight	33,000	34,000	44,000	lb
$C_{Lmax,landing}$	*2.058*	*2.046*	*2.119*	
Safety factor (S_f)	*1.241*	*1.237*	*1.228*	

*values in italics are estimations

Actual stall and approach speeds of all three versions of the F/A-18 were found from [201] as summarized in Table 23. Using the tropical day air density of 0.00224 slugs/ft^3, $C_{Lmax,landing}$ and the safety factors for each of the versions were calculated. It is important to note that $C_{Lmax,landing}$ is different from C_{Lmax} discussed in §7.6.2.2. During approach for landing, all landing gear is lowered and LE and TE flaps are deflected fully

at 34° and 45° respectively, while C_{Lmax} was calculated with LE flaps at 34° and TE flaps at 0°. Estimated $C_{Lmax,landing}$ and S_f are different from version to version. Apparently, the F/A-18E/F shows higher $C_{Lmax,landing}$ than other versions due to its improved LEX design.

7.6.5.2 Launch Wind Over Deck

According to MIL-STD-3013, minimum launch wind over deck ($V_{LWOD,min}$) is defined as catapult minimum end airspeed (V_c) minus catapult endspeed (V_A). Operational launch WOD ($V_{LWOD,op}$) uses catapult operational end airspeed (V_{op}), which is V_A plus 15 knots as a safety margin.

$$
\begin{aligned}
V_{LWOD,min} &= V_c - V_A \\
V_{LWOD,op} &= V_{op} - V_A
\end{aligned}
\tag{57}
$$

where $V_{op} = V_c + 15$ knots.

Catapult end speed (V_A) is the speed to which a vehicle can accelerate with the aid of a catapult and its own thrust and is determined by catapult performance, vehicle weight, thrust, and drag. V_A can be calculated using the following equation:

$$
V_A = \sqrt{\frac{22.5888\frac{S_C(F_n - D)}{W_{sys}} + \sqrt{\left[22.5888\frac{S_C(F_n - D)}{W_{sys}}\right]^2 + 4V_{DL}^4}}{2}}
\tag{58}
$$

where

S_c	=	catapult power stroke, ft (302 ft for C13-2 catapult)
F_n	=	net thrust, lb
D	=	aerodynamic drag, lb
W	=	air vehicle weight, lb
CEW	=	catapult equivalent weight, lb (6680 lb for C13-2 catapult)
W_{sys}	=	system weight, lb = $W + CEW$
V_{DL}	=	deadload velocity, knots (Catapult endspeed without thrust)
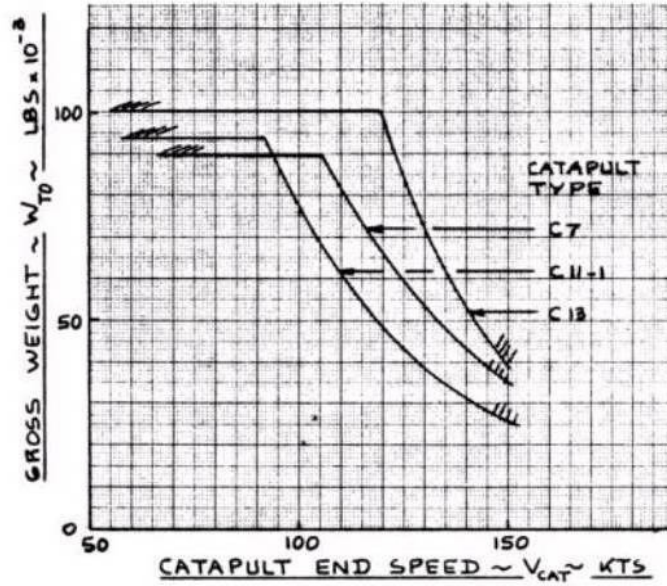
Figure 56: Effect of Takeoff Weight on Catapult End Speed [7]

In addition, thrust and drag are to be evaluated at 0.7 V_{DL}; primary mission is used for drag calculation, and minimum engine is used for thrust calculation. Deadload velocity (V_{DL}) is solely determined by the catapult performance and the weight that is accelerated by the catapult. The relationship between V_{DL} and aircraft gross weight for three types of catapults—C7, C11-1, and C13—is shown in Figure 56. For the C13 catapult, the limit on weight is 100,000 lb and the absolute speed limit is 150 knots.

Catapult minimum end airspeed (V_c) is the minimum air speed required at the end of the catapult at which a vehicle can safely fly away and is primarily a function of the vehicle's maximum lift capability and wing loading. For conceptual design of a carrier-based aircraft, V_c is estimated based on "the speed represented by 90-percent of the maximum lift coefficient, power-off, out-of-ground effect," according to MIL-STD-3013 [172].

Using the equations presented above, F/A-18's launch wind over deck (LWOD) was calculated. Launch configuration was assumed to be the attack configuration as

illustrated in Figure 51 with all landing gear down and LE and TE flaps approximately half deflected. The drag increment due to external stores, landing gear, and high lift devices was assumed to be 300 counts from the clean configuration. According to NASA TM-107601 [173], F/A-18 LE and TE flaps are deflected by 12 and 30 degrees during launch and 34 and 45 degrees during landing. The maximum lift coefficient during maneuvering with only LE flaps fully defected at 34 deg is 1.82 as described in §7.6.2.2, and $C_{Lmax,landing}$ is 2.05 as estimated in §7.6.5.1. Here, the maximum takeoff lift coefficient ($C_{Lmax,takeoff}$) of 1.9 is assumed, considering that it should be larger than 1.82 and smaller than 2.05. Finally, the maximum afterburner thrust of one engine was used for thrust calculation. The F/A-18E/F is launched and recovered using a C13-2 catapult and MK7-Mod3 arresting gear [203], and launching and recovery performance calculations for all F/A-18 versions were based on these systems.

Table 24: F/A-18 Launch WOD Calculation

	A/B	C/D	E/F	Units
Gross Weight	47,783	50,375	63,331	lb
Wing Area	400	400	500	ft^2
S_c	302	302	302	ft
F_n	16,000	17,754	22,000	lbf
C_{Do} at takeoff	0.055	0.055	0.055	
ρ (tropical day)	0.00224	0.00224	0.002244	slug/ft^3
V_{DL}	143.6	141.9	134.3	knot
$Wsys$	54,463	57,055	70,011	lb
V_A	147.0	145.6	138.2	knot
$C_{Lmax,takeoff}$ (assumed)	1.9	1.9	1.9	
V_c	147.8	151.8	256.9	knot
V_{op}	162.8	166.8	152.2	knot
Launch WOD, op	15.9	21.2	29.0	knot

Based on the assumptions listed above, the F/A-18's LWOD was calculated on a sea level tropical day. For validation purposes, calculated WOD was compared against the actual F/A-18 data, which was only known for E/F. As shown in Table 24, the calculated operational LWOD of E/F is 29 knots when the maximum takeoff lift coefficient of 1.9 is assumed, which is close to the actual value of 28 knots.

Figure 57 illustrates the relationship between aircraft weight and various launch related speeds for the F/A-18A/B/C/D. Minimum launch WOD, determined by the difference between catapult operational end airspeed (V_{op}) and catapult endspeed (V_A), is zero when the aircraft gross weight is about 41,000 lb and increases to 30 knots when the aircraft gross weight reaches 54,300 lb.
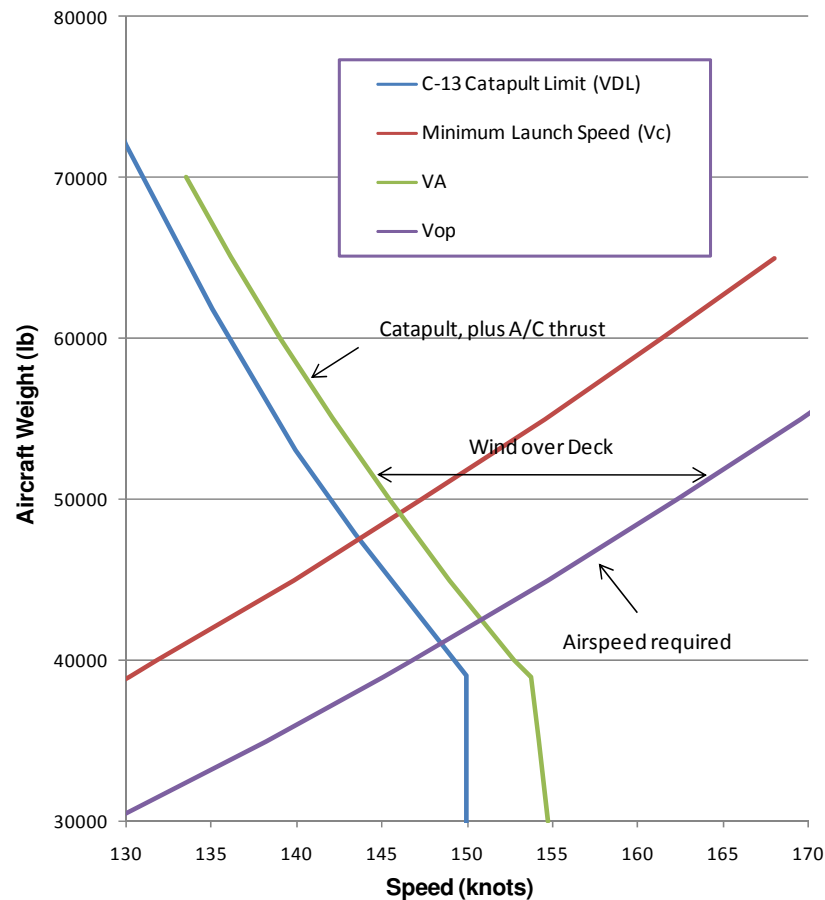
Figure 57: The F/A-18A/B Launch Airspeed/Catapult End Speed Envelope

7.6.5.3   Recovery Wind Over Deck

Speeds related to approach and recovery of the US Navy aircraft are defined by MIL-STD-3013 [172] as follows:

- Recovery Wind Over Deck (RWOD): Recovery wind-over-deck is defined as the difference between touchdown speed and shipboard engaging speed.
- Touchdown Speed (V_{td}): For design purposes, touchdown speed is defined as that speed equal to 105-percent (105%) of carrier approach speed (V_{pa}). For operational air vehicles, touchdown speed will be determined using fleet survey data.
- Shipboard Engaging Speed (V_e): The shipboard engaging speed is defined as the arresting gear engaging speed measured relative to the ship.

In other words,

$$V_{RWOD} = V_{td} - V_e$$
$$V_{td} = 1.05 V_{pa}$$

$$(59)$$

These relationships are also graphically presented in Figure 58. As shown in the figure, while an aircraft is approaching a carrier, the carrier itself moves away from the aircraft. The touchdown speed is the true airspeed experienced by the aircraft, while the speed of the aircraft relative to the ship (shipboard engaging speed) is less by the amount of WOD. Therefore, minimum RWOD is determined by the maximum speed limit of the arresting gear and minimum safe airspeed of the aircraft. Low minimum RWOD and LWOD requirements are preferred, since high values limits the way the ship is operated.
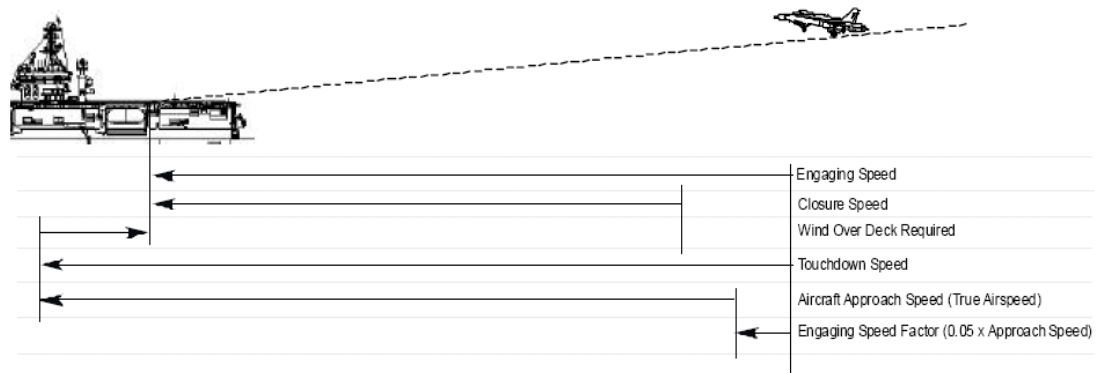
Figure 58: Carrier Aircraft Recovery Speed Relationships [201]

Shipboard engaging speed is determined by the arresting gear maximum performance. MK7-Mod3 arresting gear performance from NAEC-MISC-06900 [204] is depicted in Figure 59. The arresting gear has the speed limit of 145 knots regardless of aircraft weight and has the cylinder pressure limit of 10,000 Pascal. Due to the cylinder pressure limit, the maximum engage speed is lowered from 145 knots when the aircraft is more than 40,000 lb.
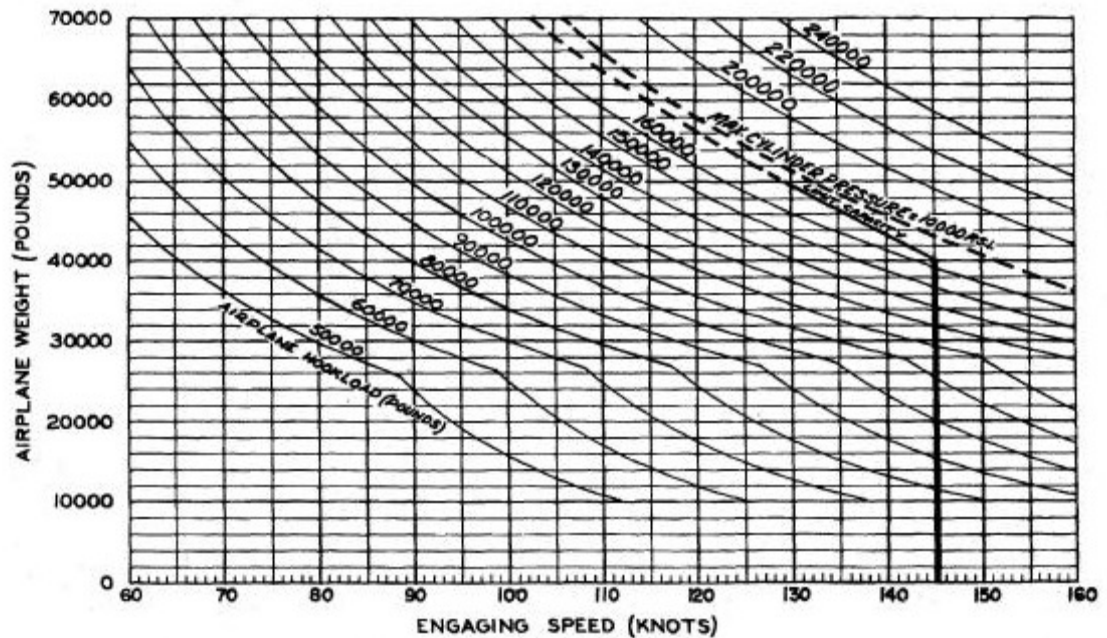
Figure 59: MK 7 Mod 3 Arresting Gear Performance [204]

Since approach speeds for F/A-18s are already calculated in §7.6.5.1, recovery WOD is readily calculated using Eq. (59). Table 25 shows the calculated recovery WOD of the F/A-18. With a MK7-Mod3 arresting gear, required WOD was calculated to be less than 10 knots for all versions. Calculated E/F WOD matched the actual WOD of 8 knots as in Table 62.

Table 25: F/A-18 Recovery Wind Over Deck

	A/B	C/D	E/F	Units
Landing Weight	33,000	34,000	44,000	lb
Wing Area	400	400	500	ft^2
Approach Speed	139	141	140	knots
Touchdown Speed	146	148	147	knots
Engaging Speed	145	145	139	knots
Recovery WOD	1	3	8	knots

7.6.5.4   Carrier Recovery Payload

MIL-STD-3013 [172] defines the carrier recovery payload (CRP), or bring back capability, of a carrier-based air vehicle as

> … the maximum combination of fuel and expendable payload an air vehicle can land with, and not exceed its maximum landing weight. This is the maximum carrier/arrested landing weight less the operating weight.

The maximum carrier/arrested landing weight for the F/A-18A/B/C/D was 33,000 lb until 1994 when it was raised to 34,000 lb with restrictions [191]. The F/A-18A's carrier recovery payload with an operating weight of 24,993 lb was 8,007 lb initially. However, as the F/A-18 gained weight over time, the bring back weight decreased accordingly. The 27,535 lb operating weight of the F/A-18C allowed only 5,465 lb of fuel and payload to be brought back upon carrier landing. That was a serious concern to the Navy, especially when training missions were forced to expend expensive, unused

weapons in order not to exceed the maximum landing weight. Raising the maximum carrier landing weight from 33,000 lb to 34,000 lb in 1994 did not solve the problem and further increasing maximum carrier landing weight would have required strengthening of landing gear and airframe and the addition of a larger wing to keep the approach speed at the same level. This poor bring back capability of the F/A-18C/D was one of the main reasons why the US Navy had to pursue a new aircraft, the F/A-18E/F. For the F/A-18E/F design, a bring back weight of 9,000 lb was required, while the maximum landing weight was set at 44,000 lb [191]. The F/A-18E/F's operating weight of 34,481[*] lb provides the bring back capability of 9,519 lb, exceeding the requirement. This calculated value is very close to the published value of 9,500 lb as in Table 62.

7.6.6 Synthesis and Validation of the F/A-18 Model

Geometry, aerodynamics, weight, and propulsion models of the F/A-18 have been developed in the previous sections. In addition, the KPPs related to carrier suitability were calculated and compared to the published data. In this section, those previously developed elements are synthesized, forming a complete aircraft model to calculate both the fighter's mission and point performance. To confirm the validity of the F/A-18 model, the calculated point and mission performance are compared to the published data. Fighter performance depends in part on the difference between thrust available and thrust required. Therefore, accurate fighter performance calculation requires an accurate engine model and drag model. Correct estimation of the mission radius is only achievable

---

[*]The definition of operating weight is different in the context of carrier recovery payload. Here, operating weight is landing weight less fuel and expendable payload such as missiles and bombs. See Table 31 for the F/A-18E weight breakdown.

when aerodynamics, engine efficiency, weight, external stores weight and drag, and, most importantly, the mission itself are all accurate. All the procedures, methods, and assumptions are documented to provide traceability of the work, and calculated vehicle performance is compared to the actual F/A-18 performance when such data are available.

7.6.6.1   Fighter Performance

Fighter performance metrics of interest are combat ceiling, specific excess power, acceleration, and turn rate. All of these metrics are calculated for the standard fighter configuration (two AIM-9s and two AIM-7s only) with 60 percent internal fuel, unless otherwise noted. These point performance metrics are essentially a function of engine thrust available and engine thrust required, which is equal to drag. For the F/A-18C, the engines are two F404-GE-402s at maximum afterburner thrust.

Combat ceiling is defined as "the altitude at which the maximum steady-state rate-of-climb potential is 500 ft per minute for a specified configuration, weight, speed, and thrust (power) setting", in MIL-STD-3013. The F/A-18A/B combat ceiling is about 53,600 ft, according to the NATOPS Flight Manual, and the calculation using FLOPS was 53,374 ft for the A version and 53,141 ft for the C version.

MIL-STD-3013 also defines specific excess power (P_s) as

> … the time rate of change of specific energy and is a measure of the capability of the air vehicle to change energy levels for a specified configuration, altitude, speed, and thrust (power) setting. Specific excess power is usually expressed in feet per second, and is defined as follows:

$$P_s = 1.6878 \frac{(F_n - D)V_{tas}}{W} \qquad (60)$$

where F_n is net thrust in pounds; D is aerodynamic drag in pounds; V_{tas} is true airspeed in knots; and W is air vehicle weight in pounds.

NAVAIR reports in a GAO document [191] some of the F/A-18C's point performance measured at the combat weight of 33,325 lb with maximum afterburner thrust of two F404-GE-402 engines: P_s is 699 ft/sec at Mach 0.9, 10,000 ft; acceleration capability is to take 55.8 seconds from Mach 0.8 to 1.2 at 35,000 ft; and turn rate is 12.3 degrees/sec at 15,000 ft.

The FLOPS model calculated these three fighter performance measures at the same condition: P_s was 686.7 ft/sec; the acceleration time was 66.54 seconds; and the turn rate was 12.393 degrees/second. While calculations of the two measures were close to the actual values, the acceleration time was noticeably higher. It seems that the aerodynamics model overestimates the wave drag at around Mach 1.

7.6.6.2 Mission Performance

To confirm the validity of the F/A-18 computer model, the calculated mission performance is compared to the published mission performance. Mission performance was compared in terms of the mission radius rather than the fuel quantify burned to fly a designed range. Correct estimation of the mission radius is only achievable when aerodynamics, engine efficiency, weight, external stores weight and drag, and most importantly the mission itself are all correct.

The F/A-18A/B/C/D NATOPS Flight Manual [183] provides the amount of fuel required for each of the mission segments, such as engine start, warm-up, takeoff, acceleration to climb speed, climb, cruise, and reserve, based on a series of flight tests in various combinations of flight conditions, such as weight, external stores, etc. For example, the combinations of best cruise Mach number and altitude and climb speed schedule for minimum time-to-climb are databased under different weight and drag

conditions. All the mission segments that comprise the fighter and attack mission profiles were modeled in the F/A-18 FLOPS model and validated against the NATOPS Flight Manual. The segment-by-segment comparison of the fuel consumption confirmed accuracy of the FLOPS model.

Then, as the next step, the F/A-18 model was flown for five different mission profiles. They are hi-lo-lo-hi interdiction as in Figure 37, hi-hi-hi interdiction, fighter escort as in Figure 38, ferry, and combat ferry missions. The standard hi-hi-hi interdiction mission profile from MIL-STD-3013 is shown in Figure 60. It is identical to the hi-lo-lo-hi interdiction described in §7.2.1 except that the 50 nm penetration and withdrawal is conducted at a fixed altitude, which is the end altitude of the cruise out segment. The ferry/combat ferry mission profile is depicted in Figure 61. A (combat) ferry mission is defined as "a range mission conducted without payload to depict the maximum range capability of the air vehicle [172]." The combat ferry mission is performed with internal fuel only while the ferry mission uses all external fuel tanks. For complete mission descriptions of these missions, see MIL-STD-3013.
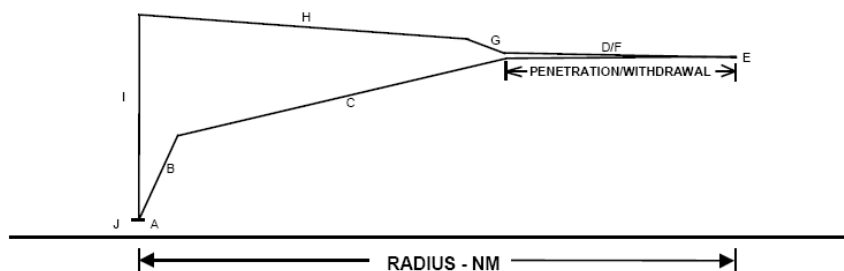
Figure 60: Interdiction (Hi-Hi-Hi)
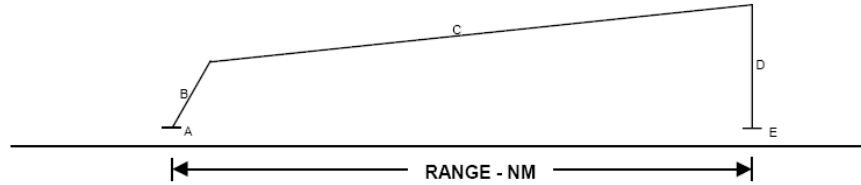
Figure 61: Ferry Mission

Mission analyses were performed for the five mission profiles for both the F/A-18A and C with various external store and reserve fuel conditions. For the fighter and ferry missions, land-based reserve mission fuel of 20 minutes loiter plus 5 percent of initial fuel was assumed among other standard reserve conditions. For the interdiction missions, either the land-based reserve fuel, fixed fuel between 3,500 lb to 4,000 lb, or 100 nm BINGO was assumed appropriately. Assumptions on external stores also had to be made for some cases, but the error in fuel consumption caused by an incorrect external store is insignificant as long as the number of external fuel tanks used is correct.

Mission radius (range for the ferry missions) calculated from the mission analyses are compared to the actual data as shown in Table 26. For each comparison, actual or assumed external store conditions and reserve conditions are listed. The shaded entries in the table are assumptions. The calculated and actual mission radius match very closely for all ten different cases analyzed with the F/A-18C model, which approves the validity of the vehicle model created in this study. On the other hand, the calculated radius for the interdiction and ferry mission are significantly lower than the published numbers in the case of the F/A-18A model. Calculated ferry range was 1,763 nm and calculated interdiction (hi-lo-lo-hi) was about 500 nm, which are about 10% lower than the published 1,800+ or 2,000+ nm and 550 or 575 nm.

This rather large difference seems to be attributed to two reasons: First, the published performance is based on the F/A-18A empty weight lower than the 21,830 lb

that was used in the analyses. The published mission radius could have been based on the weight of the very early production version of the F/A-18A or even the prototype version. The second explanation is that the published data are estimation rather than actual flight test data. This argument is supported by the fact that the 550 nm interdiction radius was initially mentioned by Lenox in 1976 [77], which was four years before the first delivery in 1980 and two years before the first test flight occurred on November 18, 1978. Thus, the author claims that the 10% difference between the published and calculated mission radius with the F/A-18A model does not undermine the validity of the vehicle models created in the study.

Table 26: Comparison of Calculated and Published Mission Performance

Mission Type	Version	Published	Calculation	Fuel Tanks	Stores	Source/Year	Reserve Type	Reserve Condition	Mission Profile
Interdiction (Hi-Lo-Lo-Hi)	A	550	496	(3) 330 gallon	Note 1.	Lenox 1976/ Janes 81	Land-based	20 min + 5% of initial fuel	As in Figure 37
	C	290	294	(2) 330 gallon	Note 1.	Janes 1992-93	Carrier-based	4000 lb of fixed fuel	
	C	304	305	(2) 330 gallon	Note 2.	DoD 1996	Carrier-based	3800 lb of fixed fuel	
	C	325	320	(2) 330 gallon	Note 1.	Hornet 2000 Study1988	Carrier-based	3500 lb of fixed fuel	
	C	369	372	(3) 330 gallon	Note 2.	DoD 1996	Carrier-based	4000 lb of fixed fuel	
	C	415	412	(3) 330 gallon	Note 1.	CRS 2007	Carrier-based	3500 lb fixed	
Interdiction (Hi-Hi-Hi)	C	395	395	(2) 330 gallon	Note 2.	DoD 1996	Carrier-based	3800 lb of fixed fuel	As in Figure 38
	C	470	462	(3) 330 gallon	Note 2.	DoD 1996	Carrier-based	4000 lb of fixed fuel	
Fighter Escort	A	400+	401	None	Note 3.	Lenox 1976/ Jane80-87	Land-based	20 min + 5% of initial fuel	As in Figure 60
	C	366	360	None	Note 3.	CRS 2007	Land-based	20 min + 5% of initial fuel	
Ferry	A	2000+	1763	(3) 330 gallon	(2) AIM-9	Janes 1980-91	Land-based	20 min + 5% of initial fuel	As in Figure 61*
	A	1800+	1763	(3) 330 gallon	(2) AIM-9	Janes 1992-3	Land-based	20 min + 5% of initial fuel	
	C	1546	1564	(3) 330 gallon	(2) AIM-9	Navy 2008	Land-based	20 min + 5% of initial fuel	
Combat Ferry	C	1089	1106	None	(2) AIM-9	Navy 2008	Land-based	20 min + 5% of initial fuel	As in Figure 61

Note 1. (2) AIM-9, FLIR, Laser Spot Tracker Pod, (4) MK-83

Note 2. (2) AIM-9, FLIR, NAVFLIR, (4) MK-83LDGP

Note 3. (2) AIM-9, (2) AIM-7

*2500 lb of combat fuel was assumed for the combat segment following Jane's All the World Aircraft 1987-1988

7.6.7 Summary of Modeling and Simulation I

In **Step 5**, a computer model of the F/A-18C was constructed using FLOPS. The validity of the model was confirmed by comparing the calculated aircraft performance to the published data at both the subsystems level and the systems level. As a summary, the mission performance, carrier suitability, and fighter performance as in the KPPs defined in **Step 1** are compared in Table 27. The review of the actual F/A-18C data is provided in APPENDIX B.

Table 27: F/A-18C Performance Comparison

Category	Key Performance Parameters	Published	Calculated	Units
Mission	Fighter escort radius	366	360.35	nm
Performance	Interdiction mission radius	369	371.9	nm
Carrier	Recovery payload	5,623	5,465	lb
Suitability	Launch wind over deck	not listed	21.23	knots
	Recovery wind over deck	not listed	3	knots
	Approach speed	141	141	knots
Fighter	Combat ceiling	53,141	52,339	ft
Performance	Specific excess power at 0.9M/10,000 ft	699	686.7	ft/sec
	Acceleration from 0.8M to 1.2M at 35,000 ft	55.8	66.54	sec
	Turn rate at 15000K	12.3	12.039	deg/sec

7.7 Modeling and Simulation II: Step 6

As the future requirements are expected to grow in the future, the baseline vehicle is also expected to grow to meet or exceed the evolving requirements. To model physical growth of the vehicle, a set of scaling laws are established and validated in this step.

FLOPS has the capability to capture the effects of parametric variations of vehicle characteristics to some degree. For example, FLOPS has some logics to evaluate changes in weight, aerodynamics, engine performance, etc. FLOPS was used as a primary means

to model the upgrades whenever possible. However, FLOPS is limited in handling the issue of volume requirement and availability of a fighter aircraft. Thus, a computer code to volumetrically size the F/A-18 baseline was written. In addition, scaling laws for aft-body size, tail size, weight change, and external stores weight and drag changes were developed and calibrated. The scaling laws were validated by applying them to the F/A-18C model created in **Step 5** to model the F/A-18E and by comparing the performance of the F/A-18E model to published data.

In addition to ensuring physical scalability of the model, it is essential to create a model to capture the cost of vehicle upgrade. The cost model of the notional fighter was created primarily through the use of Military Aircraft Life Cycle Cost Analysis (MALCCA) [205], a FORTRAN code developed by the Aerospace Systems Design Laboratory at Georgia Tech. The software was developed to work with FLOPS seamlessly and automatically reads the vehicle definitions from the FLOPS input file. Moreover, since MALCCA was developed based on supersonic fighters such as the F-18 and the F-16, the code is quite suitable to model a notional fighter based on the F-18. While MALCCA has the functionality to model the cost of developing a derivative aircraft as well as a new aircraft, it requires a pre-process to provide the necessary inputs to calculate aircraft upgrade cost. A set of logics was established and written as a computer code to prepare inputs to MALCCA.

7.7.1 Volumetric Sizing

One of the aspects of aircraft sizing is balancing aircraft internal volume available and required. During the sizing process, those volumes available within the wings and

fuselage are calculated and the fuselage is sized to make sure that available volume is larger than required volume. This imposes a constraint in aircraft sizing as follows:

$$\text{Internal volume required} - \text{Internal volume available} \leq 0 \qquad (61)$$

It is customary in aircraft design to allow some margin or growth potential in volume to allow for redesign or repackaging in the case of requirement growth and/or error in estimating either the volume required or available. However, for fighter aircraft that are required to fly supersonically, cross-sectional areas are minimized to reduce wave drag by packaging the internal area as tight as possible. Cases studies in Chapter 3 showed that for fighter aircraft limited volume available inside the airframe had posed great challenges in modifying existing available versus the volume required is very likely an *active constraint* and, therefore, must be accounted for. This section discusses volume issues of the F/A-18 and how to calculate both required and available volume when design changes are made.

7.7.1.1   *Actual F/A-18 Internal Volume Available and Required*

The F/A-18 was originally designed with room for growth in terms of the volume, although the exact magnitude is unknown. Wood's [206] indication of the F-18 A being designed with 15-20 years of growth potential gives a rough idea, but the allocation of such growth potential had to be assumed. Over time, a series of upgrade programs added more avionics, leaving very little room for growth eventually. By the time when the need for the E/F was established, the F/A-18C/D was expected to have only 0.2 ft^3 of usable volume remaining when all the planned avionics upgrades had been executed through the mid-1990s [191]. The fact the C/D version would reach its growth potential in terms of

the volume availability was one of the major reasons why the E/F program was initiated.

In the design of the F/A-18E/F, additional internal volume was needed over C/D's internal volume to accommodate 573 gallons of additional internal fuel. In addition to the extra internal fuel, 17 ft^3 extra room was required to provide volume for P^{3}I avionics upgrades from the F/A-18C/D's FY 1998 avionics package [191]. The required internal volume was appropriated from both the wings and the fuselage. The F/A-18E/F's 25 percent larger wing provided a 244 gallon fuel tank in each wing, which is a 187 percent increase from the 85 gallon fuel tank of the F/A-18A/B/C/D. In addition to a larger wing, a 34 inch fuselage plug was added to acquire more volume for fuel and equipment. Figure 62, taken from the F/A-18A/B/C/D and E/F NATOPS Flight Manuals [175, 183], shows the internal fuel tanks of the F/A-18A/C (one seat version) at the top and the F/A-18E/F (both one seat and two seat versions) at the bottom. The bottom figure shows that the difference between the E and F versions is that the F version has a shorter fuselage tank (tank 1) with 138 gallons less capacity in order to accommodate the second pilot. It is clearly seen from the figure that E has larger wing fuel tanks and longer fuselage tanks. The fuel capacity of each tank is summarized in Table 28.
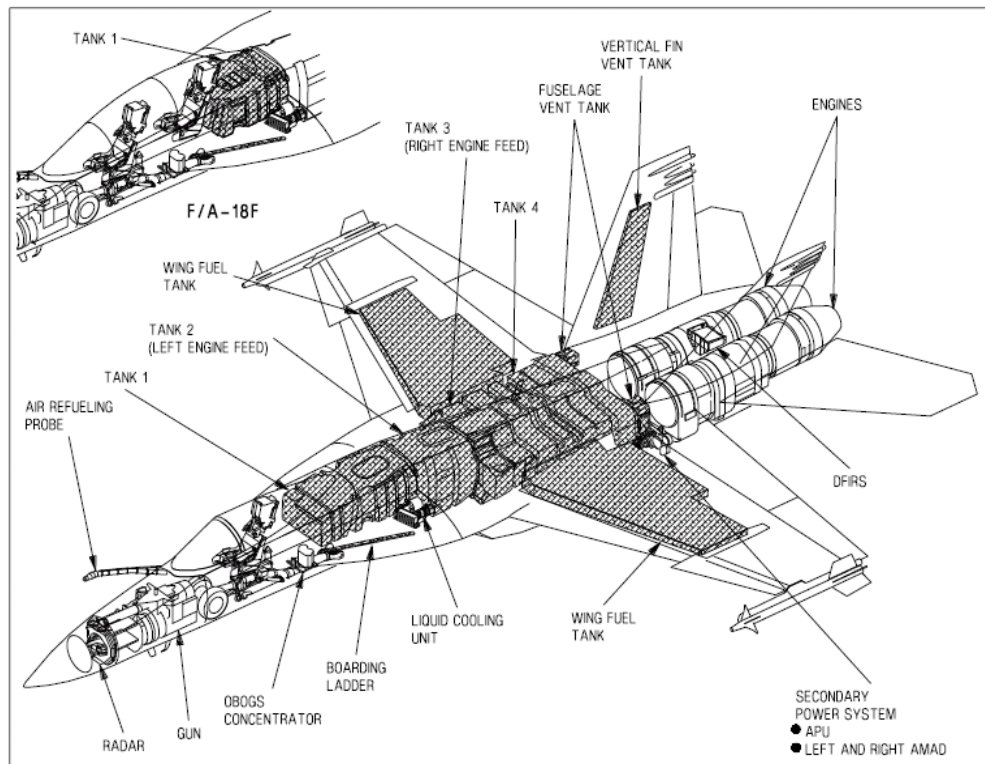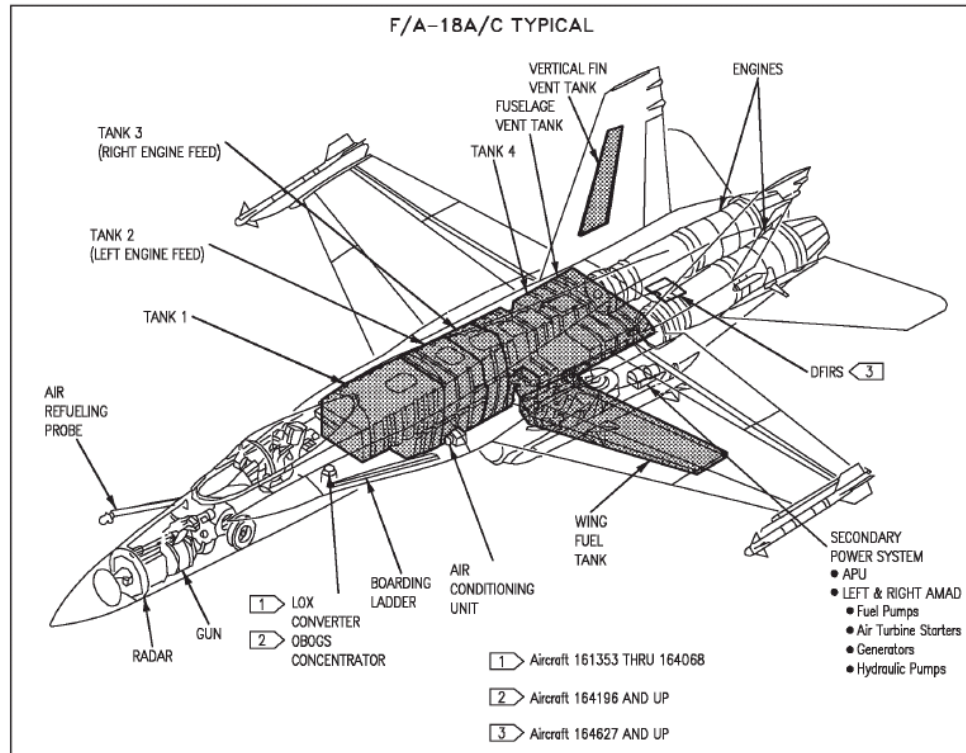
Figure 62: The F/A-18A/C (Top) and the E/F (Bottom) Fuel Tanks [175, 183]

Table 28: F/A-18 Internal Usable Fuel Volume in US Gallon [175, 183]

Tank Number	F/A-18A/C	F/A-18E
Tank 1	418	350
Tank 2	263	383
Tank 3	206	385
Tank 4	532	555
Total Fuselage	1,419	1,673
Internal Wings	170	489
Total Internal	1,589	2,162

7.7.1.2   Calculation of Extra Internal Volume Available and Required

Based on the F/A-18's volumetric information, collected and summarized in the previous section, a set of rules to calculate volume required and available are developed in this section. The point of interest here is not the total volume available and required but the change of those volumes due to the change in the need for internal fuel capacity and avionics. As in the case of the F/A-18E/F, the extra volume needed is acquired by stretching the fuselage and/or enlarging the wing.

First, extra volume available by stretching the fuselage ($\Delta V_{A,fuse}$) was calculated as follows:

$$\Delta V_{A,fuse} = d \cdot h \cdot \Delta l \cdot \frac{\kappa}{4} \cdot C_f \tag{62}$$

where d is fuselage maximum width; h is fuselage maximum height; Δl is length of the fuselage plug; κ is sectional shape factor, e.g. π for a circle or an ellipse, 4 for a square; C_f is the fraction of usable volume out of total internal volume.

It was assumed that for this particular fighter application, additional fuel and avionics were located using following rules:

- Additional internal fuel is stored in the wing if any volume is available

- The rest of the additional fuel, if any, is stored in the fuselage
- Avionics are only placed in the fuselage

Then, volume available within the wing ($W_{fuel,wing}$) by increasing the wing area is all reserved for extra fuel and is calculated using a formulation in FLOPS.

$$\Delta W_{fuel,wing} = R_f + P_f \cdot \Delta S \tag{63}$$

where R_f is reference fuel capacity in pounds (1,156 lb for F/A-18A/B/C/D); P_f is a factor to convert wing volume available to fuel capacity in pounds (21.692 for F/A-18); and ΔS is wing area change in ft^2 (100 ft^2 for F/A-18).

All the additional avionics and required fuel less the extra fuel that went to the wing are placed in the fuselage. The fuselage volume required ($V_{R,fuse}$) to house these items is calculated by

$$\Delta V_{R,fuse} = 1.05\rho_{fuel}(\Delta W_{fuel} - \Delta W_{fuel,wing}) + \rho_{eq}W_{eq} \tag{64}$$

where ΔW_{fuel} is additional internal fuel capacity required in pounds; ρ_{fuel} is fuel density; ΔW_{equip} is additional equipment in pounds; ρ_{equip} is average density of additional equipment.

In order to apply the proposed formulations on the baseline F/A-18, the extra volume available using the fuselage plug was estimated first. Figure 63 shows the F/A-18 Hornet's planform view and cross-sectional geometry at various fuselage stations (FS). The fuselage starts with a circular cross-section at the nose (FS 68) and is stretched longitudinally to form an ellipse before the cockpit is attached. As it passes the cockpit, the shape becomes close to square. The cross-section at FS 357 covers a larger area than an ellipse but a smaller area than a square. In general, fuselage plugs are inserted in the middle of the vehicle section to minimize the longitudinal variation of the center of
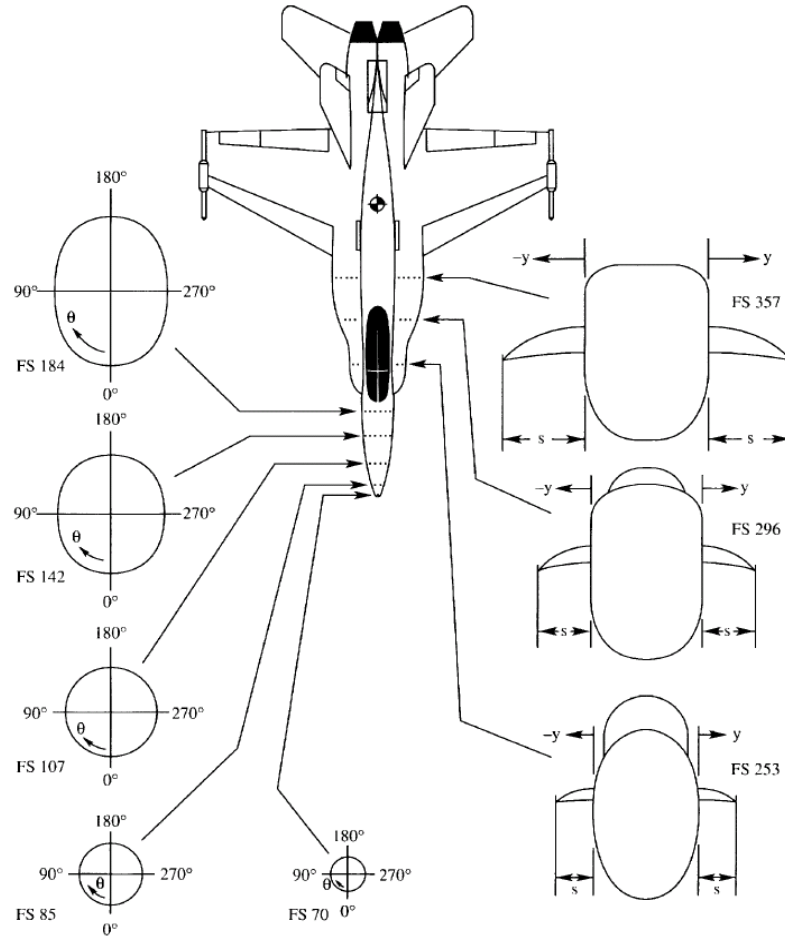
Figure 63: F/A-18A/B/C/D Planform and Cross-Sectional Geometry [207]

gravity. Considering the CG location of the F/A-18 marked in the figure, it was assumed that the 34-inch fuselage plug that was inserted in the mid fuselage section uniformly follows the cross-sectional shape of the FS 357. The 34-inch fuselage plugq using FS 357 sectional geometry, gives 55.257 ft^3 of volume under the skin. Subtracting 5 percent of assumed unusable volume, 52.49 ft^3 of usable fuselage volume was obtained.

As for calculating required volume, it was assumed that all the fuel goes to the wing volume first and any remainder goes to the fuselage. Knowing the fuel weight that should go to the fuselage, the volume for fuel is calculated assuming JP-5 jet fuel at standard temperature density of 6.8 lb per gallon. In addition, the volumes required for avionics and equipment are calculated based on the weight of the system multiplied by

the average density. The average density of avionics and equipment was assumed at 25 lb per cubic foot, which is approximately the density of the F404-GE-400 engines.

Finally, volume growth potential is calculated by subtracting required volume from available volume. Table 29 shows the calculated growth potential of the F/A-18A, C, and E with C avionics and E with its upgraded avionics. The avionics weights of the C and E versions are from [4]. The avionics weight of the F/A-18A was not available, and thus an assumption had to be made. With 1,089 lb of assumed avionics weight, it can be said that the F/A-18A was designed with 8.2 ft^3 of volume growth potential. As avionics weight increased over time, the F/A-18C reached a point where remaining volume available was only 0.2 ft^3. The F/A-18E's growth potential—when equipped with the F/A-18C's avionics package—was calculated to be 17.1 ft^3, which is close to the published value of 17 ft^3. Finally, the current F/A-18E growth potential after the P^{3}I avionics upgrade was calculated to be 12.2 ft^3.

Table 29: F/A-18 Volume Growth Potential Calculation

Version	A	C	E (w/C avionics)	E	Unit
Wing area	400	400	500	500	ft^2
Wing fuel capacity	1,156	1,156	3,325	3,325	lb
Fuselage plug length	0	0	2.83	2.83	ft
Fuselage fuel capacity	1,419	1,419	1,673	1,673	lb
Avionics weight	1,089*	1,289	1,289	1,411	lb
Growth potential	8.2	0.2	17.1	12.2	ft^3

*F/A-18A avionics weight was assumed.

7.7.2 Aft-Body Sizing

For a fighter aircraft with air breathing propulsion systems integrated into the airframe, the sizing of the structure that houses the engines, induces air flow into the engines, and discharges the air from the engine exit is one of the most important aspects of aircraft

sizing. History has shown that it is very likely that the engine thrust of a given aircraft would grow over time. Engine manufacturers usually provide a series of upgraded derivative engines by increasing the mass flow while keeping the core of the baseline engine. Engine upgrade might be easier if the engines are mounted in nacelles that are outside of the wing or fuselage, which are common cases for the commercial transports. However, upgrading propulsion systems could cause huge challenges if they start to interfere with other components. As shown in the case studies in §3.3, re-engining of the F-4K/M phantom for the Royal Navy required the entire redesign of aft-fuselage, inlets, and ducts.

Considering the very high possibility of upgrading the engines later on, it is a common engineering practice to provide some extra room for growth provisions as Northrop did on the F-5G as introduced in §3.1.1.1. For the F/A-18, the original inlet and nacelle design seems to have some level of growth potential, considering the fact that engine enhancement from F404-GE-400 to F404-GE-402 was done without modifying airframe structures, while thrust increased by approximately 11 percent. Then, during the next round of upgrade program (the E/F program), nacelle length, measured from the tip of the inlet to the end of the nozzle, increased from 25.65 ft to 30.48 ft, while engine thrust increased from 17,754 lb to 22,000 lb.

To properly size the aft-body structure related to engine mount and operation, it is necessary to define a way to scale those structures and measure their growth potentials. In this study, the entire structure including engine compartment, inlets, ducts, and nozzles are viewed as a nacelle assembly and sized together. The aft-body of the FA-18 is two nacelle assemblies attached side-by-side.

The dimension of nacelle assembly is represented by its diameter (d_n) and length (l_n). A scaling law to size a nacelle assembly is proposed and validated based on the F/A-18 data. A nacelle assembly is scaled based on the engine thrust following the formulation:

$$l_n = l_{n,ref} \cdot (T / T_{ref})^k$$
$$d_n = d_{n,ref} \cdot (T / T_{ref})^k$$

$$(65)$$

where l_n and $d_{n,ref}$ are the length and diameter of the baseline nacelle assembly; T is engine thrust; T_{ref} is baseline engine thrust; and k is the exponential factor to scale nacelle size. For the value of k, 0.5 is selected, considering that engine thrust is proportional to the mass flow rate if the core is the same and mass flow rate is proportional to the engine cross-sectional area, which is proportional to the engine diameter squared.

To identify reference nacelle size and engine thrust, it was assumed that growth potential of 12 and 15 percent were embedded in the design of the F/A-18A/B's and E/F's aft-body, respectively. Finally, since actual F/A-18's nacelle diameter was hard to measure, 48-inch diameter was assumed to give room for structure, installation, and maintenance of 36-inch diameter F404-GE-400/402 engines. Based on these assumptions, nacelle length and diameter were calculated as shown in Table 30 Calculated nacelle lengths matched actual nacelle assembly lengths of all F/A-18 versions.

In summary, the notional fighter's aft-body is scaled using two parameters, engine thrust and nacelle assembly growth potential. As those two parameters change, nacelle assembly length and diameter are calculated and inputted to FLOPS. Then, FLOPS estimate the weight and drag effect of the new aft-body size.

Table 30: F/A-18 Nacelle Assembly Size

	A/B	C/D	E/F	Unit
Engine thrust	16,000	17,754	22,000	lb
Ref. thrust for aft-body sizing	*17,920*	*17,920*	*25,300*	lb
Nacelle growth potential	*12*	*0.94*	*15*	%
Actual nacelle length	25.65	25.65	30.48	ft
Calculated nacelle length	25.65	25.65	30.48	ft
Calculated nacelle diameter	48	48	57	in

Note: Values in italics are assumptions.

7.7.3   Horizontal and Vertical Tails

Horizontal and vertical tail areas are determined considering stability and control aspects of the aircraft at all expected flight conditions. During conceptual design of aircraft, however, it is conventional to estimate required tail surface areas based on historical trend. By understanding that the function of horizontal and vertical tails is to counteract the movement about the center of gravity of the aircraft, mainly produced by the wing, a consistent trend between the wing geometry and required tail areas is observed. This trend is formulated into two non-dimensional parameters called tail volume coefficients [6].

In FLOPS, tail areas are either hard-coded or calculated based on the tail volume coefficients, wing area, aspect ratio, and fuselage length. Knowing those geometric variables of the F/A-18A/B/C/D (as in Table 15) and the F/A-18E/F including horizontal and vertical tail areas[*], tail volume coefficients were calculated and inputted into FLOPS to model the C/D version. Then, the tail areas of a notional aircraft are calculated by FLOPS as wing area and other geometry varies. The volume coefficients

---

[*]"The E/F … have a 25-percent larger wing, a 35-percent larger horizontal tail, a 15-percent larger vertical tail, and a 34-ince fuselage extension [75]."

were linearly interpolated with respect to the wing area from the settings of the C/D and E/F versions.

7.7.4 Weight

F/A-18E weight breakdown is also constructed as shown in Table 31. The empty weight of 30,564 lb from reference [153] was used, since the performance metrics listed in Table 35 are based on that production model. Crew, unusable fuel, gun, chaff, etc. were assumed equal to those of the F/A-18C. External stores and usable fuel weight is from the F/A-18E/F NATOPS Flight Manual [175].

Using the F/A-18C FLOPS model, the weight of the F/A-18E was calculated by setting the design parameters at the E's values as listed in Table 34. Subsystem weight scaling factors that were used to calibrate the F/A-18C model remained unchanged. Table 32 compares the calculated and actual weights of the F/A-18E in attack configuration. Using the same calibration factors, FLOPS estimated the weight empty with less than one percent of error.

Table 31: F/A-18E Weight Breakdown

		Weight per Unit	# in Attack	# in Fighter	Attack Weight	Fighter Weight
Weight Empty					**30,564**	**30,564**
Crew					180	180
Crew Equipment					59	59
Unusable Fuel					207	207
Engine Fluid					114	114
Gun					204	204
400 Rounds Ammo					100	100
Chaff					52	52
SUU-80 w/BRU-32	LD Pylon	181	2	0	362	0
SUU-80 w/ADU-773	LD Pylon	123	2	0	246	0
SUU-79/A w/BRU-32	STD Pylon	310	2	0	620	0
ARR-55	Nav. FLIR pod	214	1	0	214	0
AAS-46	Target FLIR	370	1	0	370	0
SUU-78/A w/BRU-32	Centerline Pylon	139	1	0	139	0
Operating Weight					**33,431**	**31,480**
480 GAL. Tank	Wing Tank	350	2	0	700	0
480 GAL. Tank	Centerline Tank	350	1	0	350	0
MK-83	1000 lb Bomb	1005	4	0	4,020	0
AIM-9	Sidewinder	195	2	2	390	390
AIM-120	AMRAAM	345	0	2	0	690
Payload					**5,460**	**1,080**
Internal Fuel					14,700	14,700
External Fuel	Wing Tank	3260	2	0	6,520	0
	Centerline Tank	3220	1	0	3,220	0
Usable Fuel					**24,440**	**14,700**
Takeoff Gross Weight					**63,331**	**47,260**

Table 32: F/A-18E/F Weight in Attack Configuration

	Actual	Calculated
Weight Empty	30,564	30,832
Payload	7,411	7,411
Usable Fuel	24,440	24,440
Takeoff Gross Weight	63,331	63,599

7.7.5 Weight and Drag of External Stores

Geometric growth of a vehicle affects both weight and aerodynamic properties of the vehicle. For the major subsystems, FLOPS updates weight and aerodynamics parametrically as design changes. However, the weight and drag changes due to external stores must be pre-calculated and inputted to FLOPS.

In the case of the F/A-18, externally carried payloads are missiles, bombs, pods, and fuel tanks. Drag contribution of pods is relatively small, since they are attached at the fuselage stations without pylons. Drag increment due to missiles and bombs and associated pylons can be calculated using the data in the flight manual. For example, drag contribution of two AIM-7s and two AIM-9s is 8 counts and increases to 24.8 counts if two AIM-120s are installed instead of two AIM-7s.

Among the externally carried items, drag contribution is dominated by external fuel tanks, and the contribution from bombs and missiles is relatively small. Drag contribution from an external fuel tank is significant enough to affect aircraft performance in a very meaningful way. Table 33 lists the drag and weight of fuel tanks and pylons for both the F/A-18C/D and E/F. As fuel capacity per tank increases from 330 gallons to 480 gallons, drag increases more than a hundred percent. When all three external fuel tanks are carried, storage drag due to fuel tanks and pylons is 86.8 counts

for the 480-gallon tanks and 39.5 counts for the 330-gallon tanks. Total weight increases from 870 lb. to 1,050 lb. Using these actual C/D and E/F fuel tank data, weight and drag for a *rubberized* fuel tank were interpolated according to its fuel capacity and inputted to FLOPS for mission analysis.

Table 33: Weight and Drag of F/A-18 External Fuel Tanks and Pylons

Version	Item	Name	Weight (lb)	Drag (count)
C/D	330 GAL Tank	External Fuel Tank	290	$10.5^*/14.5^\dagger$
	SUU-63	Wing Pylon	310	7.5
	SUU-62	Centerline Pylon	139	3
E/F	480 GAL. Tank	External Fuel Tank	350	$25^*/30.9^\dagger$
	SUU-79/A w/BRU-32	STD Pylon	310	9.4
	SUU-78/A w/BRU-32	Centerline Pylon	139	1

* When attached to the centerline pylon

† When attached to the wing pylon

7.7.6 Performance Validation

The set of scaling laws presented in the sections above were written in a computer code and integrated with FLOPS. The integrated aircraft performance analysis tool was specifically prepared for a notional carrier-based multi-role fighter based on the F/A-18 Hornet. To check the validity of the computer model's scalability, an F/A-18E model was created by scaling up the C model developed in **Step 5** and then compared against actual weight and performance data.

Table 34 lists the design changes from F/A-18C to the E version in accordance with the design variables that were defined in **Step 3**. All the values for the vehicle system level design variables increased noticeably. It is important to note that the E model was not created independent to the C model, but it was a scaled-up version of the C model following the set of scaling laws proposed in this chapter.

Table 34: F/A-18 Changes from the C to E Versions

Design Variables	F/A-18C	F/A-18E	Units
Wing area	400	500	ft^2
Thrust	17,754	22,000	lb
Ref. weight for DLF of 7.5 g	32,000	42,097	lb
Operational landing weight	33,000	44,000	lb
Internal fuel capacity	10,810	14,700	lb
External fuel capacity	6,720	9,740	lb
Fuselage length	53	55.83	ft
Avionics weight	1,289	1,411	lb

The validity of the scaling laws is confirmed by comparing the performance analysis results of the created F/A-18E model and actual data. Actual F/A-18E performance data are based on the flight tests conducted by the US Navy in 1998 and are from references [153, 208]. Two important assumptions were made on the reserve conditions. For the fighter mission, reserve fuel for 20 minute loiter at sea level, plus 5% of initial fuel was assumed. For the attack mission, the fixed 3,500 lb of reserve fuel was assumed. Table 35 shows both actual and calculated mission and point performance of the F/A-18E. Both fighter escort radius and interdiction mission radius with three 480-gallon fuel tanks using the hi-lo-lo-hi profile matched very closely. All other performance parameters were very close to the actual values.

Table 35: F/A-18E Key Performance Parameters

Category	Key Performance Parameters	Actual	Calculated	Units
Mission	Fighter escort radius	462	468.45	nm
Performance	Interdiction mission radius	498	499.20	nm
Carrier	Recovery payload	9,125	9,251	lb
Suitability	Launch wind over deck	29.9	29.51	knot
	Recovery wind over deck	9	9.56	knot
	Approach speed	142	141.48	knot
Fighter	Combat ceiling	52,300	52,992	ft
Performance	Specific excess power at 0.9M/10,000 ft	648	674.80	ft/sec
	Acceleration from 0.8M to 1.2M at 35,000 ft	64.85	64.62	min
	Turn rate at 15,000K	11.6	11.90	deg/sec
Others	Volume growth potential	12.21	12.21	ft^3
	Usable load factor	7.5	7.52	g

7.7.7 Development of the Cost Model

The F/A-18 cost model was created using FLOPS, Military Aircraft Life Cycle Cost Analysis (MALCCA), and a code written by the author. MALCCA [205] is a weight- and process-based military cost analysis code with a capability to model derivative aircraft by specifying detailed input of design ancestors. To construct and validate the cost model, numerous public domain sources were consulted. Although the sources for the numbers used in this study are mentioned in the following sections as necessary, some of the sources found to be useful in studying military cost in general are introduced in §C.2 for future reference. Some of the definitions of military cost terms such as program acquisition cost, procurement cost, operation and support (O&S) cost, and life-cycle cost are also referred to §C.1. The test and evaluation programs of the F/A-18A/B/C/D and E/F are summarized in §C.4.

7.7.7.1 RDT&E Cost and Duration

The focus of the cost model was accurate calculation of RDT&E and production cost. Since this study excluded retrofitting of existing aircraft, the production cost model is for new manufactures. Therefore, RDT&E cost is the only factor that differentiates a new design and a derivative design, and particular effort was made to develop an activity- and process-based RDT&E model.

7.7.7.2 Flight Test and Wind Tunnel Test

RDT&E cost is calculated utilizing MALCCA. MALCCA is integrated into FLOPS and reads the vehicle properties automatically. The research and development (R&D) cost is mainly calculated based on the engineering hours. Engineering hours are estimated for major aircraft subsystems based on weight-based empirical relationships and are summed up. Engineering hour estimation for a subsystem is strongly related to its own weight and to key design parameters that define such a subsystem. If the aircraft development is a follow-on program, a certain portion of the required engineering hours is saved, depending on the amount of design commonality to its predecessor.

Then, test and evaluation (T&E) cost is mainly decided by the number of test vehicles, flight test hours, types of ground test, and wind tunnel test hours, which are all inputs to MALCCA. To determine these parameters, all the potential design change options are mapped to the list of test activities using a flight test matrix (FTM), a wind tunnel test matrix (WTM), and a ground test matrix (GTM).

While the EvoLVE process identifies the aircraft design upgrade options and technologies in **Step 4**, this study compiled the list of the design change options by benchmarking the Hornet 2000 study introduced in §C.3 and the F/A-18E/F program.

The cost data from these sources are used to validate the RDT&E cost model later. The list of the design changes are:

1. Wing photographic scaling
2. Wing design change
3. LEX design change
4. Engine upgrade
5. Wing structural stiffening
6. Design landing weight
7. Inlet/nacelle (aft-body)
8. External fuel tank redesign
9. Fuselage plug
10. Avionics upgrade
11. New armament
12. Conformal fuel tank
13. Internal fuel capacity

The review of the F/A-18A/B and E/F test programs is provided in §C.4. The F/A-18A/B flight test program used eleven test articles logging 305 aircraft months. The C/D program used two flight test vehicles and the E/F program used seven flight test and three ground test articles [71, 209]. Figure 109 in §C.4 provides the list of test activities and the schedule of the F/A-18A/B's full-scale development flight test program for each of the eleven flight test articles. These flight test activities or tasks were used to construct a FTM.

Table 36 is the FTM created for the notional fighter. The flight test activities of the F/A-18A/B program are listed in the left column, and all the design change options are listed in the header row. Then, each cell of the matrix maps the degree of effort needed to perform the flight test activity for a specific design change. The amount of effort required is measure in flight year for the FTM. The goal here is to calculate the total

flight year, which is obtained by activating the columns associated with the design changes and summing up all flight years that are in the active columns. For example, if engine and avionics upgrades are made, the fourth and tenth columns become active. If the new engine grows more than the capacity of aircraft aft-body assembly that houses the engine, the aft-body needs to be redesigned and the seventh column is activated, too. Then, all the elements in the active three columns are added to get the total flight year.

The relationship between the flight test activities and design changes would be ideally mapped by the team of experienced experts from related disciplines. An integrated product team (IPT) consisting of test pilots, test engineers, managers, and design engineers would be able to estimate the types of tests required in order to upgrade a specific aircraft subsystem, such as avionics, external fuel tanks, landing gears, etc. In this study, however, the author's own judgment was used to fill the FTM using the following rationales.

When aircraft wing and/or LEX change, all the flight tests evaluating aerodynamic characteristics of the vehicle are triggered. The degree or intensity of test required varies if the change is a new LEX design, wing scaling, or a completely new wing design. Design landing weight is related to landing gears and the fuselage frame that landing gears are mounted to. A change in landing weight will require more capable landing gear, and the airframe structure needs to be changed too; the landing gear door size and structural strength should be increased. Thus, it will require carrier suitability, structural tests, and MEI. A performance flight test is required when the vehicle aerodynamics and/or engine/inlet changes. Weight increase does not require a performance flight test. So, any external geometry change would require a performance

test. Drag increase due to a new type of external stores also requires some level of performance test. Raising fuselage dorsal does not affect aircraft structure, as its impact is mostly on lift independent drag. Thus, it would not require high AOA tests or carrier suitability tests.

The calculated flight test year is then converted into aircraft months by multiplying by twelve. Then, total aircraft months are used as the basis to calculate total flight test hours, the number of flight test vehicles required, and the flight test duration. In practice, how much time and how many aircraft a flight test program would need is estimated based on experience with aircraft of the class.

Table 36: The Flight Test/Wind Tunnel Test Matrix (FTM/WTM)

Flight Test Name	1 Wing Scaling	2 Wing redesign	3 LEX redesign	4 Engine upgrade	5 Wing structural stiffening	6 Design landing weight	7 Inlet/ nacelle	8 External fuel tank redesign	9 Fuselage plug	10 Avionics upgrade	11 New armament	12 Conformal fuel tank
Flying qualities, flutter	0.6	0.8	0.2					0.2				0.7
Propulsion, performance				0.5			0.5					
Carrier suitability, ECS	0.6	0.7	0.2			0.1						
Structural	0.7	0.7			0.5	0.15			0.15			
Avionics										1		
High AOA	0.6	0.8	0.2									
Armament, systems											1	
Armament, avionics										1		
Performance, systems	0.5	0.5	0.2				0.2	0.15	0.15			0.7
Engine accel. service test				1								
MEI/EMC						0.2	0.3		0.1	0.4		
Wind tunnel test required	yes	yes	yes	no	no	no	yes	yes	yes	no	yes	yes
Wind tunnel test level	0.3	1	0.5	0	0	0	0.3	0.2	0.3	0	0.3	0.3

The key flight test program attributes—flight test aircraft required, total flight test hours, and FT duration—of a notional fighter are calculated using the statistics of the E/F test program data as given in §C.4. Total aircraft month, ACM, calculated from FTM is converted to total flight hours (t_f), assuming 18.9 available test hours per month, which was the case of the F/A-18E/F flight test program.

$$t_f = \frac{ACM}{\left(\frac{ACM_{ref}}{t_{f,ref}}\right)} \tag{66}$$

The number of aircraft required (N_{fv}) is calculated as:

$$N_{fv} = \frac{ACM}{\left(\frac{ACM_{ref}}{N_{fv,ref}}\right)} \tag{67}$$

where the ratio between total aircraft month to the number of total aircraft is average aircraft month flown by a flight test aircraft, which is 30.5 for the F/A-18E/F program. Finally, the DT duration in month (t_{DT}) is calculated as:

$$t_{DT} = \frac{ACM}{\left(\frac{ACM_{ref}}{t_{DT,ref}}\right)} \tag{68}$$

The total DT duration from the first flight to the end of DT was 40 months for the F/A-18A/B program and 40 months for the F/A-18E/F program, excluding the operational evaluation (OPEVAL) periods.

A required wind tunnel test hour is calculated using the WTM, constructed as a sub-matrix of the FTM in Table 36. In constructing WTM, the relative or absolute level of wind tunnel test required is measured for each category of design change by a team of

experts. In the case of the WTM of a notional fighter, the level of wind tunnel test required to upgrade the wing design was set to one, and the relative effort of upgrading LEX, fuselage, etc. was assessed accordingly. For example, photographic scaling of the wing was assumed to take only 30 percent of the wind tunnel test effort compared to the effort the entirely new wing design would require. Some aircraft upgrades, such as wing structural stiffening, do not affect external geometry and thus do not require any wind tunnel test. The total effort is converted into wind tunnel test hours using the fact that the F/A-18E/F wind tunnel test program logged 4,500 hours [210].

7.7.7.3   Ground Test

MALCCA calculates the cost of ground tests based on the types of test defined by the user. A list of conventional ground test activities is shown in the left column of the ground test matrix (GTM), and the header row is the types of design change activities. The test requirements are mapped by filling out the matrix. This task would be done by an IPT of experienced engineers, technicians, and managers, who are knowledgeable about aircraft modifications. However, for this study, a GTM for the notional multi-role fighter shown in Table 37 was created by the author. The types of ground tests listed in the first column are actual inputs to MALCCA. A set of planned design changes activates the corresponding columns. Then, for each of the rows, all the numbers in the active cells are added. The total value for a row is fed into MALCCA for cost calculation.

Table 37: Ground Test Matrix (GTM) for the Notional Multi-role Fighter

Ground Test Name	1 Wing Scaling	2 Wing design change	3 LEX design change	4 Engine upgrade	5 Wing structural stiffening	6 Design landing weight	7 Inlet/nacelle	8 External fuel tank redesign	9 Fuselage plug	10 Avionics upgrade	11 New armament	12 Conformal fuel tanks	13 Internal fuel capacity
Static Test Articles	0.7	1	0.2	0	0.1	0	0	0	0	0	0	0	0
Fatigue Test Articles	0.7	1	0.2	0	0.1	0	0	0	0	0	0	0	0
Iron Bird Test Articles	1	1	0	0	0	0	0	0	0	0	0	0	0
Propulsion Test Articles	0	0	0	0.8	0	0	0.2	0	0	0	0	0	0
LG Test Articles	0	0	0	0	0	1	0	0	0	0	0	0	0
Fuel Rig Articles	0	0	0	0	0	0	0	0.5	0	0	0	0.5	0.5
Armament Test Rigs	0	0	0	0	0	0	0	0	0	0	1	0	0
Hardware/Software Integration Rigs	0	0	0	0	0	0	0	0	0	1	0	0	0
Subsystem Test Rigs	0.2	0.2	0	0.2	0	0.1	0.1	0.1	0.1	0.1	0.1	0.1	0.1

7.7.7.4   Design Commonality

In order to calculate the RDT&E cost of developing a derivative aircraft using MALCCA, the degree of design commonality of the derivative aircraft to its predecessor must be defined. MALCCA calculates the engineering hours during RDT&E for the subsystems using its weight-based, historical database. To account for savings in engineering hours by adopting previous designs, MALCCA subtracts the portion of the engineering hours already spent in the past development from the current engineering hours required. If a specific subsystem design is equal to an existing design, the engineering time in the development can be waived by utilizing the previous effort.

Therefore, it is necessary to predetermine how much the current subsystems—for example wing, engine, avionics, etc.—are common to the previous subsystems. The degree of commonality is defined by using design commonality factors (DCFs). A DCF is a non-dimensional parameter that is equal to or less than one. DCF determines the percentage of engineering hours spent in the past that can be used to save the engineering hours of the current program.

$$\left(\mathbf{t}_{eng2}\right)_{dev} = \left(\mathbf{t}_{eng2}\right)_{new} - \mathbf{f}_{dc} \cdot \left(\mathbf{t}_{eng1}\right)_{new} \tag{69}$$

where $(\mathbf{t}_{eng2})_{dev}$ is a 1-by-m vector of engineering hours required for a *derivative* aircraft in stage 2; $(\mathbf{t}_{eng2})_{new}$ is the engineering hours required if it were a *new* aircraft program; $\mathbf{f}_{dc}$ is the m-by-1 vector of DCFs; and $(\mathbf{t}_{eng1})_{new}$ is the engineering hours required of the new aircraft in the first stage.

A DCF of one means that the design is the same as its ancestor, and zero means it is a completely new design. DCF was allowed to go below zero in order to simulate

instances in which the historical database is not able to capture factors such as new technology development. A negative DCF means that additional engineering hours or cost are needed to develop such subsystems. A DCF value of one does not always imply that the number of required engineering hours for the subsystem is zero: it could be still greater than zero if the second-stage subsystem is heavier than the first-stage subsystem.

The rules to define DCFs that were created for the twelve subsystems are listed in Table 38. The degree of design commonality is determined by the difference between design variable settings of the first and second design stages. For example, fuselage design commonality decreases when design changes are made on design landing weight (landing gears), reference engine thrust for aft-body sizing, fuselage length, design load factor, and the reference weight for design load factor. The relationship between design commonality factors and design change is mapped using following equation:

$$
\mathbf{f}_{dc} = \mathbf{J}_{11\times12} -
\begin{bmatrix}
1.7 & 2 & 2 & 2 & 2 & 0 & 0 & 0 & 0 & 0 & 0 & 0 \\
0 & 0 & 0 & 0 & 0 & 0 & 0 & 1 & 0 & 0 & 0 & 2 \\
0 & 0 & 0 & 0 & 0 & 0 & 1 & 1 & 1 & 0 & 0 & 1 \\
0 & 0 & 0 & 0 & 0 & 0 & 0 & 1 & 0 & 0 & 0 & 0 \\
0 & 0 & 0 & 0 & 0 & 0 & 0 & 0 & 0 & 0 & 1 & 0 \\
0 & 0 & 0 & 0 & 0 & 1 & 0 & 0 & 0 & 0 & 0 & 0 \\
0 & 0 & 0 & 0 & 0 & 1 & 0 & 0 & 0 & 0 & 0 & 0 \\
0 & 0 & 0 & 0 & 0 & 0 & 0 & 0 & 1 & 0 & 0 & 0 \\
1.7 & 2 & 2 & 2 & 2 & 0 & 0 & 0 & 0 & 0 & 0 & 0 \\
1.7 & 2 & 2 & 2 & 2 & 0 & 0 & 0 & 0 & 0 & 0 & 0 \\
0 & 0 & 0 & 0 & 0 & 0 & 0 & 0 & 0 & 0 & 0 & 0
\end{bmatrix} \Delta\mathbf{x} +
\begin{bmatrix}
-0.3T_3 \\
0 \\
0 \\
0 \\
0 \\
0 \\
0 \\
0 \\
-0.3T_3 \\
-0.3T_3 \\
-\Delta w_{av}
\end{bmatrix} \quad (70)
$$

where $\mathbf{f}_{dc}$ is an 11-by-1 vector of DCFs as defined in Table 38; $\mathbf{J}_{12\times11}$ is a 11-by-12 unity matrix; $\Delta\mathbf{x} = \mathbf{x}_2 - \mathbf{x}_1$ is the difference between the first-stage and second-stage design parameters as defined in Table 16; T_3 is a switch for the use of new LEX technology is

one if the new LEX is used and zero if not; and Δw_{av} is avionics weight increase from the

first to the second stage.

Table 38: List of Subsystems

Number	Subsystem
1	Wing
2	Empennage
3	Fuselage
4	Landing gear
5	Nacelle
6	Engine
7	Engine accessories
8	Fuel system
9	Control surfaces
10	Hydraulics
11	Avionics
12	Armament

7.7.7.5 RDT&E Duration

The F/A-18E/F program was managed following the older versions of DoDI 5000.2. The

process shown in Figure 64 is different from the current DoD's acquisition process

presented in Figure 108. The older process clearly divided the RDT&E phase into three

sub-phases of concept exploration, demonstration and validation (Dem/Val), and the

engineering and manufacturing development (EMD), which is different from current

classification. While the first two sub-phases, concept exploration and Dem/Val, can be

stretched to years of effort, the goal of RDT&E duration modeling was limited to only

the EMD period.

Figure 65 from Fox [13] shows both EMD durations of various US military aircraft

programs. The black portion of the bars represents the time from the beginning of EMD

to the start of DT/OT. The grey areas are from the start of DT/OT to the end of EMD.

It was assumed that the first period in EMD is roughly devoted to R&D and the second period to T&E. In the case of the F/A-18E/F, total EMD duration was 7 years, or 84 months, from June 1992 to April 1999, excluding the OPEVAL from May 1999 to November 1999. The duration of DT/OT was 41 months and R&D was 43 months. Although the F/A-18E/F was a derivative aircraft, developing it took slightly more time than developing its ancestor, the F/A-18A/B.
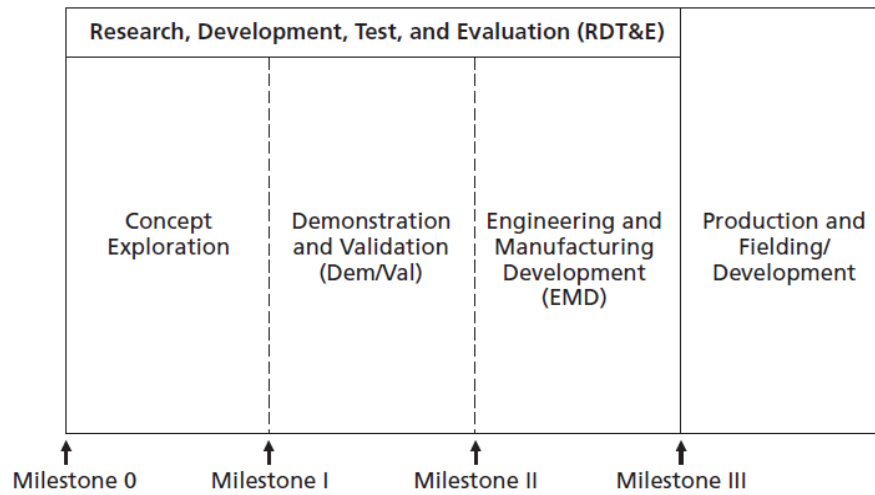
Figure 64: Old Version of DoD Acquisition Process [4]
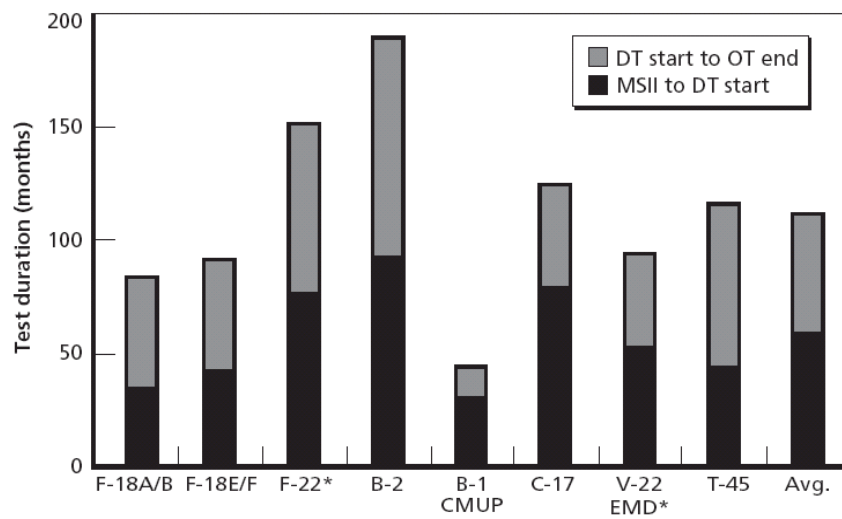
* Program in progress as of the time of publication

Figure 65: EMD Duration of US Military Aircraft [13]

MALCCA calculates engineering hours required based on the vehicle characteristics. The engineering hours calculated from MALCCA are converted to the R&D duration in months by assuming availability of the work forces. The availability of 6,000 workers on average and 1,920 average working hours per worker for a year were assumed. Then, the T&E duration calculated using Eq. (68) is added. Finally, a fixed OPEVAL duration of 7 months was assumed and added.

7.7.7.6   *Synthesis and Validation of the Cost Model*

A computer code was prepared to calculate the key cost inputs to MALCCA. Then, the computer program was integrated into FLOPS/MALCCA. Since the second-stage RDT&E cost is dependent on the first-stage vehicle characteristics, first-stage aircraft performance analysis is a prerequisite of the second-stage analysis.

Production cost was calculated using FLOPS/MALCCA. Production cost is largely dependent on the production quantity, learning curves, labor rate, etc., besides aircraft characteristics. A total of 1,479 F/A-18A/B/C/Ds were produced from 1980 to 1997, including 852 A/Bs produced from 1979 to 1991 in 7 lots and 627 C/Ds produced from 1986 to 1997 in 6 lots [88]. Since the F/A-18C/D is the basis of the first-stage notional fighter, the production quantity was set at 627 aircraft for the first-stage program. The total planned production quantity of the E/F version has been changed a couple of times from its initial plan of 1,000 aircraft to 493 as of December 2007, according to the SARs as summarized in Table 66. However, since the published production cost data that are used here for validation purposes are based on the assumption of 1,000 units, this study also assumed the production of 1,000 aircraft. In addition, since MALCCA can only handle up to 4 lots. It was assumed that all the units are produced in a single lot. Then,

annul production rate of 36 aircraft per year was assumed for all configurations. For the labor rates and learning curves, the default settings for MALCCA were used because no other information was available.

Material composition of the airframe is also an important input determining production cost. Actual F/A-18A/B, C/D, and E/F are collected from Murden [73] and Younossi [211] as given in Table 39. The A/B versions used 55.4 percent of aluminum, 8.4 percent of titanium, 10.3 percent of composites, and 14.1 percent of steel. The composition of aluminum decreased in the C/D and E/F versions. The C/D version used more titanium, and E/F used apparently more titanium and composites. For the F/A-18A, C, and E cost calculated, the actual material composition as in Table 39 was modeled in FLOPS/MALCCA. For the cost calculations of the Hornet 2000 configurations, the C/D's material distribution was assumed.

Table 39: F/A-18 Hornet Material Composition in Percentage of Structural Weight

Materials/Version	A/B	C/D	E/F
Aluminum	55.4	49	31
Titanium	8.4	13	21
Composites	10.3	10	19
Steel	14.1	15	14
Other	11.8	13	15

The fiscal year (FY) 1996 was selected as the base dollar year during all cost modeling processes. The inflation rate was determined using the US Navy inflation index [212]. The US Navy inflation index is available as a calculator that converts the dollar value between two different years for a selected cost category such as RDT&E, aircraft acquisition, operation and support, etc. FLOPS/MALCCA is based on 1988 economics and requires a fixed interest rate input. The average inflation rate of 3.32 percent

between 1988 and 1996 based on the Navy index on aircraft acquisition category was used. Actual F/A-18 cost data were also converted to 1996 dollar value using the appropriate rate category, i.e. RDT&E, production, etc.

Validation of the cost model was conducted by modeling six different F/A-18 variants including four configurations from the Hornet 2000 study, the F/A-18C, and the F/A-18E. §C.3 introduced the Hornet 2000 study in detail. Among seven configurations proposed in the Hornet 2000 study, Configuration I, II, IIIB, and IIIC were selected for the study. These four configurations are progressive upgrades to the F/A-18C. Configuration I is the F/A-18C with new armaments. Configuration II is Configuration I plus wing stiffening, F414 engines, upgraded avionics, and conformal fuel tanks by raising the dorsal. Configuration IIIB is Configuration II with a 500 ft^2 wing. Configuration IIIC uses a fuselage plug to increase internal fuel capacity instead of a conformal fuel tank. This configuration became the basis for the F/A-18E. In modeling these four configurations, the values for the design variables were set based on actual F/A-18C or E values unless they were specified in the Hornet 2000 study. The major inputs and assumptions including vehicle definitions, technologies used, and test requirements are listed in Table 40.

Table 40: Inputs/Assumptions for the RDT&E and Production Cost

	Configuration	F/A-18E	IIIC	IIIB	II	I	F-18C
Design Variables	Wing area	500	500	500	400	400	400
	Wing aspect ratio	3.5	3.5	3.5	3.5	3.5	3.5
	Wing taper ratio	0.35	0.35	0.35	0.35	0.35	0.35
	Wing t/c	0.042	0.039	0.039	0.039	0.039	0.039
	Wing sweep angle	20	20	20	20	20	20
	Thrust	22000	22000	22000	22000	17754	17754
	Ref. weight for DLF	42097	42097	42097	38000	32000	32000
	Operational landing weight	46200	46200	46200	44100	34650	34650
	Ref. thrust for aft-body	25300	25300	25300	25300	17920	17920
	Internal fuel capacity	14700	13510	14510	13510	10810	10810
	External fuel capacity	9740	6720	6720	6720	6720	6720
	Fuselage length	55.833	55.292	53	53	53	53
	Avionics weight	1411	1411	1411	1411	1289	1289
	External stores weight	6361	6361	6361	6361	6361	6637
Technologies	LEX upgrade (C_{Lmax} factor)	1.0296	1	1	1	1	1
	Conformal fuel tank	0	0	1	1	0	0
	RCS reduction	1	0	0	0	0	0
	New engine core	1	1	1	1	0	0
RDT&E Inputs	Number of flight test vehicles	7.99	6.74	7.58	5.79	2.79	2.42
	Wind tunnel test hours	4500	2250	2250	1688	563	0
	Flight test hours	5797	4901	5511	4215	2029	1763
	DT/OT duration (months)	40.8	34.5	38.8	29.7	14.3	12.4
	Engine newness	0.51	0.51	0.51	0.51	0.055	0.055
	Software newness	0.86	0.86	0.86	0.86	0.53	0.53
	Percent Aluminum	31	55.4	55.4	55.4	55.4	49
	Percent Titanium	14	8.3	8.3	8.3	8.3	13
	Percent Composite	19	10.3	10.3	10.3	10.3	10
	Static test articles	1.2	0.7	0.7	0.2	0	0
	Fatigue test articles	1.2	0.7	0.7	0.1	0	0
	Iron bird test articles	1	1	1	0	0	0
	Propulsion test articles	1.0	1.0	1.0	1.0	0.4	0.4
	LG test articles	1	1	1	1	0	0
	Fuel rig articles	1	0.5	1	1	0	0
	Armament test rigs	0.5	0.5	0.5	0.5	0.5	0
	Hardware/Software Int. Rigs	1	1	1	1	1	1
	Subsystem Test Rigs	1.1	1.0	1.0	0.8	0.3	0.2

The RDT&E and unit production costs of the six models—F/A-18C, F/A-18E, and four Hornet 2000 configurations—were created using the code developed in the sections from §7.7.7.1 to §7.7.7.5 and FLOPS/MALCCA. Calculated costs of the six F/A-18 variants are compared to the published numbers. The process of collecting and selecting a set of F/A-18 cost data is presented in §C.2. The comparisons between the published and calculated costs are shown in radargrams in Figure 66. The blue lines represent published data, and the calculated values are shown in red lines. The radargram on the left represents the production cost, and each of the six vertices are labeled with the corresponding vehicle. Production cost calculated for the six variants fell within 3.6% of error. The radargram for RDT&E cost on the right compared only five variants, since RDT&E cost of the F/A-18C was not available. The error of RDT&E cost calculation also fell under 1.6%. Actual data in 1996 million dollars are provided in Table 41.
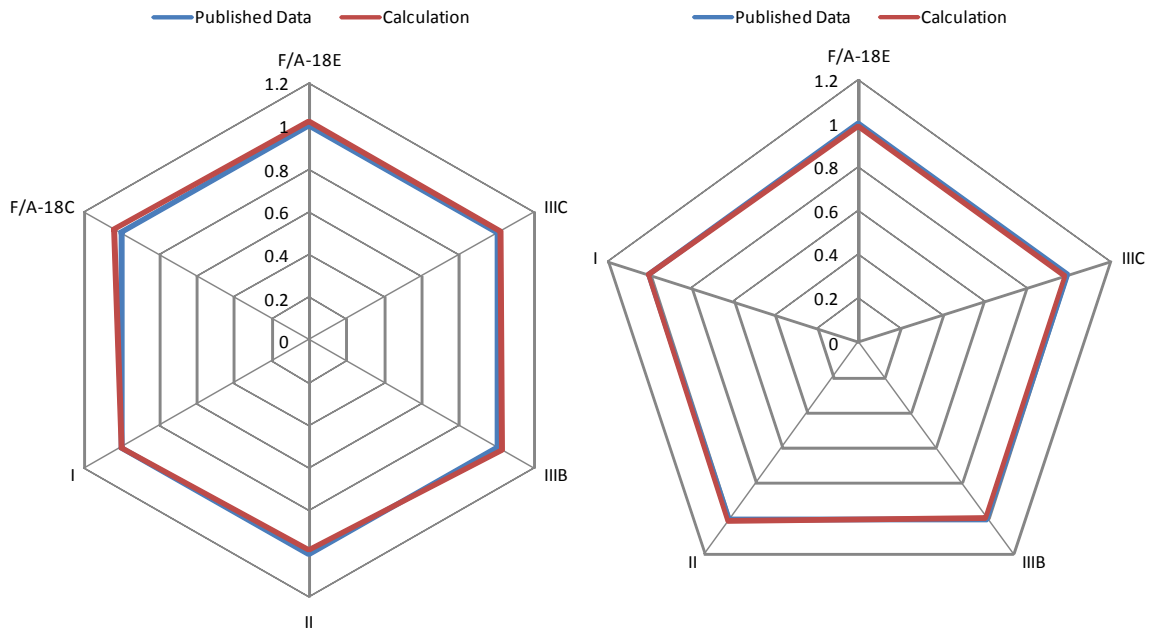
Figure 66: Radargrams of Production Cost (Left) and RDT&E Cost (Right)

Table 41: The RDT&E and Unit Production Cost Comparison

		F/A-18E	IIIC	IIIB	II	I	F-18C
Published Data (See §C.3 and §C.4)	Unit Production	48.7	1.39	1.4	1.3	1.14	27.2
	RDT&E	5783	2.78	2.89	2.22	1	unknown
Calculation	Unit Production ($M)	49.8	33.8	34.3	31.8	27.5	28.2
	ND Unit Production	2.06	1.398	1.418	1.268	1.140	
	RDT&E ($M)	5972.7	3932.6	4097.9	3252.7	1425.4	1224.2
	ND RDT&E	4.19	2.76	2.87	2.28	1	

7.7.8 Creation of the Two-Stage Aircraft Design Environment

The models developed in **Step 6** were written as a computer code and linked to the performance and cost models created using FLOPS/MALCCA. It was also necessary to link the first-stage and second-stage designs, since the RDT&E cost calculation at the second stage requires first-stage vehicle characteristics, such as design parameters and subsystem weights. This step was a prerequisite of two-stage aircraft performance and cost analysis and design, and actually had been done before the performance model validation presented in §7.7.6 and the cost model validation presented in §7.7.7.6.

The integration process was facilitated by using commercial software Model Center® of Phoenix Integration™. Figure 67 is the screen shot of the integrated two-stage aircraft design (TAD) environment within the Model Center® framework. The left hand of the figure shows input and output variables and their values. The main window of the programs shows DSM-like view of the boxes and lines. The boxes are contributing analyses that are either computer codes written by the author or the FLOPS/MALCCA suite. The links between the boxes indicates interdependencies between the contributing analyses. Each stage consists of an optimizer, a pre-processing module, an attack aircraft
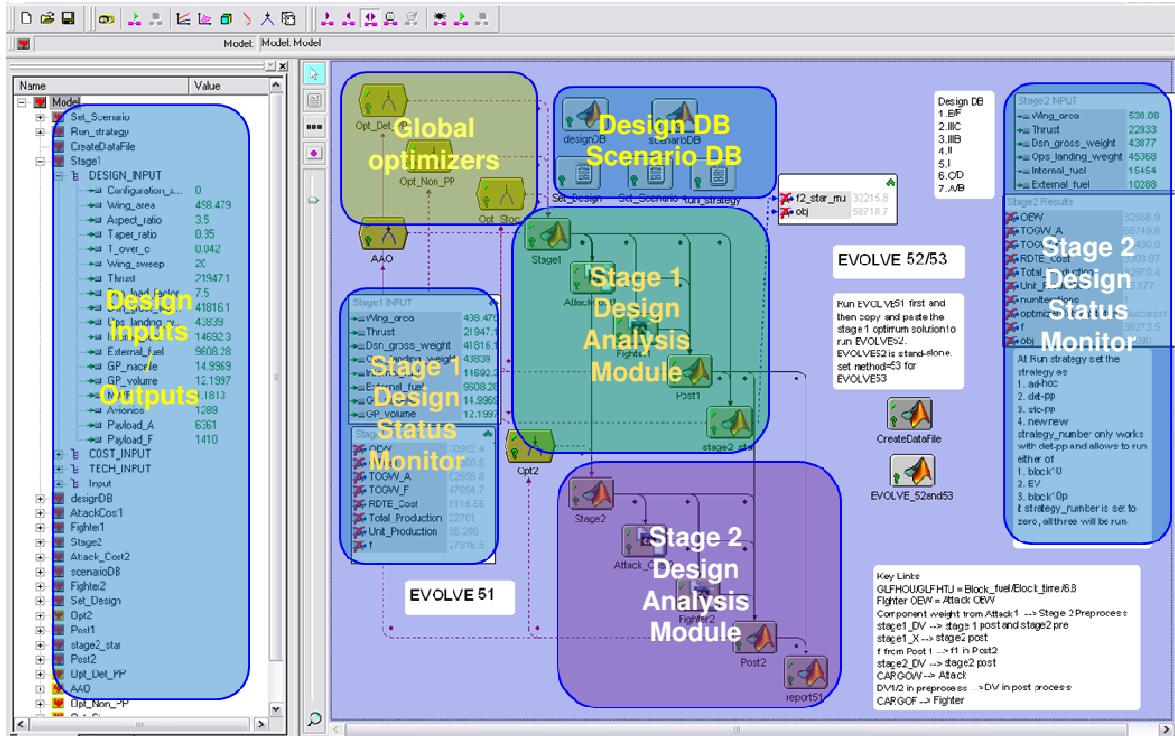
Figure 67: The Integrated Two-stage Aircraft Design (TAD) Environment

performance module, a fighter performance module, a cost module, and a post-processing

module. The pre-processing module contains the scaling-laws and prepares the inputs to

the following modules. FLOPS is run twice for performance calculations with attack

mission and fighter mission. Then, MALCCA is run for the cost calculation. The post-

processing modules collect the outputs from FLOPS/MALCCA and calculates some of

the KPPs.

7.8 A Deterministic Scenario-Based Approach to Two-Stage Aircraft Design Optimization: Step 7

Once the environment for two-stage aircraft design (TSAD) is setup, the environment can be used in three different ways in the **Steps 7-9**. In Step 7, two-stage aircraft design optimization is performed in the context of scenario-based study. Fundamentally, it is assumed that the random vector $\boldsymbol{\omega}$ can take only a finite number of outcomes, i.e. $\Theta \subset \boldsymbol{\Omega}$ is a finite set, and $\boldsymbol{\omega}_s \in \Theta, \ s = 1, \ldots, k$. Optimization is repeated for each of the scenarios $\boldsymbol{\omega}_s$. Here, all the non-stochastic strategies—ND, AH, and DetPPs—defined in **Step 4** are evaluated.

7.8.1 Optimization Problem Set-up

Optimization problem settings, such as design variables and constraints, are defined first. Some of the design variables that were considered in **Step 3** were treated as design parameters in order to limit the dimension of the design space to a manageable size. In order to keep the problem as realistic as possible those parameters that were hard coded were set to reflect the actual F/A-18 case. The first-stage design vector x1 and second-stage design vector are defined as follows, and the meaning of each symbol is listed in Table 42.

The objective function was acquisition cost for each stage. Acquisition cost is sensitive to production quantity. While production quantity could have been one of the biggest uncertainty sources, it was fixed at 492 for the first stage and 627 for the second stage, which are actual production quantities of the F/A-18C/D and E/F as of December 2007 according to SARs. Otherwise, inclusion of production quantity as a

random variable made it difficult to compare a design over a design optimized for different production quantity assumptions. In addition, since the optimum solution is sensitive to production quantity, it made the design space complicated and the creation of a surrogate model of optimum solutions very difficult. While the production quantities were fixed in the study, to investigate the extreme case of zero production quantities, EvoLVE **Steps 7** and **8** were repeated with RDT&E cost as objective function in APPENDIX D.

$$\mathbf{x}_1 = \begin{bmatrix} x_{11} \\ \vdots \\ x_{1n_1} \end{bmatrix} \text{ and } \mathbf{x}_2 = \begin{bmatrix} x_{21} \\ \vdots \\ x_{2n_2} \end{bmatrix}$$

Table 42: Design Variable Vectors ($\mathbf{x}_1$ and $\mathbf{x}_2$)

Symbol	Name	Unit
x_{11} and x_{21}	Wing area	ft^2
x_{12} and x_{22}	Engine thrust	lb
x_{13} and x_{23}	Ref. weight for DLF	lb
x_{14} and x_{24}	Operational landing weight	lb
x_{15} and x_{25}	Internal fuel weight	lb
x_{16} and x_{26}	External fuel weight	lb
x_{17} and x_{27}	Ref. thrust for aft-body sizing	lb
x_{18} and x_{28}	Fuselage length	ft^3

Some other assumptions were made. For the second-stage problem, in order to make the deigns closest to F/A-18E, fixed amount of growth potentials on the aft fuselage and forward-mid fuselage were embedded in the designs. Therefore, design thrust nacelle x_{27} sizes the aft fuselage based on the engine size and 15% of engine growth potential. Fuselage length is determined by x_{28} after balancing the vehicle's internal volume

required and available and then by adding 12.2 ft^3 of additional volume for growth potential.

Combinations of technology options were not investigated through optimization study, since they introduce discrete variables to the optimization loop, which require more time-consuming optimization algorithms to solve. Rather, among the technologies identified in **Step 4**, low RCS, new LEX design, and new engine core were used on all second-stage designs. The assumptions are summarized in Table 43.

Table 43: Second-Stage Design Assumptions

Technologies or Requirements	Value
Aft fuselage growth potential	15%
Internal volume growth potential	12.2 ft^3
Low RCS	yes
Conformal fuel tank	no
New LEX design for higher C_{Lmax}	yes
New engine core	yes
Production quantity	429

The key performance parameters identified in **Step 1** as in Table 12 constitute the constraint vectors $\mathbf{g}_1$ and $\mathbf{g}_2$ during optimization except for the combat ceiling. The thresholds for the constraints were redefined in this step. Thresholds for the constraints—fighter escort radius, interdiction mission radius, and recovery payload—are from the requirements for the first stage and are random variables ω_1, ω_2, and ω_3 in the second stage. All other constraint thresholds were setup as the calculated performance of the F/A-18E model as presented in Table 44.

Table 44: Constraint Vectors ($\mathbf{g}_1$ and $\mathbf{g}_2$)

Symbol	Constraint Name	Stage 1/2	Type	Unit
g_{11}	Fighter escort radius	$350/\omega_1$	lower	nm
g_{12}	Interdiction mission radius	$410/\omega_2$	lower	nm
g_{13}	Recovery payload	$4{,}500/\omega_3$	lower	lb
g_{14}	Launch wind over deck	28.657	upper	knots
15	Recovery wind over deck	9.5567	upper	knots
g_{16}	Approach speed	141.48	upper	knots
g_{17}	Specific excess power at 0.9M/10,00- ft	682.9	lower	ft/sec
g_{18}	Acceleration from 0.8M to 1.2M at 35,000 ft	63.6	upper	min
g_{19}	Turn rate at 15,000	12.044	lower	deg/sec
g_{110}	Usable load factor	7.6089	lower	g

7.8.2 MDO Techniques and Optimization Algorithms

As the DSM shows Figure 25, solving the two-stage problem involves optimization loops at two levels; it seems naturally suitable for the multidisciplinary design optimization (MDO) techniques. Among them, the All-At-Once (AAO) method was utilized in this study to test the efficacy of MDO techniques as proposed in **Hypothesis 6**. The entire optimization structure was transformed using AAO. In the two-stage aircraft design formulation as in Eqs. (28) and (29), optimization is solved in two hierarchical levels. The use of AAO transforms the two-level optimization problem into a single-level problem.

$$
\begin{aligned}
&\min_{\mathbf{x}_1,\mathbf{x}_2} f_1(\mathbf{x}_1) + f_2(\boldsymbol{\omega}_k,\mathbf{x}_1,\mathbf{x}_2) \\
&\text{s.t.} \quad g_{1i}(\mathbf{x}_1) \leq 0 \; (i=1,\dots,l_1) \\
&\text{and} \quad g_{2j}(\boldsymbol{\omega}_k,\mathbf{x}_1,\mathbf{x}_2) \leq 0 \; (j=1,\dots,l_2)
\end{aligned}
\tag{71}
$$

The performance of AAO was compared to the original formulations in Eqs. (28) and (29), and the computational time to converge was reduced by the order of

magnitude from hours to about tens of minutes. Although the benefit of MDO versus traditional solution techniques to two-stage aircraft design was not thoroughly investigated, the limited comparisons demonstrated the compatibility and efficacy of AAO to two-stage aircraft design, and thus proved **Hypothesis 6**.

Optimization in **Step 7** was performed without using surrogate models, but the models created in **Steps 5** and **6** were directly utilized. To confirm the global convergence, optimizations were attempted from multiple initial points, and the solution with lowest objective function value was chosen.

As for the optimization algorithm, Sequential Quadratic Programming (SQP) and Method of Feasible Direction (MoFD) were used along with the central finite different method for gradient calculation. The relative constraint violation criteria was one thousandth of the constraint value so that designs with any constraint values 0.1 % larger than the threshold would be considered as infeasible designs. In general, SQP converged much faster than MoFD and was used as the primary algorithm. MoFD was used as an auxiliary algorithm when SQP failed to find optimum solutions. SQP makes second order approximation of the objective function and first order approximations of the constraints, and sometimes it fails to capture the valley around the optimum point. MoFD more directly deals with constraints, and makes first order approximation of the objective function. Since it is cheaper to create first order approximations than second order approximations, MoFD tends to update the model more often. SQP builds the Hessian matrix gradually as it gains more knowledge about the objective function. Therefore, if the starting point is close to the optimum point, SQP makes a large first step and goes out of the valley, because of the incompletely constructed Hessian matrix.

7.8.3 Under Presence of Uncertainty: The Here-and-Now Solutions

The results of TSAD optimizations are the optimal first-stage decision vector for each strategy $(\mathbf{x}_1^*)^p$, where $p = 1, \ldots, 5$ is the strategy number, and a set of second-stage decision vectors $(\mathbf{x}_2^*)_s^p$, $s = 1, \ldots, 5$ and $p = 1, \ldots, 5$. The first-stage optimization results are summarized in Table 45. The table includes the first-stage optimal design $(\mathbf{x}_1^*)^p$, constraints $(\mathbf{g}_1^*)^p$, and the objective function $(f_1^*)^p$, $p = 1, \ldots, 5$. Also, aircraft empty weights and gross weights in both fighter and attack configurations were included. Among the five strategies, the first two—Ad-hoc and New design—are non-preplanning strategies, and those two columns were shaded to differentiate them from the other three preplanning strategies.

Several interesting observations are made from the first-stage optimum results. First of all, the two non-preplanning strategies (Ad-hoc and New-design) yielded the same design such that $(\mathbf{x}_1^*)^1 = (\mathbf{x}_1^*)^2$ since both of them minimize only f_1 in the first-stage optimization, which is the acquisition cost. This design is the optimal solution meeting all currently imposed constraints if the goal is to minimize the first-stage acquisition cost. Therefore these designs are *Perfect-fit Designs* (*PfDs*). When compared to New-design and Ad-hoc, all DetPP strategies show larger design variable settings in general. Among DetPPs the Block10p yielded the largest, heaviest, and most expensive aircraft, followed by Block10. All first-stage designs under DetPPs are *Perfect over-Design* (*PoDs*) as discussed in the subsequent sections along with second-stage optimization results.

Table 45: Optimization Results for the Five Deterministic Strategies

	Strategies	New Design	Ad-Hoc	DetPP (Block10)	DetPP (Avg.)	DetPP (Block10p)	Unit
x_{11}	Wing area	396.6	396.6	449.4	464.0	498.5	ft^2
x_{12}	Thrust	18355	18355	20441	20855	21947	lb
x_{13}	Ref. weight for DLF	34131	34131	38251	39170	41816	lb
x_{14}	Landing weight	33248	33248	39539	40830	43839	lb
x_{15}	Internal fuel	10827	10827	12777	13190	14692	lb
x_{16}	External fuel	6724	6724	6691	7920	9608	lb
x_{17}	Ref. thrust for aft-body	18355	18355	23508	23982	25238	lb
x_{18}	Fuselage length	53.08	53.08	54.68	54.79	55.60	ft
g_{11}	Fighter escort radius	350.1	350.1	409.6	423.5	478.8	nm
g_{12}	Interdiction mission radius	410.9	410.9	431.4	461.4	505.8	nm
g_{13}	Recovery payload	4508	4508	7910	8547	9846	lb
g_{14}	Launch wind over deck	22.06	22.06	22.29	24.47	28.14	knots
g_{15}	Recovery wind over deck	-0.01	-0.01	3.55	4.80	9.27	knots
g_{16}	Approach speed	138.1	138.1	141.5	141.5	141.4	knots
g_{17}	Specific excess power	708.7	708.7	699.2	696.2	685.9	ft/sec
g_{18}	Accel. from 0.8 to 1.2M	63.66	63.66	63.60	63.54	63.42	sec
g_{19}	Turn rate	12.042	12.042	12.066	12.112	12.093	deg/sec
g_{110}	Usable load factor	7.609	7.609	7.609	7.610	7.609	g
R	OEW	25738	25738	28628	29282	30992	lb
E	Attack TOGW	50520	50520	55325	57699	62697	lb
S	Fighter TOGW	37975	37975	42815	43882	47095	lb
U	RDTE	4639	4639	4904	4963	5116	$m
L	RDTE year	8.58	8.58	8.82	8.87	9.01	year
T	Production	20172	20172	21595	21897	22701	$m
S	f_1	24811	24811	26499	26859	27817	$m

It is interesting to see how each strategy places growth potential to the first-stage designs. Growth potential is essentially the difference between what is required and what is available. Growth potential can be measured from two different perspectives: degree of over-design and margins on the constraints. Figure 68 compares the growth potential in terms of degree of over-design beyond the *Perfect-fit Design* (*PfD*). Among the DetPP
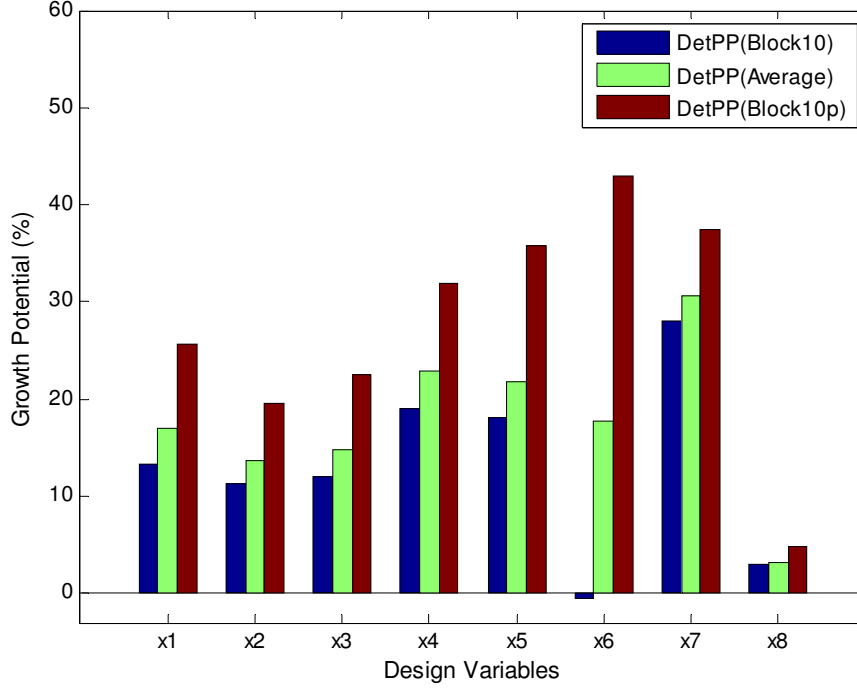
Figure 68: Growth Potential Measured by Margins on the Design Variables

strategies, the DetPP(Block10) strategy placed the most growth potential. Wing area was 498.5 ft^2, more than 100 ft^2 larger than *PfD* value of 396.6 ft^2, and the empty weight was about 30,992 lb., about 5,000 lb heavier than the *PfD*. It has the largest values on all design parameters, followed by DetPP(Block10) and DetPP(Average) such that

$$(\mathbf{x}_1^*)^5 > (\mathbf{x}_1^*)^4 > (\mathbf{x}_1^*)^3 > (\mathbf{x}_1^*)^1 = (\mathbf{x}_1^*)^2 \tag{72}$$

The inequality holds for the weight and cost metrics, too. An exception was external fuel capacity x_{16}, which is discussed in detail in the next section. The cause of this pattern is discussed again in the next section when the second-stage results are presented.

An important observation from the above results is not the fact that DetPP(Block10p) over-designed the most among other strategies, but the fact that *all* design variables followed the pattern as in Eq. (72) with only one exception. This observation has a significant meaning because it can be induced that if a designer wants

to embed growth potential on a subsystem such as wing or engine, he or she has to oversize all other subsystems. The nature of aerospace systems is that the performance and cost are very sensitive to weight. Therefore, it is impossible to improve one dimension of the design without affecting other dimensions, because the impact of weight increase propagates throughout the system. If the baseline design was optimal and thus was close to or on the constraints, the design becomes quickly infeasible if one variable deviates from the baseline value. Thus, if overdesigning of a subsystem such as engines or wings is desired, all the variables must move together to make the design feasible.

Observation 7: *For aerospace systems of which subsystems are tightly coupled, one variable cannot deviate from a feasible and optimal solution without hurting the feasibility and optimality. Therefore, overdesigning effort must be coordinated in such a way that all design variables move together towards a new feasible and optimal solution.*

The vehicles' growth potential is discussed by comparing how far the performance of first-stage aircraft is from the threshold performance. Since $(\mathbf{x}_1^*)^1$ and $(\mathbf{x}_1^*)^2$ inherently do not account for future events, they have little or no growth potential, so that $(\mathbf{g}_1^*)^1 = (\mathbf{g}_1^*)^2 \approx \mathbf{0}$. Growth margin on aircraft performance is compared among the DetPP strategies in Figure 69. The bar graphs shown in Figure 69 exhibit different patterns from the patterns observed in Figure 68. The first observation is that growth potential was not equally allocated to the performance parameters for a given evolution strategy. All three DetPPs placed large margins on the carrier suitability performance metrics (g_{13}-

g_{15}), moderated degree of margins on the mission performance parameters (g_{11} and g_{12}), and virtually no growth potential on the fighter point performance measures (g_{17}-g_{110}).

A more interesting observation is the inconsistency in the degree of growth potential among the DetPPs. The color patterns of the bar graphs show that DetPP(Block10p) in red placed the largest growth potential in the first three performance measures (g_{11}-g_{13}) followed by the DetPP(Average) and DetPP(Block10). This order is completely reversed for the fourth and fifth constraints so that the DetPP(Block10) in blue shows the largest growth potential on these constraints. Especially, the bar graph patterns of the recovery payload (g_{13}) and RWOD (g_{16}) requirements are distinctively contrasted, revealing a strong negative correlation between the two. The large growth margin on the recovery payload degraded the RWOD performance. These observations are formalized as follows:

$$(g_{13})^5 > (g_{13})^4 > (g_{13})^3 > (g_{13})^1 = (g_{13})^2 \text{ for recovery payload}$$
$$(g_{14})^3 > (g_{14})^4 > (g_{14})^5 > (g_{14})^1 = (g_{14})^2 \text{ for LWOD} \tag{73}$$
$$(g_{15})^3 > (g_{15})^4 > (g_{15})^5 > (g_{15})^1 = (g_{15})^2 \text{ for RWOD}$$

Observation 8: *The scenario-based study revealed the correlations between the growth potential in terms of margins on performance parameters. The negative correlations showed that growth potential in one performance parameter could inadvertently hurt the performance in other dimensions. System level integration of growth margins would prevent the performance degradation results in design infeasibilities.*
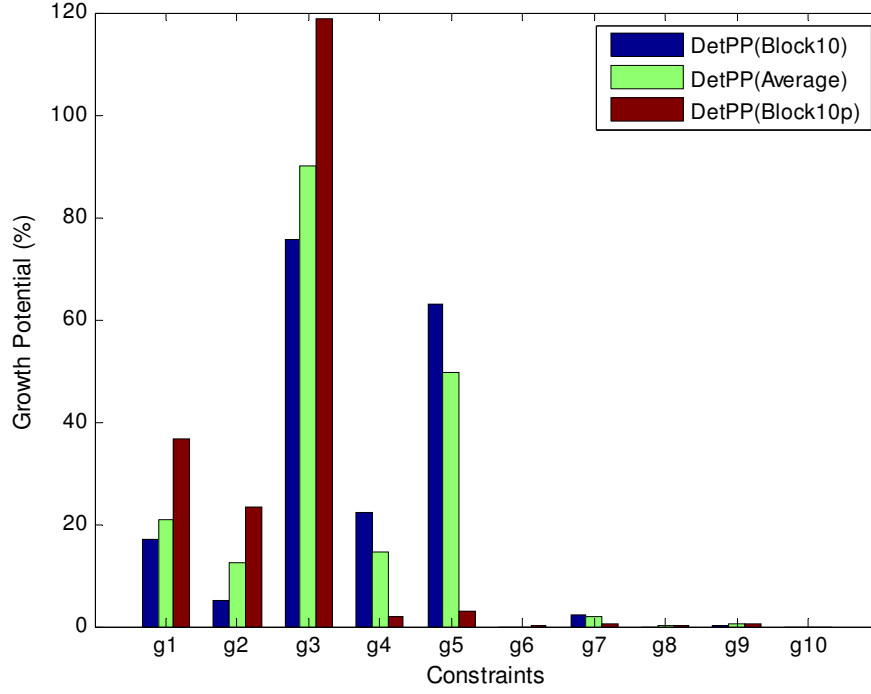
Figure 69: Growth Potential Measured by Margins on the Constraints

7.8.4 After Realization of Randomness: The Wait-and-See Solutions

Finally, the optimal second-stage strategies after the realization of the randomness are studied. The five deterministic strategies respond in the second stage after the randomness is revealed in such a way that it minimizes the second-stage cost function f_2 by solving:

$$
\begin{aligned}
&\text{for a given } (\mathbf{x}_1^*)^p \text{ and } \forall \hat{\boldsymbol{\omega}}_s, \ p = 1,\ldots 5, \ s = 1,\ldots,5 \\
&\min_{\mathbf{x}_2} f_2(\hat{\boldsymbol{\omega}}_s, (\mathbf{x}_1^*)^p, \mathbf{x}_2) \\
&\text{s.t. } g_{2j}(\hat{\boldsymbol{\omega}}_s, (\mathbf{x}_1^*)^p, \mathbf{x}_2) \le 0 \ (j = 1,\ldots,l_2)
\end{aligned}
\tag{74}
$$

Since only five scenarios were assumed to exist and apply to the five deterministic strategies, a total of twenty-five optimization problems were solved, yielding twenty-five WS solutions $(\hat{\mathbf{x}}_2^*)_s^p, \ s = 1,\ldots,5, \ p = 1,\ldots,5$. The optimization results are provided from

Table 46 to Table 50 in the following pages. Each of the tables includes the first-stage optimal solutions in the shaded column for easy comparison purposes. The results are analyzed from cost and design point-of-views in the subsequent sections.

Table 46: TAD Optimization Results for the New-Design Strategy

	Stage	1	2					
	Requirement/Scenarios	Block 0	S1	S2	S3	S4	S5	Unit
x_{21}	Wing area	396.6	426.5	453.0	465.0	500.0	530.1	ft^2
x_{22}	Thrust	18355	19691	20551	20920	22064	22933	lb
x_{23}	Ref. weight for DLF	34131	36345	38533	39416	42138	43876.8	lb
x_{24}	Landing weight	33248	37522	39865	40921	43990	45367.7	lb
x_{25}	Internal fuel	10827	11485	12846	13193	14731	15453.6	lb
x_{26}	External fuel	6723	7096	6669	7997	9692	10288	lb
x_{27}	Ref. thrust for aft-body	18355	22645	23634	24058	25374	26373	lb
x_{28}	Fuselage length	53.08	53.81	54.80	55.00	55.87	56.09	ft2
g_{21}	Fighter escort radius	349.7	350.2	410.1	420.0	475.9	493.9	nm
g_{22}	Interdiction mission radius	410.3	410.0	430.1	460.2	504.2	510.0	nm
g_{23}	Recovery payload	6489	6999	8000	8400	9698	9800	lb
g_{24}	Launch wind over deck	22.70	22.36	22.22	24.91	28.65	28.65	knots
g_{25}	Recovery wind over deck	3.55	3.54	3.56	4.94	9.52	9.56	knots
g_{26}	Approach speed	141.5	141.5	141.5	141.5	141.5	139.5	knots
g_{27}	Specific excess power	709.4	709.1	697.7	694.3	684.7	682.9	ft/sec
g_{28}	Acceleration from 0.8M to 1.2M	63.48	63.60	63.60	63.54	63.24	62.88	sec
g_{29}	Turn rate	12.049	12.122	12.063	12.069	12.047	12.176	deg/sec
g_{210}	Usable load factor	7.609	7.609	7.609	7.610	7.608	7.609	g
	OEW	25738	27522	28864	29520	31290	32567	lb
R	Attack TOGW	50520	53358	55607	58021	63122	65749	lb
E	Fighter TOGW	37975	40417	43120	44123	47432	49430	lb
S	RDTE	4639	6490	6635	6704	6887	7023	$m
U	RDTE year	8.58	9.35	9.49	9.55	9.72	9.85	year
L	Production	20172	27594	29238	29973	32126	33860	$m
T	f1/f2	24811	34084	35874	36677	39012	40883	$m
S	Total cost	-	58894	60684	61488	63823	65693	$m

Table 47: TAD Optimization Results for the Ad-Hoc Strategy

	Stage	**1**	**2**					
	Requirement/Scenarios	Block 0	S1	S2	S3	S4	S5	Unit
x_{21}	Wing area	396.6	426.5	453.4	465.0	499.8	530.1	ft^2
x_{22}	Thrust	18355	19699	20569	20920	21998	22933	lb
x_{23}	Ref. weight for DLF	34131	36348	38594	39416	42082	43877	lb
x_{24}	Landing weight	33248	37527	39899	40921	43955	45368	lb
x_{25}	Internal fuel	10827	11488	12851	13193	14708	15454	lb
x_{26}	External fuel	6724	7097	6694	7997	9610	10288	lb
x_{27}	Ref. thrust for aft-body	18355	22654	23655	24058	25298	26373	lb
x_{28}	Fuselage length	53.08	53.81	54.80	55.00	55.85	56.09	ft2
g_{21}	Fighter escort radius	350.1	350.2	410.0	420.0	475.7	493.9	nm
g_{22}	Interdiction mission radius	410.9	410.1	430.5	460.2	503.2	510.0	nm
g_{23}	Recovery payload	4508	7001	8009	8400	9703	9800	lb
g_{24}	Launch wind over deck	22.06	22.37	22.26	24.91	28.43	28.65	knots
g_{25}	Recovery wind over deck	-0.01	3.55	3.55	4.94	9.44	9.56	knots
g_{26}	Approach speed	138.1	141.5	141.5	141.5	141.4	139.5	knots
g_{27}	Specific excess power	708.7	709.4	697.8	694.3	683.1	682.9	ft/sec
g_{28}	Acceleration from 0.8M to 1.2M	63.66	63.60	63.60	63.54	63.60	62.88	sec
g_{29}	Turn rate	12.042	12.123	12.065	12.069	12.044	12.176	deg/sec
g_{210}	Usable load factor	7.609	7.609	7.615	7.610	7.608	7.609	g
	OEW	25738	27525	28890	29520	31251	32567	lb
R	Attack TOGW	50520	53365	55664	58021	62973	65749	lb
E	Fighter TOGW	37975	40423	43151	44123	47368	49430	lb
S	RDTE	4639	2830	3724	4018	4609	5101	$m
U	RDTE year	8.58	4.87	6.36	6.75	7.32	7.79	year
L	Production	20172	27099	28768	29499	31738	33597	$m
T	f_1/ f_2	24811	29929	32492	33517	36347	38697	$m
S	Total cost	-	54744	57306	58332	61161	63512	$m

Table 48: TAD Optimization Results for the DetPP(Block10) Strategy

	Stage	1	2					
	Requirement/Scenarios	Block 0	S1	S2	S3	S4	S5	Unit
x_{21}	Wing area	449.4	426.4	453.5	465.0	499.8	530.1	ft^2
x_{22}	Thrust	20441	19694	20569	20923	21998	22933	lb
x_{23}	Ref. weight for DLF	38251	36341	38594	39423	42082	43877	lb
x_{24}	Landing weight	39539	37522	39899	40920	43955	45368	lb
x_{25}	Internal fuel	12777	11487	12851	13199	14708	15454	lb
x_{26}	External fuel	6691	7094	6694	7987	9610	10288	lb
x_{27}	Ref. thrust for aft-body	23508	22648	23655	24061	25298	26373	lb
x_{28}	Fuselage length	54.68	53.82	54.80	55.01	55.85	56.09	ft2
g_{21}	Fighter escort radius	409.6	350.3	410.0	420.3	475.7	493.9	nm
g_{22}	Interdiction mission radius	431.4	410.0	430.5	460.2	503.2	510.0	nm
g_{23}	Recovery payload	7910	6999	8009	8397	9703	9800	lb
g_{24}	Launch wind over deck	22.29	22.37	22.26	24.91	28.43	28.65	knots
g_{25}	Recovery wind over deck	3.55	3.55	3.55	4.93	9.44	9.56	knots
g_{26}	Approach speed	141.5	141.5	141.5	141.5	141.4	139.5	knots
g_{27}	Specific excess power	699.2	709.2	697.8	694.2	683.1	682.9	ft/sec
g_{28}	Acceleration from 0.8M to 1.2M	63.60	63.60	63.60	63.54	63.60	62.88	sec
g_{29}	Turn rate	12.066	12.122	12.065	12.067	12.044	12.176	deg/sec
g_{210}	Usable load factor	7.609	7.608	7.615	7.610	7.608	7.609	g
	OEW	28628	27521	28890	29522	31251	32567	lb
R	Attack TOGW	55325	53358	55664	58019	62973	65750	lb
E	Fighter TOGW	42815	40419	43151	44131	47368	49431	lb
S	RDTE	4904	2273	1341	2961	3583	4041	$m
U	RDTE year	8.82	4.37	2.26	5.67	6.35	6.77	year
L	Production	21595	26934	28820	29151	31354	33201	$m
T	f_1/ f_2	26499	29206	30161	32112	34936	37242	$m
S	Total cost	-	55705	56660	58611	61435	63740	$m

251

Table 49: TAD Optimization Results for the DetPP(Average) Strategy

	Stage	1	2					
	Requirement/Scenarios	Block 0	S1	S2	S3	S4	S5	Unit
x_{21}	Wing area	464.0	426.6	461.1	465.0	499.8	530.1	ft^2
x_{22}	Thrust	20855	19703	20814	20920	21998	22933	lb
x_{23}	Ref. weight for DLF	39170	36365	39189	39416	42082	43877	lb
x_{24}	Landing weight	40830	37532	40572	40921	43955	45368	lb
x_{25}	Internal fuel	13190	11491	13168	13193	14708	15454	lb
x_{26}	External fuel	7920	7093	7901	7997	9610	10288	lb
x_{27}	Ref. thrust for aft-body	23982	22659	23936	24058	25298	26373	lb
x_{28}	Fuselage length	54.79	53.82	54.97	55.00	55.85	56.09	ft2
g_{21}	Fighter escort radius	423.5	350.3	421.6	420.0	475.7	493.9	nm
g_{22}	Interdiction mission radius	461.4	410.0	460.7	460.2	503.2	510.0	nm
g_{23}	Recovery payload	8547	7000	8264	8400	9703	9800	lb
g_{24}	Launch wind over deck	24.47	22.36	24.92	24.91	28.43	28.65	knots
g_{25}	Recovery wind over deck	4.80	3.55	4.41	4.94	9.44	9.56	knots
g_{26}	Approach speed	141.5	141.5	141.5	141.5	141.4	139.5	knots
g_{27}	Specific excess power	696.2	709.4	695.0	694.3	683.1	682.9	ft/sec
g_{28}	Acceleration from 0.8M to 1.2M	63.54	63.54	63.60	63.54	63.60	62.88	sec
g_{29}	Turn rate	12.112	12.123	12.053	12.069	12.044	12.176	deg/sec
g_{210}	Usable load factor	7.610	7.611	7.611	7.610	7.608	7.609	g
	OEW	29282	27531	29306	29520	31251	32567	lb
R	Attack TOGW	57699	53370	57681	58021	62973	65750	lb
E	Fighter TOGW	43882	40432	43885	44123	47368	49431	lb
S	RDTE	4963	2300	1306	1355	3401	3854	$m
U	RDTE year	8.87	4.40	2.23	2.27	6.18	6.59	year
L	Production	21897	26964	29256	29511	31285	33131	$m
T	f_1 / f_2	26859	29265	30562	30866	34686	36986	$m
S	Total cost	-	56124	57421	57725	61546	63845	$m

Table 50: TAD Optimization Results for the DetPP(Block10p) Strategy

	Stage	**1**	**2**					
	Requirement/Scenarios	Block 0	S1	S2	S3	S4	S5	Unit
x_{21}	Wing area	498.5	426.5	453.1	465.0	499.8	530.1	ft^2
x_{22}	Thrust	21947	19699	20557	20920	21998	22933	lb
x_{23}	Ref. weight for DLF	41816	36348	38535	39416	42082	43877	lb
x_{24}	Landing weight	43839	37526	39867	40921	43955	45368	lb
x_{25}	Internal fuel	14692	11488	12847	13193	14708	15454	lb
x_{26}	External fuel	9608	7092	6665	7997	9610	10288	lb
x_{27}	Ref. thrust for aft-body	25238	22654	23641	24058	25298	26373	lb
x_{28}	Fuselage length	55.60	53.82	54.80	55.00	55.85	56.09	ft
g_{21}	Fighter escort radius	478.8	350.2	410.1	420.0	475.7	493.9	nm
g_{22}	Interdiction mission radius	505.8	409.9	430.0	460.2	503.2	510.0	nm
g_{23}	Recovery payload	9846	7000	8000	8400	9703	9800	lb
g_{24}	Launch wind over deck	28.14	22.36	22.21	24.91	28.43	28.65	knots
g_{25}	Recovery wind over deck	9.27	3.55	3.55	4.94	9.44	9.56	knots
g_{26}	Approach speed	141.4	141.5	141.5	141.5	141.4	139.5	knots
g_{27}	Specific excess power	685.9	709.4	697.9	694.3	683.1	682.9	ft/sec
g_{28}	Acceleration from 0.8M to 1.2M	63.42	63.54	63.60	63.54	63.60	62.88	sec
g_{29}	Turn rate	12.093	12.123	12.064	12.069	12.044	12.176	deg/sec
g_{210}	Usable load factor	7.609	7.609	7.609	7.610	7.608	7.609	g
	OEW	30992	27525	28866	29520	31251	32567	lb
R	Attack TOGW	62697	53360	55606	58021	62973	65750	lb
E	Fighter TOGW	47095	40423	43124	44123	47368	49431	lb
S	RDTE	5116	2381	2863	2899	1389	3303	$m
U	RDTE year	9.01	4.49	5.71	5.74	2.30	5.98	year
L	Production	22701	27009	28426	29113	31593	32970	$m
T	f_1/f_2	27817	29390	31289	32012	32983	36273	$m
S	Total cost	-	57206	59105	59829	60799	64090	$m

7.8.4.1   *Discussions from the Cost Point of View*

Figure 70 shows the total program cost, i.e. the sum of first-stage acquisition cost (Acq_1) and second-stage acquisition cost (Acq_2), in 1996 billion dollars. Five different colors represent the five scenarios. The general trend is that the New-design strategy costs the most regardless of scenarios but the difference is not very large. The difference is mainly due to the savings in RDT&E cost in the second stage when modifications to existing design are pursued rather than a completely new design. Within each strategy, cost increases as the scenario number increases—and thus the second-stage requirement gets more challenging—regardless of the strategies. However, it is not clear to see which strategy cost the least in general or for a specific scenario in this figure.

To facilitate further observations, the same bar graph was plotted with respect to the scenarios instead of the strategies as shown in Figure 71. Now, the total costs are grouped with respect to the scenarios, and five colors represent the five strategies.
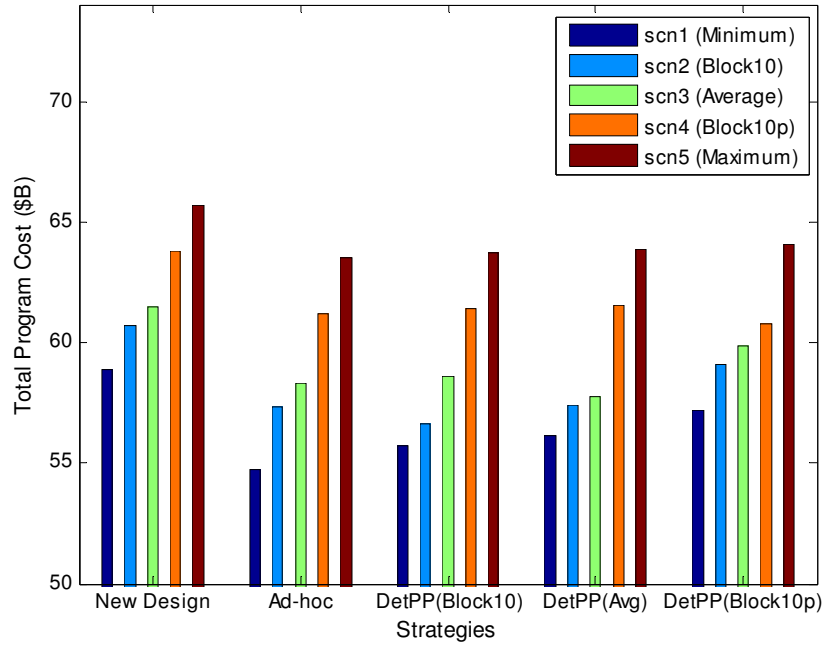
Figure 70: Total Program Cost Comparison w.r.t. the Strategies

Obviously again, the New-design strategy incurred the largest cost regardless of the scenarios. For the scenarios 2, 3, and 4, the best strategies were DetPP(Block10), DetPP(Average), and DetPP(Block10p) respectively. This result implies that a deterministic preplanning strategy works the best when the predicted scenario $\boldsymbol{\omega}_u$ matches the realized scenario $\hat{\boldsymbol{\omega}}_s$. On the other hand, when the predicted scenario was different from the actual scenario, Ad-hoc strategy was the best. For scenarios 1 and 5, Ad-hoc strategy incurred the least cost among five strategies because no DetPP predicted those scenarios, and for scenarios 2, 3, and 4, it was the second best choice. These patterns are expresses with the following inequalities:

$$
\begin{aligned}
&if\ \boldsymbol{\omega}_u = \hat{\boldsymbol{\omega}}_s, \quad (f_1^* + f_2^*)_s^{DetPP} < (f_1^* + f_2^*)_s^{Ad-hoc} < (f_1^* + f_2^*)_s^{ND} \\
&if\ \boldsymbol{\omega}_u \neq \hat{\boldsymbol{\omega}}_s, \quad (f_1^* + f_2^*)_s^{Ad-hoc} < (f_1^* + f_2^*)_s^{DetPP} < (f_1^* + f_2^*)_s^{ND}
\end{aligned} \tag{75}
$$
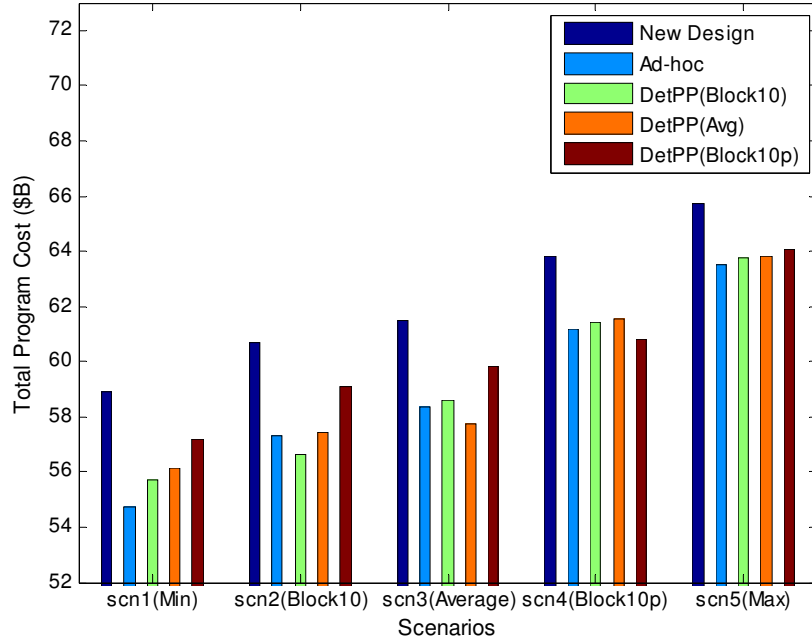
Figure 71: Total Program Cost Comparison w.r.t. the Scenarios

In reality, it is almost impossible to predict the future requirement with certainty unless it is determined from the beginning. Thus, this study suggests that under the

presence of uncertain future requirements, it is the best strategy to pursue the Ad-hoc strategy, and thus the first-stage design is a *PfD*. However, if the second-stage requirement is known, it is best to incorporate that from the beginning. The conclusion about how much growth potential would be necessary is discussed later. This pattern is true and might be only true when the objective function is acquisition cost and all second-stage aircraft are new manufactures. Therefore, hasty generalizations should be avoided. The conclusion is formally stated as follows:

Observation 9: *When acquisition cost is the objective function, incorporating growth potential into the first-stage design was not beneficial unless one could predict the future requirement with certainty or unless the future requirement was given from the beginning. Under presence of uncertainty, the least costly way to meet both the first and second requirements is to design only for the current requirement in the first stage, and then modify the design later after the second-stage requirement is revealed.*

To provide more explanations to the above observation, the first- and second-stage cost were plotted separately as shown in Figure 72. The wide, gray bar is $\$Acq_1$, and narrow bars are $\$Acq_2$ for the corresponding scenarios. Gray bars show that DetPPs incurred more cost than New-design and Ad-hoc in the first stage. Among the DetPPs, the Block10p spent the most, followed by the Average. In the second stage, the New-design cost the most as expected, and DetPPs cost less than New-design and Ad-hoc. By comparing the DetPPs, one can conclude that the pattern in Eq. (75) was achieved because the saving on $\$RDTE_2$ was greater than the penalty of over-designing when the
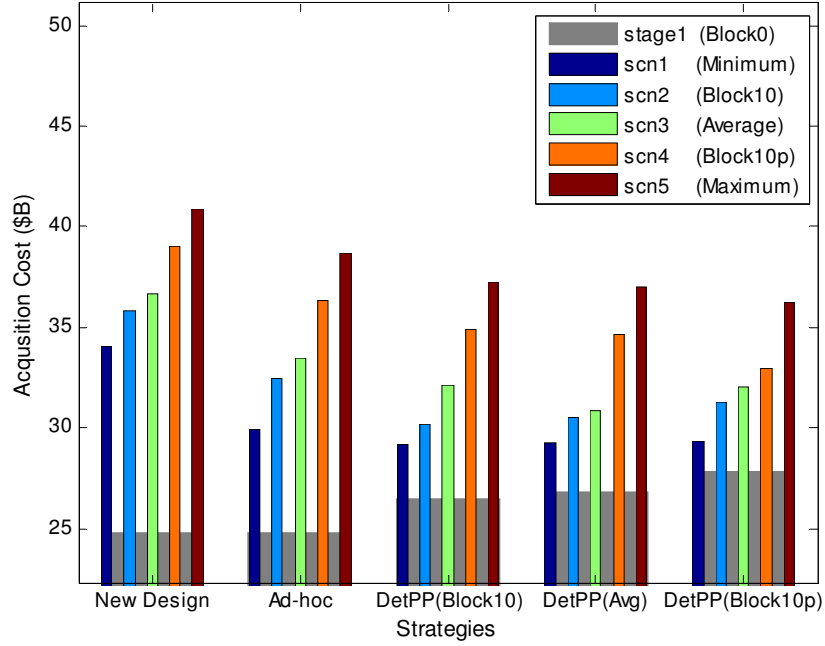
Figure 72: Stage 1 and Stage 2 Acquisition Cost Comparison

growth potential was adequately embedded in the original design. For example, the Block10p spent more than any other strategies in the first stage, but it cost the least in the second stage as well as overall under Scenario 4.

7.8.4.2   Discussions from the Design Point of View

In order to gain insight as to how different strategies decided the optimal first and second designs, the patterns among the design variables are investigated here. All the bar graphs in this section separately show the first-stage design in wide, grey bars, and the second-stage design in narrow bars of five different colors. The definition of color codes are provided in the legends of the graphs.

Figure 73 compares the wing area in the first stage $(x_{11}^*)_s^p$ and the second stage $(\hat{x}_{21}^*)_s^p$, where $s = 1, \ldots, 5$ is the scenario number and $p = 1, \ldots, 5$ is the strategy number. The New-design and Ad-hoc strategies had the same wing areas for a same scenario such that $(x_{11}^*)_s^1 = (x_{11}^*)_s^2$ and $(\hat{x}_{21}^*)_s^1 = (\hat{x}_{21}^*)_s^2$ for $\forall s$. The three DetPPs overdesigned the wing

in the first stage to the extent that they match the second-stage wing area under the predicted scenarios $\boldsymbol{\omega}_u$.

$$\text{if } u = s, (x_{11}^*)_u^{DetPP} = (\hat{x}_{21}^*)_s^{DetPP} \text{ for } \forall u \in \{2,3,4\}, \forall s \in \{2,3,4\} \tag{76}$$

where u is the predicted scenario number and s represents the realized scenario number. Eq. (76) implies that the DetPPs overdesigned the wing area to meet the second-stage requirement so that it did not have to be resized in the second stage. Figure 74 compares engine thrust in the first and second stage and is qualitatively identical to the wing area graphs. Essentially, when the same types of bar graphs as in Figure 74 are generated with other design variables, all the graphs are qualitatively identical to those in Figure 74 with the exception of external fuel tank capacity. Indeed, Eq. (76) holds for all design variables and is generalized as:

$$\begin{aligned} &\text{for } p = 3,\dots,5 \text{ if } u = s, \\ &\text{then } (\mathbf{x}_1^*)_u^p = (\hat{\mathbf{x}}_2^*)_s^p \text{ for } \forall u \in \{2,3,4\}, \forall s \in \{2,3,4\} \end{aligned} \tag{77}$$

Eq. (77) implies that all three first-stage designs under DetPP can meet the second-stage requirement without modification, and therefore they are *PoDs*.

Between the second-stage wing areas in Figure 73, a common inequality is that the wing area monotonously increases as the scenario number increases under a certain strategy.

$$(\hat{x}_{21}^*)_1^p < (\hat{x}_{21}^*)_2^p < (\hat{x}_{21}^*)_3^p < (\hat{x}_{21}^*)_4^p < (\hat{x}_{21}^*)_5^p \tag{78}$$
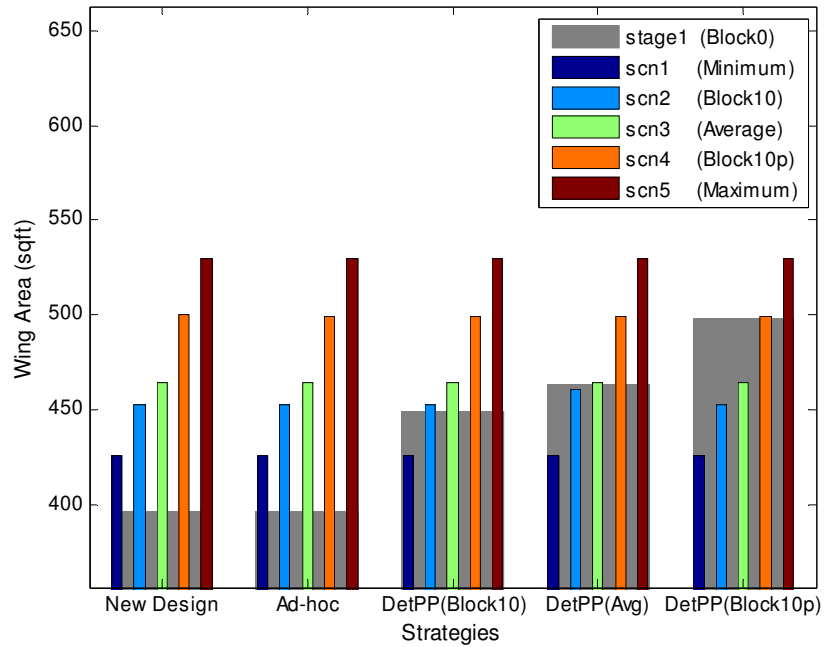
Figure 73: Wing Area Comparison
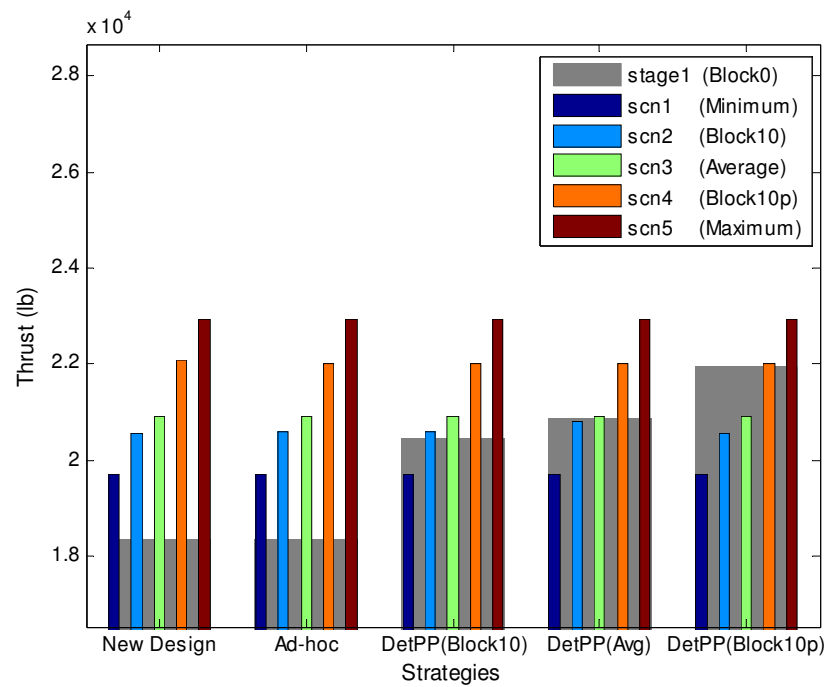
Figure 74: Engine Thrust Comparison

More importantly, all strategies had the same wing areas for a given scenario except for only $(\hat{x}_{21}^*)_2^4$. The wing area for DetPP(Average) under scenario 2 was equal to all wing areas under scenario 3. These patterns are true for all other design variables and are generalized as

$$
\begin{aligned}
&\text{for a given } s = 1,...,5 \\
&(\hat{\mathbf{x}}_2^*)_s^1 = (\hat{\mathbf{x}}_2^*)_s^2 = (\hat{\mathbf{x}}_2^*)_s^3 = (\hat{\mathbf{x}}_2^*)_s^4 = (\hat{\mathbf{x}}_2^*)_s^5
\end{aligned}
\tag{79}
$$

with an exception of,

$$
(\hat{\mathbf{x}}_2^*)_2^1 = (\hat{\mathbf{x}}_2^*)_2^2 = (\hat{\mathbf{x}}_2^*)_2^3 = (\hat{\mathbf{x}}_2^*)_2^5 \neq (\hat{\mathbf{x}}_2^*)_2^4 = (\hat{\mathbf{x}}_{21}^*)_3^p, \ p = 1,...,5
\tag{80}
$$

reminding that the second-stage optimization problem is the same for all strategies except that they might have different starting points $(\mathbf{x}_1^*)^p$. The result shows that, if only one exception is excluded, the optimizer decided to have the same $(\mathbf{x}_2^*)_s^p$ regardless of the previous design $(\mathbf{x}_1^*)^p$ for a given scenario.

Essentially, if the second-stage requirement is more stringent than the one predicted initially or $u < s$, the design is inevitably infeasible without modification. Thus, it is no option to keep the first-stage design unchanged. However, in the opposite situation where $u > s$, $(\mathbf{x}_1^*)_u^p$ could be still feasible in the second-stage. Therefore, $(\mathbf{x}_1^*)_u^p$ can either be retained to save RDT&E cost or be reduced to save production cost. It is the role of the optimizer to find the balanced solution which minimizes the sum of RDT&E and production cost. Out of the six cases where $u > s$, five cases decided to change $(\mathbf{x}_1^*)_u^p$ despite the RDT&E cost, because savings from production cost was larger. Only the DetPP(Average) decided to keep the first-stage design unchanged under scenario 2 such that $(\mathbf{x}_1^*)_u^4 = (\mathbf{x}_2^*)_2^4, u = 1,...,5$.

Figure 75 was prepared for the external fuel capacity $(\hat{x}^*_{26})^p_s$. A clear difference from previous graphs is that the smallest value occurs under Scenario 2 not Scenario 1, thus it does not follow the inequality as in Eq. (78). Intuitively, this result looks erroneous since Scenario 2 demands more attack radius than Scenario 1 does. Indeed, Scenario 2 required 19,545 lb of total fuel while Scenario 1 required 18,585 lb. This somewhat confusing result was caused by the fact that total fuel requirement is divided into internal and external fuel tanks under the following rules. External fuel tank capacity is determined by the total fuel required under the attack mission less the internal fuel capacity. Internal fuel capacity is mainly determined by the fighter mission radius, simultaneously considering wing area, fuselage length, and avionics weight. This unexpected result demonstrates the difficulty of intuitively preparing growth provisions even in a qualitative manner for a complex system such as a fighter aircraft.
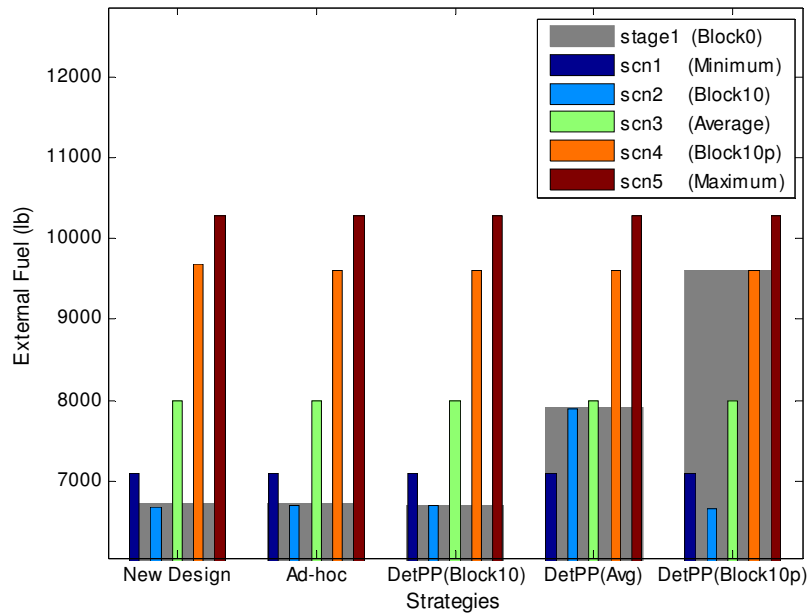
Figure 75: External Fuel Amount Comparison

Finally, aircraft empty weight (OEW) and takeoff gross weight (TOGW) in attack configurations were compared in Figure 76 and Figure 77, respectively. These two charts also are qualitatively identical to those plotted with the design variables. Therefore, all the equalities and inequalities identified in Eqs. (76)-(80) are valid for these weights. This result indicates strong, positive correlations not only between the input variables but also between input and output variables.

Observation 10: *The patterns among the optimal designs under various strategies and scenarios revealed that the second-stage design mostly dictated the realized scenario such that most first-stage design was modified to meet the second-stage requirement best, because the production cost reduction was larger than the RDT&E cost incurred.*
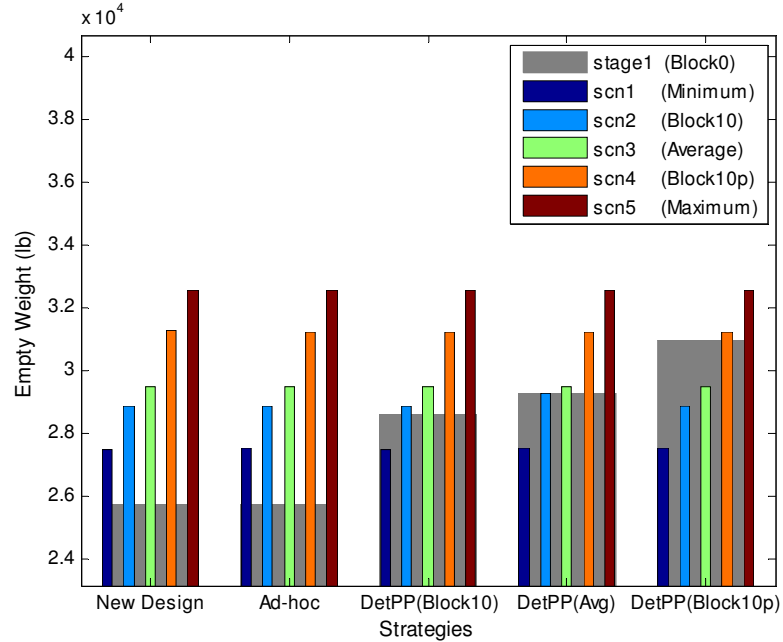
Figure 76: Empty Weight Comparison
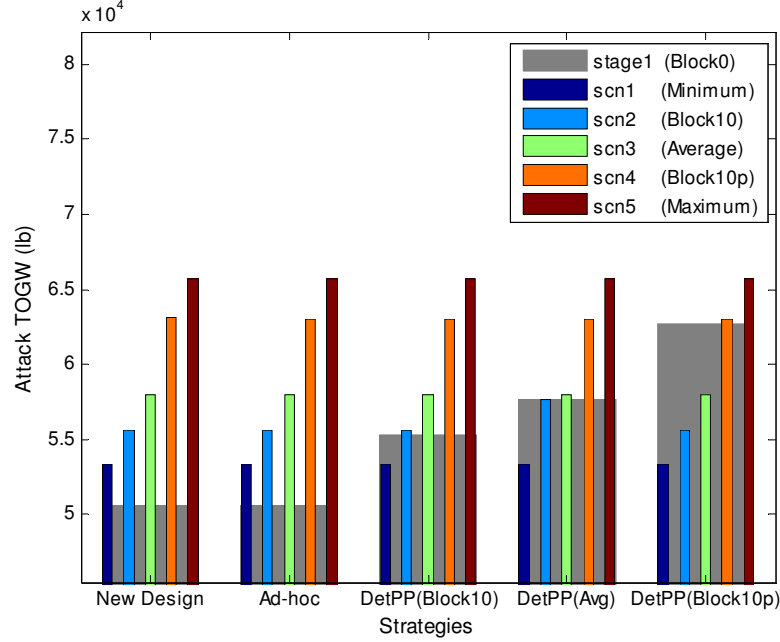
Figure 77: Takeoff Gross Weight Comparison

7.9 A Stochastic Approach Two-Stage Aircraft Design Optimization: Step 8

Step 8 incorporates the uncertainty in the second-stage requirement by directly solving two-stage aircraft design optimization for the random variables defined as PDFs. The stochastic preplanning strategy is solved to find the HN solution before realization of uncertainty. Since the StoPP minimizes $f_1 + \mathbb{E}(f_2^*)$, and evaluation of true $\mathbb{E}(f_2^*)$ is impractical, estimation is made through the use of both surrogate models and numerical integration using the Monte Carlo technique. Once the approximation process is established with reasonable accuracy, the two-stage stochastic optimization is solved and discussed. Then, the WS solutions are sought for not only the StoPP but also all other strategies solved in the previous step.

7.9.1 Surrogate Modeling

Two Artificial Neural Network (ANN) models were created—the optimum second-stage objective f_2^* under derivative aircraft strategies and New-design strategy. Under derivative strategies, the second-stage objective function f_2 is dependent on the first-stage design $\mathbf{x}_1$ and the random variables $\boldsymbol{\omega}$. Table 51 lists parameters and their ranges within which the ANNs are created. The bounds were carefully set through iterations to ensure they are large enough to include the design space necessary and they are not too large unnecessarily. The bounds for the random variables are the minimum and maximum limits of the PDFs. The lower bound of x_1 is slightly smaller than the smallest optimal first-stage design $(\mathbf{x}_1^*)^1$, and the upper bound is slightly larger than the largest optimal first-stage design $(\mathbf{x}_1^*)^5$. When, the New-design strategy is pursued, the second-stage objective function f_2 is independent to the first-stage design $\mathbf{x}_1$. Therefore, only the random variables were used in creating the ANN of f_2^*.

Table 51: List of Parameters and Bounds for Surrogate Modeling

Parameters	Lower Bound	Upper Bound
x_{11}	390	510
x_{12}	18300	22200
x_{13}	34000	42500
x_{14}	33000	44500
x_{15}	10000	15000
x_{16}	6600	10000
x_{17}	18250	25750
x_{18}	53	56
ω_1	360	490
ω_2	410	510
ω_3	7000	9800
ω_4	1300	1500

For the sampling techniques, the LHS technique was used. Two separate sets of LHS samples were created to combine 1,000 sampling points. The first set of 750 samples was used to train the model, and the remaining 250 samples were used to validate the model.

For each of the sampling points, the second-stage optimization problem as defined in Eq. (32) was solved for a given sample of x_1 and $\boldsymbol{\omega}$. To ensure local optimality, optimization results were automatically checked to see whether they satisfied all convergence, constraint, and side constraint violation criteria. For each of the sampling points, the optimization problem was solved from two different initial points, and the better answer was selected to increase the change of finding the global optimum.

ANN models were trained with various training options, and the best models were selected. As far as the architecture of the ANN is concerned, the single-layer ANN was used for both cases. The training algorithm was the Levenberg-Marquardt with Bayesian Regularization algorithm. The number of hidden nodes determines the complexity of the NN architecture. In general, more complicated functions require more hidden nodes. Final training results are summarized in Table 52, including basic statistics such as R-squares and the mean and standard deviation of model fit error (MFE) and model representation error (MRE). The numbers of hidden nodes were eight and five for each of the models, respectively.

The statistics are graphically represented in Figure 78 and Figure 79, showing histograms of error distributions, actual by predicted, and residual by predicted plots. The histograms are close to normal distribution with reasonably small mean and standard deviation values. The actual by predicted plots show tight fit around the perfect fit line without any sign of patterned behavior. The residual by predicted plots

shows random scatter of residuals without noticeable patterns. All the residuals fall

below 2% of the actual response value.

Table 52: Neural Network Training Statistics of f_2^*

Second-Stage Development Type	Derivative Design	New Design
Number of hidden nodes	8	5
R-square of Training Set	0.980528	
R-square of Validation Set	0.970675	
Model Fit Error (Mean)	0.003758	
Model Fit Error (Standard Deviation)	0.607262	
Model Representation Error (Mean)	0.016637	
Model Representation Error (Standard Deviation)	0.746351	
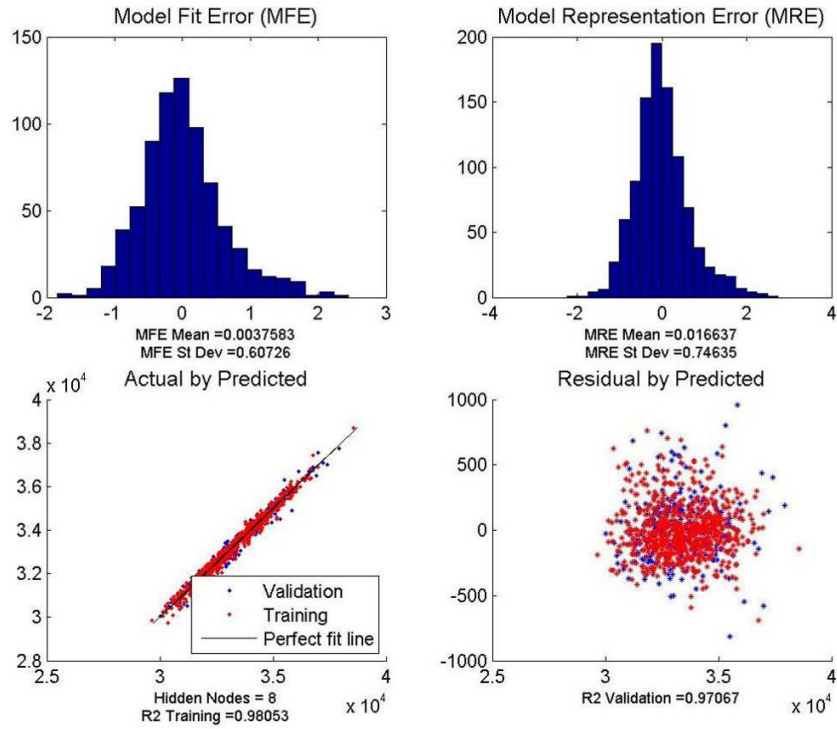
Figure 78: Neural Network of f_2^* for the Derivative Design Strategies

266
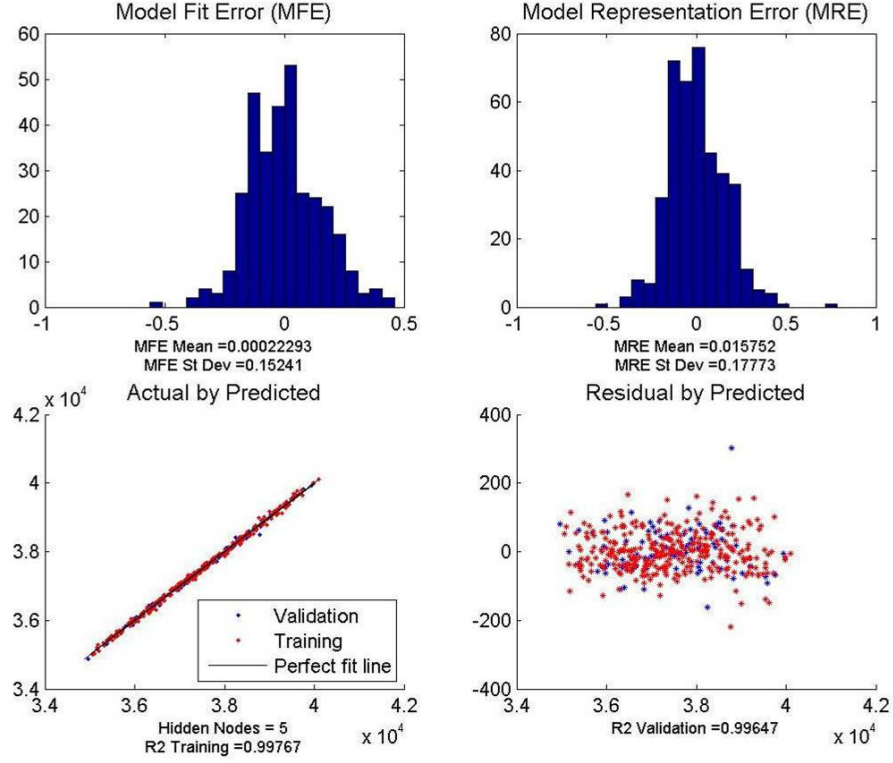
Figure 79: Neural Network of f_2^* for the New-Design Strategy

7.9.2 Monte Carlo Simulation

Since the random variables are continuous, the number of possible combinations are infinite. The expectation of the optimum second-stage cost $\mathbb{E}(f_2^*)$ is approximated using the Monte Carlo (MC) technique. Two sampling techniques—Latin Hypercube Sampling (LHS) and Simple Random Sampling (SRS)—were compared with various sample sizes in order to investigate their convergence properties. The commercial software package Crystal Ball® was utilized as the framework for MCS and sampling methods. Random samples of the four random variables—fighter escort radius, interdiction radius, recovery payload, and avionics weight—were generated using LHS and SRS following the PDFs defined in **Step 2**.

For the experiment, the first-stage design was fixed at $(\mathbf{x}_1^*)^1$. Then, Monte Carlo simulation was repeatedly performed to calculate $\mathbb{E}(f_2^*)$ with the sample size increasing from 1,000 to 500,000 using LHS and SRS. Since true value of $\mathbb{E}(f_2^*)$ is not known, it was assumed that the estimated $\mathbb{E}(f_2^*)$ would be closest to the true value when the sample size is the largest. Then, error was defined as the difference from the $\mathbb{E}(f_2^*)$, calculated using 500,000 samples.

Experiment results are provided in Table 53. It was concluded that $\mathbb{E}(f_2^*)$ converged faster with the LHS technique than it did with SRS. With only 1,000 samples, the error with LHS was less than 10^{-5}, and it was close to 10^{-6} with 5,000 samples. SRS showed considerably larger errors than LHS with the equal number of samples or converged to a similar degree of errors with considerably larger samples than LHS did. This study is limited to only a point in the first-stage design space, however it was concluded that LHS would work better than SRS in terms of approximating $\mathbb{E}(f_2^*)$, and the sample size of 5,000 was used in solving *stochastic* optimizations in the next step.

Table 53: $\mathbb{E}(f_2^*)$ Convergence Comparison with LHS and SRS Sampling Methods

	LHS		SRS	
N	$\mathbb{E}(f_2^*)$	Error	$\mathbb{E}(f_2^*)$	Error
1,000	32,516.29	0.0000504	32,596.81	0.002522
5,000	32,514.23	-0.0000128	32,529.98	0.000466
10,000	32,513.70	-0.0000291	32,530.60	0.000485
100,000	32,515.30	0.0000199	32,517.41	0.000080
500,000	32,514.65	not applicable	32,514.82	not applicable

Finally, the PDF of f_2^* was plotted with both 5,000 and 100,000 scenarios for comparison. PDF with 100,000 samples as shown in the bottom of Figure 80 is a quite smooth distribution that is close to a normal distribution slightly skewed to the left. It

does not show any irregularity from normal distribution except for the skewness, and even both tails are well represented. On the other hand, the PDF created using only 5,000 samples in the top of the figure is not smooth, while the overall trend agrees to the higher fidelity counterpart. Especially, if the point of interest were at the tails of the distribution, the PDF with 5,000 samples would be a poor representation of the true behavior. Comparison of these two PDFs shows that although 5,000 samples would be sufficient in estimating the average of the distribution, it does not guarantee the same level of accuracy with other types of statistics, and further investigation is warranted if the point of interest is something other than the average value.
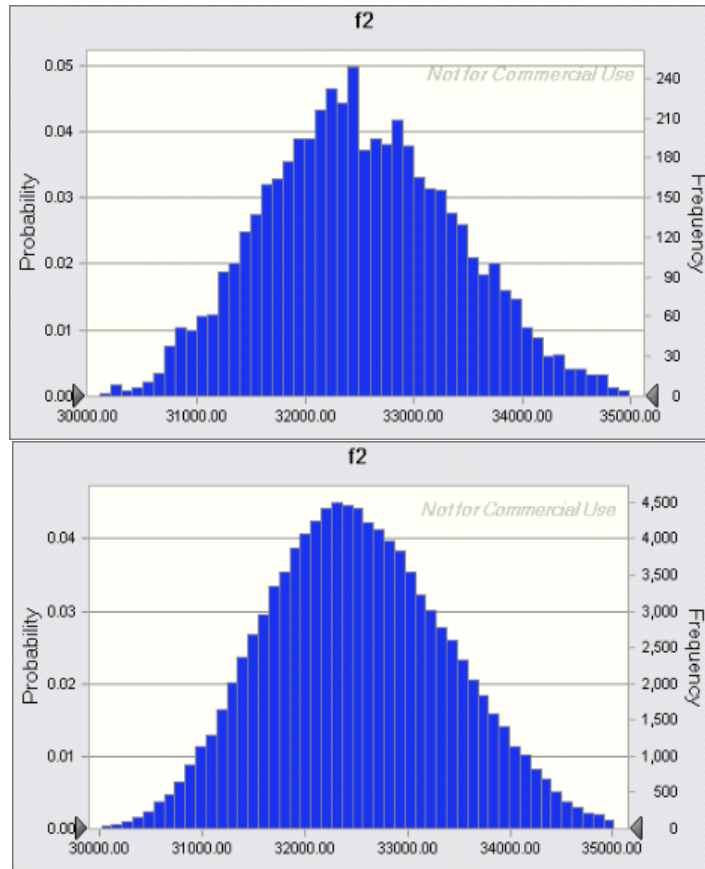
Figure 80: PDFs of f_2^* using 5,000 (Top) and 100,000 Scenarios (Bottom)

7.9.3 Before Realization of the Random Variables: The Here-and-Now Solutions

The results of SPR are a single first-stage optimal solution and a group of second-stage recourse decisions that match a specific realization of random variables. The first-stage optimal decision under StoPP $\left(\mathbf{x}_1^*\right)^6$ constraints and some of the design outputs evaluated at $\left(\mathbf{x}_1^*\right)^6$ are presented in Table 54. Deterministic optimization results that are in Table 45 are repeated in the shaded columns for easier comparison. It is observed that under stochastic strategy, the optimizer decided to overdesign more than the Ad-hoc and New-design strategies did, but not as much as any DetPPs did. Eq. (72) is expended to

$$\left(\mathbf{x}_1^*\right)^1 = \left(\mathbf{x}_1^*\right)^2 < \left(\mathbf{x}_1^*\right)^6 < \left(\mathbf{x}_1^*\right)^3 < \left(\mathbf{x}_1^*\right)^4 < \left(\mathbf{x}_1^*\right)^5 \tag{81}$$

with an exception of external fuel capacity. This inequality also holds for the weight and cost outputs.

Table 54: First-Stage Optimum Design under the Stochastic Strategy

	Strategies	Stochastic	ND	Ad-hoc	Block10	EV	Block10p	Unit
x_{11}	Wing area	413.4	396.6	396.6	449.4	449.4	498.5	ft^2
x_{12}	Thrust	19230	18355	18355	20441	20441	21947	lb
x_{13}	Ref. weight for DLF	35566	34131	34131.3	38251	38251	41816	lb
x_{14}	Landing weight	36375	33248	33247.7	39539	39539	43839	lb
x_{15}	Internal fuel	11270	10827	10826.5	12777	12777	14692	lb
x_{16}	External fuel	6951	6724	6723	6691	6691	9608	lb
x_{17}	Ref. thrust for aft-body	21384	18355	18355	23508	23508	25238	lb
x_{18}	Fuselage length	53.50	53.08	53.08	54.68	54.68	55.60	ft
g_{11}	Fighter escort radius	349.7	350.1	350.1	409.6	409.6	478.8	nm
g_{12}	Interdiction mission radius	410.3	410.9	410.9	431.4	431.4	505.8	nm
g_{13}	Recovery payload	6489	4508	4508	7910	7910	9846	lb
g_{14}	Launch wind over deck	22.70	22.06	22.06	22.29	22.29	28.14	knots
g_{15}	Recovery wind over deck	3.55	-0.01	-0.01	3.55	3.55	9.27	knots
g_{16}	Approach speed	141.5	138.1	138.1	141.5	141.5	141.4	knots
g_{17}	Specific excess power	709.4	708.7	708.7	699.2	699.2	685.9	ft/sec
g_{18}	Accel. from 0.8 to 1.2M	63.48	63.66	63.66	63.60	63.60	63.42	sec
g_{19}	Turn rate	12.049	12.042	12.042	12.066	12.066	12.093	deg/sec
g_{110}	Usable load factor	7.609	7.609	7.609	7.609	7.609	7.609	g
R	OEW	26885	25738	25738	28628	28628	30992	lb
E	Attack TOGW	52353	50520	50520	55325	55325	62697	lb
S	Fighter TOGW	39566	37975	37975	42815	42815	47095	lb
U	RDTE	4744	4639	4639	4904	4904	5116	$m
L	RDTE year	8.68	8.58	8.58	8.82	8.82	9.01	year
T	Production	20728	20172	20172	21595	21595	22701	$m
	f_1	25472	24811	24811	26499	26499	27817	$m

7.9.4 The Wait-and-See Solutions and Evaluation of the Strategies from the

Risk Point-of-View

When the random variables are defined as PDFs, an infinite number of optimal second stages exist for every corresponding realization of random variables. Here, realizations of all the combinations of random variables are simulated on top of the already found optimal first-stage decisions $(\mathbf{x}_1^*)_\omega^p$, $p = 1,...,6$. The realization of random variables were approximated by running Monte Carlo simulation with 5,000 randomly sampled scenarios. Due to a large volume of information, PDFs and CDFs are used for visualization and interpretation rather than for the bar graphs. In addition, statistics of the distributions, such as mean and variance are discussed here. With the CDFs and the statistics, the strategies can be ranked in terms of various criteria that the decision maker would choose as a risk-measure. In this study, the strategies were ranked with the following risk-measures: probability to exceed total cost limit, the probability to exceed second-stage cost limit, average total cost, and average second-stage cost.

7.9.4.1   Probability of Exceeding Total Spending Limit

The PDFs of total program cost under the six different strategies are prepared in Figure 81. The PDFs are histograms of the total program costs after the realization of all 5,000 scenarios that were generated using the LHS technique. The figure shows the location of the peak points from the right, namely, the ND strategy followed by the DetPP(Block10p), DetPP(Average), DetPP(Block10), AH, and StoPP strategies. The location of the peak point suggests that the StoPP strategy costs least in general under the realization of all future scenarios. The shapes of the PDFs are different. In terms of the degree dispersion, The Ad-hoc shows a wider distribution than any other does,
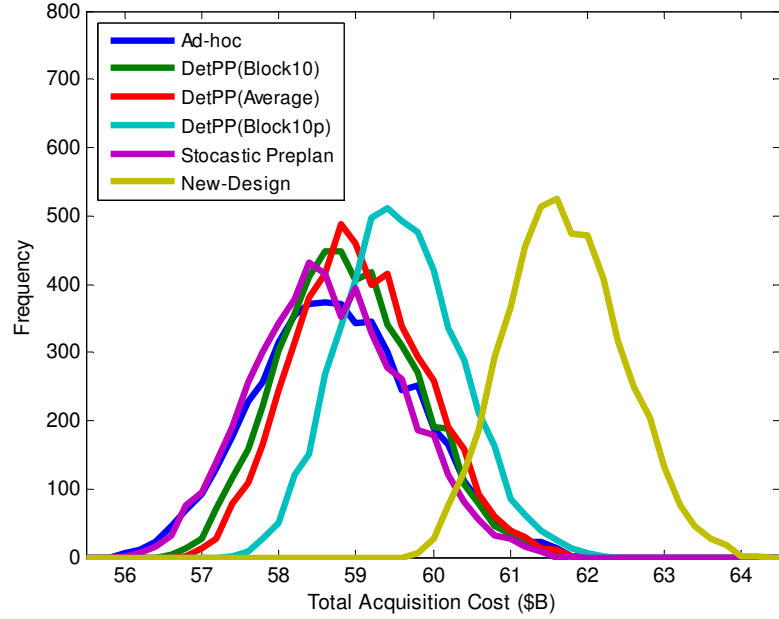
Figure 81: PDFs of Total Program Cost

indicating the largest variability. These observations are discussed again later with the statistics.

By numerically integrating the PDFs in Figure 81, the complimentary CDFs of total program cost were obtained as shown in Figure 82. Superimposed with a spending limit, the CDFs can show the probability of exceeding the cost limit. For example, the probability of spending more than 59 billion dollars for the acquisition of the notional fighter can be read by superimposing a vertical line through the $59 on the horizontal axis then reading the values on the vertical axis where the line intersects with the CDFs. Then, the probabilities are 31.42% with StoPP, 36.78% with AH, 40.4% with DetPP(Block10), 46.04% with DetPP(Average), 72.48% with DetPP(Block10p), and 100% with ND. In general, all five strategies except for the New-design spent more than $56 billion and less than $62 billion with 100% probability. The total spending of New-design strategy fell between about $60 and $64 billion.
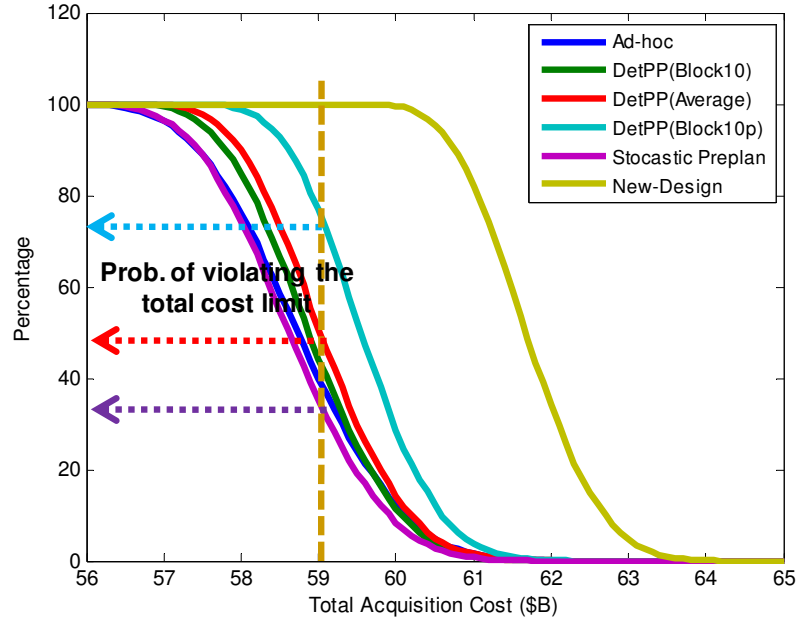
Figure 82: CDFs of Total Program Cost

If the probability of exceeding the spending limit is repeated with varying spending limits from \$56 to \$64 billion, one can see that the StoPP strategy in the purple line has the lowest probability of exceeding the spending limit than any other strategy in most of the region. In fact, a closer look at the CDFs reveals that the Ad-hoc could be the best in specific ranges, and the top three ranked strategies are provided in Table 55. When the cost limit is less than 55.9 or more than 62 billion dollars, all strategies violate or meet the constraint with one hundred percent probabilities. Then, when the spending limit is lower than 55.7 billion, the Ad-hoc strategy is safer than any other. For a limit of more than 55.7 billion dollars, the Stochastic can be selected as the best strategy.

Then, if the decision-maker is risk-averse and spending more than a certain amount is perceived as risky, then the provided rankings can give the decision-makers a handle to evaluate and select the best strategy among six of them accounting for risk. As the rankings show, it could be the StoPP strategy or the AH strategy or any other strategy, depending on the spending limit.

Another notable observation from Table 55 is that the rank of the Ad-hoc strategy gradually goes down as the spending limit increases. It is easier to see the trend in the graphical representation of the rankings as given in Figure 83. The ranking of the Ad-hoc strategy in the blue line steps down as the total cost limit increases from left to right. On the other hand, the DetPPs follow the opposite trend. These trends imply that if the spending limit is high, it is better to pursue a strategy that overdesigns the first-stage vehicle, and if the spending limit is low, it is safer not to overdesign in the first stage.

Observation 11: *The graphical representation of strategy rankings with respect to the probability of exceeding the total program cost limit revealed that no preplanning for growth was better when the cost limit was low, and more growth potential was better as cost limit increased.*

Table 55: Top Three Picks

	Ranking		
Spending Limit	1st	2nd	3rd
Less than 55.9	All equal		
55.9 - 55.7	Ad-hoc	Stochastic	All equal
55.7 - 59.7	Stochastic	Ad-hoc	Block10
59.7 - 60.7	Stochastic	Block10	Ad-hoc
60.7 - 61.9	Stochastic	Block10	Average
More than 62	All equal		
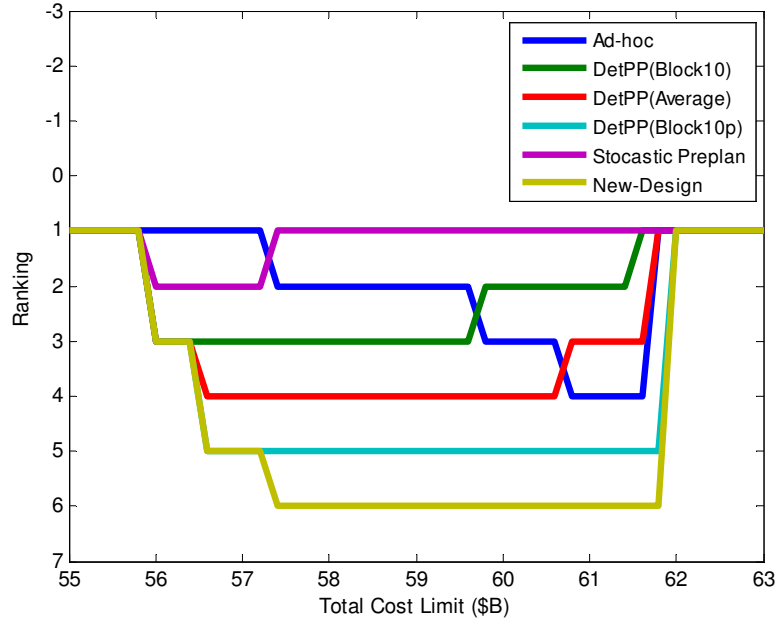
Figure 83: Rankings by the Probability of Exceeding Total Cost Limit

7.9.4.2   Probability of Exceeding the Second-Stage Spending Limit

The ranking criteria or the risk-measure can be different from organization to organization, and now the study in the previous section is repeated with the definition of risk being the probability of incurring more than a certain amount in the second stage. The premise behind this risk-measure is that the first-stage cost is under control and the decision maker is solely concerned about the second-stage cost. This scenario would be plausible when a manufacture has a firm first-stage contract already from an entity, and it is seeking to maximize its profit by selling the derivative versions to other agencies. Alternatively, the manufacturer is competing for the first-stage contract and trying to win it at a loss in hopes of recovering the loss at the second stage. While the situation involving competitors would further complicate the decision-making process, a game theoretic approach would help in making better decisions. The value of EvoLVE is to provide quantitative information to support such decision-making processes.
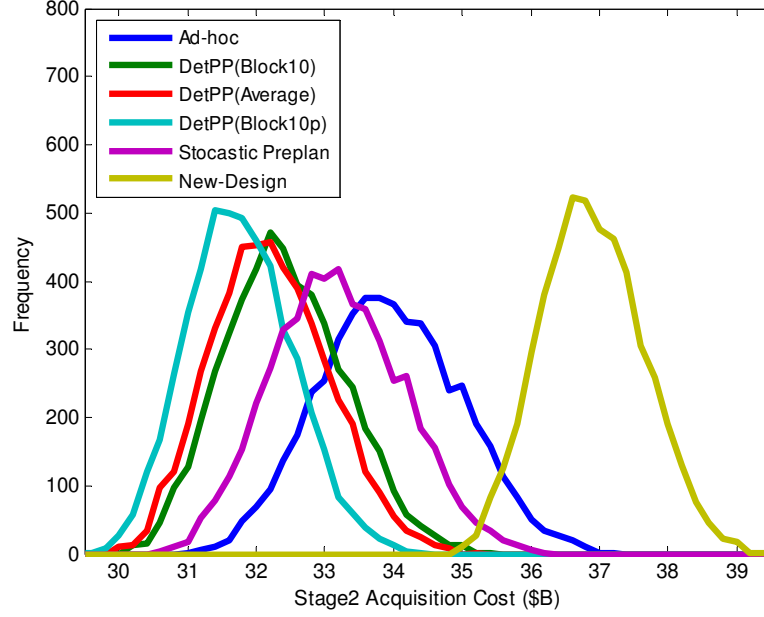
Figure 84: PDFs (Top) and CDFs (Bottom) of the Second-Stage Acquisition Cost

The outcome of the Monte Carlo simulation is now investigated focusing on the second-stage cost. Figure 84 is the PDFs of the second-stage acquisition cost of the six different strategies. One can observe general properties of the distributions, such as location of the peak, dispersion, tails etc. In general, the New-design strategy costs the most, but the dispersion was the smallest. DetPPs cost less than both StoPP and AH, because of larger second-stage RDT&E cost savings. In addition, among the derivative strategies, DetPP(Block10p) showed the greatest possibility to cost the least with the smallest dispersion. The Ad-hoc strategy was the opposite and cost the most with the least variability.

The CDFs in Figure 85 can be used to evaluate the probability of exceeding a certain second-stage cost limit. As an example, for the spending limit of 33 billion dollars, the probability with DetPP(Block10p) is 4.48%; with DetPP(Average) is 15.18%; with DetPP(Block10) is 21.86%; with StoPP is 51.92 %, with Ad-hoc is 78.94%; and with New-design is 100%.
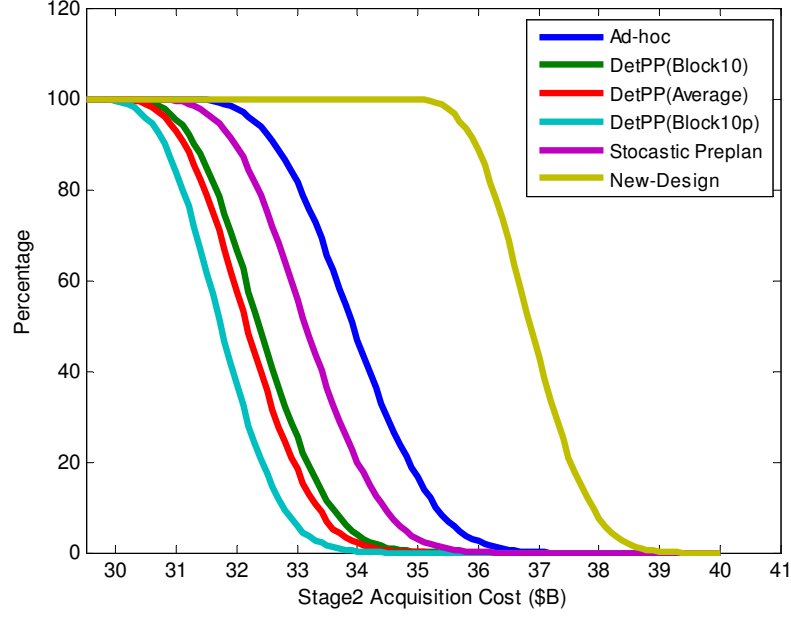
Figure 85: CDFs of the Second-Stage Acquisition Cost

Finally, the strategies are ranked in terms of the probability of exceeding the second-stage cost limit and the best strategy is found with the lowest probability. Formally, this concept is derived from the Risk-Averse Strategy Selection formulations in Eqs. (20) and (21), and they are reduced to

$$\min_{p} \text{Prob}\{Q((\mathbf{x}_1^*)^p, \boldsymbol{\omega}) > \tau\} \tag{82}$$

where $Q((\mathbf{x}_1^*)^p, \boldsymbol{\omega})$ is the optimal value of the second-stage problem or the given first-stage optimal solution $(\mathbf{x}_1^*)^p$ under strategy $p = 1, ..., 6$ defined as

$$Q((\mathbf{x}_1^*)^p, \boldsymbol{\omega}) = \min_{\mathbf{x}_2} f_2(\boldsymbol{\omega}, (\mathbf{x}_1^*)^p, \mathbf{x}_2)$$
$$\text{s.t. } g_{2j}(\boldsymbol{\omega}, (\mathbf{x}_1^*)^p, \mathbf{x}_2) \le 0 \ (j = 1, ..., l_2) \tag{83}$$

The solutions of these equations are sought using Monte Carlo simulation and are graphically represented in Figure 86. The ranking is quite different from the ones done by the total cost. When the cost limit was lower than 30 billion dollars, all strategies

violated it with 100% probability. Then, all strategies could meet the cost limit of 39.5 billion dollars under all scenarios. The DetPP(Block10p) was ranked on the top regardless of the cost limit. However, some other strategies were as good as DetPP(Block10p) in some areas. If the strategies are sorted by the rankings, the order exactly coincides with the order by the degree of overdesign as in Eq. (81) , which implies that the larger the first-stage aircraft, the smaller the probability of over-spending the second-stage cost limit.

Observation 12: *When the risk is measured by the probability of the second-stage program costing more than a certain limit, the strategy ranking corresponds with the first-stage aircraft size. Therefore, the larger the growth potential in the first-stage design, the smaller the expected risk in the second stage.*
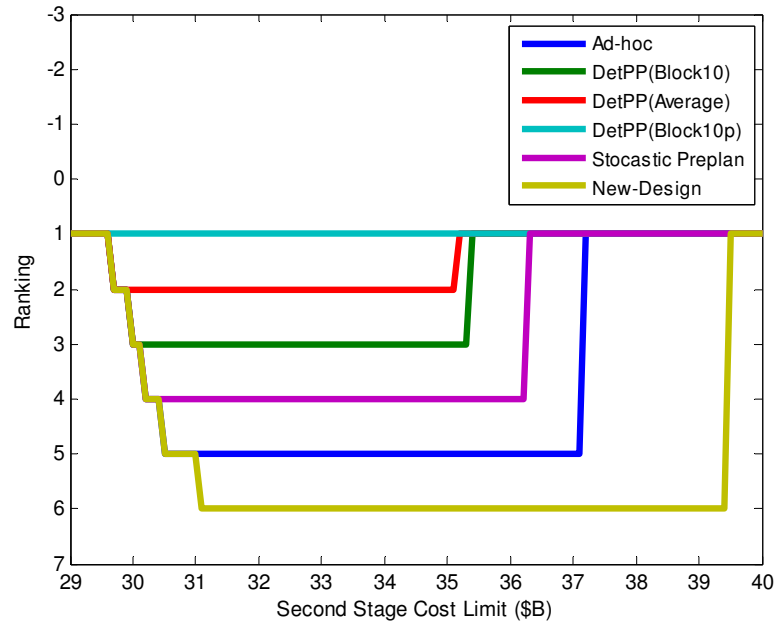
Figure 86: Rankings by the Probability of Exceeding the Second-Stage Cost Limit

7.9.4.3   Strategy Selection by Robustness

The statistics of the distributions of the total cost and second-stage cost are provided in Table 56. The strategies were also ranked in terms of either low mean or variance values. The Stochastic strategy was the best in terms of the mean total cost. However, when only the second-stage cost was considered, DetPP(Block10p) showed the lowest mean.

The variability of the distribution has been used as a measure of risk in the community of stochastic programming. However, the engineering design community regards the variability due to uncertainty is as a measure of *robustness*. When the strategies are ranked by the their robustness to future requirement growth, DetPP(Block10p) is the best, followed by DetPP(Average), DetPP(Block10), StoPP, and Ad-hoc. Interestingly, this order also matches the order by level of overdesign in Eq (81) and the probability of overspending the second-stage cost limit.

Observation 13: *The Stochastic Strategy is the best on average. However, either Ad-hoc or DetPP can be better under certain circumstances. Depending on the risk-measure the best strategy changes. Risk-averse DMs can choose other strategies in order to mitigate risk.*

Table 56: Rankings by Mean and Variance

Criteria	Total Cost (f_1+f_2)				Second-Stage Cost (f_2)			
Strategy	Mean	Rank	Variance	Rank	Mean	Rank	Variance	Rank
New-design	61803	6	550390	-	36993	6	550390	-
Ad-hoc	58860	2	1044700	5	34049	5	1044700	5
DetPP(Block10)	59011	3	756640	3	32512	3	756640	3
DetPP(Average)	59162	4	713290	2	32303	2	713290	2
DetPP(Block10p)	59681	5	583880	1	31864	1	583880	1
Stochastic PP	58751	1	889690	4	33279	4	889690	4

7.10 Framework for Interactive Decision Making Support:

Step 9

While the outcomes of EvoLVE **Steps 7** and **8** were the series of optimum solutions under various conditions, it is often more valuable to have a way to explore the design space in two time-phased stages simultaneously to investigate the options with greater flexibilities than the two approaches **Steps 7** and **8** had offered. The ultimate goal of the final step of EvoLVE is to provide tools with which stakeholders can change the assumptions, apply the scenarios, and trade-off various requirements and figures of merits. While interactive, visual representation of the design space can take many different forms, two-stage contour plots and two-stage multivariate profilers among many are proposed in this study. The benefit of this environment compared to the **Steps 7** and **8** is that it is interactive, giving instantaneous feedback to the user. The use is able to perform "what if" studies for a wide range of scenarios beyond the scenarios used for the optimization.

7.10.1 Two-Stage Constraint Analysis

While the contour profilers can be generated in many different ways and can be used in many different ways, this document demonstrates the historical example of the upgrade of the F/A-18C/D to the E/F, the history of which was briefly introduced in §3.1.1.3, and the requirements of the two versions are summarized in APPENDIX B. Two-stage constraint analysis of the F-18 was performed using the contour profilers generated using JMP®. Using the environment for TSAD created in **Steps 5** and **6**, the data for the demonstration were generated by sampling the design points in the first- and second-

stage design space, assuming uniform PDFs. With the data set, response surface equations (RSEs) were fitted in the JMP, and contour profilers were created.

The demonstration starts from Figure 87, which shows the list of design variables in the current and future stages at the top, the list of performance and cost measures in the middle, and a contour profiler plotted with engine thrust and wing area at the bottom of the figure. The plot was set at the F/A-18C/D's design along with the assumed performance limits. Since the actual F/A-18C/D's performance thresholds were not known, some of them were set at its actual performance less some margin, and some others were set at actual F/A-18E/F's thresholds. For identification purposes, the baseline design along with the setting is designated as Notional Fighter A.

Figure 87 shows that the design is highly constrained. Since the baseline vehicle's performance is very close to the limits, changing either wing area or engine thrust would cause infeasibilities. For example, if the wing area is reduced or wing loading increases, then the turn rate requirement is violated. Engine thrust cannot be reduced without violating the acceleration requirement. However, Notional Fighter A still has some room for growth on carrier operability metrics, such as launch WOD, recovery WOD, and approach speed, as is easily observed from the relative locations of the red diamonds and shaded area next to the list of each of the requirements. This suggests that the wing area could be reduced or wing loading could be increased if relaxation on the turn rate requirement was allowed.
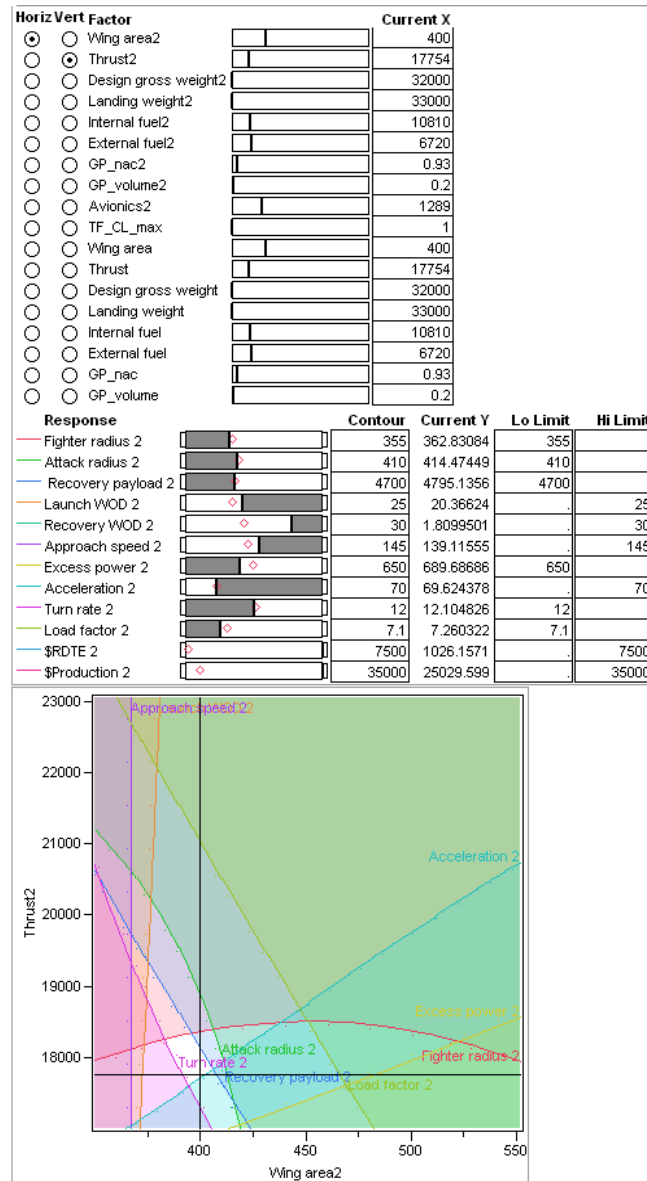
Figure 87: Contour Plot of the Notional Fighter A

The key improvements that the U.S. Navy wanted make on the F/A-18C/D were to bring back capability and interdiction mission radius. The bring back weight became more important in the late 1980s as highly advanced bombs were fielded, and the cost of jettisoning those weapons sharply increased. The Navy also wanted at least 430 nm of interdiction mission radius flying the Hi-Lo-Lo-Hi mission profile with three external fuel
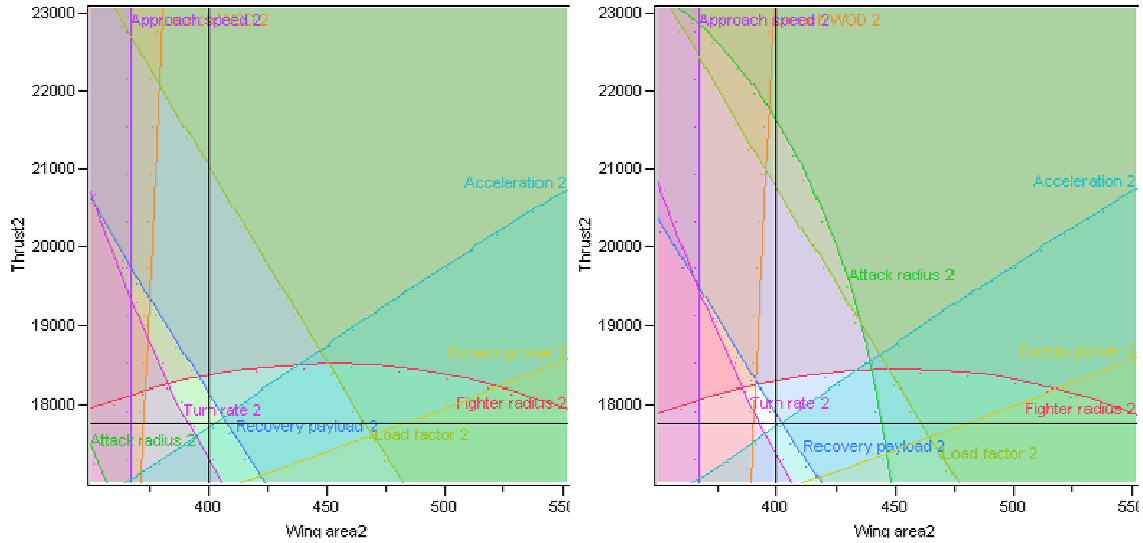
Figure 88: Fighter A with 430 nm Attack Radius (Left) and Fighter B (Right)

tanks as the mission spectrum of the Hornet was extended to complement and eventually

replace the aging A-7.

To investigate the possibility of these two improvements to the Notional Fighter A,

the attack radius is increased from 410 nm to 430 nm, which gives rise to infeasibilities

as shown in the left of Figure 88. Then, in order to increase the mission range, external

fuel tank capacity is increased from 6,720 lb to 8,000 lb, which opens up the feasible

space back as shown in the right side of Figure 88. Thus, the requirement growth is

fulfilled by upgrading external fuel tanks without modifying the aircraft itself.[*]

Notional Fighter B is then challenged by increasing its recovery payload capability

from about 4,800 lb to 9,000 lb, which is from the F/A-18E/F OSD. Recovery payload is

solely determined by the landing weight. The landing weight of the F/A-18 Hornet was

33,000 lb initially, and then increased to 34,000 lb with restriction. The U.S. Senate

---

[*]Fuel tank upgrade on F/A-18C/D was suggested by the U.S. Congress. However, the DoD opposed the idea, arguing that the use of 480 gallon tanks instead of 330 gallon tanks would cause physical interference and thus require substantial modification to the airframe itself. [191]
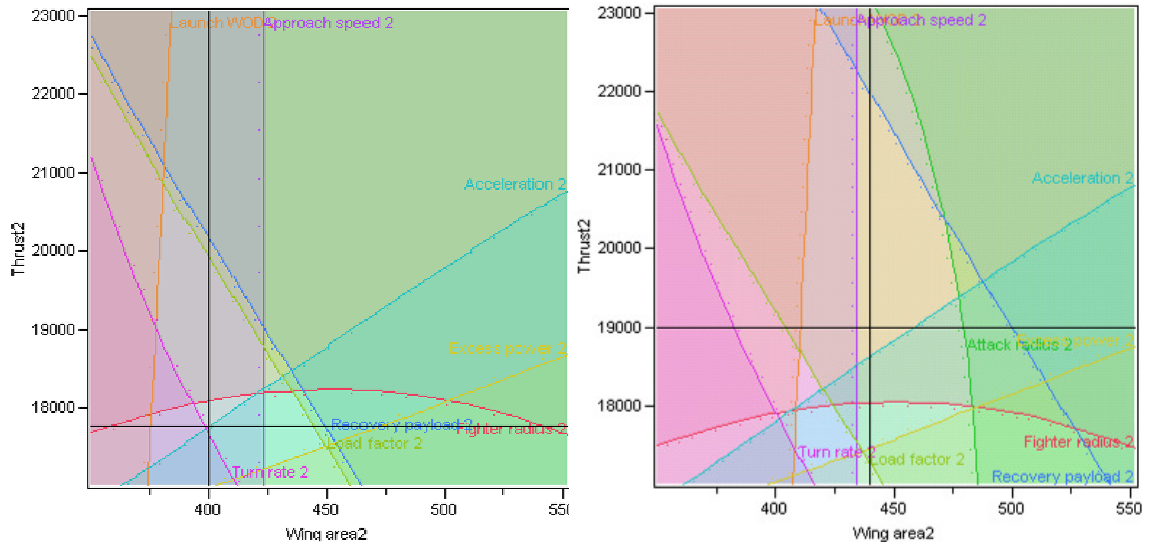
Figure 89: Fighter B with 38,000 lb Landing Weight (Left) Fighter B' (Right)

suggested increasing the landing weight further by strengthening landing gears to improve the recovery payload capacity of the Hornet. To investigate such a possibility, the landing weight of Notional Fighter B is increased to 39,000 lb. The updated contour plot is presented in Figure 89, on the left.

Upgrading landing gears caused unfavorable side effects; due to the increase in aircraft empty weight, turn rate and acceleration constraints were not met; higher landing weight also constrained the lift capability of the wing, and approach speed constraint is violated. To quickly resolve the issues, engine thrust was increased to 19,000 lb and wing area was increased to 440 ft^2 as shown in Figure 89, on the right. However, increase in engine thrust advertently degraded mission performance, and fighter mission radius was violated. In addition, further increase in empty weight due to a larger wing and engines caused violation of the load factor constraint.

As a remedy, a series of design modifications were applied. Since fighter mission profile does not use external fuel tanks, fighter mission range increased by increasing internal fuel capacity to 11,500 lb. The load factor issue was directly addressed by

increasing design gross weight. Higher design gross weight was achieved by augmenting the structural strength of the airframe so that the aircraft could pull the required maximum gravitational force with a heavier body. Strengthening the airframe gave rise to unfavorable side effects because it increased the empty weight. Therefore, to resolve newly introduced infeasibilities, some other design parameters were changed but then caused additional infeasibilities in some other dimensions. Eventually, this spiral effect converged to feasible solutions near the design of F/A-18E/F.

However, easier and lower cost solutions were also possible if some of the less important requirements were relaxed. For example, reducing the maximum load factor to 7 g's from the current 7.5 g's and increasing the design gross weight to 33,000 lb reopens up the design space as shown in Figure 90. The new feasible design is designated as Notional Fighter D. Notional Fighter D is somewhere in between the F/A-18C/D and E/F and meets most of the F/A-18E/F's requirement. Therefore, Notional Fighter D can be viewed as a de-rated, lower cost alternative of the F/A-18E/F.

Finally, the contour profiler of the Super Hornet is created as presented in Figure 91. The Super Hornet was designed to carry heavier avionics, to pull the maximum load factor of 7.5 g's, and to reduce RCS. It also features improved LEX with higher C_{Lmax} and uses a new engine core with a higher thrust to engine weight ratio than F404-GE-402. The contour plot of the F/A-18E/F indicates that it had growth margins on carrier suitability metrics but might lack some fighter performance, such as acceleration, turn rate, and excess power in the future, if weight growth is realized.

The series of demonstration in this section showed that the F/A-18E/F's requirement could not be fulfiled by retrofitting existing F/A-18C/D's with better

landing gears and larger external fuel tanks as suggested by the U.S. Congress. Rather, completely resizing the vehicle at the system level was necessary because upgrading at a subsystem level causes infeasibilities in some other dimensions. However, if some of the non-critical requirements of the F/A-18E/F were relaxed, possibility of extending the life of the F/A-18C/D by fixing some of the most critical capability defficiencies.

Observation 14: *The mission performance, fighter performance, and carrier suitability requirements are highly conflicting each other, limiting the feasible design space. Since it is very difficult to improve performance in one dimension without sacrificing the others, a system-level resizing would be necessary to upgrade a vehicle, rather than retrofitting at the subsystem level. On the other hand, relaxation of non-critical requirements can open up the design space and offer less capable and less expensive alternatives.*

Horiz	Vert	Factor		Current X
⊙	○	Wing area2		440
○	⊙	Thrust2		19000
○	○	Design gross weight2		33000
○	○	Landing weight2		39000
○	○	Internal fuel2		11500
○	○	External fuel2		9000
○	○	GP_nac2		0.93
○	○	GP_volume2		0.2
○	○	Avionics2		1289
○	○	TF_CL_max		1
○	○	Wing area		400
○	○	Thrust		17754
○	○	Design gross weight		32000
○	○	Landing weight		33000
○	○	Internal fuel		10810
○	○	External fuel		6720
○	○	GP_nac		0.93
○	○	GP_volume		0.2

Response		Contour	Current Y	Lo Limit	Hi Limit
Fighter radius 2		355	383.36146	355	.
Attack radius 2		430	467.13216	430	.
Recovery payload 2		9000	9349.144	9000	.
Launch WOD 2		25	22.510121	.	25
Recovery WOD 2		30	6.5816731	.	30
Approach speed 2		145	144.08924	.	145
Excess power 2		650	699.5355	650	.
Acceleration 2		70	67.018936	.	70
Turn rate 2		12	12.490222	12	.
Load factor 2		7	7.0831299	7	.
$RDTE 2		5000	2141.5379	.	5000
$Production 2		300000	26454.942	.	300000

Figure 90: Contour Profiler of Notional Fighter D

Horiz	Vert	Factor		Current X
⊙	○	Wing area2		500
○	⊙	Thrust2		22000
○	○	Design gross weight2		42097
○	○	Landing weight2		44000
○	○	Internal fuel2		14700
○	○	External fuel2		9740
○	○	GP_nac2		15
○	○	GP_volume2		12.2
○	○	Avionics2		1411
○	○	TF_CL_max		1.029
○	○	Wing area		400
○	○	Thrust		17754
○	○	Design gross weight		32000
○	○	Landing weight		33000
○	○	Internal fuel		10810
○	○	External fuel		6720
○	○	GP_nac		0.93
○	○	GP_volume		0.2

Response		Contour	Current Y	Lo Limit	Hi Limit
Fighter radius 2		355	475.71674	355	.
Attack radius 2		430	505.24017	430	.
Recovery payload 2		9000	9733.0734	9000	.
Launch WOD 2		30	28.572993	.	30
Recovery WOD 2		30	9.3394763	.	30
Approach speed 2		145	141.4834	.	145
Excess power 2		650	682.69988	650	.
Acceleration 2		70	61.557364	.	70
Turn rate 2		12	12.048016	12	.
Load factor 2		7.1	7.6079801	7.1	.
$RDTE 2		7500	7395.0446	.	7500
$Production 2		35000	31311.527	.	35000

Figure 91: Contour Profiler of the F/A-18E/F Super Hornet

7.10.2 Multi-Dimensional, Multi-Stage Design Tradeoff

Another useful tool to interactively investigate the evolution paths of a system simultaneously is a multivariate profiler (MVP). A multivariate plot is a relationship between multiple variables shown at a time. Therefore, it allows simultaneous consideration of desing variables and system attributes in all developing stages. In contrast to the contour profilers shown in the previous sections, where only two dimensions of multi-dimensional design space can be visualized at a time, the multivariate plot shows a designer the view of entire design space interaction simultaneously.

For the notional fighter study, three different types of MV plots were created. The first two types, called MVPI and MVPII respectively, are created based on the optimal first-stage solutions of the five evolution strategies. The third type, called MVPIII, does not start from a specific baseline design but freely investigates the first- and second-stage design space. The benefit of this environment is that it is interactive and gives instantaneous feedback to the user. "What if" studies can be performed using a wide range of scenarios beyond the scenarios used for the optimization. All MVPs were created and analyzed using the multivariate analysis feature of the JMP® software package.

7.10.2.1 Optimum First-stage Strategies and Future Design Alternatives

The New-Design strategy was identical to Ad-hoc strategy in terms of the first-stage design and was excluded. On top of the five optimal first-stage decisions, $(\mathbf{x}_1^*)^p$, $p = 2, ..., 6$, the potential derivative aircraft designs are applied by running MCS with the 1,000 second-stage designs for each of the optimal first-stage designs. The 1000

samples were obtained by LHS techniques, assuming uniform distributions on the second-stage design variables. The outcome is 5,000 derivative aircraft options that are presented in Figure 92. The MVPs are symmetrical along the diagonal. Variable names appear in the diagonal starting from design variables, aircraft performance, and RDT&E cost. Since the figure is hard to read, subsets of Figure 92 are presented in following figures.
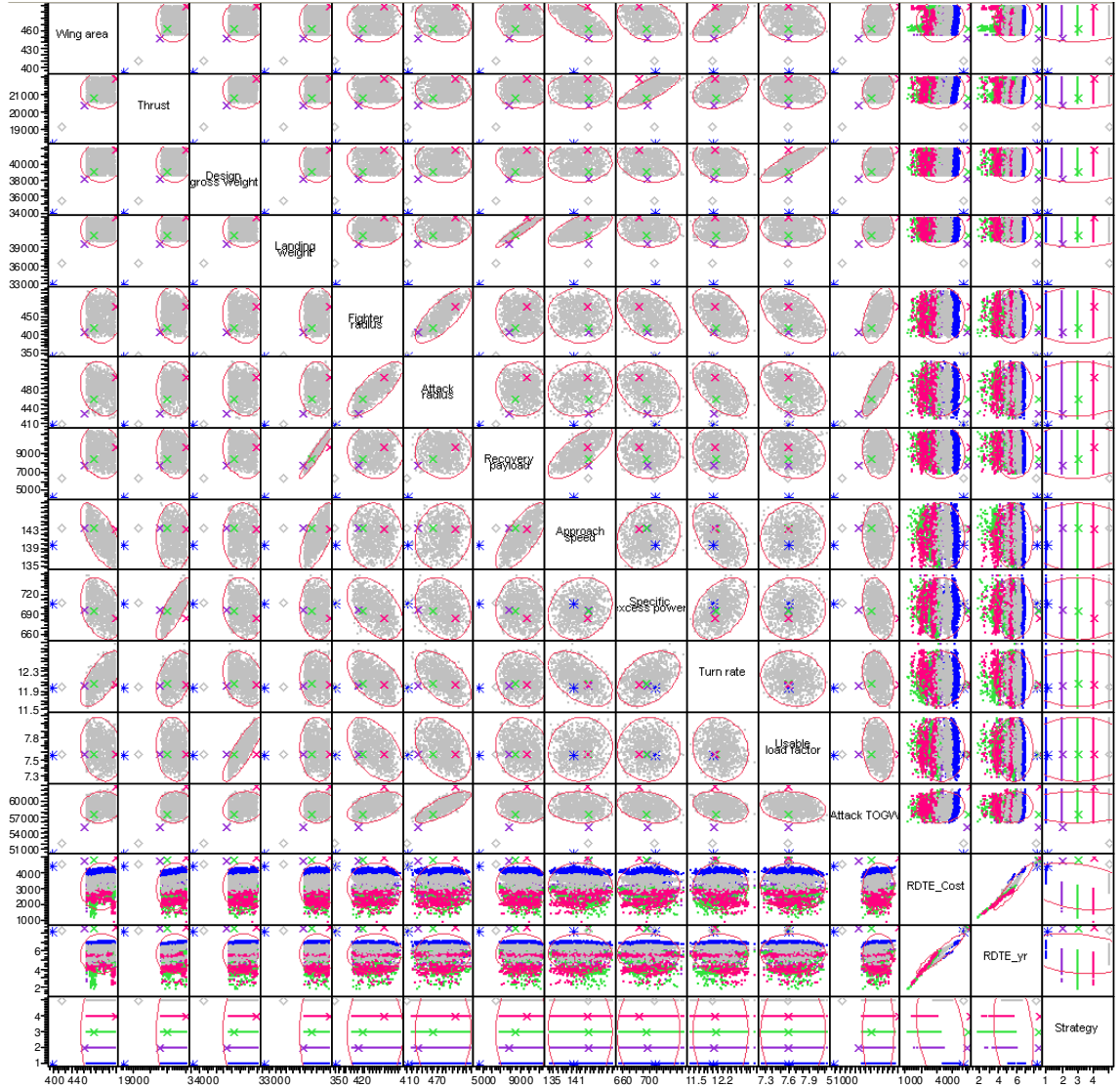
Figure 92: Entire View of Multivariate Profiler Type I

One observation from the MVP is the correlation between any two variables. The scatter patterns of the design points in a box reveal either positive, negative, or no correlation between the two variables. The variables with no correlation show randomly scattered points. A more accurate way of examining the correlation is through the correlation map. The correlation map of MVPI is presented in Figure 93. The right side of the figure is the correlation color scale from -1 to +1. Negative one in the scale in blue is complete negative correlation, and positive one in the scale in red is complete positive correlation. Some of the noteworthy correlations are highlighted with yellow-outlined boxes. External fuel has a very strong positive correlation with attack radius but no correlation with fighter radius. Approach speed performance and Recovery Wind-Over-Deck (RWOD) is highly correlated. In addition, engine thrust shows strong correlation with excess power and acceleration. Fighter performance metrics are closely correlated with each other. RDTE cost and duration are very strongly correlated to each other.

Figure 94 is the subset of MVPI that only shows the design variables. The plot shows both the first-stage designs of the five strategies and the second-stage designs. The locations of the first-stage and second-stage designs illustrate relative and absolute size of the aircraft. For example, the first-stage design under the Ad-hoc strategy $(\mathbf{x}_1^*)^{\text{Ad-Hoc}}$, shown by a blue dot, appears at the low left corner, indicating the smallest aircraft in the design space. On the other hand, the first-stage design under the DetPP(Block10p), $(\mathbf{x}_1^*)^{\text{Ad-Hoc}}$, shown by an orange cross, is at the top right corner of the design space, indicating that it is even larger than most of the second-stage designs shown in grey dots.
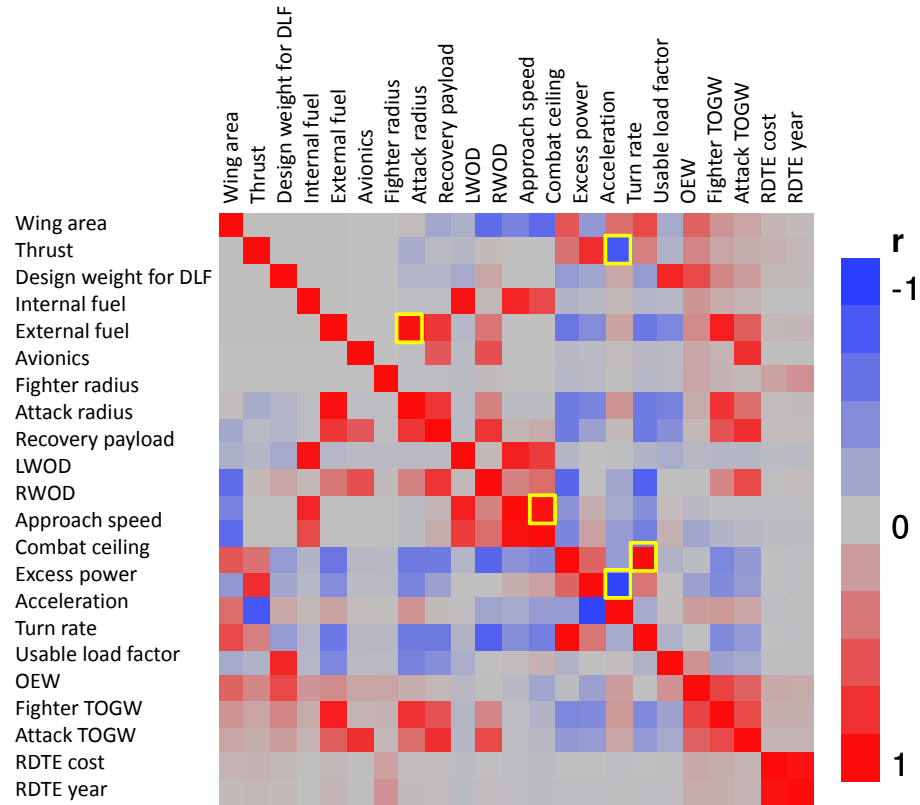
Figure 93: The Correlation Map of Multivariate Profiler I
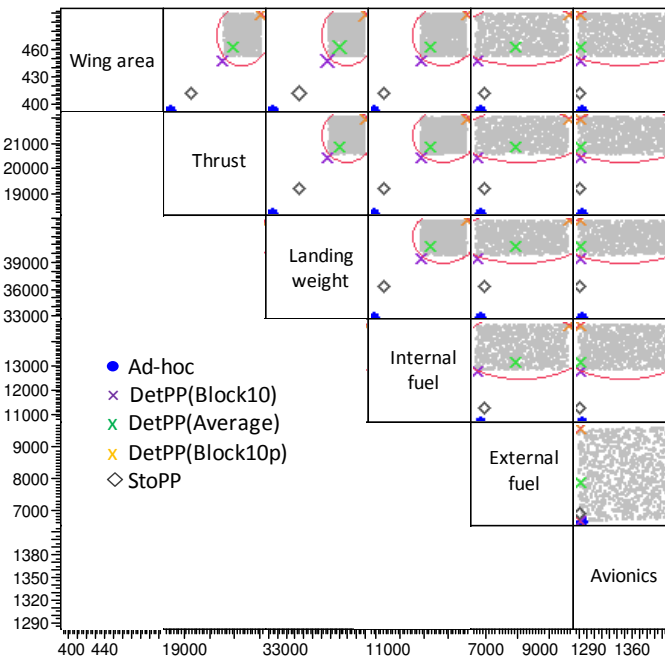
Figure 94: The Design Variables of Multivariate Profiler I

293

Once the future aircraft states are populated for each of the five optimum strategies, the next step is to apply future requirement scenarios to see which strategy offers feasibly design modification options under a specific scenario. MVPI was tested with the scenario of more emphasis on air-to-air combat. In this hypothetical scenario, a need for a dedicated air-to-air combat fighter has established by an international Air Force. The capability specifies the minimum fighter radius of 430 nm, minimum of 12.5 degrees per second turn rate, and minimum usable load factor of 7.5 g's in combat weight. The RDT&E cost to acquire such capability is limited to $2,500, which will be paid by the customer. The scenario is applied on MVPI via the use of scenario filter. Figure 95 shows the performance and cost before the filter is applied, and Figure 96 is the same plot after the filter is applied. Figure 96 shows that only a few design upgrade options survived, and most of them are based on the first-stage design under the DetPP(Block10p) strategy in orange dots. One blue dot is the upgrade option from the DetPP(Average) design, and none of the upgrade options by the Ad-hoc, DetPP(Block10), and Stochastic strategies met the new requirement.
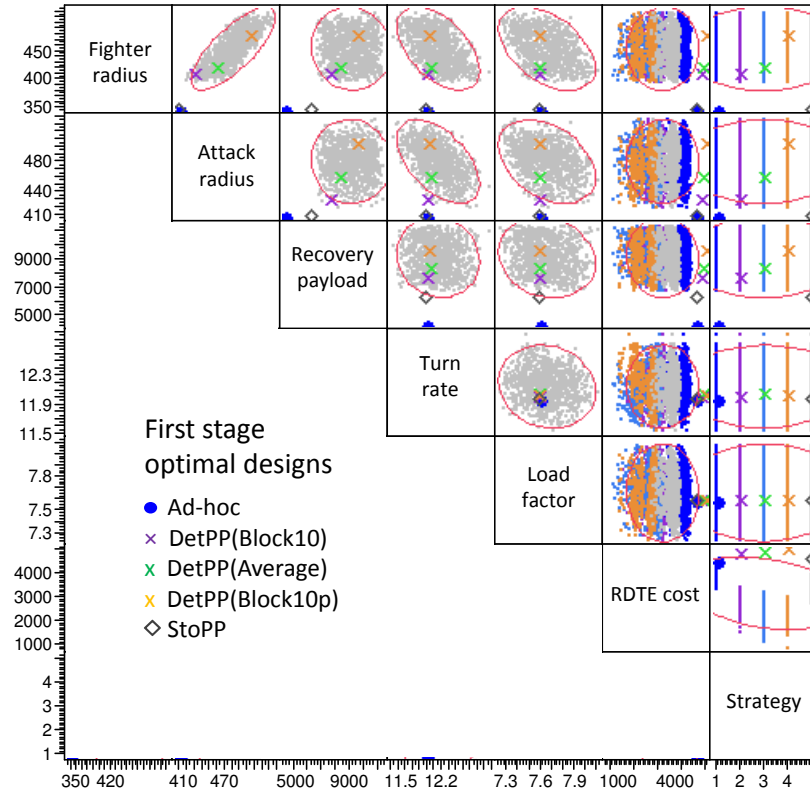
Figure 95: The Notional Fighter Upgrade Options
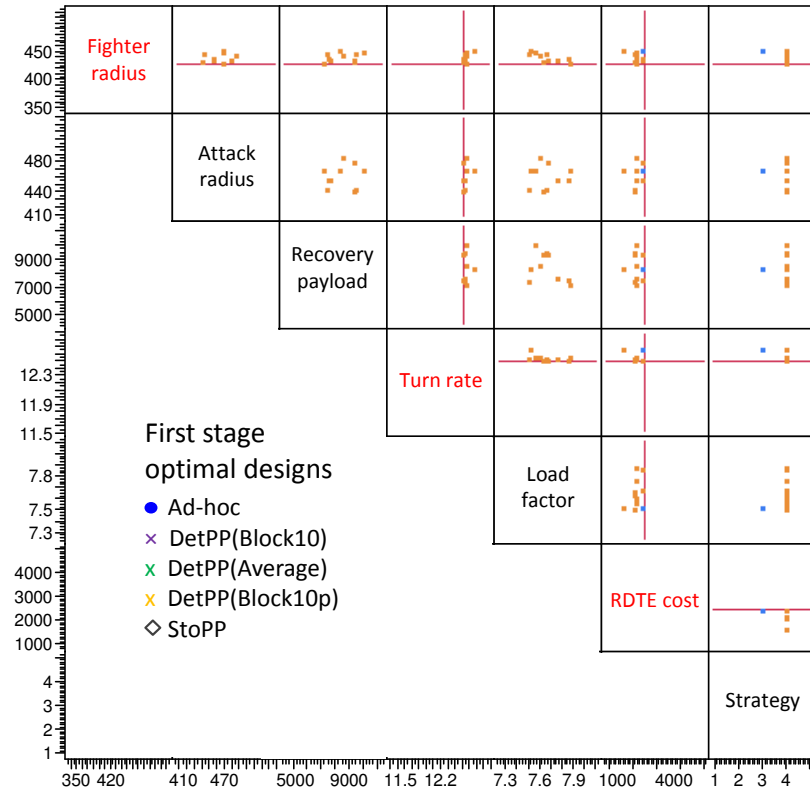
Figure 96: The Notional Fighter Upgrade Options with Scenario Filter

Robustness of Optimum First-Stage Strategies on Future

Requirement and Technology Evolution

The second type of MVP, or MVPII, is also built on the optimum first-stage designs from the five strategies as the MPVI is. Random variation on the requirement is applied on the five baseline designs to see how they react to the future requirement evolution. Here the design itself remains unchanged in the second stage. Aircraft performance, however, changes due to either more stringent requirements or the introduction of new technology. The random variables were fighter payload, attack payload, avionics weight, and technology factor on C_{Lmax}. One thousand random requirement evolution scenarios were sampled using LHS following the uniform distributions.

Figure 97 is the subset of the created MVPII, showing the four random variables. The highlighted points are the original values of the four variables in the first stage. All other points are the future deviations from the original point simulating the evolution of the requirement and technology. Since the random variables were assumed independent
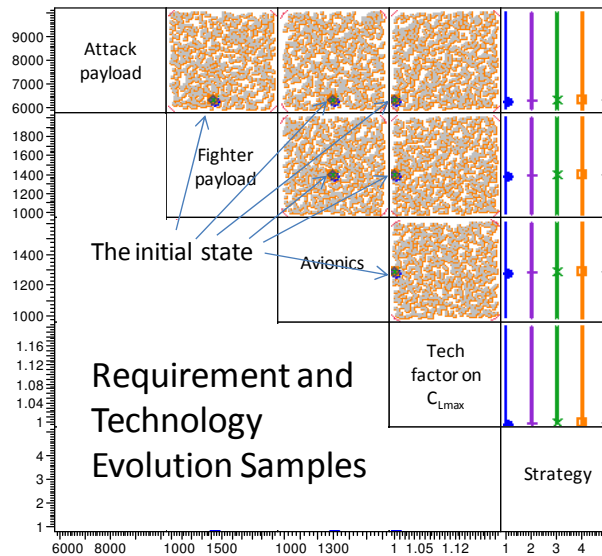
Figure 97: Uniform Variations of Requirement and Technology

of each other and the sampling takes uniform distribution, no correlation is observed from the figure. The color code shown in the far right column is to differentiate the five strategies.

Here, a hypothetical mid-ocean air-to-air scenario was applied. In this scenario, enemy threat has advanced to a degree that the Navy fleet is under potential attack in the mid-ocean. It is desired that the enemy aircraft is intercepted at a distance, and a need for a carrier-based aircraft with long stand-off capability has risen. The notional fighter, originally designed to perform light air-to-air fighter missions, is reconfigured to add Phoenix missile capability and long-range active radar. The retrofit increased avionics weight to 1,400 lb and air-to-air missile weight to 1,500 lb excluding pylons. The scenario also requires the minimum fighter radius of 410 nm, minimum turn rate of 12 degrees per second, and the usable load factor of 7.5 g's. Again, the scenario is applied using a scenario filter. Figure 102 compares the performance variation of the five optimum designs under the five strategies before the filter is applied. Then, Figure 103 is the same MVP after the mid-ocean combat scenario is applied. By comparing the two figures, one can identify which strategy meets such new capability requirements, which does not, and what the impact of the scenario on other performance metrics such as carrier suitability is. No initial design under the Ad-hoc and StoPP strategies could meet the new requirement, while all three DetPPs showed potential to meet it. One can also trade-off some less important requirement, such as attack radius and recovery payload for example, to see how such constraint relaxation opens up new opportunities.
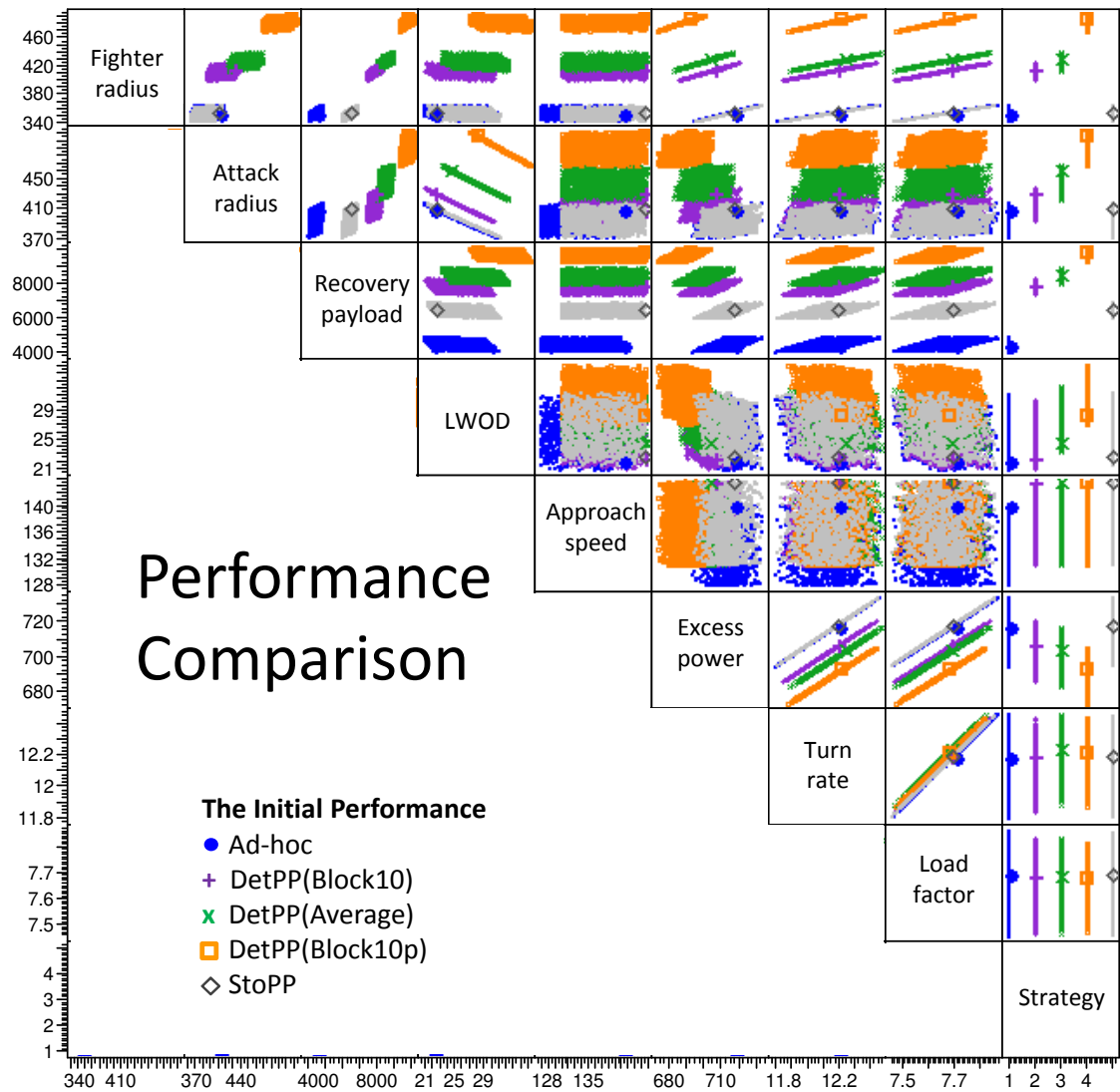
Figure 98: Feasible Designs after Applying Limits on $RDTE and Time to IOC
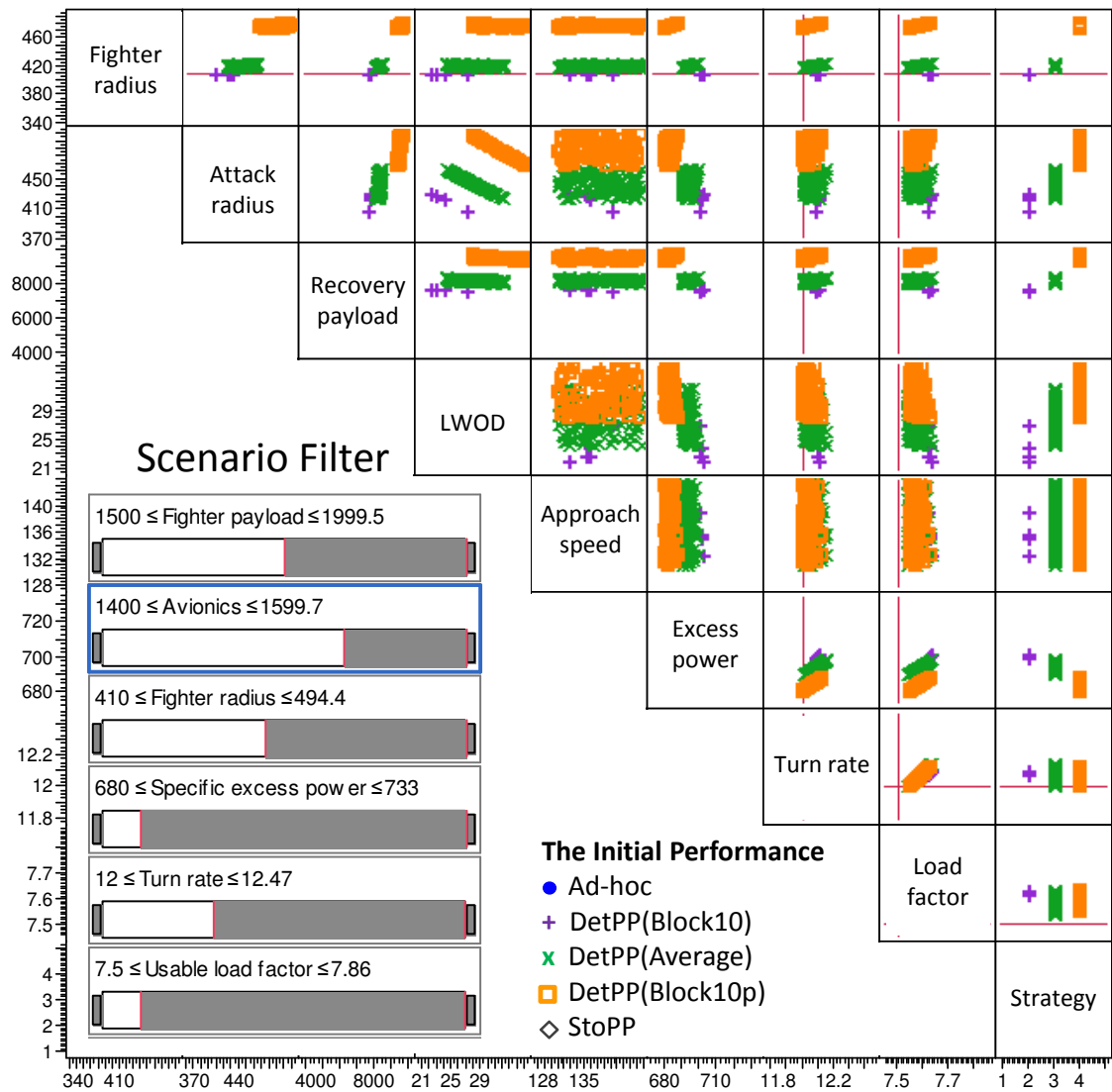
Figure 99: Feasible Designs after Applying Limits on $RDTE and Time to IOC

7.10.2.3 Simultaneous Exploration of Current and Future Design Space

The third type of multivariate profiler or MVPIII was created by running Monte Carlo simulation with 15,000 design samples. The samples were generated using LHS, assuming uniform distributions on both the first-stage and second-stage design variables. The requirement was unchanged in this case, and they are applied as scenarios after MVPIII is created. Compared to MVPI and II, MVPIII allows larger degrees of freedom in the first-stage design and enables a reverse way of defining the baseline aircraft, working back from the future to the current time frame.

Because of the increased degrees of freedom, the size of the matrix is very large and it is hard to display the entire view of MVPIII in a document. Figure 100 is the snapshot of the entire MVPIII that was created for the notional fighter study. The plot includes both first- and second-stage design variables, performance metrics, cost, and weight. It also includes the new requirement and technology that are applied in the second stage. The 15,000 data points were classified into three groups. The criteria were whether the designs meet the Block0 and Block10p requirements. The first group, in blue points, meets both the Block0 and Block10p requirements. The second group, in green points, only meets the Block0 requirement. The last group, in red dots, fails to meet either requirement.
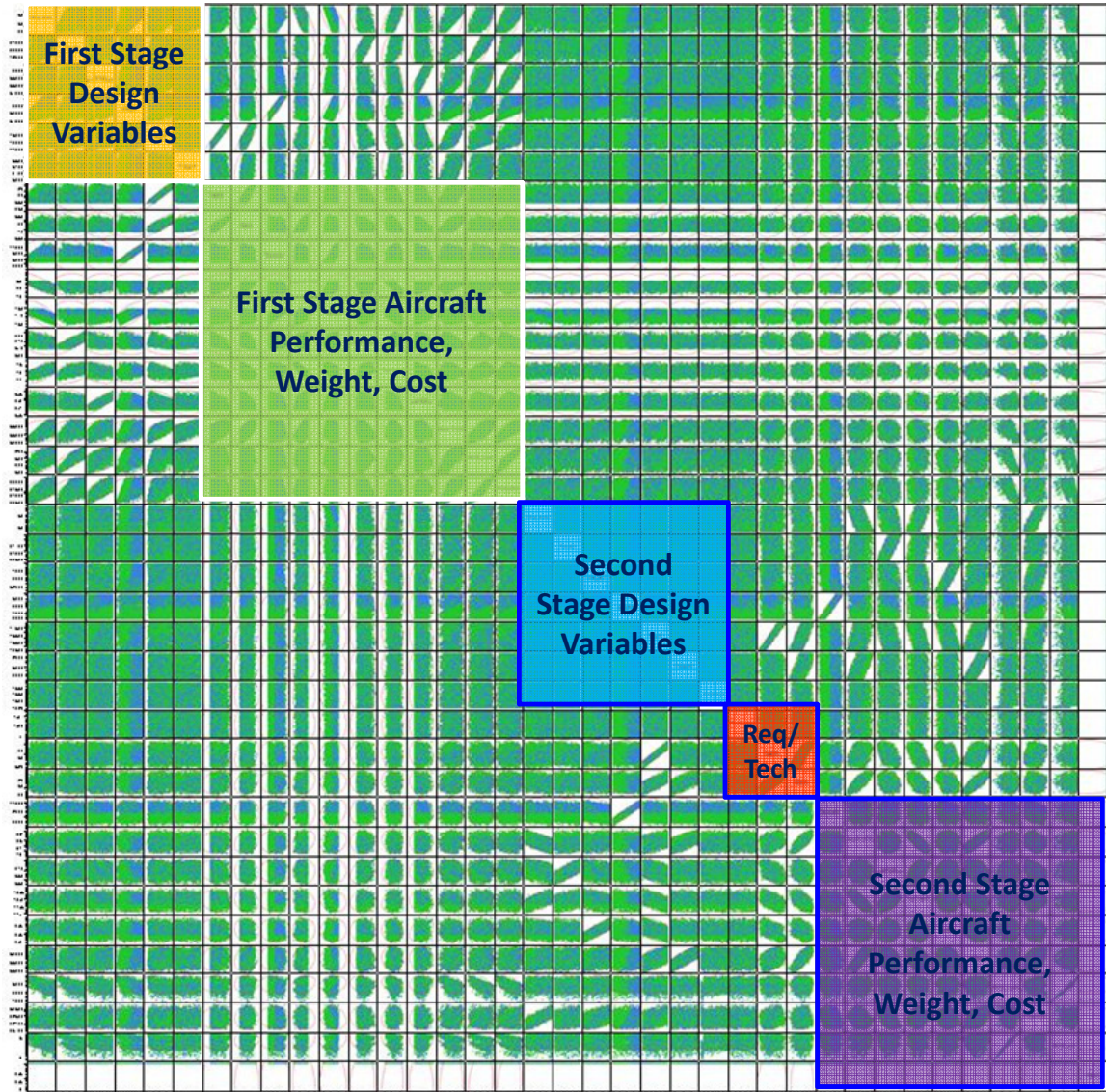
Figure 100: Entire View of Multivariate Profiler Type III

An example usage of MVPIII is to impose only cost and schedule limits on the future programs and then see what is available in the present stage design pool. Here, the RDT&E cost limit of $2500 million and RDT&E period less than 4 years is applied. After applying these two restrictions, the trends in the designs that met these two conditions are observed in Figure 101.

An observation from the thrust and wing area diagram is that only those combinations of high engine thrust and large wing area from the beginning survived the

RDT&E cost and duration constraints imposed in the second stage. The combinations of small wing and engine did not qualify. The cost of changing wing and engine was too expensive so that the aircraft designed with small wing and engine were not viable options in the future. Another observation is made on the avionics system in the second stage. The avionics system weight in the first stage was fixed at 1,289 lb as in the F/A-18C/D, and the second-stage avionics system weight was varied from 1,411 lb as in the F/A-18E/F. While viable designs are found all across the avionics weight values, more data points are clustered around the low avionics weight region. The correlation between the second-stage avionics and the first-stage design shows that keeping the exisiting avionics suite of the baseline aircraft in the second stage brings many first-stage designs viable in the future development programs. The U.S. Navy followed the spiral development strategy in the development of the F/A-18E/F. The F/A-18E/F's avionics system is 90% common to the C/D's avionics initially, and then it was upgraded later.

Observation 15: *The density plots reveal that a combination of high thrust and large wing ensures better probability of responding to requirement evolution with less time and cost. When a derivative aircraft development is under tight budget and schedule constraints, keeping the avionics suite of the baseline aircraft and upgrading it later opens up the solution space.*
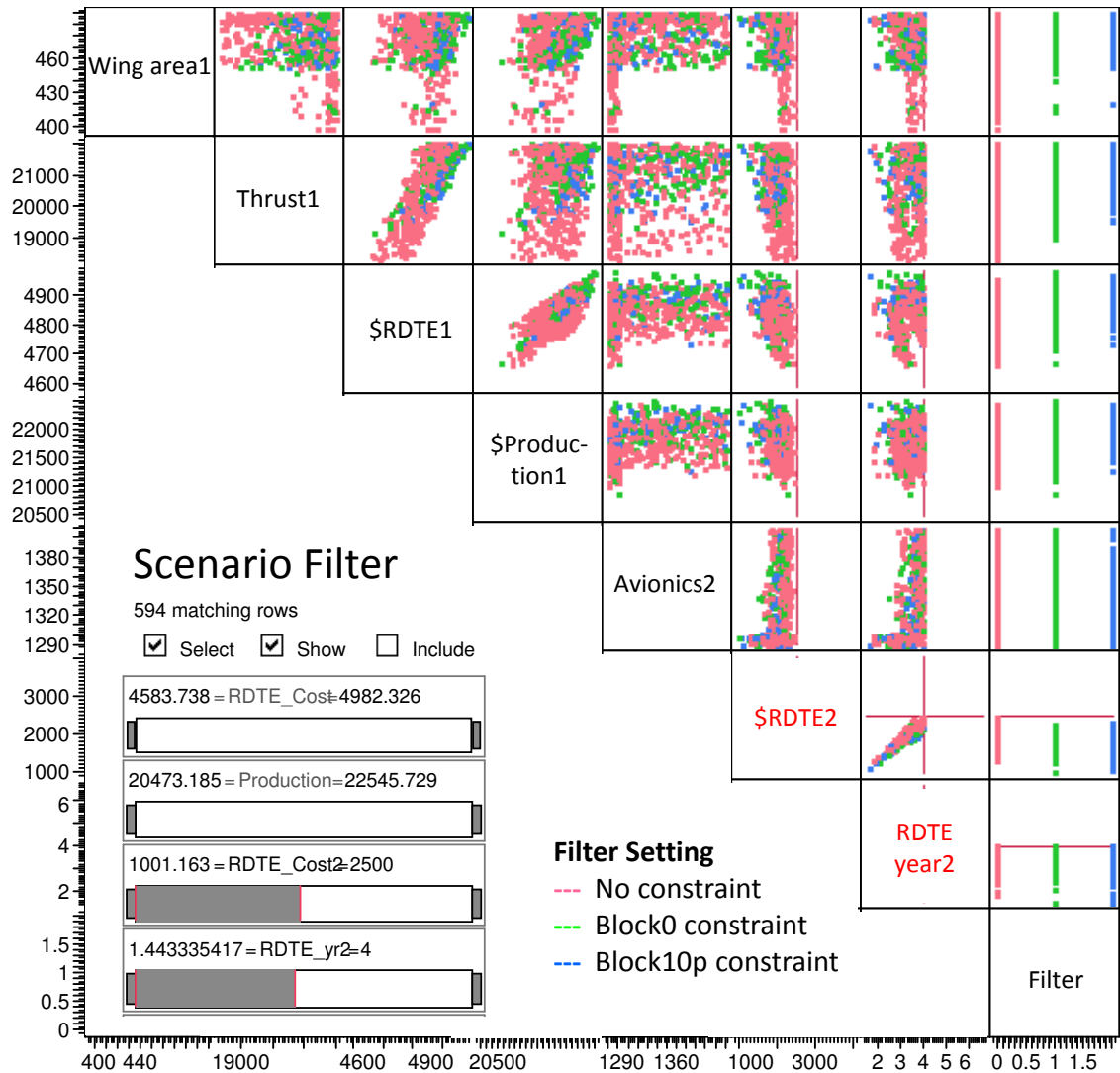
Figure 101: The MVPII after the RDT&E Cost and Duration Filter

7.11 Lessons Learned from the Notional Fighter Design

Study

These findings are obtained as the result of the study. The author hopes that these findings will help in guiding future implementations of EvoLVE both qualitatively and quantitatively; improving the EvoLVE process itself; and simply guiding the engineers and decision makers to provide better products for a longer future.

7.11.1 The Issue of Objective Function

As observed during the experiments in **Step 4** of the EvoLVE process, the optimum solution is sensitive to the objective function that the user wants to optimize for. Two different objective functions—RDTE cost and acquisition cost—were tested in this study, and they yielded quite different results. It is very important and sometimes difficult to determine what would be the most important objective. The paradigm of *design for lifecycle cost* (LCC) would place emphasis on the entire LCC of a product rather than RDT&E or acquisition cost. The largest portion of LCC is O&S cost, and it is further broken down to personnel, maintenance, fuel, etc. While not documented, optimization including O&S was attempted in this study. The conclusion was that O&S cost is not sensitive to aircraft definition when the design parameters vary at a sizing level. Which means, aircraft using a common platform do not have very distinguishable O&S cost because one has a 400 ft^2 wing and the other has a 410 ft^2 wing, because they may not differ in terms of personnel cost and maintenance cost. Fuel cost might be different, but it is only a small portion of O&S cost. In conclusion, the author hypothesizes that

inclusion of O&S cost as part of objective function in aircraft design optimization would not provide much insight.

7.11.2 Technical Challenges Experienced

Considering aircraft design in two stages required more than twice the effort of a single-stage design approach. Creation of modeling and simulation environment encompassing a very large design space required much rigorous modeling and validation processes. In addition, development and validation of the cost model was especially demanding. Fitting surrogate model was difficult because of the two reasons: wide design space and unsmooth behavior of the second-stage RDT&E cost. The use of ANNs instead of polynomial-based surrogate models could handle more complex, non-linear behaviors. The surrogate modeling process had to be repeated many times to adjust the range of the input parameters. When the bounds were too broad, many sampled cases crashed in FLOPS because they could not perform the given mission. Optimization in the setting of two-stage aircraft design was very demanding. Considering optimization at two different design stages simultaneously meant double the number of design variables. Too many design variables not only exponentially increase the computational time, but also the possibilities of human errors since the problem gets too big to grasp by a human decision maker.

CHAPTER VIII

CONCLUSION AND FUTURE WORK

In an attempt to provide a more cohesive study and follow a scientific research process, this document encapsulated important findings, research objectives, contributions, tasks, and lessons-learned. This is shown in the form of **Observations**, **Research Questions**, and **Hypotheses**. The final chapter of the manuscript revisits these formal statements to draw conclusions. Finally, future research opportunities in the context of design for lifelong vehicle evolution are proposed.

8.1 Contribution to Aerospace Systems Design

This long journey started by observing the trend in the aerospace community for many successful aircraft designs to survive a lot longer than was expected when the design was originally created. Extended design life has made it necessary to change the design over time as the operational environment, and thus the customer requirements, changes as noted in **Observation 1**. The modern trend in aircraft development raised **Question 1**: *Can existing aerospace design methods address the issues of requirement and design evolution throughout the lifecycle of a product?* Not surprisingly, review of current acquisition policies and design methods found that the same issue has been discussed amongst the government officials in acquiring major weapon systems since the early 1980s. The culmination of such questions was formalized as acquisition policies, namely Evolutionary Acquisition (EA) and Spiral Development (SD). These became official DoD policy to develop future weapon systems in 2000. While the review on the traditional

and modern design methods identified some of the potentially useful elements, a formal method to incorporate future requirements, design, and technologies into the current system following the philosophy of EA and SD has been missing. This finding was stated in **Observation 2**, citing the need for a new design method that considers the vehicle's long-term growth.

Questions 2 and **3** asked *How can the traditional, single-stage design setting be expanded to allow integration of future designs?* and *What are the barriers and key enablers?* Case studies solicited on past aircraft modifications in the areas of military aircraft, commercial aircraft, and military rotorcraft demonstrated some common issues and vehicle-type specific issues summarized in **Observations 3** and **4**. Past successes and failures were affected by many technical and non-technical factors, such as competition, international collaboration, and politics. However, uncertainty in future requirements was identified as the key challenge when one tries to incorporate future properties into a present physical entity. The goal of the study was then solidified and bound as the development of a new design methodology, capable of quantitative evaluation of the evolution paths of a vehicle while incorporating requirement uncertainties at the vehicle systems level.

Question 4 asked *How can an aircraft designer plan for design evolution under the presence of requirement uncertainty?* The issue of uncertainty, inevitable when one makes a decision involving properties of a future timeframe, historically has been studied by other fields. A review of this topic identified two areas of research that seemed particularly relevant to the problem at hand: stochastic programming with recourse (SPR) and scenario planning. In particular, the remedial approach of SPR in its two

distinctive problem solving steps seemed intrinsically compatible to aircraft design problems. This occurred where derivatives, retrofits, and upgrades have been the "remedial" ways to fix the once optimal but later infeasible and incompetent original design stated in **Observation 5**.

As a backbone of the new design methodology, **Hypothesis 1** proposed a Two-stage Aircraft Design (TAD) formulation by expanding the traditional, single-stage design optimization setting. Then, **Hypothesis 2** indicated that the adoption of SPR to TAD would find the optimum aircraft design that would best respond to the uncertain future on average. While SPR and TAD seemed a promising solution, the intrinsic assumptions behind SPR and its limitations in numerical optimization, in general, imposed restrictions in pursuing the path of SPR as summarized in **Observation 6**. The series of questions induced from the observation asked: *What if the decision-maker is risk-avert? What if the random space is too complicated to model or it is too time-consuming to solve stochastic optimization? What if the decision-maker is willing to accept infeasible designs?*

To address the issue of non-risk-neutral decision makers, **Hypothesis 3** proposed a Risk-Averse Strategy Selection (RASS), adopting the formulation of risk-averse stochastic programming and providing a means to preemptively identify and mitigate risk associated with aircraft development. **Hypothesis 4** proposed a deterministic, scenario-based approach of capturing the full spectrum of possibilities with a few scenarios and with less computational overhead, yet providing a clear perspective of the future. Lastly, **Hypothesis 5** proposed a flexible, interactive framework for decision-

making support that allows concurrent exploration of two-stage design space free from the restrictions imposed on objective function, constraints, and design variables.

Implementation of the proposed tasks in **Hypotheses 1-6** into an actual aircraft design exercise required recasting of all the abstract elements of the mathematical formulations into tangible ones. A nine-step process of Evaluation of Lifelong Vehicle Evolution (EvoLVE) identifies and defines the current and future problems in steps 1 and 2 and synthesizes the short-term and long-term solutions and strategies in steps 3 and 4. EvoLVE also creates and validates a modeling and simulation in steps 5 and 6 that evaluates candidate solutions in terms of the imposed requirement. The last three steps, 7-9, offer a two-stage design space exploration in three different perspectives as per **Hypotheses 2-6**.

The proposed methodology was demonstrated with two engineering problems. The two-stage beam design problem was a simple proof-of-concept of compatibility and efficacy of SPR in the context of the engineering design problem proving **Hypotheses 1**, **2**, and **4**. Then, EvoLVE was implemented in its full range to a notional multi-role fighter based on the F/A-18C Hornet, selected for its unique evolution history and abundance in public data. A hypothetical requirement called for a new carrier-borne, multi-role fighter for the U.S. Navy. EvoLVE steps 1 and 2 created a set of requirements based on F/A-18C and F/A-18E performance characteristics. Evolution of the requirements was defined following the transformation of F/A-18C to F/A-18E resulting in random variables in PDFs and five scenarios. EvoLVE steps 3 and 4 defined the baseline platform, the design space, six aircraft evolution strategies, and a set of technologies.

Steps 5 and 6 created computer models and an integrated TAD environment, which were validated against F/A-18 Hornet and Super Hornet data.

Based on the TAD platform, steps 7-9 performed a series of experiments and tested hypotheses. The use of AAO reduced the convergence time from hours and minutes, proving **Hypothesis 6**, by converting the optimization problem of two hierarchical levels into a single hierarchical level. The deterministic, scenario-based study in step 7 made it possible to observe structured patterns in aircraft attributes, which solidified as inequalities. An important lesson learned was that in a system for which all the major subsystems are highly coupled, a design change in one dimension propagates throughout the entire system. Therefore, a lack of coordinated effort results in infeasibilities in other dimensions. The study showed that overdesigning landing gear systems to obtain growth potential in carrier suitability inadvertently hurt fighter performance. More importantly, preplanning for the future was beneficial in terms of total acquisition cost only if the future requirement is known from the beginning. Otherwise, not having a growth provision in the first-stage design or pursuit of the Perfect-fit Designs (*PfDs*) was the best strategy among others. The scenario-based study was repeated with RDT&E cost as the objective function. This complementary study, provided in APPENDIX D, showed how much design and long-term strategy is affected by the stakeholder's interest. The findings from the scenario-based study, summarized in **Observations 7-10** and **16**, collectively supported **Hypothesis 4**.

Exposition of the optimum designs using six strategies to explore the entire random space through Monte Carlo Simulation yielded the clouds of optimal recourse decisions. These decisions were then represented using PDFs and CDFs revealing the frequency

and severity of the strategies' performance in the randomly evolving future. This holistic approach also enabled quantifications of risk, yielding ranking functions in terms of low risk using three different measures supporting **Hypothesis 3**. The low-risk-rankings varied significantly depending on how risk was defined, suggesting that the difficulty in decision-making with multiple stakeholders had different risk perceptions and conflicting goals. Lastly, the stochastic preplanning strategy was the best among others in terms of the average total cost, proving **Hypothesis 2**.

The final step of EvoLVE created the proposed Decision Making Framework (DMF) in two different formats: two-stage contour plots and multivariate profilers. The two-stage plot built based on the F-18C proved its efficacy by reproducing the F-18C's evolution history to the F-18E. The step-by-step demonstration examined some of the background stories behind the development of the F-18E and other F-18C upgrade options considered by the U.S. Congress. The study showed that the retrofitting of the F-18C, as suggested by the U.S. Congress, was not a feasible option to meet the F-18E's requirement. However, relaxation on some of the fighter performance parameters could have lead to cost and time saving solutions, avoiding the development of the F-18E. The multivariate plot based on TAD enabled simultaneous exploration of the first and second design space in one view. The inverse design approach demonstrated with the multivariate plot showed that the combination of high thrust with large wings from the beginning ensures higher probability of responding to requirement growth with less time and cost. These two demonstrations proved **Hypothesis 5**.

Above all, the experiments performed in EvoLVE steps 7-9 were possible because of the expansion of the traditional, single-stage design process to a two-stage design process

proposed in **Hypothesis 1.** This is approved by all the derivative hypotheses proven to be true. Table 57 is the summary of how each of the observations induced research questions, tasks, observations, and lead to more observations or hypotheses. Also, the tasks are documented and the specific page numbers of the observations, research questions, and hypotheses are given in the table. Finally, Table 58 summarizes the solutions each of the hypotheses proposed in an attempt to improve the identified deficiencies and how each solution was tested. The test of Hypotheses 7 and 8 are proposed as future research.

Table 57: Mapping of Observations, Research Questions, and Hypotheses

Observation	Research Question	Tasks Performed	Where	Outcome
Obs1	Rq1	Literature review on design methods for aircraft evolution	Ch2	Obs2
Obs2	Rq2-3	Case study on past aircraft upgrade programs	Ch3	Obs3-4, Hyp1
Obs3	Rq4	Literature review on decision making under uncertainty	Ch4	Obs5, Hyp2
Obs4	Rq5	Future work	Ch8	Hyp7-8
Obs5	Rq6	Case studies/interview of engineers, military officials	Ch4	Obs6
Obs6	Rq7	Literature review on decision making under risk	Ch4	Hyp3
	Rq8	Literature review on strategic planning	Ch4	Hyp4
	Rq9	Literature review on modern design methods	Ch2	Hyp5

Table 58: Summary of Hypothesis Test

Hypothesis	Proposed Solution	Tasks Performed	Outcome	Proved?
Hypothesis 1	TAD	EvoLVE Steps 1-9	Obs7-16	yes
Hypothesis 2	SPR + TAD	EvoLVE Step 8	Obs13	yes
Hypothesis 3	RASS	EvoLVE Step 8	Obs11-12	yes
Hypothesis 4	Scenario Planning + TAD	EvoLVE Step 7	Obs7-10, 16	yes
Hypothesis 5	DMF + TAD	EvoLVE Step 9	Obs14-15	yes
Hypothesis 6	MDO + TAD	EvoLVE Step 7	-	yes
Hypothesis 7	EvoLVE in SoS Level	Future work	-	n/a
Hypothesis 8	Minefield Mapping of HQ	Future work	-	n/a

8.2 Future Research Opportunities

This thesis is not a completion to the quest for a design method for lifelong aircraft evolution. Rather, it is the beginning of the research in the sense that it has brought up more questions than answers. Also, some of the research questions were left unanswered. This section identifies several areas of possible improvements to the current study, proposes the use of EvoLVE in different perspectives, and opens up new research opportunities in the context of design for lifelong evolution.

8.2.1 Consideration of Retrofitting Existing Airframe

One of the limitations of this study was that the option of retrofitting existing airframes was not considered due to the lack of the cost model of retrofitting. Inclusion of such cases would make the study more realistic and valuable. Furthermore, consideration of combinations of both newly manufactured and retrofit aircraft, e.g. 350 retrofits and 400 new manufactures, can be studied within the EvoLVE framework and is identified as a future research opportunity.

8.2.2 Family of Aircraft Design

It is a common practice of a military aircraft or engine manufacturer to develop a new product for the U.S. government and then sell the variants to other countries after the export license is cleared. Some of the foreign orders can be firm from the beginning if such development is supported by an international alliance as in the case of the Joint Strike Fighter. It is very common in commercial aircraft development that multiple variants are planned from the beginning to maximize the market capture as the case study on the Boeing 737 series in §3.1.3 exhibited. A typical case in commercial transport is to offer variants by the use of fuselage plugs, different engines, and equipments. For example, most of the Boeing aircraft can be configured as passenger transport, cargo aircraft, an executive jet, etc.

While the current implementation of EvoLVE considered only one design solution for each stage, it can handle more than one first and/or second-stage design. For instance, the TAD optimization can be set up in a way that the first-stage design is the baseline aircraft and the second-stage problem prepares for multiple variants of the baseline. The time gap between the first and second-stage development can be set at zero if all the versions are developed in the same timeframe. The design of family of aircraft would be a trade-off between the degree of design commonality among the family members, the cost of development, and profit. These metrics from the manufacturer's viewpoint are determined by market, competition, and essentially customer satisfaction.

8.2.3 Weight and Balance Issue Affecting Stability and Control

The F/A-18E/F was designed from the beginning for growth potential. The ORD specifically required internal volume growth potential of 17 ft^3 to accommodate future

avionics. While the most critical physical constraint is the availability of the volume, provisions for the avionics upgrade must be coordinated with other systems and subsystems aspects. For example, adding more avionics creates more electrical power consumption and a need for additional cooling capacity. Growth provisions on those two subsystems must be planned from the beginning to ensure a successful avionics upgrade.

Another important matter that should not be neglected is the issue of weight and balance. The 17-ft^3 of room is most likely appropriated from the forward fuselage section. When the once empty room is filled with additional equipment, the weight increase in the forward part of aircraft will shift the center of gravity (CG) point forward. The relative location of the CG point to the neutral point (NP) of the aircraft, defined as static margin (SM), determines the vehicle's longitudinal static stability and controllability. Since fighter aircraft are designed with very tight or negative static margin to increase agility, even a slight shift in SM can lead to less than desired performance. The issue raised here was not included in this study, but it warrants further investigation to avoid unexpected project failures and delays as in the case of the T-45 introduced in §3.3. To address the issue of the mass property change due to upgrade, it is further discussed in §0 along with a proposed solution.

8.2.4 Systems-of-Systems Research to Identify the Uncertainties at Vehicle Systems Level

In the notional fighter study, the random variables were defined by the author based on the actual evolution history of the F/A-18. However, implementation of EvoLVE on a real-world problem would require a different way to come up with the random future requirements. Considering the fact that the functional requirements are from higher

hierarchical levels than the level in which design solutions are synthesized, expanding EvoLVE to the SoS level would enable a more systematic and quantitative approach to define aircraft design requirements both deterministically and probabilistically.

Figure 102 shows an example of a hierarchical structure involving a U.S. Navy fighter such as the F/A-18 Hornet. At higher levels, there are U.S. Navy Air Wings below which are Navy Combat Aircraft Fleets, consisting of fighter aircraft such as the F-14 Tomcat, F/A-18 Hornet, and A-7. Finally, the F-18 is at the vehicle systems level. The requirements for the F/A-18E/F as summarized in APPENDIX B were defined deterministically as threshold and objective values for each performance parameter. Although such behind-the-scene information is not available publicly, it is not hard to imagine that some higher level studies (for example the CBO study in 0) led to the definition of the F/A-18E/F's requirements.

The author hypothesizes that if such campaign level studies that defined E/F's requirements had been conducted in a probabilistic manner by running a Monte Carlo Simulation with respect to probabilistically defined conflict scenarios, it would have been possible to provide the KPPs in the form of PDFs. This idea is formally stated as:

Hypothesis 7: *Observing the fact that the requirements at a certain hierarchical level in engineering design come from higher level problems, Monte Carlo Simulation at a System-of-Systems level would enable quantification of the probability density functions of the random variables at the air-vehicle systems level.* (**Research Question 6**)
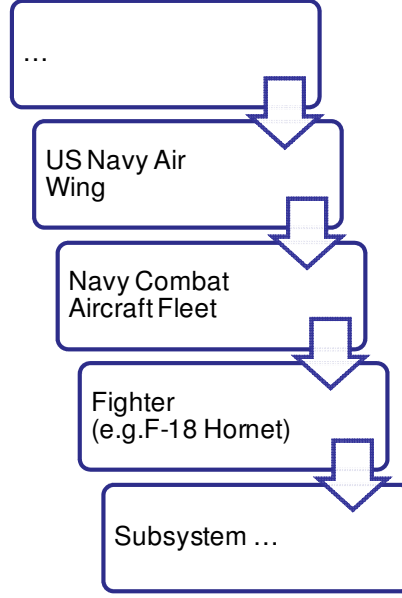
Figure 102: The Hierarchy of the Naval Fighter Design Problem

8.2.5 Risk-Averse Stochastic Programming

While systematic integration of risk associated with uncertainty, proposed by **Hypothesis 3**, had proved its usefulness, the degrees of freedom were limited to which strategy the decision makers could choose among the finite number of strategies. A more rigorous treatment of risk would require the use of the risk measure as part of an objective function.

$$
\begin{aligned}
&\min_{\mathbf{x}_1} \ f(\mathbf{x}_1) + \mathbb{E}_{\omega \in \Omega}\left[Q(\mathbf{x}_1, \boldsymbol{\omega})\right] + \lambda \cdot \mathrm{Prob}\left\{\mathbb{E}_{\omega \in \Omega}\left[Q(\mathbf{x}_1, \boldsymbol{\omega})\right] > \tau\right\} \\
&\text{s.t.} \ \ g_{1i}(\mathbf{x}_1) \leq 0 \ (i = 1,...,l_1)
\end{aligned}
\tag{84}
$$

where $Q(\mathbf{x}_1, \boldsymbol{\omega})$ is the optimal value of the second-stage problem defined as

$$
\begin{aligned}
&Q(\mathbf{x}_1, \boldsymbol{\omega}) = \min_{\mathbf{x}_2} f_2(\boldsymbol{\omega}, \mathbf{x}_1, \mathbf{x}_2) \\
&\text{s.t.} \ \ g_{2j}(\boldsymbol{\omega}, \mathbf{x}_1, \mathbf{x}_2) \leq 0 \ (j = 1,...,l_2)
\end{aligned}
\tag{85}
$$

This formulation is particularly compatible with the situation where a fixed contract stipulation is amended by monetary penalty on the occurrence of schedule slippage and

cost overrun. Once the model of such penalty is developed, the equations can be readily applied to the notional fighter example.

8.2.6 MDO Techniques for Deterministic Two-Stage Aircraft Design

The use of AAO to solve the deterministic two stage aircraft design optimization problems in §7.8.2 demonstrated the order-of-magnitude reduction in time to converge; the application of an MDO technique was only limited to AAO. A more comprehensive study is proposed to compare the performance of widely accepted MDO techniques, such as CO and BLISS. Since a comparative study of MDO techniques requires solving the same problem with various different methods at numerous optimization settings, such as convergence criteria, optimization algorithm, finite difference methods, and finite difference step sizes, this study would be ideally conducted with a simpler problem than aircraft design, such as the two-stage beam problem.

8.2.7 Design for Lifelong Vehicle Evolution Ensuring Satisfactory Handling Qualities

Finally, a completely different approach than the current EvoLVE process is proposed herein. A current design practice in the helicopter industry is that the high-level design parameters are determined during conceptual design considering high-level design metrics such as performance. Then, some of the lower level constraints, such as handling qualities, are analyzed, and control gains are fine tuned at later phases. If it turns out that Level-1 Handling Qualities (HQ) cannot be achieved within the current design setting, the design is changed at the higher level until it reaches a convergence. This traditional approach is essentially serial rather than parallel in that HQs are *fall-outs* rather than *designed-in* from the beginning of the design process. This ad-hoc or trial-

and-error type of approach might take longer than a parallel process but might be inevitable because a lack of vehicle definition, lack of disciplinary analysis, test data, etc. at an early phase of design renders HQ analysis very difficult or meaningless. This traditional approach has proved to be practical as past successful rotorcraft developments have shown.

However, modern trends in helicopter development include that the helicopters are operated longer than initially planned, and they are often reconfigured as the customer's needs evolve over time. In most instances, the vehicle is not operated at the point where it was originally designed. The evolution of rotorcraft has been that the derivatives are heavier and carrying more payloads and fuel than the original version did. This weight increase often compromised agility, HQ, safety, and survivability.

For instance, assume that the random variable under investigation is the gross weight of the vehicle including airframe, crews, payload, and fuel weight. When it is likely that the gross weight of the vehicle will increase in the future by as much as one hundred percent as shown in the case of the CH-47 in §3.1.2, it will not change aerodynamic properties of the vehicle or engine characteristics much. However, in the case of military aircraft, degraded agility and/or handling qualities due to sluggish response of the body can cause mission failure and loss of life. A research question that can be asked is: how can a design evolution path(s) be identified, with which future design changes or operational mission changes are safely implemented without compromising safety? Is there a systematic and efficient way to prevent poor HQ in derivative rotorcraft?

A solution is proposed by creating a map of design space showing the probability of design infeasibilities, for example having poor HQ. The idea is named "mine-field mapping" to indicate that the goal is not to *find* an optimum solution but to *avoid* bad designs. It would be possible to create such a mapping of the design space using an inverse design technique along with a Monte Carlo Simulation in a two-stage design setting. The use of a classification neural network can divide the design space into the regions of Level-1, Level-2, and Level-3 HQ. With the map, the designer can identify not only the original design point with Level-1 HQ, but also the potential evolution paths with high probability of Level-1 HQ.

Hypothesis 8: *Early identification and integration of the key physical constraints into the aircraft sizing and synthesis loop would reduce the possibility of technical infeasibility being identified during later stages.* (**Research Question 5**)

Sub-Hypothesis 8-1: *Expansion of the traditional single-stage design process to a time phased design process along with the inverse design technique and classification neural network technique would enable identification of the design space mapping with which the designer can find safer design evolution paths and reduce the probability of unexpected system failure.*

8.3 Concluding Remarks

While our lives are full of decisions made under growing, uncertain needs, the author would like to claim that this thesis is the first solidified, analytic effort to address the paradigm shift to design for lifelong system evolution in the aerospace systems design

domain. While the work presented here is not complete, let alone perfect, the author hopes that it will make a small stepping-stone that researchers in the future will find helpful in their quest for better design methodology or processes incorporating lifelong system evolution.

APPENDIX A

SYSTEM-OF-SYTEMS STUDY EXAMPLES

Example SoS level studies that can be potentially used in identifying aircraft system level requirements are introduced here. A U.S. Navy Air Wings level study involving the F/A-18 conducted by the Congressional Budget Office (CBO) in 1987 is introduced first. The Cost and Operational Effectiveness Analysis (COEA) required by the DoD in major DoD acquisition programs and the system specific System Threat Assessment Report (STAR) prepared by the Defense Intelligence Agency (DIA) are also examples of SoS level studies involving the friendly force structure and enemy capability projection in the future.

A.1 A CBO Study on US Naval Combat Aircraft

In 1987, the Congressional Budget Office (CBO) [80] conducted a study at the U.S. Navy Air Wings level, encompassing the U.S. Navy fighter aircraft fleet including the F/A-18. The goal of the study was to formulate and evaluate the modernization strategies of the U.S. Navy combat aircraft into the 1990s in terms of aircraft types and mission roles they would perform, production quantity, and the time frame they would be needed. The study started by projecting enemy threat into the future and simulating conflict scenarios. Figure 103 is the mission radii of various Soviet Union bombers and fighters launched from Kola Peninsula, covering most of Europe including the United Kingdom. The geographical region was the main theater they considered to identify the needed capability of the U.S. Naval combat aircraft fleet beyond the 1990s.

After the evolution of the threat was evaluated, the means to counter the increasing threat was sought. The alternatives were sought by projecting the friendly force structure at the Navy Air Wing fleet level. Table 59 from [80] lists the spectrum of missions performed by naval aircraft in the late 1980s. For example, the feet air defense and strike warfare missions were conducted by the F-14, F/A-4, F/A-18A/B/C/D, A-6, and AV-8. The CBO study examined the retirement/procurement schedule and the performance of the existing fleet, and then offered the options to fill the projected deficiency. For details on the alternatives and comparisons, refer to [80].
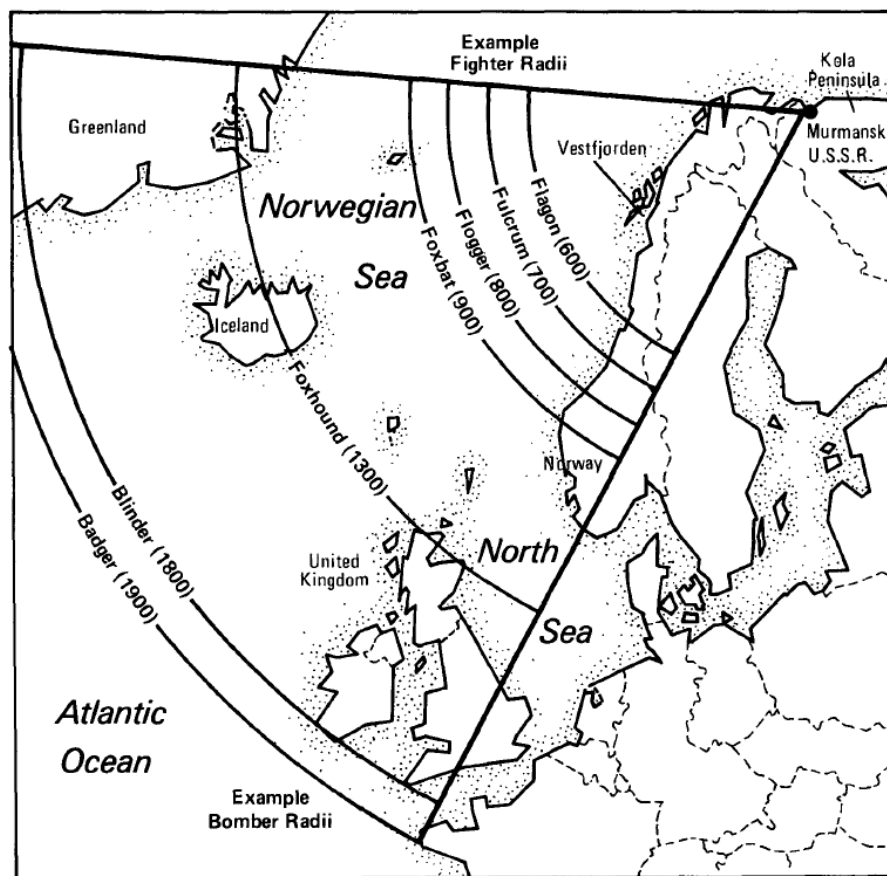
Figure 103: Mission Radii of Unrefueled Soviet Union Bombers and Fighters [80]

Table 59: Naval Aircraft and Their Primary Missions [80]

Fleet Air Defense	Strike Warfare	Anti-submarine Warfare	Electronic Warfare	Amphibious Assault
F-14	F/A-18	P-3	E-2	CH-46
F-4	A-6	S-3	EA-6	CH-53
F/A-18	AV-8	SH-2	ES-3	V-22
	F-4	SH-3		AH-1
	A-4	SH-60B/F		

A.2 Cost and Operational Effectiveness Analysis (COEA)

DoD's system acquisition process requires a cost and operational effectiveness analysis (COEA) to be conducted for the Milestone I review as a means to determine whether a new acquisition program is warranted [14, 213]. The goal of COEA is to compare performance, cost, and schedule of alternatives under various operational and threat scenarios. Scenarios are generated to reflect the wide spectrum of possible operations. Alternatives are candidate systems and mixes of candidate systems that can fulfill the anticipated missions. The candidate systems include both the new system under consideration and the existing systems. The threat is developed by the entity conducting COEA and approved by the Defense Intelligence Agency (DIA). In particular, a system specific System Threat Assessment Report (STAR), produced during Phase 0, can be used as the basis for the threat in the COEA. Drivers of performance, cost, and schedule are identified as Measure of Effectiveness (MoE). Then, parametric variations of the threats are studied to see the impact on the effectiveness. The COEA that was prepared for the acquisition of the U.S. Marine Co.'s Medium Lift Replacement (MLR) concept is provided as an example case in Table 60.

A STAR was created by the Naval Maritime Intelligence Center (NAVMIC) for the F/A-18E/F program*. However, the formal COEA was waived since it entered the EMD (Phase II) directly. Although a formal COEA was waived, the Navy conducted extensive analysis to compare cost and benefit alternatives as provided in [83]. The study evaluated combinations of F-14 variants and F/A-18E/F to compare performance, cost, and program schedule. The MoEs for the F/A-18E/F COEA were [83]:

- Survivability (measured by RCS)/Vulnerability (vulnerable area)
- Unit cost
- Strike mission radius
- Carrier suitability (recovery and launch wind-over-deck)
- Fighter performance (such as turn rate, climb rate, and excess power)
- Weapons system features
- Armament flexibility

---

*F/A-18E/F STAR, NAVMIC TA#037-92 is not available publicly.

Table 60: COEA Study for the USMC Medium Lift Replacement Program [214]

Scenarios	For Amphibious Assault • Ship ranges of 50, 75, and 100 nm • Operation Size of Marine Expeditionary Force (MEF) and Marin Expeditionary Brigade (MEB) For Marine Expeditionary Unit (MEU) Missions • Ship ranges of 25, 200, and 400 nm.
Threat	Use MLR STAR and following documents • Strike/Surface/Air Warfare Intelligence Compendium, NAVMIC Compendium #2-92 • F/A-18E/F STAR, NAVMIC TA#037-92 • Advanced Interdiction Weapon System STAR, NAVMIC TA#031-92
Alternatives (Mix of CH-53E and)	• Upgrade of existing helicopters • Major modifications of existing helicopters • New helicopter developments • V-22 • V-22 and helicopter alternatives
Measures of Effectiveness	For MEB/MEF Vertical Assault Elements: • Combat power delivered over time • Correlation of forces/means (COF/M) For MEU Operations: • Time in/time out with objective met
Cost Analysis	RDT&E, procurement, military construction, and operation and support assuming a 20-year lifecycle

APPENDIX B

F/A-18 DESIGN REQUIREMENT

Military combat aircraft design requirements are prepared in terms of both mission performance and point performance requirements [215]. The point performance requirement decides the aerodynamic characteristics and the two important design parameters, thrust to weight ratio (T/W) and wing loading (W/S). The mission performance requirement sizes the air vehicle by matching fuel required and available. The mission requirement determines how much fuel an air vehicle needs to carry.

The F/A-18 Hornet, conceived as a multi-role strike fighter to replace both the F-4 and the A-7, was designed and sized by two different mission profiles. Those "primary" or "design missions" are fighter escort mission as a fighter aircraft and carrier-based interdiction mission using the hi-lo-lo-hi profile as an attack aircraft. These two missions dictated the design of the F/A-18 and its fuel requirement. Lenox [77] stated about the design missions of the F/A-18A/B in 1976 as follows:

> The basic design of the airplane comes out of an operational requirement, which, in its call for an airplane to replace the F-4 and the A-7, identified a fighter escort mission and an interdiction mission—with certain store requirements, certain range requirements, certain fuel reserve requirements, etc. So, it's those two missions which determined the basic airplane design and internal fuel requirements.

For the interdiction and fighter escort missions, the following external store conditions were specified:

<u>F/A-18A/B/C/D</u> [183]

Attack configuration: two AIM-9s, FLIR, LTD, four MK-83 bombs, and three 330-gallon fuel tanks

Fighter configuration: two AIM-9s and two AIM-7s

<u>F/A-18E/F</u> [175]

Attack configuration: two AIM-9s, FLIR, NAVFLIR, four MK-83 bombs, and three 480-gallon fuel tanks

Fighter configuration: two AIM-9s and two AIM-120s

The F/A-18 A, C, and E versions' mission performance data were collected from various sources and summarized in Table 61[*]. The sources include a paper by Lenox in 1976 [77], a paper by Young in 1998 [76], a CRS report in 2007 [74], the DoD data found in the appendix of a GAO report in 1996 [191], another GAO report in 2000 [208], the Navy Fact File [216], and the annual Jane's All the World Aircraft published from 1981 to 1993. The table shows mission radius, external store conditions, and reserve condition for four different missions: the hi-lo-lo-hi interdiction, the hi-hi-hi interdiction, the fighter escort, the ferry, and the combat ferry missions. Data for the F/A-18A was most difficult to obtain, while C and E data were relatively abundant.

---

[*]all mission radius in nautical miles, range for the ferry missions

Note 1.	(2) AIM-9, FLIR, Laser Spot Tracker Pod, (4) MK-83
Note 1-1.	includes but may not be limited to (2) AIM-9, (4) MK-83
Note 1-3.	includes but may not be limited to FLIR and Laser Tracker
Note 2.	(2) AIM-9, FLIR, NAVFLIR, (4) MK-83LDGP
Note 3.	(2) AIM-9, (2) AIM-7
Note 4.	(2) AIM-9, (2) AIM-120

Table 61: Published F-18 Mission and Range

Mission Type	Version	Radius	Fuel Tanks	Stores	Source and Year	Reserve Type	Reserve Condition	Other
Interdiction	A	550/575	(3) 330 gallon	Note 1	Lenox 1976/Janes 80-87	not listed	not listed	Includes sea-level dash
(Hi-Lo-Lo-Hi)	C	290	(2) 330 gallon	not listed	Janes 1992-93	not listed	not listed	
	C	304	(2) 330 gallon	Note 2	DoD 1996	Carrier-based fixed fuel	not listed	Standard profile
	C	325	(2) 330 gallon	Note 1-1	Young 1998	Carrier-based fixed fuel	not listed	
	C	369	(3) 330 gallon	Note 2	DoD 1996	Carrier-based fixed fuel	not listed	Standard profile
	C	415	(3) 330 gallon	not listed	CRS 2007	not listed	not listed	
	E	468	(2) 480 gallon	Note 2	DoD 1996	Land-based	1900~2200 lb of fuel	Standard profile
	E	524	(3) 480 gallon	Note 2	DoD 1996	Land-based	1900~2200 lb of fuel	Standard profile
	E	490	(3) 480 gallon	not listed	CRS 2007	not listed	not listed	
	E	444	(2) 480 gallon	not listed	GAO 2000	not listed	not listed	
	E	496	(3) 480 gallon	not listed	GAO 2000	not listed	not listed	
Interdiction	C	395	(2) 330 gallon	Note 2	DoD 1996	Carrier-based fixed fuel	not listed	Standard profile
(Hi-Hi-Hi)	C	470	(3) 330 gallon	Note 2	DoD 1996	Carrier-based fixed fuel	not listed	Standard profile
	E	597	(2) 480 gallon	Note 2	DoD 1996	Land-based	1900~2200 lb of fuel	Standard profile
	E	666	(3) 480 gallon	Note 2	DoD 1996	Land-based	1900~2200 lb of fuel	Standard profile
Attack	A	575	not listed	Note 1-3	Janes 1980-87	not listed	not listed	
Fighter Escort	A	400+	None	Note 3	Lenox 1976	Land-based	20 min+5% of initial fuel	2500 lb of combat fuel
	C	366	None	not listed	CRS 2007	not listed	not listed	
	E	420	None	not listed	CRS 2007	not listed	not listed	
	E	462	None	not listed	GAO 2000	not listed	not listed	Standard profile
Ferry	A	1800+	not listed	not listed	Janes 1992-3	not listed	not listed	
	A	2000+	not listed	not listed	Janes 1980-91	not listed	not listed	
	C	1546	(3) 330 gallon	(2) AIM-9	Navy 2008	not listed	not listed	
	E	1660	(3) 480 gallon	(2) AIM-9	Navy 2008	not listed	not listed	
Combat Ferry	C	1089	None	(2) AIM-9	Navy 2008	not listed	not listed	
	E	1275	None	(2) AIM-9	Navy 2008	not listed	not listed	

See the previous page for Note 1, Note 1-1, Note 1-2, Note 2, Note 3, and Note 4

As shown in Table 61, mission radii for the same version of the F/A-18 flying the same mission varies noticeably from source to source. The F/A-18 C's mission radii for the hi-lo-lo-hi interdiction with two 330-gallon external tanks are reported as 290, 304, and 325 nm from three different sources. With three 330-gallon tanks, the discrepancy is even larger, ranging from 415 to 468 nm. Jane's All the World Aircraft has been publishing F/A-18 performance data every year since 1980, and F/A-18 A ferry range has been listed as "2,000+ nm" from 1980 to 1991 and reduced to "1,800+ nm" after 1992. The book also listed the attack radius of the F/A-18 A to be 575 nm from its 1980 to 1987 issues, except for the 1981 issue at 550 nm.

Possible sources of discrepancies include the difference in aircraft empty weight within the version, published data being based on estimation rather than flight test, and different reserve conditions being used. Aircraft empty weight varies (usually increases) production lot after lot, and it is not certain which mission radius is based on a vehicle from which lot. For a vehicle in development phases, its performance data is based on estimation and optimistic performance estimation is very common. Some of the F/A-18A's and the F/A-18E's performance data published while the concepts were still in development seems to be based on estimation. This issue is discussed in more detailed in §7.6.6.2.

The most critical source of the mission radius variations from data source to data source seems to be attributed to the inconsistent use of reserve types and conditions. While it is standard to have reserve fuel for 20 minute loiter at sea level, plus 5% of initial fuel for a land-based aircraft, a carrier-based aircraft is typically required a more stringent reserve mission profile in order to ensure adequate fuel to an alternate airport

during mid-ocean operations. According to MIL-STD-3031 [172], a reserve profile for a carrier-based aircraft should choose from following three types:

1. Any number of visual flight rules (VFR) and/or instrument flight rules (IFR) passes in the landing configuration (flaps and gears down; speed break at final turn and approach)
2. 100 nm BINGO fuel (the minimum fuel required to divert to an alternate landing site using an emergency flight profile)
3. A specified quantity of fuel (typically 3000 to 4000 lb)

Most published mission performance did not specify what the reserve type was, but the inconsistent use of reserve type in the DoD's documents was identified. The DoD compared F/A-18 C's and E's mission performance to illustrate the performance deficiency of the C version and to justify the Super Hornet program. Such comparison, appearing in Appendix III of the 1996 GAO report [191] and provided in Figure 104, shows that the F/A-18E's promises 42 to 54 percent mission radius increase over the C version. The DoD stated the that standardized mission profiles were used for the comparison "in order to get an apples to apples valid comparison with other platforms." However, it seems that the DoD used the less stringent land-based reserve type for the F/A-18E's performance estimation, while they used the carrier-based reserve type for the F/A-18C's performance. The land-based reserve only requires about 1,900 to 2,200 lb of fuel, while the carrier-based reserve requires about 3,500 to 5,000 lb of fuel. The GAO report [191] caught this discrepancy, stating that

> According to NAVAIR data, in the E/F Early Operation Assessment, the E/F's first pass fuel level for determining combat range varies from approximately 1,900 pounds to about 2,200 pounds, depending on the mission profile. If the higher 5,000-pound reserve fuel DoD stated is needed for carrier recovery payload were used for range calculations, the range would be lower than reported.

Hi-Lo-Lo-Hi Interdiction Mission

(2)AIM-9 SIDEWINDERS, FLIR/NAVFLIR, (4)MK-83LDGP (1000 LB. Bombs)

	SPEC	CDR[Note 1]	% OVER C/D
F/A-18E	390		
2(480 TANKS)		468	54%
3(480 TANKS)		524	42%
F/A-18C (LOT XIX)	ACTUAL		
2(330 TANKS)	304		
3(330 TANKS)	369		

Hi-Hi-Hi Interdiction Mission

(2)AIM-9 SIDEWINDERS, FLIR/NAVFLIR, (4)MK-83LDGP (1000 LB. Bombs)

F/A-18E		CDR[Note 1]	% OVER C/D
2(480 TANKS)		597	51%
3(480 TANKS)		666	42%
F/A-18C (LOT XIX)	ACTUAL		
2(330 TANKS)	395		
3(330 TANKS)	470		

Note: (1) Status based on design and simulation at Critical Design Review. Models used to predict range were verified via flight test during EOA Jan - Feb 1996.

Figure 104: F/A-18C and E Mission Range Comparison by the DoD [191]

What is more interesting is that the DoD used the stringent carrier-based reserve fuel weight in order to justify the improvement of the F/A-18 Hornet's bring back capability. The DoD stated in the GAO report that "Air Wings consistently set operating procedures for first pass fuel at 4,000 lbs. day/5,000 lbs. night during early work ups. As the experience base increases, first pass fuel is brought down to 3,500 lbs. day/4,500 lbs. night."

On March 22, 2000, the honorable Colye [217], Director of Operational Test and Evaluation, testified before the Senate Armed Services Committee about the issue:

> ... the ORD-defined specification missions using a 2000-lb. reserve fuel... Associated with these KPP range requirements, as established by the ORD, are specific flight profiles. These are the Fighter Escort Mission and Interdiction Mission flight profiles established by the F/A-18E/F Specification. These profiles are well defined in the system specification and are documented in the F/A-18E/F

TEMP. All computations of ORD profile ranges were conducted to include the 100 nautical mile divert leg to arrive overhead at the divert location with 2000 lbs. of fuel. In contrast, the CNO/operational missions did not have a reserve fuel specified, and as such the threshold values were interpreted relative to current F/A-18C/D practices. For these missions, the peacetime training reserve fuel of 4000 lbs. was used.

The difference in reserve fuel amount directly affected mission radius. Considering the fact that specific range of the F/A-18 in attack configuration is about 0.1 nautical miles per pound of fuel at best cruise altitude and Mach number [183], the aircraft gains roughly 50 nm in mission radius if the reserve fuel requirement is reduced by 1,000 lb.

The key performance parameters (KPPs) are the most critical performance measures of a given system. The KPPs are often defined as objective and failure to meet the threshold value can cause the program to be terminated [153]. The list of KPPs of the F/A-18E/F Super Hornet was obtained along with the threshold, objective, and demonstrated values. All the values related to F/A-18E/F are either from a GAO report in 2000 [208] or from a DoD report in 1999 [153]. In addition, the F/A-18 C's performance data were collected from [74, 175, 183, 191, 201, 218]. The actual performance values of both F/A-18C and E are provided in Table 62. The F/A-18 C's performance is for the LOT XIX production model with the F404-GE-402 engines, except for the combat ceiling. The combat ceiling data was from the F/A-18A/B/C/D NATOPS Flight Manual with the F404-GE-400 engines [183].

Table 62: F/A-18C and E Performance Requirements

| Constraint \ Data Type | F/A-18E | | | F/A-18C | |
	Objective	Threshold	Actual	Actual	Units
Fighter escort radius*	>425	>410	462	366	nm
Interdiction mission radius†	>450	>430	496	369	nm
Combat ceiling	>50,000	>50,000	52,300	53,141	ft
Recovery payload	>9000	>9000	9,125	5,623	lb
Launch wind over deck	< 25	< 30	28	not listed	knots
Recovery wind over deck	<10	< 15	8	not listed	knots
Approach speed	<140	< 150	142	141	knots
Specific excess power‡ at 0.9/10,000 ft	> 650	> 600	648	699	ft/sec
Acceleration from 0.8M to 1.2M at 35,000 ft	< 60	< 70	65	55.8	sec
Turn rate at 15,000 ft	not listed	not listed	11.6	12.3	deg/sec

*One way unrefueled range using internal fuel and no external fuel tanks

†One way unrefueled range using external fuel tanks (3-480 gallon for E and 3-330 gallon for A and C)

‡1 g level flight in fighter configuration, maximum thrust, 60% total fuel remaining; 2 AIM-9 and 2 AIM-120 for E and 2 AIM-9 and 2 AIM-7 for C; 33,325 lbs of combat weight for C

APPENDIX C

F/A-18 COST DATA

APPENDIX C.1 provides some military cost definitions and some useful data sources for military cost analysis in general. To construct and validate the cost model of the F/A-18, numerous public domain sources were consulted. The F/A-18 specific cost data are collected and reviewed in APPENDIX C.2. Validation of the cost model was conducted by modeling the four aircraft configurations proposed in the Hornet 2000 study that is introduced in APPENDIX C.3. Finally, APPENDIX C.4 reviews the F/A-18A/B/C/D and E/F test and evaluation programs.

C.1 Military Cost Definitions and Data Sources

US Code, Title-10, Chapter 44 on major defense acquisition programs [219] presents cost definitions with respect to a major defense acquisition program:

> Program acquisition (unit) cost: the total cost for development and procurement of, and system-specific military construction for, the acquisition program, (divided by the number of fully-configured end items to be produced for the acquisition program.)
>
> Procurement (unit) cost: the total of all funds programmed to be available for obligation for procurement for the program, (divided by the number of fully-configured end items to be procured.)
>
> Full life-cycle cost: all costs of development, procurement, military construction, and operations and support, without regard to funding source or management control.

Congressional Budget Office (CBO) [220] defines O&S costs as

The total of the operation and maintenance accounts, the military personnel accounts, and the portion of the family housing accounts aimed at short-term maintenance of DoD family housing.

Operation and maintenance includes: fuel, spare parts, supplies to run and maintain the equipments, transportation, logistics, training, education, recruiting, medical, administration, salaries for civilian personnel, etc. Operation and maintenance cost and military personnel cost account for 99 percent of the total O&S cost [220].

The Selected Acquisition Reports (SARs) are quarterly status reports from the Department of Defense to the Congress on major defense acquisition programs in accordance with Title 10, US Code 2432 [219]. SARs present "each system program manager's current best estimate of key performance, schedule, and cost goals from the total program [221]." SARs are focused on program total acquisition cost and do not provide data for O&S.

SAR summary tables from 1969 to the present are available through the DoD's Acquisition Resources and Analysis website, and it provides the total program acquisition cost and production quantity for the F/A-18. An issue with using the SAR summary table for this study is that it does not differentiate A/B and C/D programs, because the C/D program was a minor upgrade that was done through several engineering modification proposals. Also, SAR summary tables only provides the total program cost and do not break it down to RDT&E, procurement, and military construction.

RDT&E Descriptive Summary (RDDS) is the budget report on the DoD's RDT&E programs. The report is issued annually and is a very good source of studying the RDT&E cost of aircraft upgrade programs. For example, the F/A-18C/D radar upgrade

program RDT&E cost and F/A-18C/D aircraft upgrade RDT&E cost were reported in FY 1998 RDT&E, N Budget Item Justification Sheet. The F/A-18A/B/C/D improvement programs were conducted until 2005, well after the production of the last F/A-18C/D [222].

A good source of O&S cost data is the Navy Visibility and Management of Operating and Support Costs (VAMOSC) that has been established since the mid-1970s. The VAMOSC is an on-line based information management system that "collects and reports U.S. Navy and U.S. Marine Corps historical weapon system operating and support (O&S) costs. VAMOSC provides the direct O&S costs of weapon systems, some linked indirect costs (e.g., ship depot overhead), and related non-cost information, such as flying hour metrics, steaming hours, age of aircraft, etc [223, 224]." The database is accessed via www.navyvamosc.com.

The Department of the Navy reports its budget estimates annually or biennially to the Congress. These unclassified documents provide detailed RDT&E and procurement cost estimates to justify the Navy's budget request for the following fiscal year. These reports are particularly useful in studying aircraft modification cost at the sub-systems level. Procurement of upgrades to existing aircraft are done in installation kits. For example, 219 F/A-18A/B and 464 C/D were retrofitted with GPS using installation kits between 1994 and 2000 [224].

C.2 Collection of the F/A-18 Cost Data

This section introduces the F/A-18 cost data that were collected from various public domain sources. While collecting cost data, a wide range of literature was consulted from as early as 1975 to 2006, encompassing the lifecycle cost of all F/A-18 variants.

In 1975, F/A-18A/B's unit flyaway and unit acquisition costs were projected to be 5.9 and 9.97 million dollars according to [225], based on production of 800 units. In 1982,

CBO [221] studied modernization strategies for the U.S. Navy Air Wings and compared the cost for various Navy aircraft. The report listed the procurement, operation and support, and lifecycle cost estimations of the Navy aircraft of interest including the F/A-18, A-7E, A-6E, F-14, E-2C, S-3A, and others. The estimation of F/A-18's average unit procurement cost was 20 million assuming the production of 1,366 units, and 17.2 million for the last 665 aircraft, in 1983 dollars. The CBO report is also a good source for operation and support cost modeling, since it listed the number of officers and enlisted required for each aircraft type, the number of aircraft required for one squadron, and the number of squadrons for one carrier air wings, and so forth. For example, Table 63 summarizes the operation costs of various U.S. Navy aircraft for one carrier air wing per year in 1983 dollars. The readers are referred to [221] for assumptions and details.

Table 63: Operation Costs for One Carrier Air Wing per Year

Aircraft	# of A/C per Air Wing	Personnel	Operation and Maintenance	Total
F/A-18	24	4	40	44
F-14	24	6	51	57
E-2C	4	4	8	12
EA-6B	4	4	12	16
S-3A	10	6	21	27
SH-60	6	4	19	23

The F/A-18 Hornet program was included in SAR from 1976 until December 1994. The final F/A-18 Hornet program cost when the program was ended in 1994 was 36,783.4 billion in 1994 dollars [226]. The program cost includes the RDT&E and procurement of 1,026 aircraft in total [226]. The F/A-18A/B and C/D programs were not reported separately in the Navy's and DoD's budget reports. While the RDT&E cost of the F/A-18A/B was not separately available from the SARs, a Rand report [227]
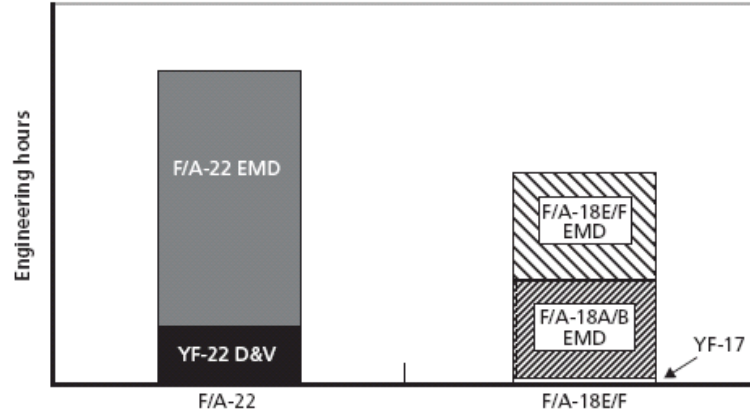
Figure 105: Comparison of F/A-22 and F/A-18 EMD Engineering Hours [227]

qualitatively compared the total RDT&E engineering hours of the F/A-18A/B and the

E/F programs as shown in Figure 105.

On June 30, 1992, the House of Armed Services Committee held a hearing to handle

the Defense Acquisition Board review of the F/A-18E/F program [83]. The hearing

discussed various U.S. Navy fleet options after the mid-1990s, including 40 F-14D carrier

air wings (CVWs); 20 F-14D and 20 F/A-18E/F CVWs; 40 F/A-18E/F CVWs; 20 F/A-

18C/D; and 20 STC-21 CVWs. The comparison included lifecycle cost of pursuing each

option. Table 64 shows the cost of acquiring and operating the F/A-18E/F, F/A-18C/D,

and F-14D in 1990 million dollars, assuming 20 years of service life. The F/A-18C/D

E&MD cost of 500 million dollars was the only number the author could come across

that separately reports the F/A-18C/D program development cost and used in cost

modeling process.

Table 64: Cost Comparison of F/A-18C/D, E/F and F-14D

	E/F	F-14D	C/D
Aircraft quantity	962	1,084	481
E&MD	4,880	330	500
Total procurement	43,480	47,150	16,550
Operations and support	23,540	31,840	11,340
Total	71,900	79,320	28,390
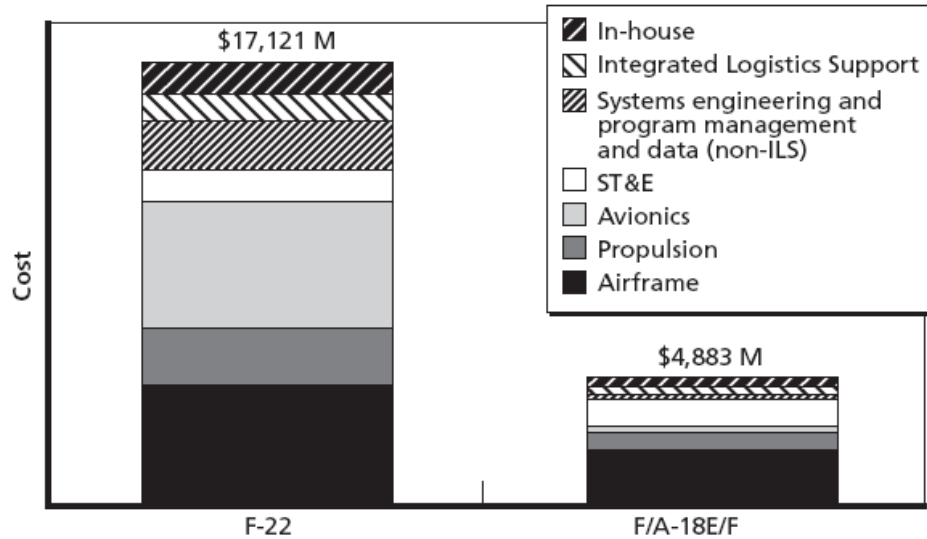
Figure 106: F/A-22 and F/A-18E/F EMD Program Cost Drivers [4]

The 4,880 million dollars spent on the F/A-18E/F EMD program is broken down into cost spent on airframe, propulsion, avionics, system test and evaluation (ST&E), and others as shown in Figure 106 along with the F-22 EMD cost. It is important to note that the portion of EMD cost spent on the F/A-18E/F's avionics is not only absolutely but also relatively small compared to the avionics cost of the F-22. The cost saving is attributed to the fact that the F/A-18E/F used 90 percent of the C/D's avionics in the beginning, followed by P^{3}I upgrades.

A Master's Thesis by Duma [228] from the Naval Postgraduate School developed a model that estimates aviation depot level repair (AVDLR) cost based on the F/A-18. In addition, a MBA professional report [229] also from the Naval Postgraduate School includes operation cost comparison of the F/A-18A/B and the F-5 E/F based on the VAMOSC data. The study broke down the operation cost into fuel, maintenance, and AVDLR costs per flight hour. These reports did not cover entire O&S cost but focused on major subsets of O&S cost elements.

In 1996, GAO [191] investigated the E/F program for the U.S. Congress and published a reliable cost breakdown of the F/A-18E/F program as provided in Table 65. It also listed the average recurring flyaway cost of 36 C/D's built in 1994 as $26.175 in 1994 million dollars. The data set in the table was used as the main source for the F/A-18E/F cost model calibration.

Table 65: F/A-18E/F Unit Cost Estimation in 1996 million dollars

	E/F
RDT&E	5.783
Recurring Flyaway	43.6
Total Flyaway	48.7
Initial Spares and Support	8.61
Procurement	57.31
Total Program	63.093
Number of Aircraft Assumed	1,000

The F/A-18E/F program has been included in SAR since December 1991. Table 66 summarizes important changes to the program classification, program cost estimation, and the production quantify found in the SARs from 1992 to 2007. The Super Hornet program was classified as a PE program from December 1991 to March 1992, then as a DE program as the EMD phase started from June 1992 to December 1997, and then as PDE after the conclusion of the EMD phase. Total production of 1,000 E/F was initially planned but reduced to 548 in December 1997. The total number of aircraft changes several times afterwards, and as of December 2007 the total planned production is 493 aircraft.

Table 66: F/A-18E/F Program Cost and Production Quantity Projections

	Dec-91	Jun-92	Dec-97	Sep-00	Dec-01	Dec-03	Dec-07
	PE	PE/DE	DE	DE/PDE	PDE	PDE	PDE
RDTE (BY1992)	1,738.6						
RDTE (TY)	5,109.9						
Program (BY1990)		53,959.6	34,292.9	43,489.6			
Program (TY)		94,583.0	46,064.1	46,825.7			
Program (BY2000)					45,289.7	41,665.3	43,257.6
Program (TY)					48,791.1	43,845.2	46,344.8
Aircraft Quantity		1,000	548	548	548	462	493

*in million Base-Year(BY) or Then-Year(TY)

C.3 The Hornet 2000 Study

In 1987, McDonnell Douglas studied the options to upgrade the F/A-18A/B under a contract to the US DoD [171]. Figure 107 from [76] shows the seven different configurations investigated as the upgrades options. By taking the 1988 version of Hornet as the baseline, a series of upgrades, such as improved avionics, new cockpits, more internal fuel volume, and higher thrust engines were considered. Table 67 lists the changes planned for each of the configurations. Configuration I was essentially the F/A-18C/D and Configuration IIIC became the basis for the F/A-18E/F. All other configurations were discarded.

The Hornet 2000 study compared both recurring and nonrecurring cost for the seven options. While the original document was not available to the author, the non-dimensionalized numbers were published by Young [76]. By combining some of the cost data found in §C.2 and the non-dimensional cost from Hornet 2000 study, dimensional cost for F/A-18 upgrade was constructed. These cost data set were used in calibrating the RDT&E and production cost model of the notional multi-role fighter in §7.7.
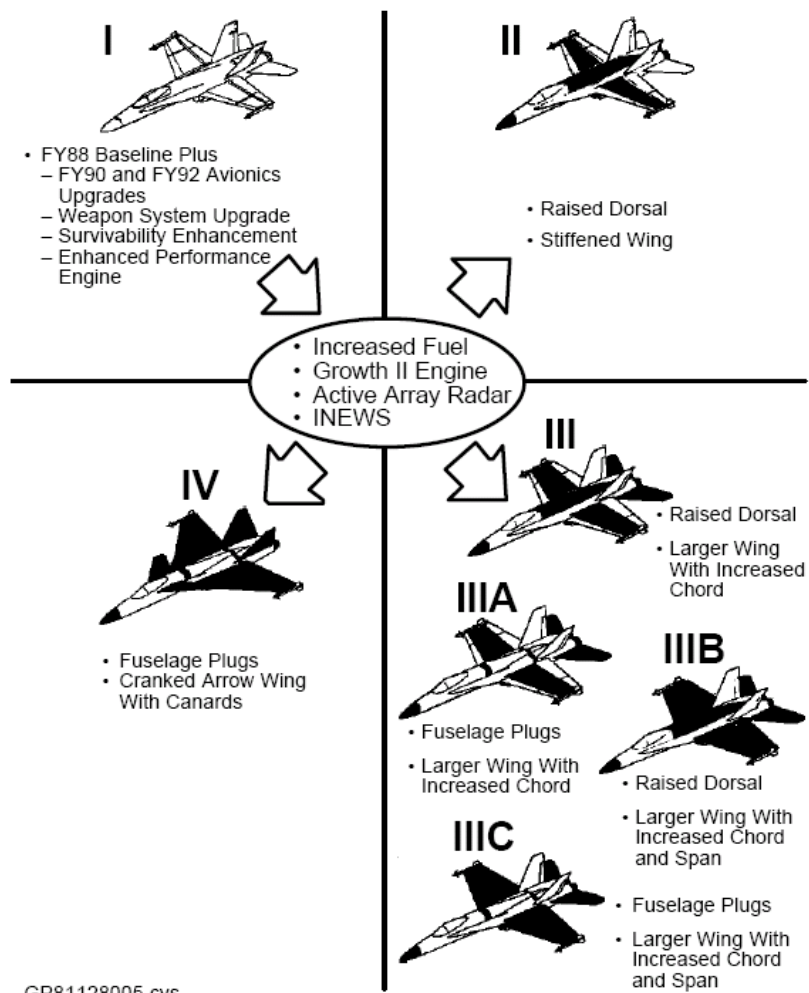
Figure 107: F/A-18 Upgrade Options from Hornet 2000 Study [76]

Table 67: F/A-18 Upgrade Cost from Hornet 2000 Study [76, 171]

Configuration	I	II	III	IIIA	IIIB	IIIC	IV
Major upgrades	FY88 plus, - Avionics upgrades - Weapon system upgrades - F404-GE-402 engines	I plus, - Increase fuel capacity - F414-GE-400 engines - Active array radar[*] - INEWS					
Configuration changes	Retrofit of new equipments and engines without modification to airframe	Raised dorsal Stiffened wing	Raised dorsal 25% Larger wing (increased chord) Larger tails	2'3.5" Fuselage plugs 25% Larger wing (increased chord) Larger tails	Raised dorsal 25% Larger wing (increased chord and span) Larger tails	2'3.5" Fuselage plug 25% Larger wing (increased chord and span) Larger tails	Fuselage plugs Cranked arrow wing with canards New V tails
Additional Internal Fuel	zero	2700 lb	3700 lb	2700 lb	3700 lb	2700 lb	3197 lb
$Recurring	1.14	1.3	1.37	1.36	1.4	1.39	1.46
$Non-Recurring	1	2.22	2.88	2.77	2.89	2.78	3.44

C.4   Overview of the F/A-18A/B and E/F Test Programs

For military acquisition programs, conformation to the specified requirements defined by the ORD is supported through a series of test and evaluation programs that are prepared in accordance with DoD Instruction 5000.2 [230]. Figure 108 from DoDI 5000.2 shows military acquisition process and testing activities at each milestone and phase. Before milestones B and C, a test and evaluation master plan (TEMP) is prepared by the program manager and approved by the Director of Testing and Evaluation (DOT&E).

---

[*]F/A-18C/D and E/F Radar upgrade to active array radar was done as one of the F/A-18 radar P^{3}I programs starting in 1999 [224]. Budget for RDT&E and procurement costs for these radars were prepared separately from the F/A-18C/D and E/F programs. Thus, the F/A-18 cost model in this study also excluded cost related to the radar upgrade.
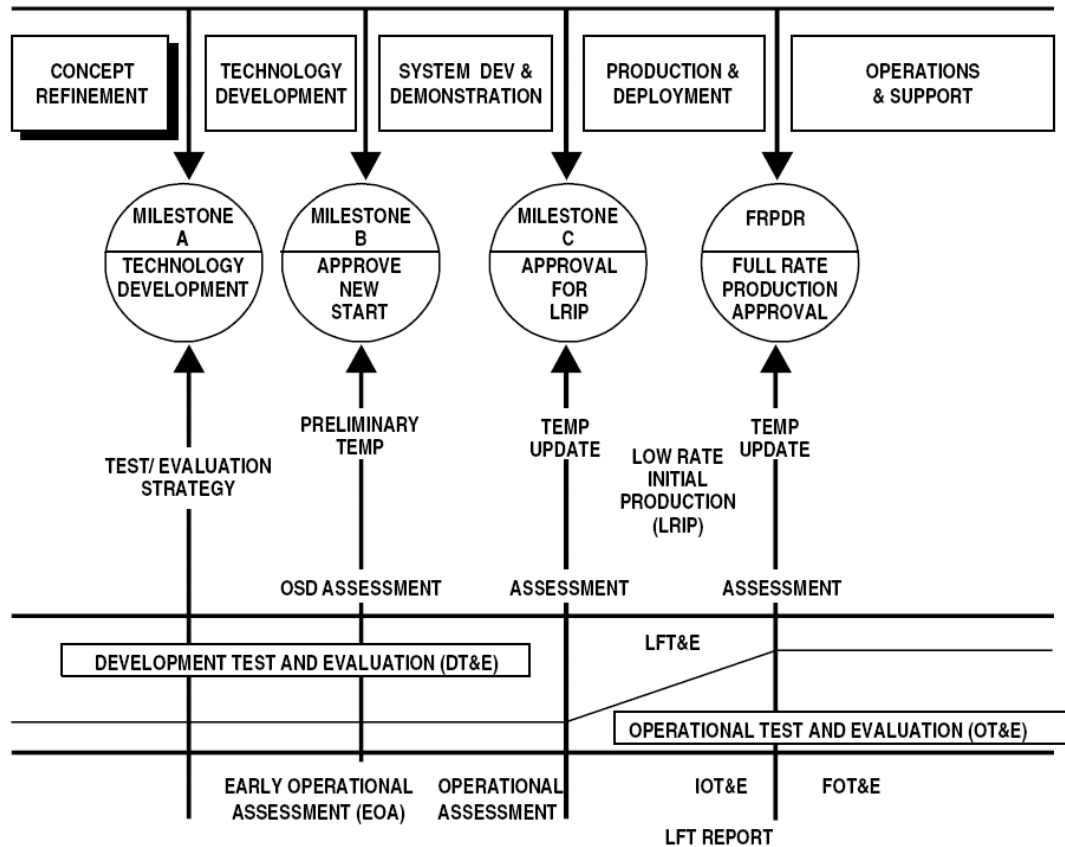
Figure 108: Testing and the Defense Acquisition Process in DODI 5000.2

The testing and evaluation process for a major acquisition program can be divided into developmental testing and evaluation (DT&E) and operational testing and evaluation (OT&E). DT&E is usually conducted by the contractors to prove that the system functions as intended and is usually completed before the approval of low rate initial production (LRIP) at Milestone C. Military Handbook 881 [231] provides work breakdown structure (WBS) for T&E programs. A typical fighter DT&E program includes but not limited to: M&S, wind-tunnel tests, static article and test, fatigue article and test, drop article and test, subsystem ground tests, avionics integration tests, armament and weapon delivery integration tests, flight tests, etc. DT&E is typically conducted using the prototype or EMD vehicle. OT&E, also called operational evaluation (OPEVAL) by the US Navy, is performed by the user of the product using

Test a/c No.	Model Build No.	Test Title	77 Q4	1978				1979				1980				1981				1982			
				1	2	3	4	1	2	3	4	1	2	3	4	1	2	3	4	1	2	3	4
	T-39	Radar test bed	HAC radar development					MCAIR radar/avionics development																
1	F1	Flying qualities, flutter																						
2	F2	Propulsion, performance																						
3	F3	Carrier suitability, ECS													BIS				BIS				
4	F4	Structural																						
5	F5	Avionics												BIS										
6	F6	High AOA												BIS										
7	TF1	Armament, systems																						
8	F7	Armament, avionics															BIS							
9	F8	Performance, systems											BIS											
10	TF2	Engine Acceleratied Service Test (AST)													Navy								
11	F9	MEI, EMC											BIS			BIS								

Legend:
- NPE
- NPA (T-39D)
- F/A-18 Test
- IOT&E
- OPEVAL

Figure 109: F/A-18A/B Flight Test Program Schedule[*] [71]

the some of the LRIP vehicles and takes much less time than DT&E. Successful evaluation will give the approval for the full-rate production (FRP).

In the case of the F/A-18A/B program, eleven test aircraft were used for its flight test program, while the C/D program used two test vehicles and the E/F program used 7 flight test articles and 3 ground test articles [71, 209]. The F/A-18A/B full-scale development flight test program tasks and schedule is shown in Figure 109. The figure shows what tests each of the test vehicles performed and how long it was scheduled to take. The radar test was conducted with a T-39.

In 1997, the Applied Physics Laboratory at Johns Hopkins published the list of the F/A-18E/F flight test categories and number of required flights based on the F/A-18E/F

[*]ECS: Environmental Control System
MEI: Maintenance Engineering Inspection
EMC: Electromagnetic Compatibility
NPE: Navy Preliminary Evaluation
NPA Navy Preliminary Assessment
IOT&E: Initial Operational Test and Evaluation
BIS: Board of Inspection and Survey

TEMP as shown in Table 68 [232]. The TEMP for the F/A-18E/F flight test program was prepared by an integrated Navy/contractor test team based on the F/A-18A/B flight test experience and the F/A-18E/F flight test requirements. According to the TEMP, 1,839 test flights in 13 categories were required to fulfill the demonstration and test objectives for the F/A-18E/F aircraft.

Table 68: F/A-18E/F Flight Test Program Projection [232]

Flight test category	No. of required flights
Flying qualities	265
Performance	125
Propulsion	130
High angle of attack	250
Flutter	255
Empennage buffet	25
Noise/vibration	30
Flight loads	195
Dynamic store release	40
Carrier suitability/ground loads	173
Mission systems	74
Weapons separation	267
New technology	10

The required number of sorties for the E/F program was more than doubled over time from the number of sorties originally planned in the TEMP. A Rand study performed in 2004 on test and evaluation cost of military aircraft [13] provides a good summary of the F/A-18E/F flight test program. The study summarized the flight test program conducted from November 1995 to April 1999. According to the study, from the first flight in November 1995 to April 1999, "eight aircraft made 3,141 flights, logging 4,620 flying hours, for a total of 244 aircraft months." Then, the OPEVAL program followed from May to November 1999 using seven aircraft and consisting of over 1,200

flight hours in 850 plus sorties [233]. Total flight test hours reached almost 6,000 hours. The actual F/A-18E/F flight test program from the first flight to the end of OPEVAL is summarized by Fox [13] and duplicated in Table 69.

Table 69: Actual F/A-18E/F Flight Test Program Summary

	Test aircraft (no.)	Sorties (no.)	Flight hours
Avionics			600
Flying qualities, flutter			1,890
Propulsion, performance			195
Aircraft systems			275
Armament			310
Structures			1,126
Carrier suitability			189
Other			35
Total EMD/FSD flight test	8	3,141	4,620
OPEVAL	7	850	1,200
Total flight test	8	3,991	5,820

F/A-18A/B and E/F test program statistics are summarized in Table 70. Most data are from Fox [13]. In the case of the F/A-18A/B and E/F test programs, 305 and 244 aircraft months were flown by 11 and 8 aircraft, respectively. Each test aircraft flew 16.1 and 18.9 hours per month on average. Also, each of the test aircraft was used for 27.7 and 30.5 months on average. Test duration measured from the first flight to the end of DT, was 40 months for the F/A-18A/B program and 40 months for the F/A-18E/F program, excluding the OPEVAL periods.

NASA Langley Research Center [96] summarized the F/A-18E/F wind tunnel test programs as follows:

> The vehicle's performance at subsonic and transonic speeds was validated in a series of wind tunnel tests at NASA Ames (11-Foot Transonic Tunnel, 1991-94). During approximately 3,000 hours of tunnel occupancy, data were obtained on four

different scale models to determine performance and stability and control characteristics. The tests included aerodynamic measurements to evaluate a series of aircraft design options, such as engine inlet studies. Stability and control characteristics at high-angle-of-attack flight conditions were evaluated in numerous wind tunnel tests at Langley (approx. 1,500 occupancy hrs in 30- by 60-Foot Full Scale Tunnel, 1993-4).

Fox [13] describes the ground test program of the F/A-18E/F as follows:

"… three ground test articles—static, drop, and fatigue—were built, and seven flight test vehicles were built and flight tested in EMD… During DT-IIA (November 1995 to November 1996), the static test article was used for initial wing-bending tests; the drop-test article was used for a series of landing-gear tests at increasing sink rates …"

Fatigue testing was completed in July 1998 before flight testing was completed in April 1999.

Table 70: F/A-18A/B and E/F Flight Test Programs

	F/A-18A/B	F/A-18E/F	Units
Total aircraft month	305	244	month
Total flight hours	4,922	4,620	hrs
Number of vehicles	11	8	ea
Average flight hours per aircraft month	16.1	18.9	hrs/month
aircraft month per vehicle	27.7	30.5	month/aircraft
DT duration	40	41	month

APPENDIX D

OPTIMIZATION WITH RDT&E COST AS OBJECTIVE

This complementary study is a repetition of **Step 7** of the EvoLVE process with the objective function as RDT&E cost instead of acquisition cost. A large portion of acquisition cost is production cost, which acts as a deterrent or penalty of overdesigning in the first stage. Therefore, the study with RDT&E cost as objective function examines an extreme case in which the cost of changing the design dominates the game. The study was conducted deterministically only. The optimization results are provides in Tables from 71 to 76. The bar graphs are also provided from Figures 110 to 118 for comparison.

General equalities and inequalities are also observed that are fundamentally different from those found in §7.8. In terms of the cost, the graphs show similar trends that were found with the optimization results conduced with the acquisition cost as the objective function. The major difference is that the second-stage cost is significantly saved by pursuing the DetPP strategies. In addition, the difference between New-design and Ad-hoc is also amplified. From the perspective of designs, a clear difference from the results with acquisition cost is that all DetPPs overdesigned $\mathbf{x}_1$ to meet the predicted requirement $\boldsymbol{\omega}_u$ and retained it in all cases in which the second-stage requirement was less rigorous than the predicted one.

$$\text{if } \hat{\boldsymbol{\omega}}_s \leq \boldsymbol{\omega}_u, \text{ then } (\hat{\mathbf{x}}_2^*)_s^p = (\mathbf{x}_1^*)_s^p \tag{86}$$

Observation 16: *The TAD optimization with RDT&E cost as an objective function showed that if the realized scenario is less demanding than the predicted scenario, the first-stage design is retained in the second stage.*

Table 71: First-Stage TAD Optimization Results

	Strategies	New Design	Ad-hoc	DetPP (Block10)	DetPP (Avg.)	DetPP (Block10p)	Unit
x_{11}	Wing area	396.6	396.6	449.4	464.0	498.5	ft^2
x_{12}	Thrust	18355	18355	20441	20855	21947	lb
x_{13}	Ref. weight for DLF	34131	34131	38251	39170	41816	lb
x_{14}	Landing weight	33248	33248	39539	40830	43839	lb
x_{15}	Internal fuel	10827	10827	12777	13190	14692	lb
x_{16}	External fuel	6724	6724	6691	7920	9608	lb
x_{17}	Ref. thrust for aft-body	18355	18355	23508	23982	25238	lb
x_{18}	Fuselage length	53.08	53.08	54.68	54.79	55.60	ft
g_{11}	Fighter escort radius	350.1	350.1	409.6	423.5	478.8	nm
g_{12}	Interdiction mission radius	410.9	410.9	431.4	461.4	505.8	nm
g_{13}	Recovery payload	4508	4508	7910	8547	9846	lb
g_{14}	Launch wind over deck	22.06	22.06	22.29	24.47	28.14	knots
g_{15}	Recovery wind over deck	-0.01	-0.01	3.55	4.80	9.27	knots
g_{16}	Approach speed	138.1	138.1	141.5	141.5	141.4	knots
g_{17}	Specific excess power	708.7	708.7	699.2	696.2	685.9	ft/sec
g_{18}	Accel. from 0.8 to 1.2M	63.66	63.66	63.60	63.54	63.42	sec
g_{19}	Turn rate	12.042	12.042	12.066	12.112	12.093	deg/sec
g_{110}	Usable load factor	7.609	7.609	7.609	7.610	7.609	g
R	OEW	25738	25738	28628	29282	30992	lb
E	Attack TOGW	50520	50520	55325	57699	62697	lb
S	Fighter TOGW	37975	37975	42815	43882	47095	lb
U	RDTE	4639	4639	4904	4963	5116	$m
L	RDTE year	8.58	8.58	8.82	8.87	9.01	year
T	Production	20172	20172	21595	21897	22701	$m
S	f_1	24811	24811	26499	26859	27817	$m

Table 72: Second-Stage Optimization Results under the New-Design Strategy

	Stage	1	2					
	Requirement/Scenarios	Block 0	S1	S2	S3	S4	S5	Unit
x_{21}	Wing area	396.8	426.6	453.1	465.0	502.6	529.9	ft^2
x_{22}	Thrust	18366	19703	20558	20910	22068	22927	lb
x_{23}	Ref. weight for DLF	34138	36359	38563	39401	42194	43865.6	lb
x_{24}	Landing weight	33246	37532	39877	40916	44046	45360.5	lb
x_{25}	Internal fuel	10827	11495	12854	13189	14729	15447.1	lb
x_{26}	External fuel	6707	7091	6664	7991	9851	10288	lb
x_{27}	Ref. thrust for aft-body	18366	22658	23642	24046	25378	26366	lb
x_{28}	Fuselage length	53.08	53.82	54.81	55.00	55.80	56.08	ft
g_{21}	Fighter escort radius	350.0	350.5	410.4	420.0	475.5	493.7	nm
g_{22}	Interdiction mission radius	410.3	410.1	430.1	460.1	504.5	509.9	nm
g_{23}	Recovery payload	4501	7000	8001	8403	9701	9800	lb
g_{24}	Launch wind over deck	22.00	22.35	22.23	24.89	28.65	28.65	knots
g_{25}	Recovery wind over deck	-0.05	3.53	3.56	4.93	9.32	9.56	knots
g_{26}	Approach speed	138.1	141.5	141.5	141.5	141.2	139.5	knots
g_{27}	Specific excess power	709.1	709.3	697.7	694.0	683.4	682.9	ft/sec
g_{28}	Acceleration from 0.8M to 1.2M	63.60	63.60	63.60	63.60	63.54	62.88	sec
g_{29}	Turn rate	12.046	12.123	12.061	12.068	12.069	12.175	deg/sec
g_{210}	Usable load factor	7.609	7.609	7.612	7.609	7.609	7.609	g
	OEW	25743	27531	28874	29513	31344	32560	lb
R	Attack TOGW	50507	53373	55619	58004	63341	65735	lb
E	Fighter TOGW	37980	40436	43139	44112	47483	49417	lb
S	RDTE	4640	6491	6636	6703	6892	7022	$m
U	RDTE year	8.59	9.35	9.49	9.55	9.73	9.85	year
L	Production	20175	27605	29249	29967	32213	33850	$m
T	f_1/f_2	4640	6491	6636	6703	6892	7022	$m
S	Total cost	-	11439	11585	11651	11841	11970	$m

Table 73: Second-Stage Optimization Results under the Ad-hoc Strategy

	Stage	1	2					
	Requirement/Scenarios	Block 0	S1	S2	S3	S4	S5	Unit
x_{21}	Wing area	396.8	426.6	453.0	465.0	502.6	532.4	ft^2
x_{22}	Thrust	18366	19698	20551	20920	22068	23011	lb
x_{23}	Ref. weight for DLF	34138	36363	38533	39416	42194	44033	lb
x_{24}	Landing weight	33246	37534	39865	40921	44046	45467	lb
x_{25}	Internal fuel	10827	11506	12846	13193	14729	15544	lb
x_{26}	External fuel	6707	7084	6669	7997	9851	10249	lb
x_{27}	Ref. thrust for aft-body	18366	22653	23634	24058	25378	26463	lb
x_{28}	Fuselage length	53.08	53.83	54.80	55.00	55.80	56.13	ft
g_{21}	Fighter escort radius	350.0	351.2	410.1	420.0	475.5	496.9	nm
g_{22}	Interdiction mission radius	410.3	410.3	430.1	460.2	504.5	510.7	nm
g_{23}	Recovery payload	4501	7001	8000	8400	9701	9802	lb
g_{24}	Launch wind over deck	22.00	22.37	22.22	24.91	28.65	28.56	knots
g_{25}	Recovery wind over deck	-0.05	3.54	3.55	4.94	9.32	9.55	knots
g_{26}	Approach speed	138.1	141.5	141.5	141.5	141.2	139.4	knots
g_{27}	Specific excess power	709.1	708.9	697.7	694.3	683.4	682.9	ft/sec
g_{28}	Acceleration from 0.8M to 1.2M	63.60	63.60	63.60	63.54	63.54	62.82	sec
g_{29}	Turn rate	12.046	12.119	12.063	12.069	12.069	12.181	deg/sec
g_{210}	Usable load factor	7.609	7.608	7.609	7.610	7.609	7.609	g
	OEW	25743	27532	28864	29520	31344	32664	lb
R	Attack TOGW	50507	53376	55607	58021	63342	65896	lb
E	Fighter TOGW	37980	40448	43120	44123	47484	49618	lb
S	RDTE	4640	2832	3716	4018	4640	5137	$m
U	RDTE year	8.59	4.87	6.35	6.75	7.35	7.83	year
L	Production	20175	27109	28739	29499	31866	33743	$m
T	f_1/ f_2	4640	2832	3716	4018	4640	5137	$m
S	Total cost	-	7472	8355	8658	9280	9777	$m

Table 74: Second-Stage Optimization Results under the DetPP(Block10) Strategy

	Stage	1	2					
	Requirement/Scenarios	Block 0	S1	S2	S3	S4	S5	Unit
x_{21}	Wing area	453.7	453.7	453.7	465.0	502.6	529.9	ft^2
x_{22}	Thrust	20564	20564	20564	20917	22068	22927	lb
x_{23}	Ref. weight for DLF	38576	38576	38576	39413	42194	43866	lb
x_{24}	Landing weight	39887	39887	39887	40920	44046	45361	lb
x_{25}	Internal fuel	12853	12853	12853	13193	14729	15447	lb
x_{26}	External fuel	6672	6672	6672	7990	9851	10288	lb
x_{27}	Ref. thrust for aft-body	23649	23649	23649	24055	25378	26366	lb
x_{28}	Fuselage length	54.66	54.69	54.79	55.00	55.80	56.09	ft
g_{21}	Fighter escort radius	411.4	411.2	410.2	420.1	475.5	493.7	nm
g_{22}	Interdiction mission radius	431.0	430.8	430.1	460.1	504.5	509.9	nm
g_{23}	Recovery payload	8082	8067	8000	8401	9701	9800	lb
g_{24}	Launch wind over deck	22.00	22.03	22.17	24.89	28.65	28.65	knots
g_{25}	Recovery wind over deck	3.48	3.48	3.48	4.93	9.32	9.56	knots
g_{26}	Approach speed	141.4	141.4	141.4	141.5	141.2	139.5	knots
g_{27}	Specific excess power	699.2	698.9	697.6	694.2	683.4	682.9	ft/sec
g_{28}	Acceleration from 0.8M to 1.2M	63.54	63.54	63.66	63.60	63.54	62.88	sec
g_{29}	Turn rate	12.096	12.091	12.069	12.068	12.069	12.175	deg/sec
g_{210}	Usable load factor	7.629	7.626	7.612	7.610	7.609	7.609	g
	OEW	28804	28819	28886	29518	31344	32560	lb
R	Attack TOGW	55557	55572	55639	58012	63341	65735	lb
E	Fighter TOGW	43067	43082	43149	44121	47483	49417	lb
S	RDTE	4920	650	1291	2910	3560	3985	$m
U	RDTE year	8.83	0.83	2.21	5.63	6.33	6.71	year
L	Production	21683	28988	28813	29127	31461	33170	$m
T	f_1/ f_2	4920	650	1291	2910	3560	3985	$m
S	Total cost	-	5570	6211	7830	8480	8905	$m

Table 75: Second-Stage Optimization Results the DetPP(Average) Strategy

	Stage	1	2					
	Requirement/Scenarios	Block 0	S1	S2	S3	S4	S5	Unit
x_{21}	Wing area	465.0	465.0	465.0	465.0	500.7	530.3	ft^2
x_{22}	Thrust	20920	20920	20920	20920	22029	22940	lb
x_{23}	Ref. weight for DLF	39416	39416	39416	39416	42127	43889	lb
x_{24}	Landing weight	40921	40921	40921	40921	43990	45376	lb
x_{25}	Internal fuel	13193	13193	13193	13193	14710	15461	lb
x_{26}	External fuel	7997	7997	7997	7997	9748	10289	lb
x_{27}	Ref. thrust for aft-body	24058	24058	24058	24058	25333	26381	lb
x_{28}	Fuselage length	54.77	54.79	54.90	55.22	55.83	56.09	ft
g_{21}	Fighter escort radius	422.2	422.0	421.0	418.1	475.2	494.1	nm
g_{22}	Interdiction mission radius	461.8	461.7	460.9	458.7	504.0	510.1	nm
g_{23}	Recovery payload	8550	8535	8468	8265	9702	9800	lb
g_{24}	Launch wind over deck	24.62	24.65	24.78	25.17	28.62	28.65	knots
g_{25}	Recovery wind over deck	4.94	4.94	4.94	4.94	9.42	9.56	knots
g_{26}	Approach speed	141.5	141.5	141.5	141.5	141.4	139.5	knots
g_{27}	Specific excess power	697.1	696.8	695.5	691.7	683.4	682.9	ft/sec
g_{28}	Acceleration from 0.8M to 1.2M	63.36	63.42	63.48	63.72	63.54	62.88	sec
g_{29}	Turn rate	12.117	12.112	12.090	12.026	12.053	12.176	deg/sec
g_{210}	Usable load factor	7.640	7.637	7.623	7.584	7.609	7.609	g
	OEW	29370	29385	29452	29655	31287	32575	lb
R	Attack TOGW	57871	57886	57953	58156	63157	65765	lb
E	Fighter TOGW	43973	43988	44055	44258	47407	49446	lb
S	RDTE	4971	654	1300	1399	3390	3835	$m
U	RDTE year	8.88	0.84	2.22	2.30	6.17	6.58	year
L	Production	21941	29609	29427	29669	31321	33134	$m
T	f_1/ f_2	4971	654	1300	1399	3390	3835	$m
S	Total cost	-	5625	6271	6370	8361	8806	$m

Table 76: Second-Stage Optimization Results under the DetPP(Block10p) Strategy

|	Stage	**1**		**2**				
	Requirement/Scenarios	Block 0	S1	S2	S3	S4	S5	Unit
x_{21}	Wing area	502.6	502.6	502.6	502.6	502.6	530.7	ft^2
x_{22}	Thrust	22070	22070	22070	22070	22070	22961	lb
x_{23}	Ref. weight for DLF	42191	42191	42191	42191	42191	43919	lb
x_{24}	Landing weight	44102	44102	44102	44102	44102	45397	lb
x_{25}	Internal fuel	14732	14732	14732	14732	14732	15474	lb
x_{26}	External fuel	9850	9850	9850	9850	9850	10290	lb
x_{27}	Ref. thrust for aft-body	25381	25381	25381	25381	25381	26405	lb
x_{28}	Fuselage length	55.54	55.56	55.67	55.78	55.80	56.09	ft
g_{21}	Fighter escort radius	478.0	477.8	476.8	475.8	475.5	494.4	nm
g_{22}	Interdiction mission radius	506.3	506.2	505.5	504.7	504.5	510.1	nm
g_{23}	Recovery payload	9919	9904	9836	9768	9753	9801	lb
g_{24}	Launch wind over deck	28.36	28.39	28.51	28.63	28.66	28.64	knots
g_{25}	Recovery wind over deck	9.50	9.50	9.50	9.50	9.50	9.56	knots
g_{26}	Approach speed	141.3	141.3	141.3	141.3	141.3	139.5	knots
g_{27}	Specific excess power	686.2	685.9	684.8	683.6	683.3	683.1	ft/sec
g_{28}	Acceleration from 0.8M to 1.2M	63.36	63.36	63.42	63.54	63.54	62.82	sec
g_{29}	Turn rate	12.118	12.113	12.093	12.073	12.068	12.180	deg/sec
g_{210}	Usable load factor	7.637	7.635	7.622	7.610	7.607	7.609	g
	OEW	31183	31197	31265	31333	31348	32595	lb
R	Attack TOGW	63182	63197	63264	63332	63347	65799	lb
E	Fighter TOGW	47325	47339	47407	47475	47490	49479	lb
S	RDTE	5133	667	1329	1363	1370	3266	$m
U	RDTE year	9.02	0.85	2.25	2.28	2.28	5.95	year
L	Production	22792	31814	31611	31692	31710	32992	$m
T	f_1/ f_2	5133	667	1329	1363	1370	3266	$m
S	Total cost	-	5799	6462	6496	6503	8399	$m
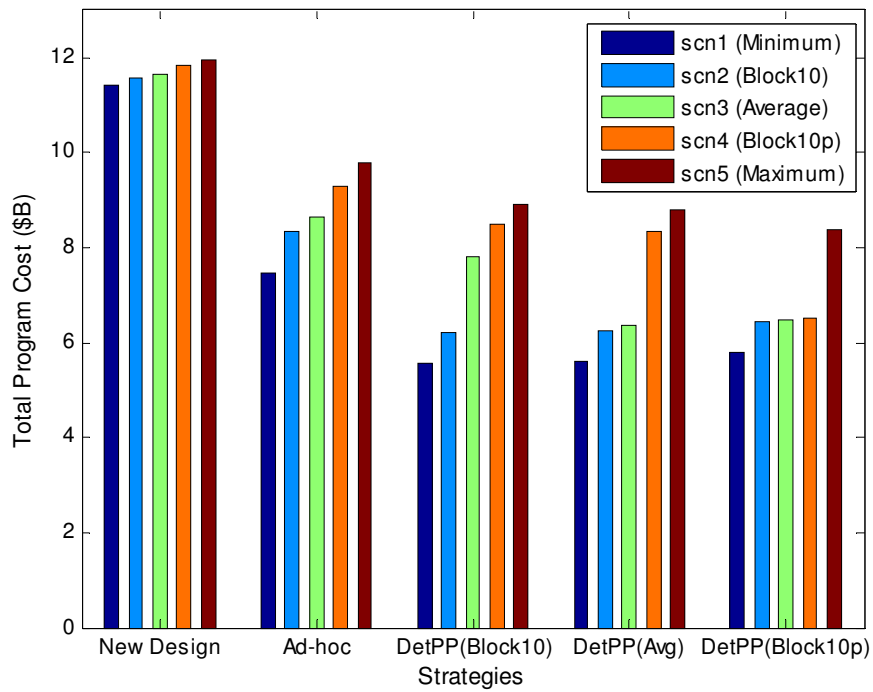
Figure 110: Total Program Cost Comparison w.r.t. Strategies
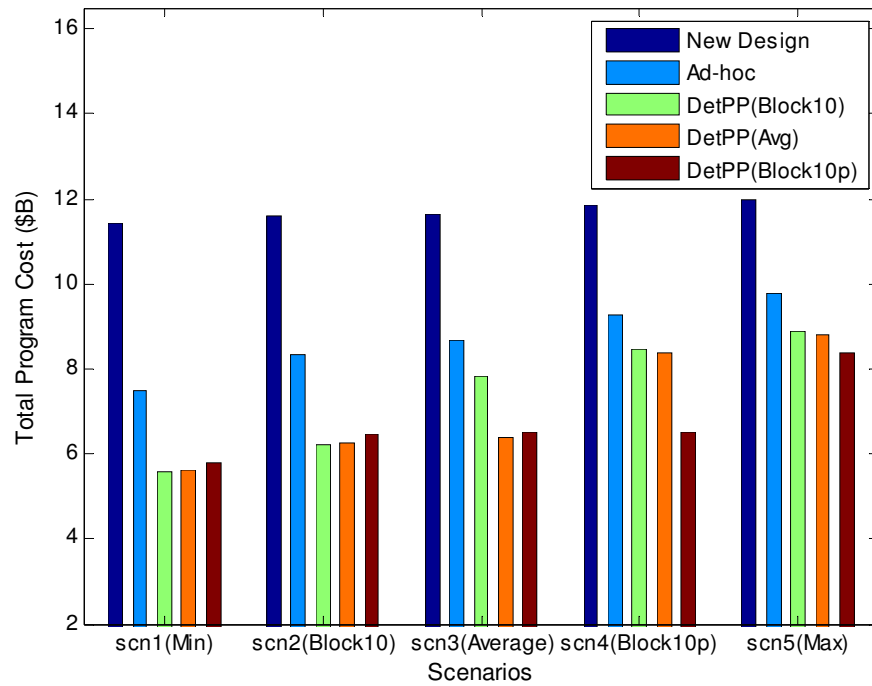

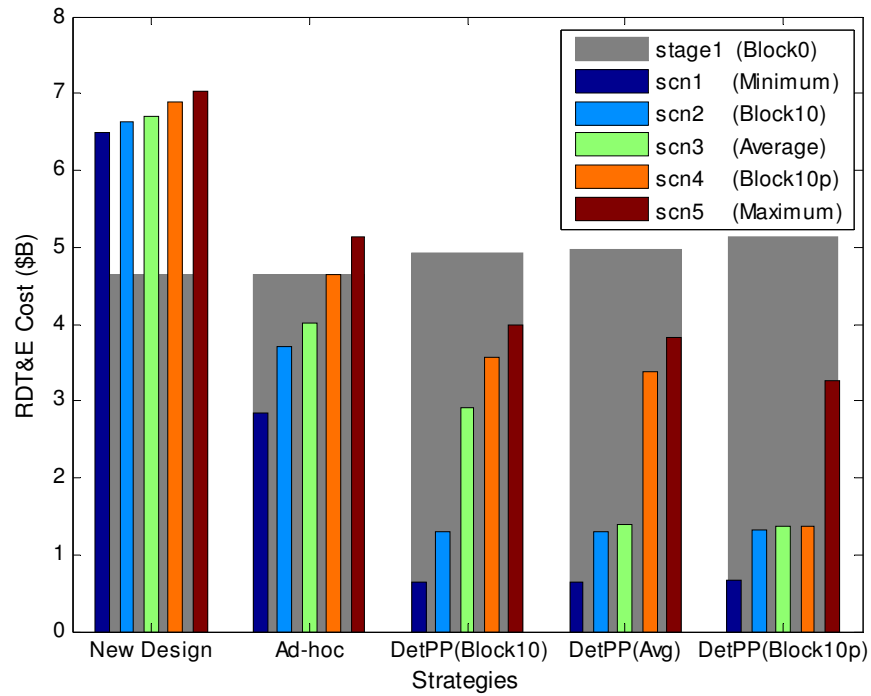Figure 111: Total Program Cost Comparison w.r.t. Scenarios
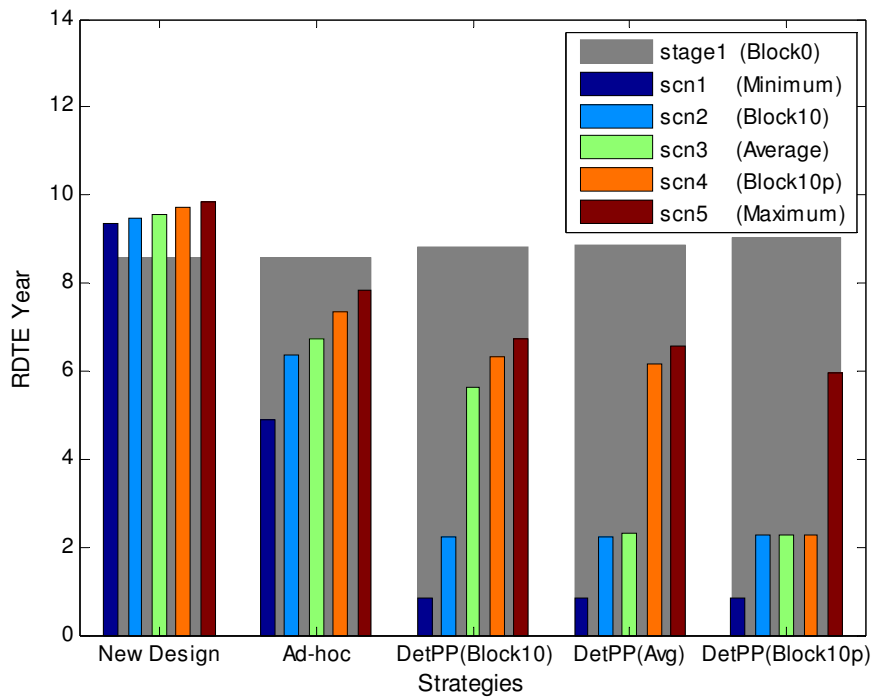
Figure 112: RDT&E Cost Comparison
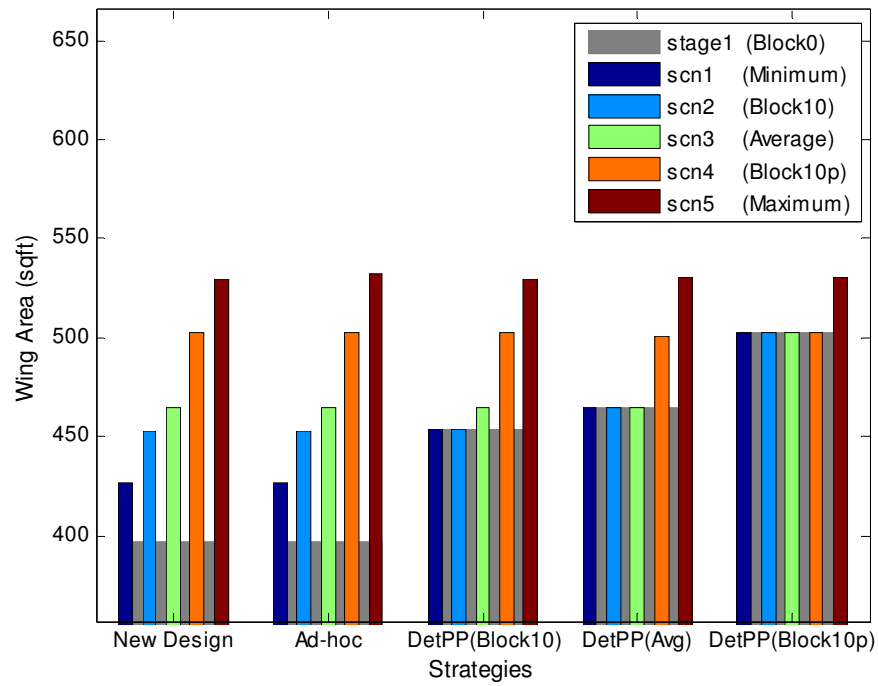

Figure 113: RDT&E Year Comparison
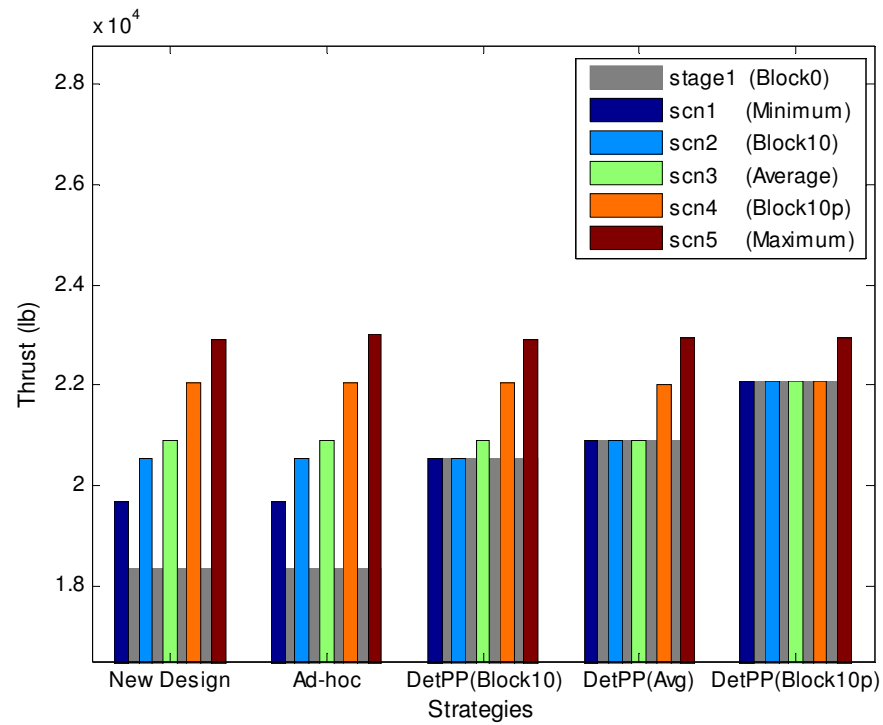
Figure 114: Wing Area Comparison

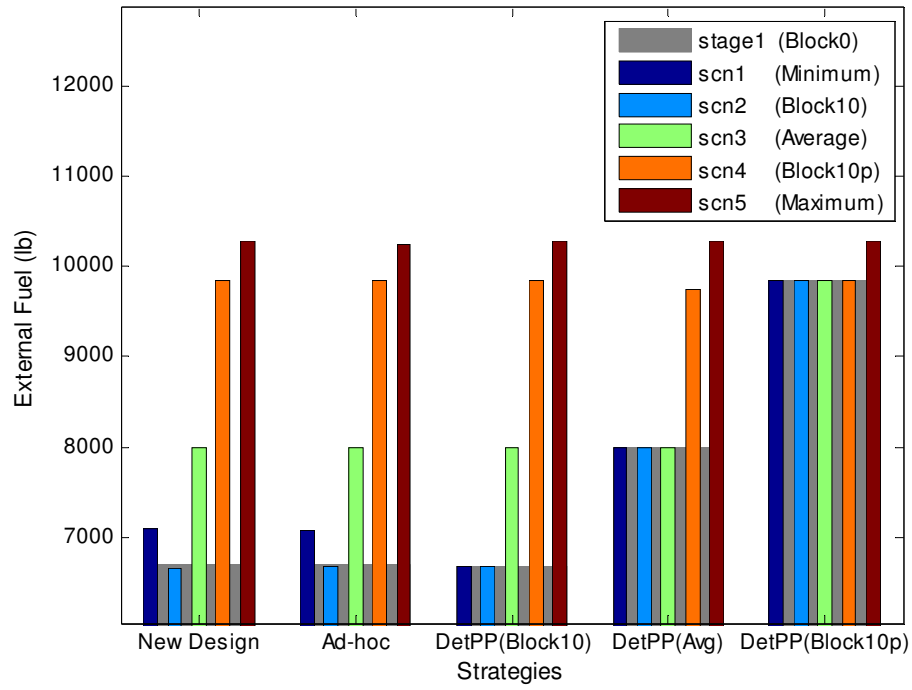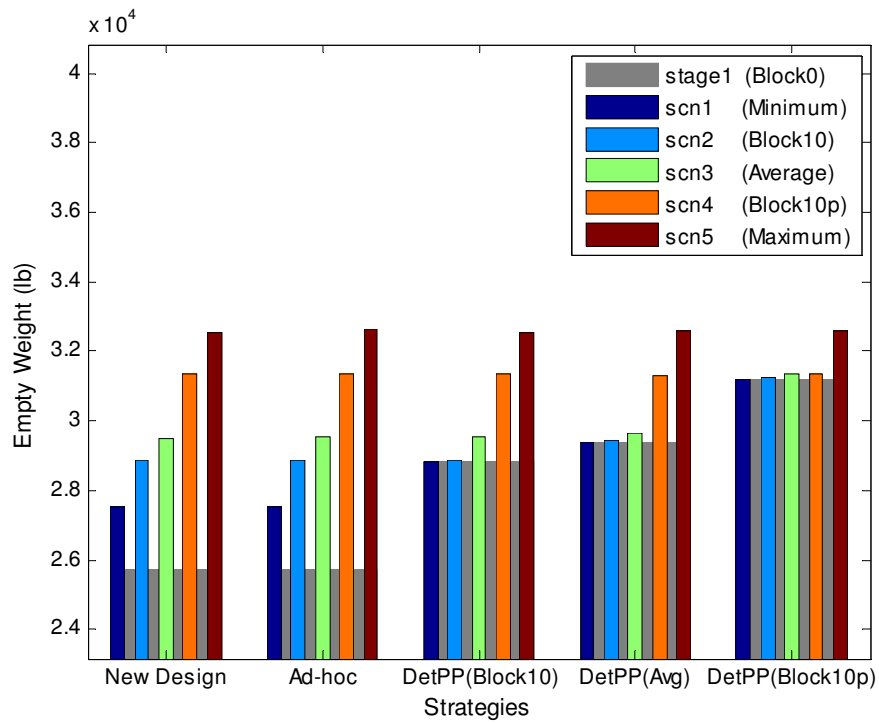Figure 115: Engine Thrust Comparison

Figure 116: External Fuel Comparison
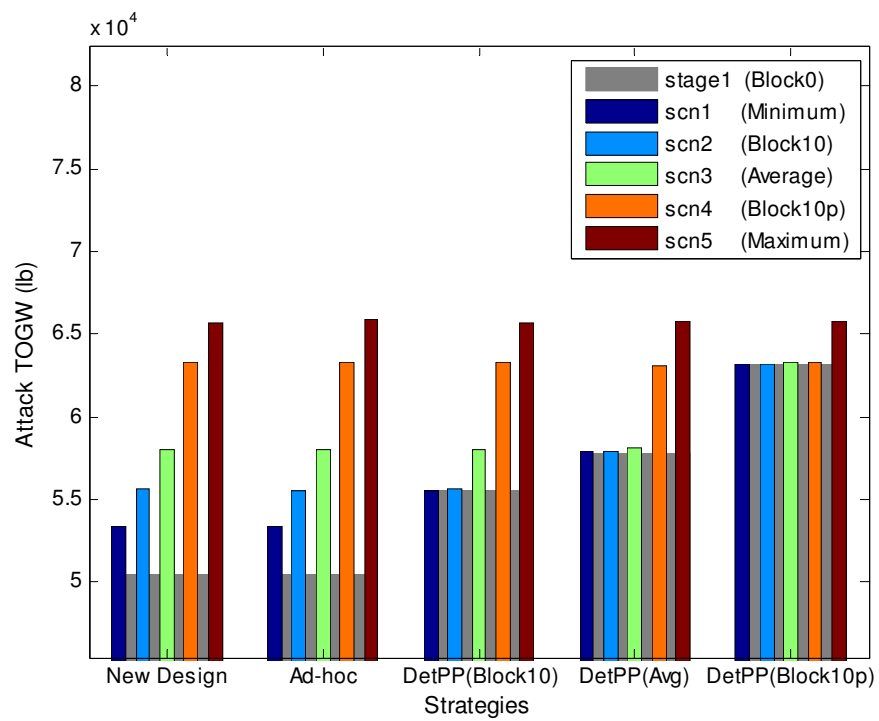

Figure 117: Empty Weight Comparison

Figure 118: Takeoff Gross Weight in Attack Configuration

REFERENCES

[1] SORENSON, D. S., *The Politics of Strategic Aircraft Modernization*, Praeger, Westport, Connecticut, 1995.

[2] JAWOROWSKI, R. and DANE, W., "The World Rotorcraft Market 2006-2015", *Vertiflite*, American Helicopter Society, 2006.

[3] BIERY, F. and LORELL, M., *Preplanned Product Improvement and Other Modification Strategies: Lessons from Past Aircraft Modification Programs, RAND-N-1794-AF*, RAND Corporation, Santa Monica, CA, 1981.

[4] YOUNOSSI, O., STEM, D. E., LORRELL, M. A., et al., "Lessons Learned from the F/A-22 and F/A-18E/F Development Programs", *Project Air Force*, Rand Corporation, 2005.

[5] MCNUTT, R., "Reducing Air Force Acquisition Response Times and Spiral Development", U.S. Air Force Briefing, Acquisition Management Policy Division, 2000.

[6] RAYMER, D. P., *Aircraft Design: A Conceptual Approach*, American Institute of Aeronautics and Astronautics, Reston, VA, 1999.

[7] ROSKAM, J., *Part I: Preliminary Sizing of Airplanes, Airplane Design*, DARcorporation, Lawrence, Kansas, 2003.

[8] FIELDING, J. P., *Introduction to Aircraft Design*, Cambridge University Press, 1999.

[9] TORENBEEK, E., *Synthesis of Subsonic Airplane Design*, Springer, 1982.

[10] STEVENS, D., DAVIS, B., STANLEY, W., et al., "The Next-Generation Attack Fighter: Affordability and Mission Needs", *Project Air Force*, Rand 1997.

[11] SCHRAGE, D. P., "Army Aircraft Requirements in the 1990s - A View Forward", *AIAA Aircraft Design, Systems, and Technology Meeting*, Fort Worth, TX, 1983.

[12] MACKEY, P. T., "Pre-Planned Product Improvement: A Better Way of Weapon System Acquisition", Master's Thesis, School of Systems and Logistics, Air Force Institute of Technology, Wright-Patterson AFB, OH, 1984.

[13] FOX, B., BOITO, M. and GRASER, J. C., "Test and Evaluation Trends and Costs for Aircraft and Guided Weapons", *Project Air Force*, Rand Corporation, 2004.

[14] "Operation of the Defense Acquisition System", Department of Defense, DoD Instruction 5000.2, 2004.

[15] "Evolutionary Acquisition For C2 Systems", Secretary of the Air Force, The US Air Force, Air Force Instruction 63-123, 2000.

[16] "Guidance for DoD Space System Acquisition Process", Under Secretary of Air Force Deputy for Space, Department of Defense, 2004.

[17] BOEHM, B., "A Spiral Model of Software Development and Enhancement", *Computer*, **1**(May), 1988, pp. 61-72.

[18] BOEHM, B., "Spiral Development: Experience, Principles, and Refinements", Carnegie Mellon Software Engineering Institute, 2000.

[19] ALDRIDGE, E. C., JR., "Evolutionary Acquisition and Spiral Development ", Acquisition Technology and Logistics, Under Secretary of Defense, 2002.

[20] SYLVESTER, R. K. and FERRARA, J. A., "Conflict and Ambiguity - Implementing Evolutionary Acquisition", *Acquisition Review Quarterly*, (Winter), 2003.

[21] ASIMOW, M., *Introduction to Design*, Prentice-Hall, 1962.

[22] DIETER, G. E., *Engineering Design: A Materials and Processing Approach*, McGraw-Hill, New York, NY, 2000.

[23] WOLLOVER, D. R., "Quality Function Deployment as a Tool for Implementing Cost as an Independent Variable", *Acquisition Review Quarterly*, 1997.

[24] BALABA, D., LIM, D. W., SCHMOLGRUBER, P., et al., "Quiet Efficient Subsonic Transport Aircraft for the American Institute of Aeronautics and Astronautics 2002-2003 Graduate Team Aircraft Design", Georgia Institute of Technology, 2003.

[25] ARMACOST, R., COMPONATION, P., MULLENS, M., et al., "An AHP framework for prioritizing customer requirements in QFD: An industrialized housing application", *Institute of Industrial Engineers Transactions*, **26**(4), 1994, pp. 72-79.

[26] SAATY, T. L., *The Analytic Hierarchy Process*, McGraw-Hill, New York, 1980.

[27] SAATY, T. L., *Decision Making for Leaders: The Analytic Hierarchy Process for Decisions in a Complex World*, RWS Publications, Pittsburgh, Pennsylvania, 1999.

[28] HAUSER, J. R. and CLAUSING, D., "The House of Quality", *Harvard Business Review*, **66**, 1988, pp. 63-73.

[29] GUINTA, L. R. and PRAIZLER, N. C., *The QFD Book, The Team Approach to Solving Problems and Satisfying Customers Through Quality Function Deployment*, AMACOM Books, 1993.

[30] ZWICKY, F., "The Morphological Method of Analysis and Construction", *Courant*, 1948, pp. 461-470.

[31] ZWICKY, F., *Discovery, Invention, Research — Through the Morphological Approach*, Macmillan, Toronto, 1969.

[32] RHYNE, R., "Whole-Pattern Futures Projection, Using Field Anomaly Relaxation", *Technological Forecasting and Social Change*, **19**, 1981, pp. 331–360.

[33] COYLE, R. and MCGLONE, G., "Projection Scenarios for South-east Asia and the South-west Pacific", *Futures*, **27**(1), 1995, pp. 65-79.

[34] RITCHEY, T., "Nuclear Facilities and Sabotage: Using Morphological Analysis as a Scenario and Strategy Development Laboratory", *44th Annual Meeting of the Institute of Nuclear Materials Management*, Phoenix, Arizona, 2003.

[35] STENSTRÖM, M., WESTRIN, P. and RITCHEY, T., "Living with UXO – Using morphological analysis or decision support in phasing out military firing ranges", Swedish Defence Research Agency, 2004.

[36] HILL, P. H., *The Science of Engineering Design*, Holt, Rinehart and Winston, New York, 1970.

[37] VANDERPLAATS, G. N., *Numerical Optimization Techniques For Engineering Design*, Vanderplaats Research & Development, Inc., Colorado Springs, 2001.

[38] SUH, N. P., *The Principles of Design, Oxford Series on Advanced Manufacturing*, Oxford University Press, New York, 1990.

[39] JONES, J. C., "A Method of Systematic Design", edited by J. C. Jones and Thornley, D., *Conference on Design Methods*, Pergamon Press, Oxford, 1963, pp. 53-73.

[40] CROSS, N., *Engineering Design Methods: Strategies for Product Design*, John Wiley and Sons, 1994.

[41] ANDERSON, J. D., *Aircraft Performance and Design*, McGraw-Hill Companies Boston, MA, 1998.

[42] NAM, T., SOBAN, D. and MAVRIS, D., "A Generalized Aircraft Sizing Method and Application to Electric Aircraft", *3rd International Energy Conversion Engineering Conference*, San Francisco, California, 2005.

[43] BORER, N. K. and MAVRIS, D. N., "Formulation of a multi-mission sizing methodology for competing configurations", *42nd AIAA Aerospace Sciences Meeting and Exhibit*, Reno, NV, 2004.

[44] MATTINGLY, J. D., HEISER, W. H. and PRATT, D. T., *Aircraft Engine Design, AIAA Education Series*, American Institute of Aeronautics and Astronautics, Inc., Reston, VA, 2002.

[45] NAM, T., "A Generalized Sizing Method for Revolutionary Concepts under Probabilistic Design Constraints", PhD Thesis, Aerospace Engineering, Georgia Institute of Technology, Atlanta, 2007.

[46] BORER, N., "Decision Making Strategies for Probabilistic Aerospace Systems Design", PhD Thesis, School of Aerospace Engineering, Georgia Institute of Technology, Atlanta, 2006.

[47] MAVRIS, D. N. and DeLAURENTIS, D. A., "A Stochastic Design Approach for Aircraft Affordability", *21st Congress of the International Council on the Aeronautical Sciences (ICAS)*, Melbourne, Australia, 1998.

[48] "Technology for Affordability: A Report on the Activities of the Working Groups", IPPD Working Groups, The National Center for Advanced Technologies (NCAT), 1993.

[49] "Department of Defense Guide to Integrated Product and Process Development", Office of the Undersecretary of Defense, Acquisition and Technology Division, 1996.

[50] SCHRAGE, D. P., "Technology for Rotorcraft Affordability Through Integrated Product/Process Development (IPPD)", *Alexander A. Nikolsky Lecture, Proceedings of the 55th National Forum of the American Helicopter Society*, Montreal, Quebec, Canada, 1999.

[51] MAVRIS, D. N., BANDTE, O. and DeLAURENTIS, D. A., "Robust Design Simulation - A Probabilistic Approach to Multidisciplinary Design", *Journal of Aircraft*, **36**(1), 1999, pp. 298-307.

[52] KIRBY, M. R., "A Methodology for Technology Identification, Evaluation, and Selection in Conceptual and Preliminary Aircraft Design", PhD Thesis, Georgia Institute of Technology, Atlanta, 2001.

[53] MAVRIS, D. N. and KIRBY, M. R., "Technology Impact Forecasting for a High Speed Civil Transport", *World Aviation Congress and Exposition*, Anaheim, CA, 1998.

[54] MAVRIS, D. N., BAKER, A. P. and SCHRAGE, D. P., "Implementation of a Technology Impact Forecast Technique on a Civil Tiltrotor", *55th National Forum of the American Helicopter Society*, Montreal, Quebec, Canada, 1999.

[55] MAVRIS, D. N., SOBAN, D. S. and LARGENT, M. C., "An Application of a Technology Impact Forecasting (TIF) Method to an Uninhabited Combat Aerial Vehicle", *4th World Aviation Congress and Exposition*, San Francisco, CA, 1999.

[56] MAVRIS, D. N., BAKER, A. P. and SCHRAGE, D. P., "Simultaneous Assessment of Requirements and Technologies in Rotorcraft Design", *56th AHS International Annual Forum*, Virginia Beach, VA, 2000.

[57] BAKER, A. P., "The Role of Mission Requirements, Vehicle Attributes, Technologies and Uncertainty in Rotorcraft System Design", PhD Thesis, School of Aerospace Engineering, Georgia Institute of Technology, Atlanta, GA, 2002.

[58] BAKER, A. P., MAVRIS, D. N. and SCHRAGE, D. P., "Assessing the Impact of Mission Requirements, Vehicle Attributes, Technologies and Uncertainty in Rotorcraft System Design", *58th Annual Forum*, Montreal, Canada, 2002.

[59] BAKER, A. P. and MAVRIS, D. N., "Assessing the Simultaneous Impacts of Requirements, Vehicle Characteristics, and Technologies During Aircraft Design", *39th AIAA Aerospace Sciences Meeting and Exhibit*, Reno, NV, 2001.

[60] MAVRIS, D. N. and DeLAURENTIS, D., "Methodology for Examining the Simultaneous Impact of Requirements, Vehicle Characteristics, and Technologies on Military Aircraft Design", *22nd Congress of the International Council on the Aeronautical Sciences (ICAS)*, Harrogate, England, 2000.

[61] MYERS, R. H. and MONTGOMERY, D. C., *Response Surface Methodology: Process and Product Optimization Using Design Experiments*, John Wiley & Sons, Inc., 1995.

[62] MCCULLOCH, W. S. and PITTS, W. H., "A Logical Calculus of the Ideas Immanent in Nervous Activity", *Bulletin of Mathematical Biophysics*, **5**, 1943, pp. 115-133.

[63] "DARPA Neural Network Study", Lincoln Laboratory, MIT, 1988.

[64] BOX, G. E. P. and DRAPER, N. R., *Empirical model-building and response surfaces*, John Wiley & Sons, Inc., New York, NY, 1987.

[65] BARROS, P. A., JR., KIRBY, M. R. and MAVRIS, D. N., "Impact of Sampling Technique Selection on the Creation of Response Surfaces", *the World Aviation Congress and Exposition*, Reno, NV, 2004.

[66] INMAN, R. L., HELSON, J. C. and CAMPBELL, J. E., "An Approach to Sensitivity Analysis of Computer Models, Part I. Introduction, Input Variable Selection and Preliminary Variable Assessment", *Journal of Quality Technology*, 1981.

[67] LIM, D. W., AHN, B. H. and MAVRIS, D., "A Comparative Study of a Multi-Gas Generator Fan to a Turbofan Engine on a Vertical Takeoff and Landing Personal Air Vehicle", *General Aviation Technology Conference & Exposition*, Wichita, Kansas, 2006.

[68] STUART, W. G., *Northrop F-5 Case Study in Aircraft Design, AIAA Professional Study Series*, AIAA, Alexandria, VA, 1978.

[69] HEHS, E., "F-16 Evolution", *Code One, An Airpower Projection Magazine*, 1997, [online] www.codeonemagazine.com/archives/1997/articles/jul_97/july4a_97.html [retrieved 24 Oct 2006].

[70] PATIERNO, J., "YF-17 design concepts", *6th American Institute of Aeronautics and Astronautics, Aircraft Design, Flight Test and Operations Meeting*, Los Angeles, California, 1974.

[71] GIBSON, C. M., "F/A-18 HORNET-A Status Report", *Interavia*, **35**(Feb), 1980, pp. 139-146.

[72] KRINGS, J. E., "F/A-18 status report", *Society of Experimental Test Pilots, Technical Review*, **14**(4), 1979, pp. 1-9.

[73] MURDEN, W. P., ALTIS, H. D. and RAMEY, M. L., "Fighter Superiority by Design", *AGARD Fighter Aircraft Design*, 1978.

[74] BOLKCOM, C., "Navy F/A-18E/F Super Hornet and EA-18G Growler Aircraft: Background and Issues for Congress", Congressional Research Service, 2007.

[75] FORD, J. T., MEREDITH, W. C., CLARK, J. W., et al., "Naval Aviation: F/A-18E/F Acquisition Strategy", National Security and International Affairs Division, General Accounting Office, Washington DC, 1994.

[76] YOUNG, J. A., ANDERSON, R. D. and YURKOVICH, R. N., "A Description of the F/A-18E/F Design and Design Process", *7th AIAA/USAF/NASA/ISSMO Symposium on Multidisciplinary Analysis and Optimization*, St. Louis, MO, 1998.

[77] LENOX, G. W., "F-18 Multi-mission Aircraft", *Society of Experimental Test Pilots, Technical Review*, **13**(2), 1976, pp. 34-41.

[78] BRINKS, W. H., "F/A-18 Full Scale Development Test", *Technical Review*, **15**(2), 1980, pp. 38-46.

[79] LAMBERT, M. (ed), *Jane's All the World's Aircraft 1992-1993*, Jane's Information Group, London, UK, 1993.

[80] "Naval Combat Aircraft: Issues and Options", Congressional Budget Office, The Congress of the United States, 1987.

[81] BOLKCOM, C., "Military Aircraft, the F/A-18E/F Super Hornet Program: Background and Issues for Congress", Congressional Research Service, 2004.

[82] "History of F-35", F-35 Joint Strike Fighter Program Office, 2008, [online] http://www.jsf.mil/history/his_prejast.htm [retrieved 10-Setember-2007].

[83] "Cost and Operational Effectiveness Analysis Summary for F/A-18 Upgrade Program", *The House Armed Service Committee*, U.S. Senate, 1992.

[84] HOLZEISEN-MULLEN, S., "Squadron Homecoming Marks End of Era for Tomcats", The US Navy, 2006, [online] http://www.news.navy.mil/search/display.asp?story_id=22637 [retrieved 16-May-2007].

[85] "Boeing Chinook", The Boeing Company, 2007, [online] www.boeing.com/rotorcraft/military/ch47d/ [retrieved 26-March-2007].

[86] TAYLOR, J. W. (ed), *Jane's All the World's Aircraft 1970-71*, Sampson Low, 1971.

[87] TAYLOR, J. W. (ed), *Jane's All the World's Aircraft, 1983-1984*, Jane's Information Group, London, UK, 1984.

[88] JACKSON, P., PEACOCK, L. T. and MUNSON, K. (eds), *Jane's All the World's Aircraft 2001-2002*, Jane's Information Group, London, 2002.

[89] "Boeing 737 Family", The Boeing Company, 2006, [online] http://www.boeing.com/commercial/737family/ [retrieved 24-March-2006].

[90] TAYLOR, J. W. (ed), *Jane's All the World's Aircraft 1966-67*, McGraw-Hill Book Co., 1967.

[91] GERVAIS, E. L., "Boeing Commercial Airplanes Current Product Overview", Presentation, Boeing Commercial Airplanes, 2007.

[92] GULCHER, R. H., "Flexibility for the Next Century - P3I and B-1B (Preplanned Product Improvement)", *AIAA, AHS, ASEE, Aircraft Design Systems and Operations Meeting*, San Diego, CA, 1984.

[93] STEINER, J. E., BOWES, G. M., MAXAM, F. G., et al., *A Case Study in Aircraft Design: The Boeing 727*, American Institute of Aeronautics and Astronautics, 1978.

[94] BIRGE, J. R. and LOUVEAUX, F., *Introduction to Stochastic Programming*, Springer, New York, 1997.

[95] DANTZIG, G., "Linear Programming Under Uncertainty", *Management Science*, **1**, 1955, pp. 197-206.

[96] BEALE, E., "On Minimizing a Convex Function Subject to Linear Inequalities", *Journal of Royal Statistical Society*, **B17**, 1955, pp. 173-184.

[97] SHAPIRO, A. and PHILPOTT, A., "A Tutorial on Stochastic Programming", School of Industrial and Systems Engineering, Georgia Institute of Technology, 2007.

[98] BASTIN, F., "Nonlinear Stochastic Programming", PhD thesis, Department de Mathematique, Faculte des Sciences, Universitaires Notre-Dame de la Paix, Namur, Belgium, 2001.

[99] BELLMAN, R. E., *Dynamic Programming*, Princeton University Press, Princeton, PA, 1957.

[100] NIEDERREITER, H., *Random Number Generation and Quasi-Monte Carlo Methods*, SIAM, 1992.

[101] WANG, W., "Sample Average Approximation of Risk-Averse Stochastic Programs", PhD Thesis, School of Industrial and Systems Engineering, Georgia Institute of Technology, Atlanta, GA, 2007.

[102] "Guiding Principles for Monte Carlo Analysis", US Environmental Protection Agency, Washington DC, 1997.

[103] IMAN, R. L. and CONOVER, W. J., "A Distribution-Free Approach to Inducing Rank Correlation among Input Variable", *Communications in Statistics, Part B-Simulation and Computation*, **11**, 1982, pp. 311-334.

[104] STEIN, M., "Large Sample Properties of Simulations using Latin Hypercube Sampling ", *Technometrics*, **29**(2), 1987, pp. 143-151.

[105] MANTEUFEL, R. D., "Estimating the Error in LHS Predictions", *46th AIAA/ASME/ASCE/AHS/ASC Structures, Structural Dynamics & Materials Conference*, Austin, Texas, 2005.

[106] MANTEUFEL, R. D., "Evaluating the Convergence of Latin Hypercube Sampling", *Proceedings of 41st AIAA Structures, Structural Dynamics, and Material Conference*, 2000.

[107] RAIFFA, H. and SCHLAIFER, R., *Applied Statistical Decision Theory*, Harvard University, Boston, MA, 1961.

[108] MANDANSKY, A., "Inequalities for Stochastic Linear Programming Problems", *Management Science*, (6), 1960, pp. 197-204.

[109] SAHINIDIS, N. V., "Optimization under uncertainty: state-of-the-art and opportunities", *Computers and Chemical Engineering*, **28**, 2003, pp. 971-983.

[110] CARINO, D. R. and ZIEMBA, W. T., "Formulation of the Russell-Yasuda Kasai Financial Planning Model", *Operations Research*, **46**, 1998, pp. 433–449.

[111] ANDERSSON, F., MAUSSER, H., ROSEN, D., et al., "Credit risk optimization with Conditional Value-at-Risk criterion", *Mathematical Programming*, **89**(2), 2001, pp. 273-292.

[112] ESCUDERO, J., KAMESAM, P. V., KING, A., et al., "Production Planning via Scenario Modeling", *Annals of Operations Research*, **43**(1-4), 1993, pp. 311–335.

[113] BIRGE, J. R. and DEMPSTER, M. A. H., "Stochastic Programming Approaches to Stochastic Scheduling", *Journal of Global Optimization*, **9**(3–4), 1996, pp. 417–451.

[114] BARBAROSOGLU, G. and ARDA, Y., "A two-stage stochastic programming framework for transportation planning in disaster response", *Journal of the operational research society*, **55**, 2004, pp. 43-53.

[115] LINDEROTH, J., "Stochastic Programming", *Class Note*, Department of Industrial and Systems Engineering, Lehigh University, 2003, [online] www.lehigh.edu/~jt13/teaching/slp [retrieved 13 Feb 2006].

[116] KALL, P. and WALLACE, S. W., *Stochastic Programming*, Wiley John & Sons, 1995.

[117] CHOI, T., "A recourse-based solution approach to the design of fuel cell aeropropulsion systems", PhD Thesis, School of Aerospace Engineering, Georgia Institute of Technology, Atlanta, 2008.

[118] LIM, D. W. and MAVRIS, D., "An Approach to Evolutionary Aircraft Design for Growth Potential", *7th AIAA Aviation Technology, Integration and Operations Conference (ATIO)* Belfast, UK, 2007.

[119] SOMMER, L., "Exposition of a New Theory on the Measurement of Risk", *Econometrica*, **22**(1), 1954, pp. 22-36.

[120] VON NEUMANN, J. and MORGENSTERN, O., *Theory of Games and Economic Behavior*, Princeton University Press, Princeton, 1947.

[121] CHARNES, A. and COOPER, W. W., "Chance-Constrained Programming", *Management Science*, **6**, 1959, pp. 73-79.

[122] Rao, S., "Structural Optimization by Chance Constrained Programming Techniques", *Computers and Structures*, **12**, 1980, pp. 777-781.

[123] Agnew, N. H., Agnew, R. A., Rasmussen, J., et al., "An Application of Chance Constrained Programming to Portfolio Selection in a Casualty Insurance Firm", *Management Science*, **15**(10), 1969, p. B512.

[124] Li, S. X., "An Insurance and Investment Portfolio Model Using Chance Constrained Programming", *Omega*, **23**(5), 1995, pp. 577-585.

[125] Enevoldsen, I. and Sorensen, J., "Reliability-Based Optimization in Structural Engineering", *Structural Safety*, **15**, 1994, pp. 169-196.

[126] Tu, J., Choi, K. K. and Park, Y. H., "A New Study on Reliability-Based Design Optimization", *Journal of Mechanical Design*, **121**, 1999, pp. 557-564.

[127] Rais-Rohan, M. and Xie, Q., "Probabilistic Structural Optimization Under Reliability, Manufacturability, and Cost Constraints", *AIAA Journal*, **43**, 2005, pp. 864-873.

[128] Ba-abbad, M. A. and Kapania, R. K., "Reliability-Based Structural Optimization of an Elastic-Plastic Beam", *AIAA Journal*, **41**, 2003, pp. 1573-1582.

[129] Nam, T. and Mavris, D., "A Non-Deterministic Aircraft Sizing Method under Probabilistic Design Constraints ", *47th AIAA/ASME/ASCE/AHS/ASC Structures, Structural Dynamics, and Materials Conference*, Newport, Rhode Island, 2006.

[130] Markowitz, H. M., "Portfolio Selection", *Journal of Finance*, **7**(1), 1952, pp. 77-91.

[131] Malcolm, S. A. and Zenios, S. A., "Robust optimization of power systems capacity expansion", *Journal of the operational research society*, **45**, 1994, pp. 1040-1049.

[132] Ahmed, S. and Sahinidis, N. V., "Robust process planning under uncertainty", *Industrial & Engineering Chemistry Research*, **37**(5), 1998, pp. 1883-1892.

[133] LAGUNA, M., "Applying robust optimization to capacity expansion of one location in telecommunications with demand uncertainty", *Management Science*, **44**, 1998, pp. S101-S110.

[134] RUSZCZYNSKI, A. and SHAPIRO, A., "Optimization of Risk Measures", In: G. Calafiore and Dabbene, F. (eds), Probabilistic and Randomized Methods for Design Under Uncertainty, Birkhäuser, 2006.

[135] BENATI, S., "The optimal portfolio problem with coherent risk measure constraints", *European Journal of Operational Research*, **150**, 2003, pp. 572-584.

[136] *Risk Metrics Technical Manual*, JP Morgan, New York, 1996.

[137] BEDER, T. S., "VAR: Seductive but Dangerous", *Financial Analysts Journal*, **51**(5), 1995, pp. 12-24.

[138] JORION, P., *Value at Risk: A New Benchmark for Measuring Derivatives Risk*, Irwin Professional Publishing, 1996.

[139] EMBRECHTS, P., KLUPPELBERG, S. and MIKOSCH, T., *Extreme Events in Finance and Insurance*, Springer, 1997.

[140] BUCAY, N. and ROSEN, D., "Credit Risk of an International Bond Portfolio: A Case Study", *ALGO Research Quarterly*, **2**(1), 1999, pp. 9-29.

[141] SCHOEMAKER, P. J. H., "Scenario Planning: A Tool for Strategic Thinking", *Sloan Management Review*, **36**(2), 1995, pp. 25-40.

[142] SCHWARTZ, P., *The Art of the Long View*, Doubleday, 1991.

[143] WILSON, I. and RALSTON, B., *Scenario Planning Handbook: Developing Strategies in Uncertain Times*, South-Western Educational Pub, 2006.

[144] SCHOEMAKER, P. J. H. and VAN DER HEIJDEN, C. A. J. M., "Integrating Scenarios into Strategic Planning at Royal Dutch/Shell", *Planning Review*, **20**(3), 1992, pp. 41-46.

[145] ERIKSSON, T. and RITCHEY, T., "Scenario Development and Force Requirements using Morphological Analysis", Swedish Defence Research Agency, 2005.

[146] ZIEGLER, R., DE CLERCQ, M. and ARIATTI, A., "Tapping the Sun: Solar Energy in the Middle East", *Executive Agenda*, A.T. Kearney, Chicago, Illinois, 2007.

[147] GASPAR, D. and PERLINGIERE, T., "Future-Proofing the Company Against Risk", *Executive Agenda*, A.T. Kearney, Chicago, Illinois, 2007.

[148] THOMAS, C., "Scenario-based Planning for Technology Investments", In: L. Fahey and Randall, R. (eds), Learning from the Future John Wiley & Sons, 1997.

[149] BOROUSH, M. A. and THOMAS, C. W., "Alternative Scenarios for the Defense Industries after 1995", *Strategy & Leadership*, **20**(3), 1992.

[150] BLAKE, M., "Baseline Future Scenarios for JPDO Evaluation and Analysis", Presentation, 2005.

[151] BORENER, S., CARR, G., BALLARD, D., et al., "Can NGATS Meet the Demands of the Future?", *ATCA Journal of Air Traffic Control*, **January-March**, 2006.

[152] THOMAS, V., "A Method for Scenario-based Risk Assessment for Robust Aerospace Systems", PhD Thesis, School of Aerospace Engineering, Georgia Institute of Technology, Atlanta, 2007.

[153] "Audit Report: Operational Testing and Evaluation of the F/A-18E/F Super Hornet", Office of the Inspector General, Department of Defense, 1999.

[154] SCHWARTZ, N. A., "Joint Capabilities Integration and Development System", Chairman of the Joint Chiefs of Staff Instruction, 2005.

[155] "Current Market Outlook 2008-2027", The Boeing Company, 2008.

[156] "Global Market Forecast 2007-2026", Airbus, 2007.

[157] BLAKE, M., "Baseline Future Scenarios for JPDO Evaluation and Analysis", Next Generation Air Transportation System, Joint Planning and Development Office, 2005.

[158] YOON, K. P. and HWANG, C.-L., " Multiple Attribute Decision Making: An Introduction", *Quantitative Applications in the Social Sciences*, 1995.

[159] ENGLER, W. O., BILTGEN, P. T. and MAVRIS, D. N., "Concept Selection Using an Interactive Reconfigurable Matrix of Alternatives (IRMA)", *45th AIAA Aerospace Sciences Meeting and Exhibit, no. AIAA 2007-32*, American Institute of Aeronautics and Astronautics, Reno, NV, 2007.

[160] SOBAN, D. and UPTON, E., "Design of a UAV to Optimize Use of Fuel Cell Propulsion Technology", *Infotech@Aerospace, no. AIAA 2005-7135*, American Institute of Aeronautics and Astronautics, Arlington, VA, 2005.

[161] MANKINS, J. C., "Technology Readiness Level", A White Paper, Advanced Concepts Office, Office of Space Access and Technology, NASA, 1995.

[162] J. S. SOBIESKI, J. S. A., R. ROBERT, ", "Bi-Level Integrated System Synthesis (BLISS)", NASA Langley Research Center, 1998.

[163] BRAUN, R. D., GAGE, P. J., KROO, I. M., et al., "Implementation and Performance Issues in Collaborative Optimization", *Proceedings of the 6th AIAA/USAF/NASA/ISSMO Symposium on Multidisciplinary Analysis and Optimization*, ASA Langley Research Center, 1996.

[164] BRAUN, R. D. and KROO, I. M., "Development and Application of the Collaborative Optimization Architecture in a Multidisciplinary Design Environment", *International Congress on Industrial and Applied Mathematics*, NASA Langley Research Center, 1995.

[165] GIUNTA, A. A., "Aircraft Multidisciplinary Design Optimization using Design of Experiments theory and response surface modeling methods", PhD Thesis, Virginia Polytechnic Institute and State University, 1997.

[166] BRAUN, R. D., MOORE, A. A. and KROO, I. M., "Use of Collaborative Optimization Architecture for Launch Vehicle Design", *Proceedings of the 6th AIAA/USAF/NASA/ISSMO Symposium on Multidisciplinary Analysis and Optimization*, NASA Langley Research Center, 1996.

[167] BROWN, N. F. and OLDS, J. R., "Evaluation of Multidisciplinary Optimization Techniques Applied to a Reusable Launch Vehicle", *Journal of Spacecraft and Rockets*, **43**(6), 2006.

[168] SOBIESKI, J. S., "Multidisciplinary Design Optimization: An Emerging New Engineering Discipline", *The World Congress on Optimal Design of Structural Systems*, Rio De Janeiro, Brazil, 1993.

[169] MAVRIS, D. N., BRICENO, S. I., BUONANNO, M., et al., "A Parametric Exploration of Supersonic Business Jet Concepts Utilizing Response Surfaces", *Presented at the 2nd AIAA ATIO Forum*, Los Angeles, CA, 2002.

[170] SCHARL, J., "Formulation and Implementation of a Methodology for Dynamic Modeling and Simulation in Early Aerospace Design", PhD Thesis, Aerospace Engineering, Georgia Institute of Technology, Atlanta, 2001.

[171] LAMBERT, M. (ed), *Jane's All the World's Aircraft 1990-1991*, Jane's Information Group, London, UK, 1991.

[172] "Glossary of Definitions, Ground Rules, and Mission Profiles to Define Air Vehicle Performance Capability", Department of Defense, MIL-STD-3013, 2003.

[173] BUTTRILL, C. S., ARBUCKLE, P. D. and HOFFLER, K. D., "Simulation model of a twin-tail, high performance airplane ", NASA Langley Research Center, NASA-TM-107601, 1992.

[174] "NATOPS Flight Manual: Navy Model F/A-18E/F 165533 and up Aircraft", McDonnell Douglas Corporation, AF-F18EA-NFM-000, 1999.

[175] "Preliminary NATOPS Flight Manual Performance Charts: Navy Model F/A-18E/F 165533 and Up Aircraft", McDonnell Douglas Corporation, AF-F18EA-NFM-200, 1999.

[176] ALLMON, A. D., II, "USAF F-15E Strike Eagle", *The Defense Imagery Server*, US Air Force, 2004.

[177] MCCULLERS, L. A., "Flight Optimization System Release 5.94 User's Guide", National Aeronautics and Space Administration, 1998.

[178] HALL, D., CHUN, S. and ANDREWS, D., "Study of Preliminary Configuration Design of F-35 using Simple CFD", 2003, [online]

http://www.aoe.vt.edu/~mason/Mason_f/F35AndrewsS03.pdf [retrieved 22-January-2008].

[179] HENRY, M. M., "Two-dimensional Shock Sensitivity Analysis for Transonic Airfoils with Leading-Edge and Trailing-Edge Device Deflections", Master's Thesis, Aerospace Engineering, the Virginia Polytechnic Institute and State University, Blacksburg, Virginia, 2001.

[180] SIEWERT, R. F. and WHITEHEAD, R. E., "Analysis of advanced variable camber concepts", *AGARD Fighter Aircraft Design 21 p*, 1978.

[181] FEAGIN, R. C. and MORRISON, W. D., "Delta method, an empirical drag buildup technique ", NASA Ames Research Center, NASA-CR-151971, 1978.

[182] SALTZMAN, E. J. and HICKS, J. W., "In-Flight Lift-Drag Characteristics for a Forward-Swept Wing Aircraft (and Comparisons with Contemporary Aircraft)", National Aeronautics and Space Administration, NASA Technical Paper 3414, 1994.

[183] "NATOPS Flight Manual Performance Charts: Navy Model F/A-18A/B/C/D Equipped with F404-GE-400 Engines", McDonnell Douglas Corporation, A1-F18AC-NFM-200, 1998.

[184] JOHN, A., JR., *Aircraft Performance and Design*, McGraw Hill, 1999.

[185] HALL, R., MURRI, D., ERICKSON, G., et al., "Overview of HATP Experimental Aerodynamics Data for the Baseline F /A-18 Configuration", NASA Langley Research Center, NASA TM 112360, 1996.

[186] LEE, B. H. K. and BROWN, D., "Wind-Tunnel Studies of F/A-18 Tail Buffet", *Journal of Aircraft*, **29**(1), 1992, pp. 146-152.

[187] LEE, B. H. K. and BROWN, D., "Aerodynamic characteristics of the F/A-18 at large roll angles and high incidence", *Journal of Aircraft (0021-8669)*, **34**(1), 1997, pp. 139-141.

[188] BROWNE, L. and ASHBY, D., "Study of the integration of wind tunnel and computational methods for aerodynamic configurations", National Aeronautics and Space Administration, NASA TM 102196, 1989.

[189] ERICKSON, G., HALL, R., BANKS, D., et al., "Experimental investigation of the F/A-18 vortex flows at subsonic through transonic speeds", *7th AIAA Applied Aerodynamics Conference*, Seattle, WA, 1989.

[190] MEYN, L. A., LANSER, W. R. and JAMES, K. D., "Full-Scale High Angle-of-Attack Tests of an F/A-18", 1992.

[191] KUHTA, S. F., CLARK, J. W., GILLIES, W. J., et al., "F/A-18E/F will Provide Marginal Operational Improvement at High Cost", *Report to Congressional Committees*, General Accounting Office, 1996.

[192] TAYLOR, J. W. (ed), *Jane's All the World's Aircraft 1981-1982*, Jane's Information Group, London, UK, 1982.

[193] DAUB, W. J., "F404/RM12 - A key step in the F404 growth plans ", *21st SAE, ASME, and ASEE, Joint Propulsion Conference*, Monterey, CA, 1985.

[194] "F404 Engine Specification", General Electric, 2008, [online] http://www.geae.com/engines/military/f404/f404-400.html [retrieved 11-January-2008].

[195] SCHOCH, E. J., "A Simulation of the I3 to D Repair Process and Sparing of the F414-GE-400 Jet Aircraft Engine", Master's Thesis, Naval Postgraduate School, Monterey, CA 93943-5000, 2003.

[196] YOUNOSSI, O. and UNITED STATES AIR FORCE, *Military jet engine acquisition : technology basics and cost-estimating methodology*, Rand, Project Air Force, Santa Monica, CA, 2002.

[197] GEISELHART, K. G. C., MICHAEL J. and MORRIS, S. J., JR., "Computer Program for Estimating Performance of Airbreathing Aircraft Engines", *Military and Aerospace Electronics*, NASA TM 4254, 1991.

[198] CADDY, M. J. and SHAPIRO, S. R., "NEPCOMP - The Navy Engine Performance Computer Program, Version I", NADC-74045-30, 1975.

[199] ANDERSON, M. R. and MASON, W. H., "An MDO Approach to Control-Configured-Vehicle Design", 1996.

[200] "Airplane Strength and Rigidity", US Department of Defense, Military Specification MIL-A-8629, 1960.

[201] RUDOWSKY, T., COOK, S., HYNES, M., et al., "Review of the Carrier Approach Criteria for Carrier-Based Aircraft – Phase I: Final Report", Naval Air Warfare Center Aircraft Division, Department of the Navy, 2002.

[202] "Flying Qualities of Piloted Aircraft", *US Dept. of Defence Handbook*, Department of Defense, MIL-HDBK-1797, 1997.

[203] "Super Hornet completes carrier suitability round", *Seapower Magazine*, Navy League of the United States, Arlington, VA 22201-5424, 1998.

[204] "Aircraft Carrier Reference Data Manual, Revision D", Naval Air Warfare Center, NAEC-MISC-06900, 1997.

[205] GARCIA, E., "Military Aircraft Life Cycle Cost Analysis", Georgia Institute of Technology, 2001.

[206] WOOD, J. and ROBERT, F., JR., "It's the Aircraft We Need", the US Navy, [online] www.tailhook.org/ACNeedSp97.htm [retrieved 25-Feburary-2008].

[207] BEYERS, M. E., "F/A-18 Nonplanar Maneuvering Aerodynamics", *Canadian Aeronautics and Space Journal*, **47**(2), 2001, pp. 57-69.

[208] "Defense Acquisitions: F/A-18E/F Aircraft Does Not Meet All Criteria for Multilayer Procurement", General Accounting Office, 2000.

[209] KUHTA, S. F., CLARK, J. W., PETRICK, W. E., JR. , et al., "Navy Aviation: F/A-18E/F Development and Production Issues ", Government Accounting Office, 1998.

[210] "NASA's Contribution to F/A-18E/F", *Langley News*, NASA Langley Research Center, 1999, [online] http://www.nasa.gov/centers/langley/news/factsheets/F-18.html [retrieved 13-June-2008].

[211] YOUNOSSI, O., KENNEDY, M. and GRASER, J. C., *Military Airframe Costs: The Effects of Advanced Materials and Manufacturing Processes*, Project Air Force, Rand, 2001.

[212] "NCCA Inflation Calculator Documentation and Update Instructions", Naval Center for Cost Analysis, The US Navy, 2006.

[213] "The Defense Acquisition System", Department of Defense, DoD Directive 5000.1, 2003.

[214] "Memorandum: Milestone I COEA Guidance for USMC Medium Lift Replacement (MLR)", The Under Secretary of Defense, 1992.

[215] BURNS, B. R. A., "The design and development of a military combat aircraft - Part 1: Design for Performance", *Interavia*, **March**, 1976.

[216] "F/A-18 Hornet Strike Fighter", *United States Navy Fact File*, Department of the Navy, 2006, [online] http://www.navy.mil/navydata/fact_display.asp?cid=1100&tid=1200&ct=1 [retrieved 13-March-2009].

[217] COYLE, P. E., "Tactical Aviation", Statement, Senate Armed Services Committee, AirLand Forces Subcommittee, 2000.

[218] DYER, J., "Use of Measurement in Managing the F/A-18E/F Acquisition", *Presented at the Practical Software and Systems Measurement Conference*, 1999.

[219] "US Code, Title 10, Chapter 44, §2432 Major Defense Acquisition Programs", Law Revision Counsel, 2008.

[220] "Operation and Support Costs for the Department of Defense", Congressional Budget Office, The Congress of the United States, 1988.

[221] "Costs of Expanding and Modernizing the Navy's Carrier-Based Air Forces", Congressional Budget Office, The Congress of the United States, 1982.

[222] "Research Development Test & Evaluation, Navy / BA-7: Exhibit R-2, RDTEN Budget Item Justification", The Department of Navy, 2004.

[223] "The Navy Visibility and Management of Operating and Support Costs (VAMOSC)", the US Navy, [online] http://www.navyvamosc.com/ [retrieved 12-May-2008].

[224] "Department of the Navy Fiscal Year 2005 Budget Estimates", Department of the Navy, 2004.

[225] "Land-based F-18 programme firms up", *Interavia*, **11**, 1976.

[226] "SAR Program Acquisition Cost Summary", Department of Defense, 1994.

[227] STEM, D., "F/A-22 and F/A-18 E/F: An Evaluation of the Acquisition Strategy and Cost and Schedule Reports", *Project Air Force*, Rand Corporation, 2005.

[228] DUMA, D. P., "A Cost Estimation Model for Commander Naval Air Forces Pacific's TACAIR F/A-18S Aviation Depot Level Repair Costs", Master's Thesis, Naval Postgraduate School, Monterey, California, 2001.

[229] BROWN, J. C., DEGUZMAN, R. K., JR., FULFORD, T. S., III , et al., "Cost Benefit Analysis of The Department of the Navy's F-5 Tiger II Contract", Naval Postgraduate School, 2003.

[230] *Defense Acquisition Guidebook*, Defense Acquisition University, 2004.

[231] "Work Breakdown Structures for Defense Materiel Items", *Department of Defense Handbook*, Department of Defense, MIL-HDBK-881, 2005.

[232] HALPIN, J. P., PANDOLFINI, P. P., BIERMANN, P. J., et al., "F/A-18 E/F Program Independent Analysis", *Johns Hopkins APL Technical Digest (0270-5214)*, **18**(1), 1997, pp. 33-49.

[233] PENFIELD, J. and RUTHERFORD, R., "Operational flight testing of the F/A-18E/F Super Hornet", *2001 Report to the aerospace profession*, Los Angeles, CA, 2001.

VITA

Dongwook Lim was born in Seoul, South Korea in 1977. He went to Seoul Science High School. He then earned his Bachelor of Science degree in Mechanical and Aerospace Engineering from Seoul National University in 2002. From May of 1999 to July of 2001, he served in the Korean Army. He was stationed at 1st Signal Brigade of the US Army Signal Co. He then enrolled at the Georgia Institute of Technology and was awarded a Master of Science degree in Aerospace Engineering in December of 2003. Dongwook Lim will be awarded his Doctor of Philosophy degree in Aerospace Engineering with Mathematics minor in May of 2009.

During his graduate study, Dongwook Lim was a Samsung Lee Kun Hee Scholarship recipient. He also won the first place in 2002-2003 AIAA Graduate Aircraft Design Competition and third place in 2005 International Micro Air Vehicle Competition. Dongwook is a member of American Institute of Aeronautics and Astronautics, American Helicopter Society, and Society of Automotive Engineers.

Throughout his life, he had a passion for the sky and everything flying in it (and yet does not have a pilot license). Dongwook is enthusiastic about all kinds of sports and music. He plays for the Korean Student Soccer Club and the Georgia Tech intramural soccer league. He plays piano and guitar and always wishes to improve his skills if he had more time. Above all, Dongwook is a very proud father of two wonderful children Heechan and Jumi, and happiest when he spends his time with them.